LincSys Ver 1.0
User's Manual

By
D. Zerihun and C.A. Sanchez

University of Arizona
Maricopa Agricultural Center
37860 W. Smith-Enke Rd
Maricopa, AZ 85138-3010

Abstract: This document presents the *LincSys* software, a computer program for simulating the hydraulics of linear-move and center-pivot irrigation systems. The name *LincSys* is a mnemonic for the phrase 'linear-move and center-pivot systems'. At the core of the *LincSys* software is a pair of executable files: a hydraulic simulation module, *HydrSimLaterals.exe*, and a graphical user interface (GUI), *LincSys.exe*, through which the user interacts with the hydraulic module. The user interface and the computational module are coupled through an application programming interface. Data exchange between the user interface and the simulation module takes place through text files.

The hydraulic module of *LincSys*, *HydrSimLaterals.exe*, is a numerical model that solves the continuity and energy balance equations (for one-dimensional steady flow through a branched hydraulic network consisting of straight and stationary pipes) to determine the lateral-wide distribution of link discharges and nodal heads and an array of additional output parameters. The model can simulate the hydraulics of a linear-move or center-pivot system that uses the following emission devices to meter outlet discharges along the lateral: *(i)* drop-tube, pressure regulator, and emitter assemblies, *(ii)* drop-tube and emitter assemblies, or *(iii)* emitters placed directly on the lateral.

The GUI of *LincSys* consists of a tabbed form with four windows, namely, the Systems-Projects, Input, Output, and Charts tabpages. Each tabpage provides access to a set of program functionalities, consisting of project management and preprocesing, processing, and postprocessing of project data.

The help utility of the *LincSys* software provides resources that the user can tap into through tooltips, a dedicated Help menu that can be activated from the Systems-Projects window, and a set of text files placed in various folders during program installation.

The content of this document is presented in six chapters. Chapter 1 provides a quick introduction to the *LincSys* software. Chapter 2 presents a concise description of linear-move and center-pivot irrigation systems. A summary of linear-move and center-pivot lateral hydraulics is presented in Chapter 3. Chapter 4 describes the features and functionalities of the *GUI* of *LincSys*. A description of the contents and format of the input-output data files and the directory structure used by *LincSys* to manage and track data files is presented in Chapter 5. A discussion on model evaluation results and application examples (sample projects), copied into the *LincSys* input-output data folders during program installation, is presented in Chapter 6.

Contents

List of Tables

List of Figures

Chapter 1. A quick introduction to the *LincSys* software

1.1. Model description, An overview

LincSys is a computer program for simulating the hydraulics of linear-move and center-pivot irrigation systems. The name *LincSys* is a mnemonic device for the phrase 'linear-move and center-pivot systems'.

The *LincSys* software is comprised of a pair of executable files: a hydraulic simulation module, *HydrSimLaterals.exe*, and a graphical user interface (GUI), *LincSys.exe*, through which the user interacts with the hydraulic module. The user interface and the computational module, are coupled through an application programming interface that uses the CreatProcess function.

Data exchange between the user interface and the simulation module takes place through text files. Input data, edited within the user interface, is transferred to the simulation module (*HydrSimLaterals.exe*) and output data from the simulation module is relayed back to the user interface (*LincSys.exe*) using space delimited text files.

1.2. System requirements and installation

1.2.1. Hardware requirements

Although not thoroughly tested, experience suggests that the CPU, memory, and graphics hardware requirements of *LincSys* are basic and hence it is unlikely that hardware constraints would be series limitations for running *LincSys* in most PC's.

Storage space requirements vary with the number of *LincSys* projects and the size of the individual projects. However, at installation, the *LincSys* folder contains software components (*LincSys.exe*, *HydrSimLaterals.exe*, and .Net Framework 4.8 utilities), *LincSys* sample project data, input data file templates, and help resources related documents, which in total require a storage space of about 60MB.

1.2.2. Software requirements

LincSys 1.0 is designed for Windows environment and it can be run on machines with Windows 7.0 or later releases of the Windows operating system. The necessary .Net framework utilities are installed along with the core executable files, thus the model has no requirements for additional software accessories.

1.3. Installation, running, quick exploration of the contents of LincSys installation folder

1.3.1. Installation of LincSys

To install *LincSys 1.0* in a PC, the user need to go to the *url* …….. and then click on the link *Install_LincSys*. This will start the installation program *Install_LincSys.exe*. The user can then follow the directions of the installer software to unzip and place *LincSys* files, .Net Framework utility files, and other files in a specified directory.

1.3.2. Running LincSys

Following a successful installation, the user may notice that the *LincSys* icon appears in the user's desktop and the start menu of Windows. In order to run *LincSys* the user simply needs to click on the *LincSys* icon in the start menu or double click on the icon in the desktop. This will

open a tabbed form (the user interface of *LincSys*) with the Systems-Projects tabpage enabled (Figure 1).

1.3.2.a. The Graphical User Interface (GUI) of LincSys

The GUI of *LincSys* consists of a tabbed form with four windows, namely, the Systems-Projects, Input, Output, and Charts tabpages (Figure 1). Each window is designed to provide access to a set of program functionalities. The user interface was developed with the Basic computer programming language in the Visual Studio Integrated Development Environment (MS, 2019) and is based on the Windows Forms for .Net Framework Ver. 4.8.

The Systems-Projects tabpage represents the main access or entry point to *LincSys*. It is the window that provides access to project management functionalities and help resources. It also enables access to the other tabpages through Windows Forms user interface control buttons. Furthermore, the Systems-Projects window is where the system configuration option for which simulation is to be conducted is specified and the current *LincSys* project is selected. Note that the term project is used in this document to refer to all the input and output data files (of a simulation problem) stored in a folder that bears the name of the project.

The Input tabpage enables access to the input functionality of the model, where input data are displayed and can be edited. If necessary, a simulation run of the current *LincSys* project is also executed from within the Input window.

The Output tabpage is the window where the output data from a successful simulation is displayed. The Charts tabpage provides access to a series of charts (eleven in all) that display a graphical rendering of computed hydraulic parameters.

Standard Windows Forms controls, namely control buttons, textboxes, a listbox, DataGridView tables, labels, chart control, a toolbar, and a dropdown menu are used to issue commands and navigate the user interface. Access to tabpages is mainly enabled through control buttons, although direct access to each tabpage through the respective tabcontrols is conditionally possible (Sections 4.2.3.c, 4.3.1, 4.4.1, and 4.5.1). Note that in this document, the user interface controls used in *LincSys* are referred to using contextually more intuitive names, in place of the general technical names used in the programming literature. A more specific discussion on this is provided in Section 4.1.1.

1.3.2.b. The hydraulic simulation module of LincSys: HydrSimLaterals.exe

The hydraulic module of *LincSys*, *HydrSimLaterals.exe*, is a numerical model that solves the continuity and energy balance equations (for one-dimensional steady flow through a branched hydraulic network consisting of straight and stationary pipes) to determine the lateral-wide distribution of link discharges and nodal heads (e.g., Zerihun and Sanchez, 2019a, 2019b). The model can simulate the hydraulics of linear-move and center-pivot systems with the following lateral outlet discharge metering apparatus configuration options: *(i)* Systems that use drop-tube, pressure regulator, and emitter assemblies to meter outlet discharges along a lateral (labeled as Droptube-Prv-Emittter in the *LincSys* user interface), *(ii)* Systems that use drop-tube

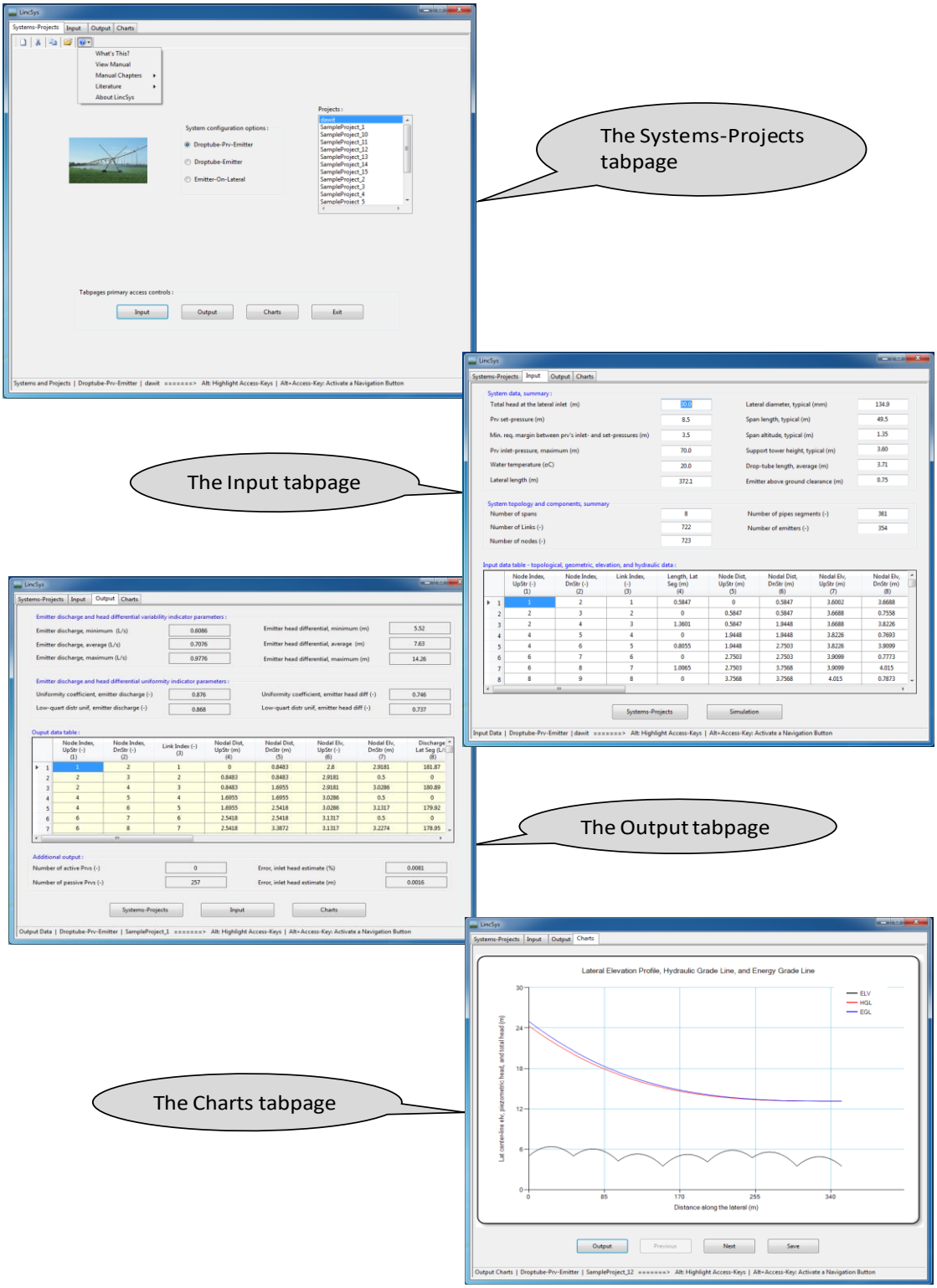

Figure 1. Features, layouts, and control elements of the tabpages (Systems-Projects, Input, Output, and Charts) that form the GUI of *LincSys*

and emitter assemblies to meter outlet discharges (named as Droptube-Emittter in the user interface), and *(iii)* Systems in which the emitters are placed directly on the lateral (described as Emitter-On-Lateral in the user interface). Note that the rather more concise phrase of, system configuration options, is often used in this document to refer to the lateral outlet discharge metering configuration options.

The hydraulic simulation module of *LincSys* was developed by the current authors as a standalone simulation model in 2017. It was written in the *C++* computer programming language, as an MS DOS application, within the Visual Studio Integrated Development Environment (MS, 2017). The model obtains its input data from a text file and output data are saved in text files. The output files can then be opened with a spreadsheet program, such as MS Excel, or any other suitable application for further processing and reporting. A limited evaluation of the computational module conducted by the authors and cooperators (Zerihun et al., 2019) showed that model performance is satisfactory.

The hydraulic simulation module of *LincSys* was initially developed for linear-move irrigation systems (Zerihun and Sanchez, 2019a,b,c). However, the geometric features and hydraulic elements of linear-move and center-pivot laterals are very similar (Martin et al., 2007), thus the hydraulics of these systems is generally considered identical. Accordingly, *LincSys* is presumed here to be equally applicable to center-pivot systems as well.

A final note here is that the angular movement of center-pivots could introduce forces that may have an effect in lateral hydraulics, which is different from those encountered in linear-move systems. However, those effects are generally not considered in center-pivot hydraulics, perhaps because of the low angular velocity of these laterals they are presumed to be of negligible effect.

1.3.3. Quick exploration of the contents of the installation folder

Opening the installation folder with Windows Explorer (or File Explorer) shows that a sizable number of files and a folder have been copied into it. These include the executable files *LincSys.exe* and *HydrSimLaterals.exe*, the program icon file *LincSys.icon*, and the program configuration file *LincSys.exe.config.xml*. In addition, a host of .Net Framework utility files with a *.Dll (dynamic link library) extension were copied to the installation folder. Furthermore, the user may notice that a folder named Projects was created under the installation folder.

LincSys uses a specific directory structure to track and manage projects. The directory structure for project data management is created under the Projects folder during installation. Directly under the Projects folder there are five subfolders: DrptubePrvEmitter, DrptubeEmitter, EmitterOnLat, HelpDocAndLiterature, and Templates_InputDataFiles. A brief description of the contents of each of these folders will be presented in the next section. However, a more detailed discussion including a description of the contents and formats of each of the files in these folders is presented in Chapter 5.

1.3.3.a. Contents of a system configuration option folder

The DrptubePrvEmitter, DrptubeEmitter, and EmitterOnLat folders are referred here as system configuration option folders and they contain the *LincSys* project data corresponding to the Droptube-Prv-Emitter, Droptube-Emitter, and Emitter-On-Lateral system configuration options, respectively.

Opening any of the system configuration option folders, say for instance the DrptubePrvEmitter folder, would show that at installation it contains fifteen sample projects (i.e.,

folders), named SampleProject_1, SampleProject_2, …, SampleProject_15, each with a complete set of input and output data files.

Further, opening a *LincSys* project folder, say for instance, the SampleProject_1 folder would show that it contains a total of 9 files with extensions Inp, Out, Dat, Txt and Xlxs, and a subfolder named Charts. The file with the extension Inp is the input data file, while the files with the extensions Dat and Out are the output data files. The file with the extension Txt is a Readme file and is intended to serve as a quick reference resource on the contents of the current project folder. It contains a quantitative and qualitative summary of the dimensions, geometries, and hydraulic characteristics of the lateral components. The excel file (extension Xlxs), has the same content as the input data file (extension Inp) and is intended to be used as an input data template that can be modified and adapted by the user as needed.

The Charts subfolder under the SampleProject_1 folder contains 12 files, comprised of 11 image files in Png format and a Readme file. Each image file corresponds to one of the 11 output charts of *LincSys*. A detailed description of the charts files is provided in Section 4.5. The Readme file contains a concise description of the contents of each of the image files in the Charts folder.

At installation, the DrptubeEmitter and EmitterOnLat system configuration folders also contain 15 sample projects with exactly the same name as those of the DrptubePrvEmitter folder. Each of the project subfolders under the DrptubeEmitter and EmitterOnLat folders contains input and output data files with the same names as the DrptubePrvEmitter folder, although the contents differ.

Note that in *LincSys* the user specifies the project name, which is used as the name of the project folder, but not the names of the input-output data files. The names and extensions of the input and output data files of a *LincSys* project are set by the program internally and do not change from one project to another. A more detailed discussion on the contents of the input and output data files of the model is provided in Chapter 5.

1.3.3.b. Contents of the HelpDocAndLiterature folder

Opening the HelpDocAndLiterature folder shows that it contains thirteen documents in Pdf format. The contents of some of these documents are used by *LincSys* as help information resources that can be accessed through the Help menu from the user interface. The documents in this folder also include a selected set of technical literature that relate to linear-move and center-pivot hydraulics that can be accessed through the Help menu of the GUI. A more detailed discussion on the contents of the HelpDocAndLiterature folder is provided in Section 5.1.2.

1.3.3.c. Contents of the Templates_InputDataFiles folder

The Templates_InputDataFiles folder contains input data files for laterals with number of spans ranging between 6 and 12. The contents and formats of these files are used by *LincSys* as templates for creating the input data file for a new project. It can be observed that directly under the Templates_InputDataFiles folder there are three subfolders: DrptubePrvEmitter, DrptubeEmitter, and EmitterOnLat. These folders contain the input data template files (text files with extension Inp) for the Droptube-Prv-Emitter, Droptube-Emitter, and Emitter-On-Lateral system configuration options, respectively.

For instance, opening the subfolder DrptubePrvEmitter (under the folder Templates_InputDataFiles) shows that it contains a total of eight text files. Seven of them have

the extension Inp and represent the input data template files. It also has a Readme file with the extension Txt, which contains information about the contents and format of the text files in the current folder.

Although the exact contents differ, the number, names, and extensions of files in the DrptubeEmitter and EmitterOnLat system configuration folders are the same as those for the DrptubePrvEmitter folder. Further discussion on the contents of the Templates_InputDataFiles folder is provided in Section 5.1.3.

1.3.4. Uninstall

LincSys can be uninstalled following standard Windows procedure for uninstalling a program. To uninstall *LincSys*, the user needs to select Control Panel from the start menu in the user's PC Windows desktop. In the control panel window, click on the option Uninstall a program under the heading Programs. This leads to the Control Panel Home window. In the Control Panel Home window move the mouse pointer to the entry Install_LincSys, which is the name of the installer, and then click the left mouse button. This opens up a dropdown menu, then selecting the option Uninstall will initiate the process of uninstalling the program.

1.4. Disclaimer

LincSys is designed to analyze and evaluate the hydraulic performance of linear-move and center-pivot irrigation systems. Authors have made significant effort to identify and correct software bugs (syntactical and logical). However, the authors cannot guarantee that the software is completely free of bugs. Furthermore, as a mathematical model, *LincSys* is based on a simplified abstraction, conditioned by limiting assumptions, of a more complex reality. Thus, judicious interpretation and application of outputs is essential for a proper use of the model, which for the most part is an engineering judgement call. Being cognizant of these facts, the authors and the University of Arizona maintain that they assume or accept no liability or responsibility of any kind arising from the installation and use of this program.

1.5. Contents of the *LincSys* User Manual

The contents of this document is presented in six chapters. Chapter 1 provides a quick introduction to the *LincSys* software, including a discussion on the features, layout, and functionalities of the user interface, system requirements and installation, and file management and directory structure. Chapter 2 presents a brief description of linear-move and center-pivot irrigation systems and their significance. A summary of linear-move and center-pivot lateral hydraulics, as implemented in the computational module of *LincSys*, is presented in Chapter 3. Chapter 4 describes the features and functionalities of the graphical user interface of *LincSys*. A description of the contents and format of the input and output data files and the directory structure used by *LincSys* to manage and track data files is presented in Chapter 5. A discussion on model evaluation results and application examples (sample projects), copied into the *LincSys* input-output data folders during installation, is presented in Chapter 6.

Chapter 2. Linear-move and center-pivot systems: Importance and system description

2.1. Importance

Center-pivot and linear-move systems are used to irrigate a wide variety of crops under a range of conditions (Gregg, 2004). These systems account for about half of the irrigated acreage in the U.S. (FRIS, 2008) and are expanding. With application efficiency exceeding 80% and coefficient of uniformity greater than 0.85 (Keller et al., 1980), linear-move and center-pivot systems can be considered among the most efficient irrigation methods.

High pressure impact sprinklers were commonly used in the early versions of center-pivot systems (New and Fipps, 2018). However, because of energy costs and efficiency considerations, impact sprinklers are now recommended only in special applications such as land application of wastewater. More closely spaced low-pressure spray nozzles coupled to pressure regulators and drop-tubes are often used in recent systems (both center-pivots and linear-moves) to minimize energy consumption and wind drift and spray evaporation losses. Mainly because of their amenability to automation these systems are considered particularly suitable for site-specific application of water and agricultural chemicals and have minimal labor requirements.

Center-pivots are much more widely used in the U.S. than linear-move systems. Linear-move systems generally have higher initial cost per unit area of irrigated land, higher labor costs, and the need for a separate guidance mechanism (Martin et al., 2007). Furthermore, linear-move systems are suitable only for terrains with moderate and gentle slopes, not exceeding 3%, while center-pivots can be used in fields with gently rolling terrains and steeper slopes. Potential complexities associated with water intake apparatus, especially when water is supplied through an underground pipeline is another limitation of linear-move systems compared to center-pivots.

Linear-move systems, nonetheless, have some advantages over center-pivots, including the capability to fully irrigate a square field without the need for additional accessories at the far-end of the system, the capability to irrigate rectangular fields, and to maintain low application rates over the entire lateral length.

2.2. System description

A linear-move or a center-pivot irrigation system is a self-propelled machine consisting of a steel or aluminum lateral that apply water to crops in the form of precipitation, as it moves across the irrigated field. Linear-move systems travel in a straight-line irrigating a rectangular field. Center-pivot systems, on the other hand, rotate about a pivot point fixed to a permanent base and irrigate a circular area, although various accessories can be used to irrigate parts of the field corners.

Linear-move and center-pivot laterals are generally placed at a suitable above ground clearance atop an elevated platform, consisting of structural elements (trusses, cables, and support towers on wheels), drive units, and alignment mechanisms that support and propel the system as well as keep it aligned. Linear-move systems also require a separate guidance system that keeps it on course along a set travel direction during irrigation.

A sketch of a typical linear-move system, obtaining its supply from a canal, with an intake apparatus, a pump, and a power unit attached to its inlet-end is depicted in Figure 2a. The lateral is comprised of a series of arched spans connected, at their lowest points, with flexible

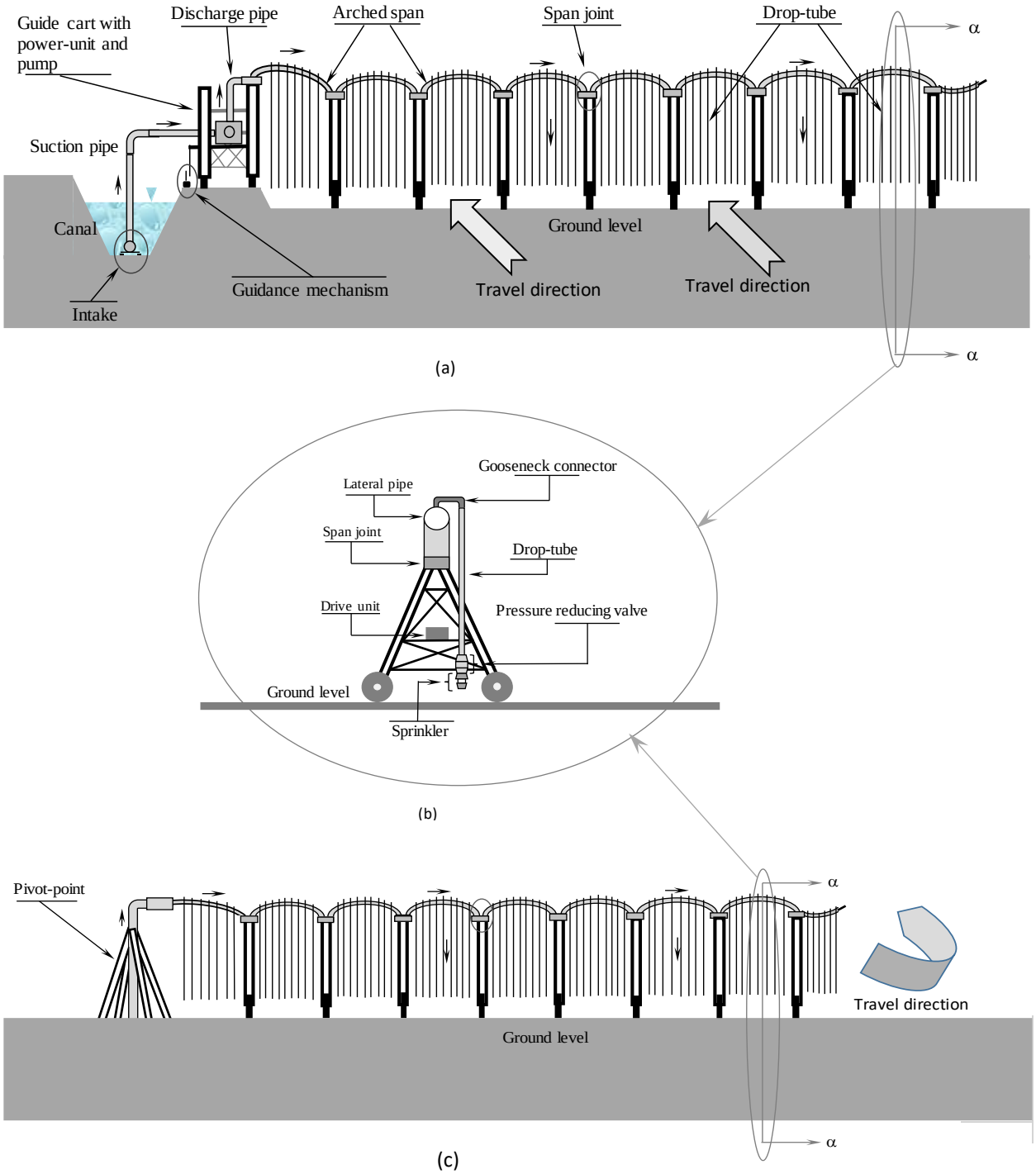

Figure 2. (a) Sketch of a linear-move system obtaining its water supply form a canal and (b) Details showing a support tower, drop-tube fitted with a *prv*-emitter assembly, and drive unit (from section at α-α, Figure 2a), and (c) Sketch of a center-pivot system

joints that allow relative movement between adjoining spans. Each span has multiple regularly or variably spaced outlet ports.

Although high pressure impact sprinklers placed directly on the lateral outlet ports were used in early versions of center-pivots, recent machines (both center-pivots and linear-moves) typically use more closely spaced low-pressure spray nozzles to meter outlet discharges along the lateral. These systems often use semi-flexible tubing (known as drop-tubes) to convey water from outlet ports down to emitters, which are suspended at a constant above ground clearance (often under the crop canopy so as to minimize droplet wind drift and evaporation losses). The spray nozzles are typically combined with accessories known as wear panels (which are fixed or rotating) to produce a range of precipitation patterns that may suit different applications.

A curved rigid tubing, called gooseneck connector, is used to connect each outlet port on the lateral with a drop-tube. Drop-tubes can be fitted with pressure reducing valves, *prvs* (Figure 2b). Some systems have *prvs* installed at the inlet-end of the drop-tube. Other systems have *prvs* placed at the lower end of the drop-tube, just upstream of the emitters (Senninger, 2017a). In the system considered in the *LincSys* software, it is assumed that *prvs* are placed immediately upstream of emitters.

As noted earlier, the use of precision applicator (droptube-prv-emitter) assemblies as emission devises to meter outlet discharges across a lateral at a preset rate has multiple advantages, including high irrigation uniformity and efficiency, a more uniform application of plant nutrients and other agricultural chemicals, and reduced energy consumption. These systems are also particularly suitable for variable application of water and agricultural chemicals.

A center-pivot irrigation system equipped with precision applicators is depicted in Figure 2c. Figure 2 shows that the structural elements, hydraulic components, and geometric features of center-pivots are the same as those of linear-move systems. The principal differences between these systems are the mobility of the inlet-end support tower (i.e., stationary or mobile), the mode of motion of the lateral (i.e., circular or linear/straight-line), and if there is a need for a separate guidance mechanism or not.

Figure 2 depicts systems equipped with precision applicator assemblies for metering outlet discharges along the lateral (i.e., systems with Droptube-Prv-Emitter configuration option). However, as noted earlier in Section 1.1.3, *LincSys* can also simulate the hydraulics of systems fitted with different types of lateral outlet discharge metering apparatuses. Note that the term emitter is used here in the broader sense to describe various water emission devices used in linear-moves and center-pivots, including high pressure sprinklers placed directly on lateral outlet ports and low pressure spray-nozzles fitted to droptube-*prv* assemblies or to drop-tubes.

Chapter 3. Hydraulic simulation module of *LincSys,* assumptions, equations, and numerical solution

3.1. A review

Flow in center-pivot and linear-move systems are generally considered steady. Accordingly, forms of the energy conservation and continuity equations applicable to one-dimensional steady flow in pipes (Granger, 1995) can be used to describe the hydraulics of such systems. Hydraulic modeling and design of sprinkler irrigation systems, including center-pivots and linear-moves, relied mainly on analytical formulations or simplified numerical approaches (e.g., Keller and Bleisner, 1990; Martin et al., 2007). A step-wise approach for computing

pressure distribution along a center-pivot lateral, with a specified outlet discharge profile, was proposed by Kincaid and Heermann (1970). Considering continuous and nonuniform outflow discharge profile, constant lateral diameter, and zero slope, Chu and Moe (1972) derived equations for the pressure head profile of a center-pivot lateral. Scaloppi and Allen (1993) extended the results of Chu and Moe by taking into account the effects of constant slope and residual outflow discharge, at the distal-end, on lateral hydraulics. Equations for computing friction head loss in center-pivot laterals were proposed by Anwar (1999) and Tabuada (2014), among others. Valiantzas and Dercas (2005) derived expressions for hydraulic analysis of variable diameter center-pivot laterals based on both continuous and discrete outflow assumptions. A model for design and evaluation of center-pivot systems, CPED, was presented by Heermann and Stahl (2006).

The design of linear-move irrigation systems was discussed by Keller and Bleisner (1990). Fraisse et al. (1995) reported the results of a simulation study, conducted using a version of the CPED model, on variable water application with linear-move systems. Published studies on hydraulic analysis of linear-move irrigation laterals are limited. However, the geometric features and hydraulic components of linear-move and center-pivot irrigation systems are generally the same. The principal differences between these systems are the mobility or lack thereof of the inlet-end support tower, the mode of motion of the lateral, and the need for a separate guidance mechanism for linear-move systems. These differences are considered not to have appreciable effect on the basic hydraulic principles governing flow in these systems and applicable equations. Thus, in practice the hydraulics of these systems is considered identical.

The hydraulic module of the *LincSys* software, *HydrSimLaterals.exe*, is based on a numerical solution of the one-dimensional steady-state pipe flow equations (Zerihun and Sanchez, 2019a,b). A unique attribute of *HydrSimLaterals.exe* model, compared to earlier center-pivot and linear-move hydraulic models, is that it takes into account the effects of span geometry and key lateral components (namely, *prvs* and drop-tubes) on the system hydraulics and also has sufficient flexibility to accommodate variabilities in lateral hydraulic parameters and field topography. The model can be used to determine the hydraulic performance of a linear-move or a center-pivot irrigation system, given the lateral hydraulic, geometric, and topographic parameters as input. Specifically, model input parameters include lateral diameter, pipe hydraulic resistance characteristics, number of spans and span geometry, field slope, spacing between outlets, and emitter hydraulic characteristics, among others. Furthermore, for systems with precision applicators, the hydraulic characteristics of the pressure reducing valves, *prvs*, are required inputs. Model outputs include the total head, lateral discharge, lateral pressure head, head differential across emitters, friction and local head losses, velocity head, and emitter discharge profiles along the lateral. Additional model outputs are the uniformity of emitter head differential and emitter discharge profiles.

As noted earlier, the hydraulic module of the *LincSys* model is capable of simulating the hydraulics of laterals with three different outlet discharge metering configurations: *(i)* systems that use *prv*-emitter assemblies, fitted to drop-tubes, as emission devices to meter outlet discharges at a pre-set rate across the lateral (labeled here as Droptube-Prv-Emitter or precision applicator configuration), *(ii)* systems that use emitters attached to drop-tubes to meter outlet discharges across the lateral (named as Droptube-Emitter configuration), and *(iii)* systems in which emitters are placed directly on the lateral (described here as Emitter-On-Lateral system configuration).

3.2. Particulars of linear-move and center-pivot laterals

From the perspective of hydraulic modeling, the pipeline that conveys water across a linear-move or a center-pivot machine is essentially an irrigation lateral. Nonetheless, these laterals differ from the conventional irrigation laterals of solid-set or set-move systems in the following respects: they move across the field as they apply irrigation water, they are comprised of arched spans placed on an elevated platform, and are often equipped with precision applicators that are suspended from the lateral at a suitable above ground clearance.

Assumptions pertaining to the effects of lateral movement and span curvature on lateral hydraulics and the approaches used in *LincSys* to model *prv* effects (in the systems that are fitted with pressure regulators) will now be discussed. Before that, however, a brief description of *prvs*, *prv* operating modes, and their effects on lateral hydraulics will be presented.

3.3. Pressure reducing valves and their effects on lateral hydraulics

Systems with precision applicators use pressure reducing valves, *prvs*, to regulate pressure at the emitter inlet. A *prv* is a hydraulic network element that reduces excess pressure at its inlet-end to a pre-set downstream pressure, known as *prv*-set pressure, provided the pressure at the *prv* inlet is within a (manufacturer) recommended range. Because emitters are placed immediately downstream of a *prv*, the *prv*-set pressure is essentially the emitter inlet pressure. The practical irrigation management implication (of such an arrangement of the system components) is that if pressure along a lateral is maintained at such a level that the inlet pressures to all the *prvs* in the lateral are within the recommended range, then the emitter head differentials, and hence the corresponding emitter discharges, will become constant along the lateral. This should then lead to a uniform application of irrigation and agricultural chemicals. However, if a *prv* is operated at an inlet pressure that falls outside the recommended range, then the *prv* will not function as a pressure regulator and it will have distinctly different effects on the hydraulics of the lateral.

For *prvs* used in linear-move and center-pivot sprinkler irrigation systems three distinct operating modes can be discerned (Zerihun and Sanchez, 2019a): *(i) Active mode* is one in which the *prv*-inlet pressure is within the recommended range and the *prv* actively regulates the emitter inlet pressure. *(ii) Passive mode* consists of a scenario in which the *prv*-inlet pressure is less than the minimum recommended for the *prv* to operate reliably in the active mode. In this operating mode, the *prv* is fully open and hence no longer regulates pressure, instead it acts as a passive network element. And *(iii) Fully-throttled mode* is one in which the *prv*-inlet pressure exceeds the maximum recommended for the *prv* to operate reliably in the active mode. In this operating mode, the *prv* is nearly or fully closed and hence emitter is no longer considered operational.

For a given *prv* model, the *prv*-set pressure can vary over a range. However, for a particular application, the *prv*-set pressure is fixed at a suitable level by the manufacturer (e.g. Senninger, 2017a). The minimum recommended *prv*-inlet pressure is defined here as the sum of the *prv*-set pressure and the minimum required pressure head margin between the *prv*-set pressure and the *prv*-inlet pressure for the *prv* to operate reliably in the active mode. The minimum required pressure head margin is often specified in the *prv* manufacturer's catalogue as well (e.g., Senninger, 2017a). The maximum *prv*-inlet pressure or its range of variation is typically specified in the manufacturers catalogue.

The *prv* operating modes, described above, have direct effect on the computational algorithms applicable to the solution of the hydraulic simulation problem of these systems. For a *prv* operating in the active mode, the attached emitter is hydraulically separated from the effects

of the flow dynamics upstream of the *prv*, hence emitter discharge can be directly calculated with the emitter head-discharge equation as a function of the *prv*-set pressure. For *prvs* operating under the passive mode, however, the attached emitters interact directly with the system hydraulics upstream and hence emitter pressure and discharge can only be computed using the same approach as that used for systems without *prvs* (Zerihun and Sanchez, 2014; Zerihun and Sanchez, 2017; Zerihun and Sanchez, 2019b). For *prvs* operating under fully throttled mode, the attached emitters are considered inoperative, thus there are no emitter discharges. A more detailed discussion on the full range of operating modes of *prvs* that are used in irrigation laterals, their effects on system hydraulics, and applicable computational methods are provide by Zerihun and Sanchez (2019a,b).

3.4. Definition of the linear-move and center-pivot lateral hydraulic simulation problem

3.4.1. Concepts and assumptions

For computational purposes a lateral is schematized here as a connected series of pipe segments, referred to as lateral (pipe) segments. A lateral segment is typically delimited by outlet ports at both ends. However, it can also be delimited by an outlet port at one end and by the inlet-end of the lateral, a span joint, or simply by a point (on the lateral) with a known elevation at the other. In cases where emitters are widely spaced, the lateral pipe segments may need to be smaller than the outlet spacing for a more precise representation of lateral geometry and elevation profile. Under such a scenario, lateral pipe segments can be delimited at both ends by points that, have known elevations but, are not outlet ports.

The configuration and modes of operation of a linear-move or a center-pivot lateral considered in *LincSys* needs to satisfy a set of requirements: (1) A lateral pipe segment is characterized by its slope, diameter, hydraulic resistance parameter, and length (in other words, the slope, diameter, and hydraulic resistance of a lateral pipe segment are constant). (2) The parameters of lateral pipe segments as well as the hydraulic characteristics of emitters can be constant or variable along a lateral. (3) The lengths of the lateral pipe segments and drop-tubes (where applicable) are sufficiently large for the flow within these network elements to be considered fully developed and hence the uniform flow friction head loss equations can be applied to calculate energy loss within them. (4) Flow velocities and the curvature of the arched spans are sufficiently small for pipe curvature effects on the hydraulic resistance of the lateral pipe to be considered negligible. (5) The travel speeds of linear-move and center-pivot machines are sufficiently small for the dynamic effects of lateral movement on its hydraulics to be considered negligible. (6) The angular velocity of center-pivots is sufficiently small not to have appreciable effects on center-pivot hydraulics. (7) For systems with *prvs*, it is assumed that each drop-tube along a lateral is fitted with a *prv*-emitter assembly at its downstream end. (8) The model, size, set-pressure, and other parameters of the *prvs* installed in a given lateral are the same. And (9) A lateral pipe segment does not contain inline devices that add energy into the system, but pipe appurtenances such as valves and couplers and bends can be placed anywhere along the lateral.

3.4.2. Irrigation lateral as a branched hydraulic network

For the purpose of hydraulic modeling, a linear-move or a center-pivot lateral is treated here as a branched hydraulic network consisting of links delimited by nodes (Figure 3a). Lateral pipe segments and outlet flow metering apparatuses are considered as hydraulic links. In Figure 3a, horizontal line segments represent lateral pipe segments, whereas outlet discharge metering apparatuses (i.e., droptube-*prv*-emitter assemblies, droptube-emitter assemblies, or emitters as the case may be) are depicted as vertical lines. Note that the link discharges, Q, are system unknowns and need to be determined as part of the hydraulic simulation.

The network nodes consist of fixed head nodes and junction nodes. The fixed head nodes are boundary nodes and include the lateral inlet and the exit ends of each emitter. These nodes either have a known total head (as in the case of the lateral inlet) or have total heads that can be defined in terms of the discharge and elevation of individual emitters, thus they do not need to be specifically treated as unknowns of the hydraulic simulation problem. On the other hand, junction nodes are points along the lateral at which two or more links are joined (Figures 3b and 3c). These include span joints and other nodes where lateral elevations are defined, but no outlet ports exist (referred here as non-offtake nodes) and nodes where drop-tubes or emitters connect to lateral outlet ports (described here as offtake nodes). The total head, H, at each of the junction nodes are system unknowns and need to be determined as part of the hydraulic computation. Note that non-offtake nodes, that do not have network elements that can cause local energy loss, are treated here as junction nodes so as to allow a more accurate representation of the lateral elevation profile and its effects on lateral hydraulics.

As can be observed from Figure 3c, for computational convenience it is assumed here that a junction node representing a non-offtake point along the lateral, such as a span joint, has a virtual link with zero discharge attached to it. Note that with this convention, each of the odd nodal indexes represent a fixed head node and all even nodal indexes represent junction nodes. Furthermore, all of the odd link indexes represent lateral pipe segments and each of the even indexes represent an outlet metering apparatus or a virtual link with zero discharge.

3.4.3. Specification of the lateral hydraulic simulation problem

The problem of interest here is hydraulic simulation of a linear-move or a center-pivot lateral that uses any of one the three outlet discharge metering configurations (described earlier in Section 3.1) and is operated under steady flow condition. Thus, the modeling objective is to determine all the link discharges and the nodal heads (heads at junction nodes), given the elevation profile and the geometric and hydraulic parameters of the lateral, including the total head at the inlet. Forms of the energy conservation and continuity equations, applicable to one-dimensional steady flow in stationary and straight pipelines, can be used to model the hydraulics of these laterals.

Accordingly, a continuity equation can be written for each junction node and an energy balance equation can be formulated across each link. For a general lateral hydraulic simulation problem these equations can be coupled to form a system of nonlinear equations that can be solved iteratively (Zerihun and Sanchez, 2017). However, the hydraulic module of *LincSys* uses computational methods applicable to hydraulic manifolds (e.g., Hathoot et al., 1994; Zerihun and Sanchez, 2014) to solve the hydraulic simulation problem of linear-move and center-pivot irrigation systems. The conventional manifold approach is applicable only to laterals with Droptube-Emitter and Emitter-On-Lateral configurations (i.e., laterals that do not have *prvs*). For

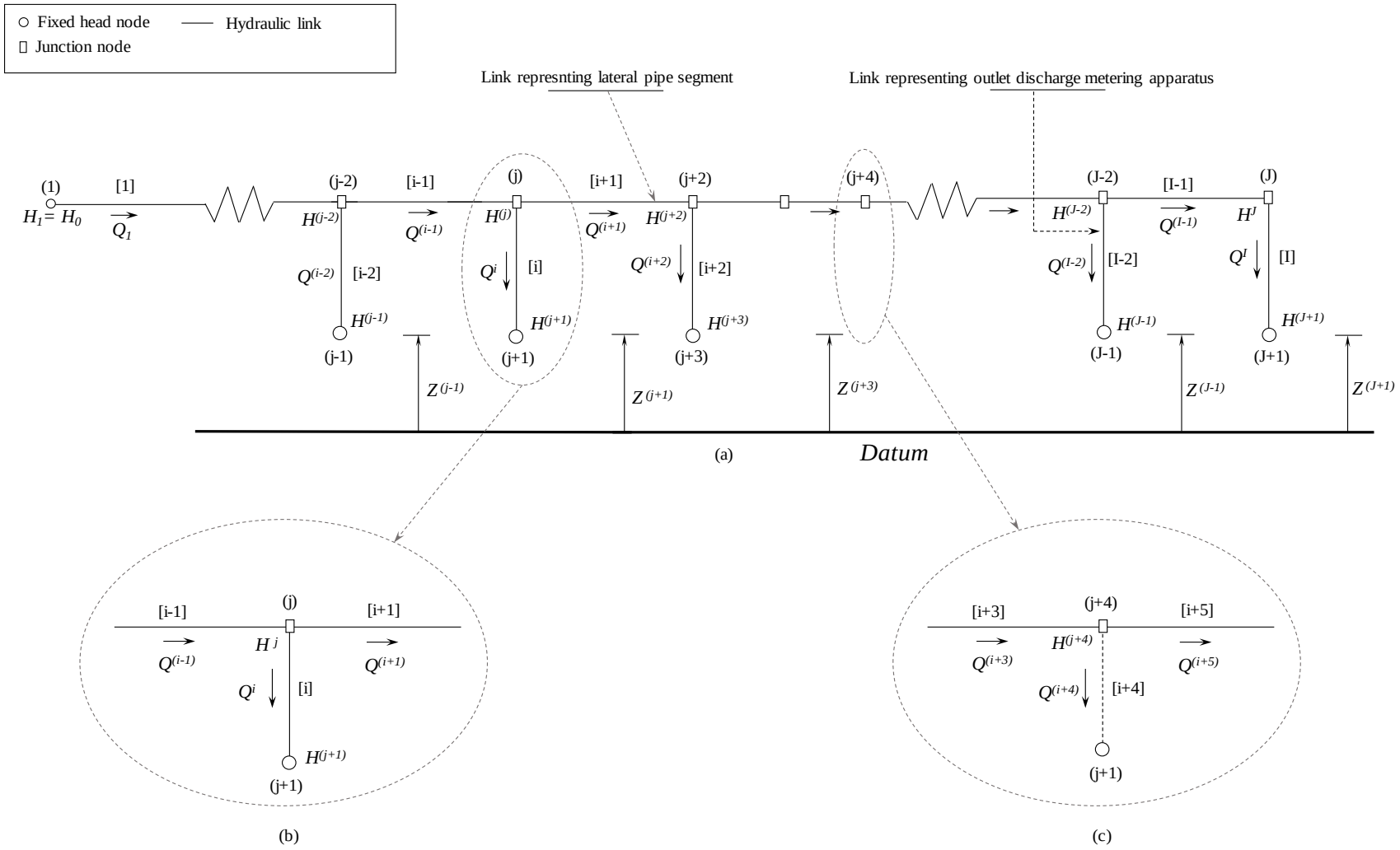

Figure 3. (a) Schematics of a linear-move or center-pivot lateral as a connected series of links delimited by nodes, (b) an offtake junction node and attached links, and (c) a non-offtake junction node (i.e., a node without an outlet) and attached links. (*Note*: *(i)* node index and *[j]* is link index, *Q* is link discharge; *H* and *Z* are nodal head and elevation, respectively, and H_0 = total head imposed at the lateral inlet. Furthermore, for computational convenience, it is assumed here that a virtual link with zero discharge is connected to each non-offtake junction node)

systems with *prvs*, on the other hand, the basic algorithm developed as such needs to be modified to account for the particular conditions that *prvs* impose on the hydraulics of these laterals.

Details on the formulation and numerical solution of the hydraulic simulation problem of linear-move laterals as implemented in *LincSys* are provided by Zerihun and Sanchez (2019a,b). Thus, only a synopsis of the hydraulic equations and numerical solutions will be presented here.

3.5. Equations

3.5.1. Link energy balance and nodal continuity equations

3.5.1.a. Equations for the junction nodes and attached links upstream of the distal-end node, offtake nodes

The basic numerical algorithm of manifold hydraulics involves a series of iterative computations that begins at the distal-end junction node and proceeds upstream sequentially through each junction node ending at the lateral inlet. At each node, the nodal continuity equation and the energy balance equations for the attached links (which form a small quasilinear system) are solved iteratively for the nodal head and the respective link discharges.

Now, consider two consecutive offtake nodes - nodes *j* and *(j+2)* – in Figure 3a and the link that carries discharge from node *j* to *(j+2)*, i.e., the *[i+1]th* link. As noted earlier, each lateral-wide hydraulic computation proceeds, sequentially through the junction nodes, in the upstream direction starting from the distal-end. Thus, the head just upstream of the *(j+2)th* node, $H^{(j+2)}$, and the discharge through the *[i+1]th* link, $Q^{(i+1)}$, would be treated here as variables whose values have already been determined in the preceding computational step. On the other hand, the head just upstream of node *j*, H^{j}, the discharge into node *j*, $Q^{(i-1)}$, and the discharge through the *ith* link, Q^{i}, would be considered as unknowns.

Considering a system with a drop-tube and emitter assembly (Droptube-Emitter system configuration option), it can be observed that for junction node *j*, three equations consisting of two link energy balance equations and a nodal continuity equation (expressed as a function of the nodal head, H^{j}, and the link discharges, $Q^{(i-1)}$ and Q^{i}) can be formulated. Substituting the nodal continuity equation in the link energy balance equations and simplifying yields a pair of nonlinear algebraic expressions as a function of H^{j} and Q^{i}.

$$\xi^{i}\left(Q^{i}\right)^{2} + \beta^{i}\left(Q^{i}\right)^{\lambda^{i}} + \sum_{q} \pi_{q}^{i} f\left(Q^{i}\right) - H^{j} + Z^{(j+1)} = 0 \qquad (1)$$

$$\sum_{q} \pi_{q}^{i} f\left(Q^{i}\right) - H^{j} + \xi^{(i+1)}\left(Q^{(i+1)}\right)^{2} + H^{(j+2)} = 0 \qquad (2)$$

Equation 1 is the energy balance equation along the path connecting a point just upstream of the *jth* junction node and the *(j+1)th* node (Figure 3a), expressed in terms the unknowns Q^{i} and H^{j}. In Eq. 1, the first term on the left-hand side is the friction head loss in the drop-tube; the second term represents the head differential across the emitter; the third term is the sum of all the local head losses (including branching loss at the *jth* junction node, bending loss at the connector if applicable, and others losses if any) that occur at the inlet to, and over, the drop-tube; and the fourth and fifth terms are the head just upstream of the *jth* junction node and elevation at the *(j+1)th* node (i.e., elevation of the emitter), respectively (Figure 3a).

Equation 2 is the energy balance equation along the path connecting points just upstream of the *jth* and *(j+2)th* junction nodes, expressed in terms Q^i and H^j. In Eq. 2, the first term on the left-hand side represents the sum of the local head losses that occur between the points just upstream of the *jth* and *(j+2)th* junction nodes, the second term is the head at the *jth* junction node, the third term is the friction head loss in the *[i+1]th* link, and the fourth term is the head just upstream of the *(j+2)th* node.

In Eqs. 1 and 2, ξ^i is the hydraulic resistance coefficient of the friction head loss equation $[T^2/L^5]$; β^i $[T^{\lambda i}L^{(1-3\lambda i)}]$ and λ^i *[-]* are parameters of the emitter head-discharge function; π_q^i is the parameter of the local head loss equation for the *qth* pipe appurtenance in the *ith* link $[T^2/L^5]$; and $f(Q^i)$ is an expression defined as some function of Q^i. The form of the $f(Q^i)$ function will be defined later in this section.

As noted earlier, Eqs. 1 and 2 apply to a system that uses a droptube-emitter assembly to meter outlet discharges along the lateral. On the other hand, if the lateral configuration is one in which the emitter is placed directly on the lateral, then the friction head loss term in Eq. 1 would become zero and the local head loss term would be reduced to that of a branching loss at the lateral outlet. Thus, the energy balance equation for the *ith* link simplifies to

$$\beta^i(Q^i)^{\lambda^i} + \pi^i f(Q^i) - H^j + Z^{(j+1)} = 0 \qquad (3)$$

Equations 1 and 2 constitute the basic set of link energy balance equations, for a system with Droptube-Emitter configuration, expressed in terms of the variables Q^i and H^j. Equations 2 and 3, on the other hand, consist of the corresponding link energy balance equations (for a system with Emitter-On-Lateral configuration), also expressed in terms of the variables Q^i and H^j.

For each junction node and attached links, Eqs. 1 and 2 (for the Droptube-Emitter system configuration option) or Eqs. 2 and 3 (for the Emitter-On-Lateral system configuration) are solved iteratively for the unknowns (Q^i and H^j) using the Newton method (Zerihun and Sanchez., 2019b). The inflow discharge, $Q^{(i-1)}$, to the *jth* node can be then determined with the nodal continuity equation

$$Q^{(i-1)} = Q^i + Q^{(i+1)} \qquad (4)$$

For a systems with Droptube-Prv-Emitter configuration option, Eqs. 1 and 2 are solved in full when a *prv* is operating in the passive mode (note that under such a scenario, local head losses associated with the *prv* needs to be taken into account in Eq. 1). If, on the other hand, the *prv* operates in the active mode, then a modified form of these equations and a different procedure is used to compute Q^i, H^j, and $Q^{(i-1)}$. Details of this procedure is provided by Zerihun and Sanchez (2019b).

3.5.1.b. Equations for the junction nodes and attached links upstream of the distal-end node, non-offtake nodes

As noted earlier, a non-offtake junction node is a point along the lateral where two lateral pipe segments join and no outlet port exists, Figure 2c. If the *jth* junction node is a non-offtake node, then the discharge in the *ith* link, Q^i, is 0. It then follows from continuity that the

discharge in the lateral pipe segment that carries flow into the node, $Q^{(i-1)}$, is equal to the discharge in the lateral segment that carries flow from the node, $Q^{(i+1)}$. Noting that $Q^{(i+1)}$ has already been determined in the preceding computational step, it can be readily observed (from the equivalence of $Q^{(i-1)}$ and $Q^{(i+1)}$) that $Q^{(i-1)}$ is also known. The implication is that for a non-offtake junction node, the nodal computational problem can be reduced to one of finding the total head just upstream of the junction node, H^j. Given that $H^{(j+2)}$ has already been determined in a preceding step, H^j can be computed directly from the energy balance equation for the *[i+1]th* lateral pipe segment, Eq. 2.

3.5.1.c. Equations for the distal-end node

Unlike the other offtake nodes, at the distal-end node there is only one link that carries discharge from the node, namely the link that represents the distal-end outlet discharge metering apparatus (which is labeled in Figure 3a as the *Ith* link). Thus, a slightly different computational approach need to be used at the distal-end node.

While the head just upstream of the distal-end node and discharges in the attached links ($Q^{(I-1)}$, Q^I, and H^J) are unknowns, only two equations (consisting of the link energy balance equation across the *Ith* link and the nodal continuity equation at the *Jth* junction node) can be formulated. However, noting that there is no lateral pipe segment that carries discharge from the node, it can be readily inferred from continuity that $Q^{(I-1)} = Q^I$.

Now, substituting Q^I for $Q^{(I-1)}$ in the energy balance equation of the *Ith* link and simplifying, results in an expression similar in form to that of Eq. 1 (for a system with a Droptube-Emitter or Droptube-Prv-Emitter configuration option) and another expression of the same form as Eq. 3 (for an Emitter-On-Lateral system configuration option). Note that a form of Eq. 1, applicable to the *Ith* link, can be applied to Droptube-Prv-Emitter configuration option only if the distal-end *prv* is operating in the passive mode. If, on the other hand, the *prv* is operating in the active mode, then a modified form of the equation and a different procedure need to be used (Zerihun and Sanchez, 2019b)

Based on a form of Eq. 1 (or Eq. 3) applicable to the distal-end junction node or some modification thereof, as the case may be, a lateral-wide hydraulic computation can be initiated at the distal-end node where a preset total head is used to compute the link discharge, Q^I. Determination of $Q^{(I-1)}$ follows automatically from the equivalence of $Q^{(I-1)}$ and Q^I.

Note that in the context of a hydraulic simulation of a lateral, the distal-end nodal head, H^J, is set to an assumed initial nodal head (in the first lateral-wide iteration) or to a revised estimate of the nodal head in subsequent iterations (Section 3.7).

3.5.1.d. Equations for the inlet-end node

As can be noted from Figure 2a, the inlet-end node is attached only to the upstream-end lateral pipe segment, i.e., link #1. There is no link that carries discharge into or an outlet metering apparatus that carries discharge from the inlet-end node. Furthermore, at the end a lateral-wide computation, the discharge in link #1, Q^1, and the head at a point just upstream of node #2, H^2, have already been determined in the preceding computational step. It, thus, follows that the only unknown left to determine at the end of a lateral-wide computation is the total head at the lateral inlet, H^1, which can be calculated directly from the energy balance equation for the upstream-end lateral pipe segment, Eq. 2.

3.5.2. Equations of friction and local head losses

Noting that the Darcy-Weisbach formula is used to calculate friction head loss in the hydraulic module of *LincSys*, the hydraulic resistance coefficient, ξ, can be given as

$$\xi = k_f \frac{f}{D^5} l \qquad (5)$$

where k_f is a dimensional constant in the friction head loss equation $[T^2/L]$; f is the friction factor for a hydraulic link *[-]*; l is the link length *[L]*; and D is the link diameter *[L]*. In the model presented here, for $R \leq 4000$, where R is the Reynolds number, the link friction factor, f, is calculated with the friction factor formula applicable to laminar flow in pipes. For turbulent flow ($4000 < R$), f is computed through iterative solution of the Colebrook-White equation. The exact formulation of the Colebrook-White equation used in the model presented here is given by Zerihun and Sanchez (2017).

As noted earlier, the expression $\sum_q \pi_q^i f\left(Q^i\right)$, in Eqs. 1 and 2, is the sum of all the local head losses that occur in a drop-tube or a lateral pipe segment. The *qth* local head loss component in a link, h_l *[L]*, which may occur across pipe transitions (such as pipe size changes, couplers, tees, bends, valves) where the flow is constrained, changes direction, or changes velocity are calculated with the equation

$$h_l = \pi Q^2, \quad where \quad \pi = k_l \frac{k_L}{D^4} \qquad (6)$$

In Eq. 6, π is local head loss parameter $[T^2/L^5]$, k_l is a dimensional constant $[T^2/L]$, and k_L is the local head loss coefficient of an appurtenance *[-]*.

Note that depending on the source of the local head loss, the link discharge, Q, and diameter, D, applicable to Eq. 6 vary. For scenarios in which the discharge and/or diameter upstream of an appurtenance are different from those downstream of the appurtenance, the link discharge, Q, and diameter, D, applicable to Eq. 6 are: *(i)* for local losses associated with branching, line-flow, and sudden expansion of the lateral cross-sectional area applicable Q and D are those associated with the link carrying discharge into the pipe appurtenance that caused the head loss and *(ii)* for losses associated with sudden contraction of the lateral cross-sectional area, applicable Q and D are those corresponding to the link that carries discharge from the appurtenance.

Alternatively, for appurtenances across which link discharges and diameters are the same (which may include losses associated with bending, couplers, valves, and equivalent head losses), the through-flow discharge and the local link diameter can be used.

Based on these observations, it can be shown that the expression $f\,(Q^i)$ in Eqs. 1 to 3 can be expressed in terms of the unknown discharge Q^i as follows

$$f(Q^i) = (Q^i)^2, \quad if\ h_l\ is\ a\ function\ of\ Q^i \qquad (7)$$

$$f(Q^i) = (Q^i)^2 + 2Q^{(i+1)}Q^i + \left(Q^{(i+1)}\right)^2, \ if\ h_l\ is\ a\ function\ of\ Q^{(i-1)} \qquad (8)$$

$$f(Q^i) = (Q^i)^0\left(Q^{(i+1)}\right)^2, \quad if\ h_l\ is\ a\ function\ of\ Q^{(i+1)} \qquad (9)$$

Note that Eq. 7 is applicable to local head losses that occur within a droptube, such as bending and valve losses. Equation 8 is applicable to losses associated with branching-flow, line-flow, and sudden expansion of the lateral cross-sectional area, all of which occur at junction nodes. Equation 9 is applicable to losses that occur at sudden contraction of the lateral cross-sectional area, which also occur at junction nodes. Equation 9 is also applicable to local head losses that occur within a lateral pipe segment across couplers, valves, and also a series of appurtenances that are placed in close proximity to one another and hence their effects are represented by an equivalent head loss coefficient.

3.6. Numerical solution

Given the head at the distal-end junction node, H^J, the lateral geometric and hydraulic parameter set, and the lateral elevation profile, a successful lateral-wide computation determines the corresponding link discharge and nodal head vector, $[\boldsymbol{Q},\boldsymbol{H}]$. Note that this implies that the total head, and hence discharge, vector of a lateral are uniquely related to the head at the distal-end node. However, the solution of a lateral hydraulic simulation problem requires the determination of a unique discharge and head vector, $[\boldsymbol{Q},\boldsymbol{H}]_0$, corresponding to a specified lateral inlet head, H_0. This requires multiple iterative sweeps across the lateral to determine the distal-end nodal head, $H^J{}_0$, that leads to the lateral discharge and head vector, $[\boldsymbol{Q},\boldsymbol{H}]_0$, with an inlet head, H_{inlet}, that is sufficiently close to H_0.

In the context of lateral hydraulic simulation, each lateral-wide hydraulic computation (iteration) begins at the distal-end junction node where an assumed initial nodal head (in the first iteration), or a revised estimate of the nodal head (in subsequent iterations), is used to compute the discharges in the attached links. Computation then proceeds upstream sequentially through each junction node, where a nodal continuity equation and link energy balance equations are solved for the nodal head and the discharges in the attached links (Zerihun and Sanchez, 2019b). A lateral-wide hydraulic computation ends with the determination of the corresponding total head at the lateral inlet. At the end of each lateral-wide sweep, an error metric that measures the difference between the computed head at the lateral inlet and the actual imposed head will be compared with a preset tolerance (0.0001m) to ascertain convergence.

If convergence is achieved, then the nodal head and link discharge vectors, $\boldsymbol{Q}$ and $\boldsymbol{H}$, computed in the current iteration will be accepted as the solution to the hydraulic simulation problem. If, on the other hand, the error in the computed lateral inlet head exceeds the tolerance, then a revised estimate of the head at the distal-end junction node is calculated and a new lateral-wide iteration is initiated. To systematize the search for the distal-end head that leads to a combination of $\boldsymbol{Q}$ and $\boldsymbol{H}$ vectors with an inlet-head that is sufficiently close to the imposed head, the simulation module of *LincSys*, *HydrSimLaterals.exe*, uses a one-dimensional error minimization (optimization) algorithm developed based on the golden-section method (Zerihun and Sanchez, 2019b).

In summary, *HydrSimLaterals.exe* uses a pair of coupled computational modules, consisting of a hydraulic module (which performs each of the lateral-wide iterative sweeps described above) and a one-dimensional error minimization module to systematize the search for the $[\boldsymbol{Q},\boldsymbol{H}]_0$ vector.

Chapter 4. *LincSys* user interface: Features and functionalities

4.1. The Graphical User Interface (GUI)

4.1.1. An overview

As noted in Section 1.1.1, the *LincSys* software is comprised of a pair of executable files: a hydraulic simulation module, *HydrSimLaterals.exe*, and a Graphical User Interface (GUI) through which the user interacts with the computational module. The user interface and the computational module, are coupled through an application programming interface that uses the CreatProcess function.

Data exchange between the user interface and the simulation module takes place through text files. Input data, edited within the user interface, is transferred to the simulation module (*HydrSimLaterals.exe*) and output data from the simulation module is relayed back to the user interface (*LincSys.exe*) using space delimited text files.

The GUI is a tabbed form designed to provide access to program functionalities, consisting of project management and preprocessing, processing, and postprocessing of project data. While the preprocessing model functionality pertains to *LincSys* capabilities and user interface features that allows the display and editing of input data and the handling of input data files, the data processing functionality refers to model capabilities related to lateral hydraulic simulation. On the other hand, software components and user interface features for displaying output data and charts and the handling of output data and charts files constitute the postprocessing functionality of the model.

The GUI of *LincSys* was developed with the Basic programming language in the Visual Studio Integrated Development Environment (VS 2019) and it is based on the Windows Forms for .Net Framework Ver. 4.8. It is comprised of four tabpages (the Systems-Projects, the Input, the Output, and the Charts tabpage, Figure 1), each providing access to a set of program functionalities of the model.

The Systems-Projects tabpage represents the main entry point to the *LincSys* model. It provides access to the other tabpages and also to project management functionalities.

The Input tabpage enables access to the preprocessing and processing functionality of the model. It is the window in which the current project's input data is displayed and can be edited. It is also the tabpage from which a simulation run of the current *LincSys* project can be conducted, if necessary.

The Output and Charts tabpages provide access to the postprocessing functionality of the model. While the Output tabpage is where the output data from a new or an earlier simulation session is displayed, the Charts tabpage provides access to a series of charts (11 in all) that display graphical renderings of computed hydraulic parameters.

Standard Windows Forms controls, namely control buttons, textboxes, a listbox, DataGridView table, a toolbar, a dropdown menu, label controls, and chart control are used to issue commands, navigate the user interface, and perform various program functionalities. Note that in this document, control buttons are referred to with names that are contextually more intuitive and meaningful, in place of the more general technical names used in the programming literature. Table 1 summarizes the names used here for the input-output controls and their technical counter parts.

Table 1. Conventional technical names of input-output controls used in *LincSys* and names used to refer to them in this document

Names of input-output controls		**Properties**	**Function**
Name used in *LincSys*	**Technical name**		
Inputbox	Textbox	Editable content	Displays and allows the editing of nontabular project input data
Outputbox	Label	Non-editable content	Displays nontabular output data
Input data table	DataGridView	Editable content	Displays and enables the editing of the hydraulic network topological data, lateral hydraulic and geometric parameters, and elevation profile data in a tabular format
Output data table	DataGridView	Non-editable content	Displays the hydraulic network topological data, lateral elevation profile data, and output parameters in a tabular format
Project listbox	Listbox	Non-editable content	Displays the list of existing projects under the currently selected system configuration option and allows selection of a project for which simulation is to be conducted
Navigation buttons	Control buttons	–	Windows Forms control buttons used to navigate the user interface
Groupbox	Groupbox	–	A windows user interface feature that contains a set of related user interface controls

4.1.2. Starting LincSys

The procedure for installing *LincSys* in the user's computer was discussed in *Section 1.2.3* of this manual. Following a successful installation, the program icon will appear in the user's computer desktop and the Windows start menu. In order to run *LincSys* the user simply needs to click on the *LincSys* icon in the start menu or double click on the icon in the desktop. This will open a tabbed form (the user interface of *LincSys*) with the Systems-Projects tabpage enabled and the Systems-Projects tabcontrol highlighted.

4.2. The Systems-Projects tabpage

The Systems-Projects tabpage is the window that the user sees when opening *LincSys*. It is the window that provides access to project management functionalities (namely, creating new *LincSys* project, copying a project, deleting an existing project, and renaming a project) and help resources. The Systems-Projects window also enables access to user interface features that allows the specification of the system configuration option for which simulation is to be conducted and the selection of *LincSys'* current project. Furthermore, the Systems-Projects

tabpage contains navigation buttons (Table 1) that serve as access points to the other tabpages: Input, Output, and Charts, although with some conditionality (Section 4.2.3.c). Note that the term project is used here to refer to all the input and output data files (of a simulation problem) stored in a folder that bears the name of the project.

4.2.1. Features and layout of the Systems-Projects tabpage

The layout of the Systems-Projects tabpage is displayed in Figures 4 and 5. The Systems-Projects tabpage has two types of features. Features that are informational and those consisting of one or more Windows user interface controls that provide access to a program functionality.

The Systems-Projects page displays a titlebar at the top and a statusbar at the bottom of the window (Figure 4), which represent features that serve only informational purpose. User interface controls associated with the Systems-Projects page consists of tabcontrols, a toolbar, a groupbox with radio buttons, project listbox, and navigation buttons (Figure 5).

The tabcontrols (Systems-Projects, Input, Output, and Charts) are positioned right under the titlebar. Underneath the tabcontrols are the toolbar icons representing project management functionalities of *LincSys* and a help icon.

In the main body of the tabpage, the image of a linear-move/center-pivot machine is depicted. Immediately to the right is a groupbox in which the three system configuration options (Droptube-Prv-Emitter, Droptube-Emitter, and Emitter-On-Lateral) are displayed. Radio button controls can be used to select the system configuration option for which a simulation is to be conducted or output data and output charts from an earlier simulation are to be displayed. Next to the right edge of the tabpage is a Project listbox displaying the list of existing projects under the currently selected system configuration option.

The Systems-Projects has three navigation buttons placed right above the statusbar (Input, Output, Charts) which represent the primary access controls to the other tabpages and an Exit button for closing the program.

4.2.2. Features of the System-Projects tabpage that are informational: titlebar and statusbar

The content of the titlebar consists of *(i)* program icon (i.e., a thumbnail of a lateral image) and the model's name displayed in the upper left-hand corner of the window and *(ii)* the standard windows buttons for minimizing and closing windows, shown in the upper right-hand corner of the tabpage (Figure 4). Note that the maximize button is deactivated in *LincSys'* user interface windows, which implies that the size of the *LincSys* user interface windows cannot be increased. The content of the titlebar remains unchanged from one tabpage to another.

At the bottom left-hand corner of the tabpage, the statusbar displays the name of the currently active tabpage, the current system configuration option, and the currently selected project separated from one another by a vertical bar. To the right, following a horizontal arrow is informational text on how to display the access keys of the navigation buttons highlighted and on how to activate the navigation buttons using access keys from the keyboard.

The default display mode for the labels of navigation buttons is one in which the access keys appear unhighlighted. However, the navigation button access keys can be highlighted (i.e., underlined) by pressing the *Alt* key on the keyboard. A navigation button can be activated from the keyboard using the access key by simply tapping on the relevant key on the keyboard, while the *Alt* key is pressed down.

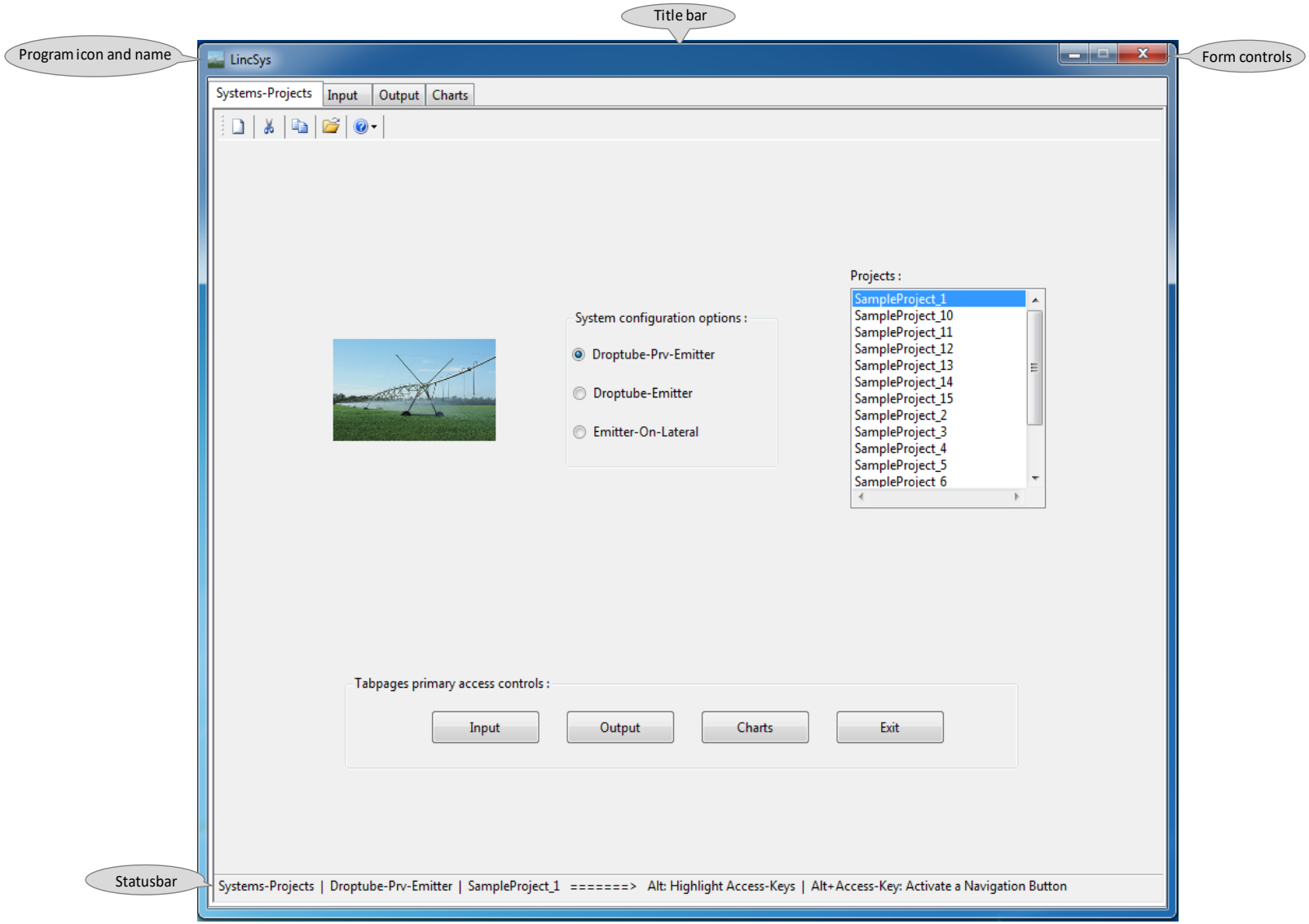

Figure 4. The Systems-Projects tabpage with the titlebar, statusbar, and the minimize and close buttons of the window highlighted

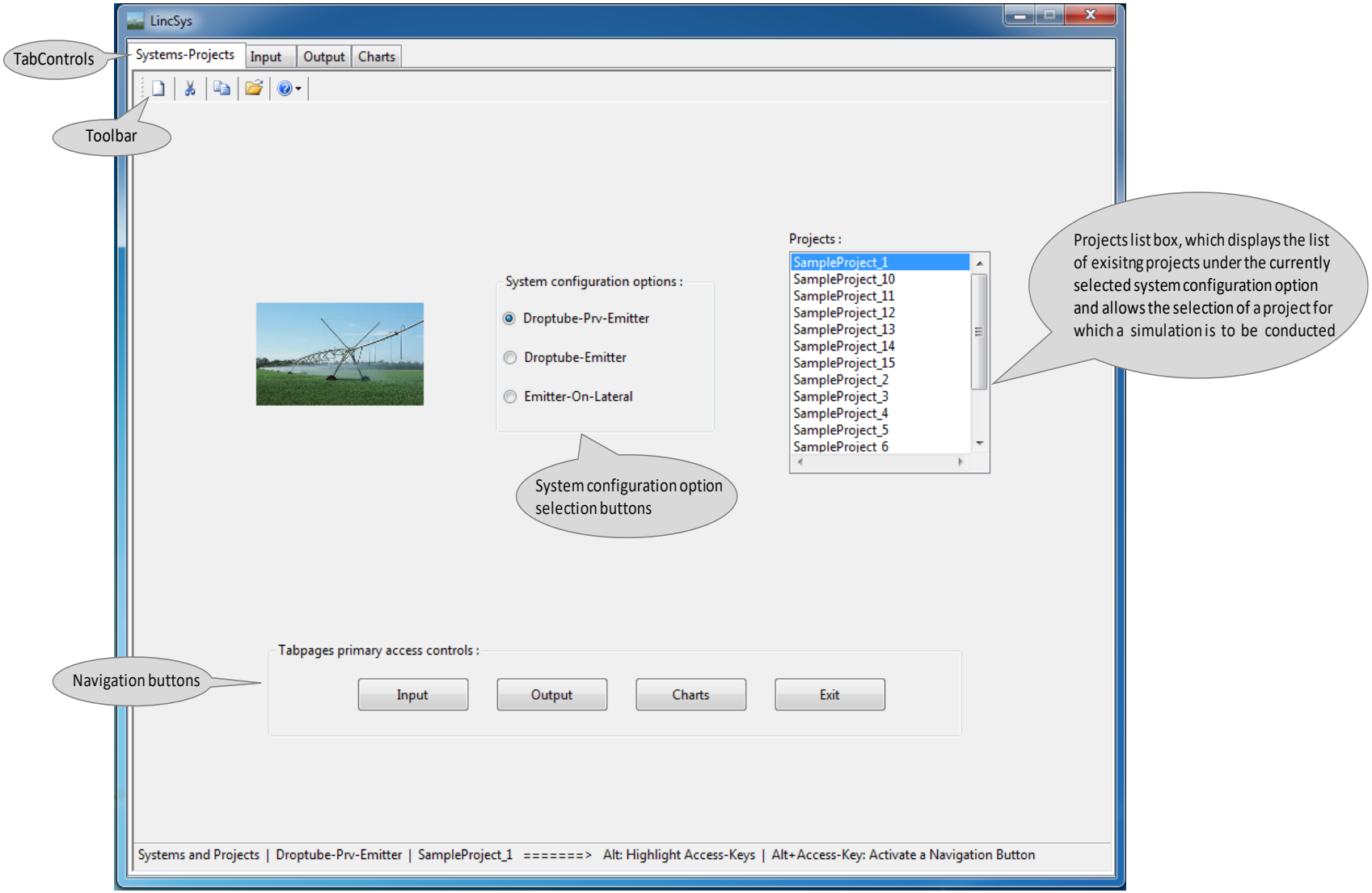

Figure 5. The Systems-Projects tabpage in which the user interface controls are highlighted

4.2.3. Program functionalities associated with the Systems-Projects tabpage and user interface controls

As noted in Section 4.2, program functionalities that are accessible from the Systems-Projects tabpage are: project management, selection of system configuration option, selection of the *LincSys* project for which a simulation is to be conducted, and access to the other tabpages.

For convenience, the discussion on program functionalities, associated with the Systems-Projects tabpage, will start with descriptions of the user interface controls that enable the selection of a system configuration option and of a project from a set of existing projects under the current system configuration option. The discussion on additional functionalities of the model will then build on those descriptions.

4.2.3.a. Selection of system configuration options and the current project

A groupbox titled System configuration options features the three different types of linear-move and center-pivot system configuration options (i.e., Droptube-Prv-Emitter, Droptube-Emitter, and Emitter-On-Lateral) that *LincSys* is capable of simulating, Figure 5.

The option Droptube-Prv-Emitter should be selected if the hydraulics of a linear-move or center-pivot lateral (that uses droptube, *prv*, and emitter assemblies for metering outlet discharges along the lateral) is to be simulated. On the other hand, if the Droptube-Emitter option is selected, *LincSys* can then simulate the hydraulics of a lateral that uses drop-tube and emitter assemblies (i.e., without *prvs*) for metering outlet discharges. The option Emitter-On-Lateral is to be selected for systems in which emitters are placed directly on lateral outlet ports.

Selection of a system configuration option is effected using the radio button controls displayed in Figure 5 adjacent to each option. The default selection, the option that is on when *LincSys* is opened, is the Droptube-Prv-Emitter system configuration option.

When the Droptube-Prv-Emitter option is selected, the projects listbox, which is right next to the Systems configuration option groupbox, displays an alphabetically ordered list of the existing projects (under the Droptube-Prv-Emitter option) with the currently selected project highlighted. The default project selection is the top entry in the list of existing projects (Figure 5). The cursor can be moved up and down the list in the Projects listbox to make a different selection. The vertical scroll can be used to browse through a longer list of projects quickly.

Similarly, if one of the other system configuration options are selected, an alphabetically ordered list of the projects that are under that system configuration option will be displayed in the Projects listbox, with the currently selected project highlighted. As is the case with the Droptube-Prv-Emitter option, the default project selection for each of the other system configuration options is also the top entry in the list of existing projects within the corresponding project configuration folder.

4.2.3.b. The LincSys toolbar icons

The toolbar provides access to the project management functionality of the model. It contains five icons, each representing a different aspect of the project management functionality of *LincSys*. Going from left to right on the toolbar, the icons represent the Create new project, Delete project, Copy project, Rename project, and Help functionalities. The images in the toolbar icons are from a standard toolbar strip commonly used in Windows applications and hence they generally provide a good idea of the program functionality that each icon represents. However, a more specific information on the function of a toolbar icon can be obtained from a tooltip, which

would appear on the screen if the mouse pointer is allowed to hover over an icon (further discussion on this is provided later in this section).

Create new project

The create new project toolbar item is represented by an icon with a blanc page image. Clicking on the New project icon would open the create New Project Name dialog box with a prompt for the user to enter the project name in an input box (Figure 6). If the New project icon is selected by mistake, then the user can click on the Cancel button in the New Project Name dialog box or the Close button at the upper right-hand corner of the dialog box to return to the Systems-Projects window.

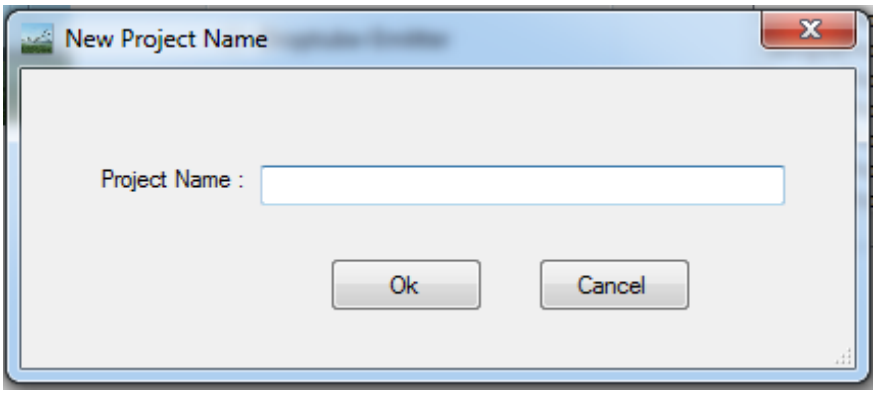

Figure 6. The New Project Name dialog box

To create a new project, however, the user needs to enter the name of the project to be created in the input box and press the Ok button. The program would then check, if the new project name is not a duplicate of the name of an existing project under the currently selected system configuration folder. If it is, then a message box will appear on the screen suggesting that a different name be used for the new project.

If, on the other hand, the new project name is different form the names of existing projects, in the current system configuration folder, then the Number of Spans dialog box (Figure 7) will appear on the screen with a prompt for the user to enter the number of spans of the lateral in an input box. If the user wants to cancel the Create new project command, then simply clicking on the Close button of the dialog box would return program control to the Systems-Projects window.

On the other hand, if the user opts to complete the command, to create a new project, then the number of spans in the lateral needs to be entered in the input box of the Number of Spans dialog box. Valid inputs are between 6 and 12 spans. If the user specified span number is in the range between 6 and 12, then a new project folder bearing the user specified project name will be created under the current systems configuration folder. The Project listbox would then be updated accordingly and the name of the newly created project will be displayed highlighted.

Opening the folder of the newly created project would show that a project input data file, InputData_LinLat.Inp, with exactly the same number of spans as that specified by the user had been created in the project folder. The user may also note that an empty folder named Charts was also created under the new project folder. This subfolder will be used by *LincSys* to store image

files, consisting of charts of output hydraulic parameters, in *Png* format following a successful hydraulic simulation.

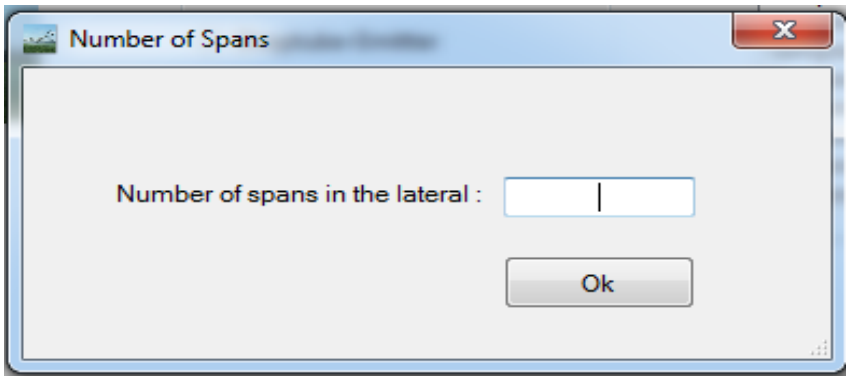

Figure 7. The Number of Spans dialog box

If the user specified span number is less than 6, the program would create a project for a lateral with 6 spans. Similarly, if the user specified number of spans exceed 12, the program would simply create a project with 12 spans only. Note that the contents and the format of the input data file saved in the new project folder, InputData_LinLat.Inp, represents an input data template for a lateral with the user specified number of spans (Sections 4.2.3.b and 5.1.3). The user can run simulations with the input data file as is, if need be. However, a more practical scenario would be consisting of one in which the input data template is modified and adapted by the user such that it represents the hydraulic and geometric parameters and elevation profile of a specific lateral for which a hydraulic simulation is to be conducted.

Delete project

The delete project functionality is represented by an icon with an image of scissors. Clicking on the Delete project icon initiates the process of deleting the currently selected project (i.e., the project that is currently highlighted in the Project listbox). Before deleting the project, however, the program displays a message box with a request for the user to confirm or cancel the delete command. Upon user confirmation the currently selected project would be deleted. The Project listbox would then be updated accordingly and the project name at the top the listbox will be displayed highlighted.

Copy project

The copy project functionality is represented by an icon featuring two partially overlapped non-blank pages. Clicking on the Copy project icon initiates the process of copying the currently selected (highlighted) project. The copy project will be placed in the currently selected system configuration option folder. The name of a copied project will be a concatenation of the name of the original project and the string "_Copy". For instance, if the name of the original project is "Project_A", the name of the copy project would be "Project_A_Copy". The Project listbox would then be updated accordingly and the name of the copy project will be displayed highlighted.

Rename project

The rename project functionality is represented by an icon featuring an open file folder. Clicking on the Rename project icon opens the New Project Name dialog box with a prompt to enter the new project name in the input box (Figure 6). To rename a project the user then needs to enter the new name of the project in the project name input box and press the Ok button. The name of the current project will then be changed to the user specified name and the new project name will be highlighted in the Projects listbox. If the Rename project icon was activated by mistake, then press the Cancel button or the Close button of the dialog box, program control will then revert back to the Systems-Projects tabpage.

Help

The Help functionality of *LincSys* is represented by an icon featuring the image of a question mark, a commonly used symbol for help resources in Windows based user interfaces. Clicking on the Help icon opens a drop-down menu with five menu titles (Figure 8a): What's this?, View Manual, Manual Chapters, Literature, and About *LincSys*.

What's This?: Clicking on the menu item What's This? (Figure 8a) enables help information, in the form of tooltips, that describe the model functionalities that underlie the user interface controls in each of the tabpages.

Tooltips popping up unprompted, during the movement of the mouse pointer over a tabpage, can be a nuisance. Thus, the default display mode for most tooltips is hidden. To activate the tooltips, click on the What's This? menu title from the drop-down menu under the Help icon of the toolbar and then just let the cursor hover over the user interface control whose function is to be queried. A concise description of the function of the particular control will then appear in a gray box below the control. The tooltips can be deactivated, if need be, by clicking on the What's This? menu title for a second time.

View Manual: Clicking on the View Manual menu item from the Help drop-down menu (Figure 8a) opens a Pdf document of the *LincSys Ver 1.0* User's Manual. Note that Adobe Acrobat reader/writer, release 2017 or later, need to be installed in the user's computer for the Help menu items to be successfully activated.

Manual Chapters: Clicking on the Manual Chapters menu title opens a dropdown menu consisting of six menu items (Figure 8b): Chapter 1, Chapter 2, Chapter 3, Chapter 4, Chapter 5, and Chapter 6. Clicking on one of these submenu items opens a Pdf document of the corresponding chapter of the user manual for a quick reference on a specific topic.

Literature: Clicking on the literature menu title opens a dropdown menu consisting of six submenu items (Figure 8c): Linear Move Hdyraulics_I, Linear Move Hdyraulics_II, Linear Move Hdyraulics_III, Linear Move Pressure Profile, Center Pivot Management, and Sprinkler System Design and Operation. Clicking on one of these submenu items opens a Pdf document of a published article, a book chapter, or a technical report. The first four documents are journal articles and are published by the authors themselves and cooperators (Zerihun and Sanchez, 2019a,b,c; Zerihun et al., 2019). These papers detail the computational framework and specific algorithms that underlie the simulation module of *LincSys*. The fifth document is a handbook on center pivot management by Martin et al. (2017) and the sixth document is a book chapter

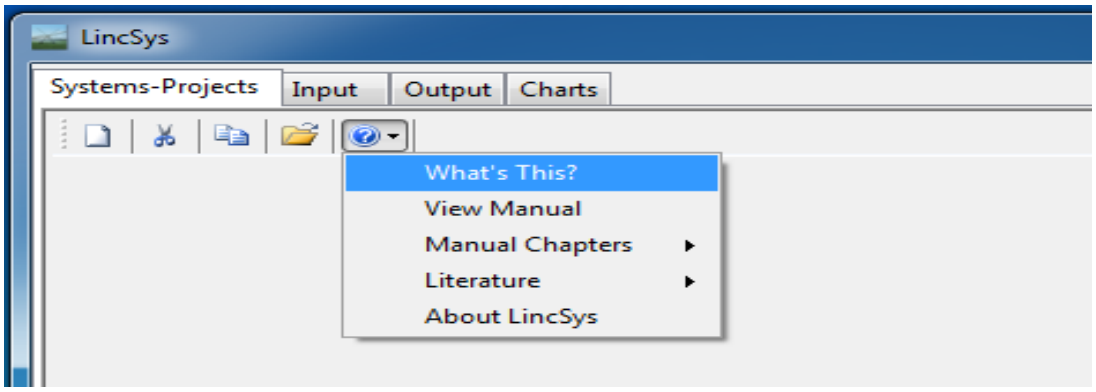

(a)

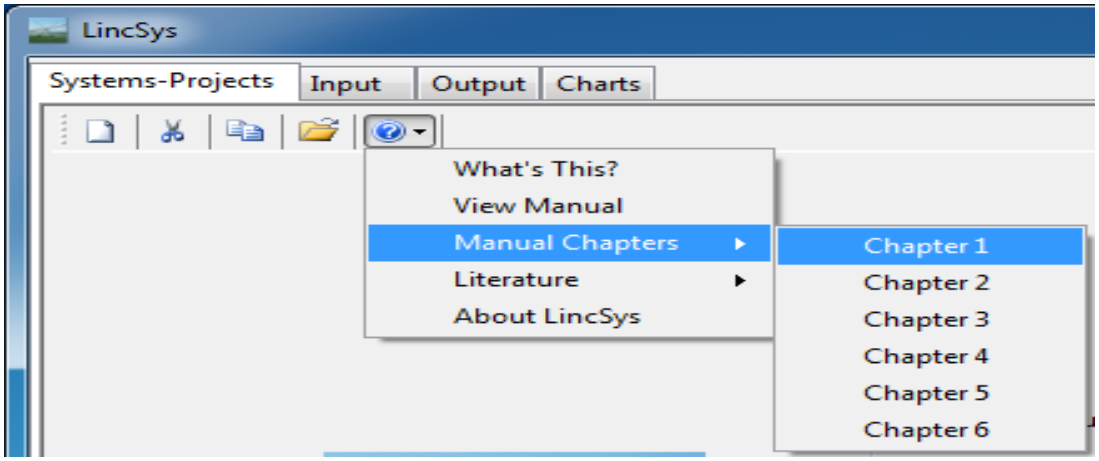

(b)

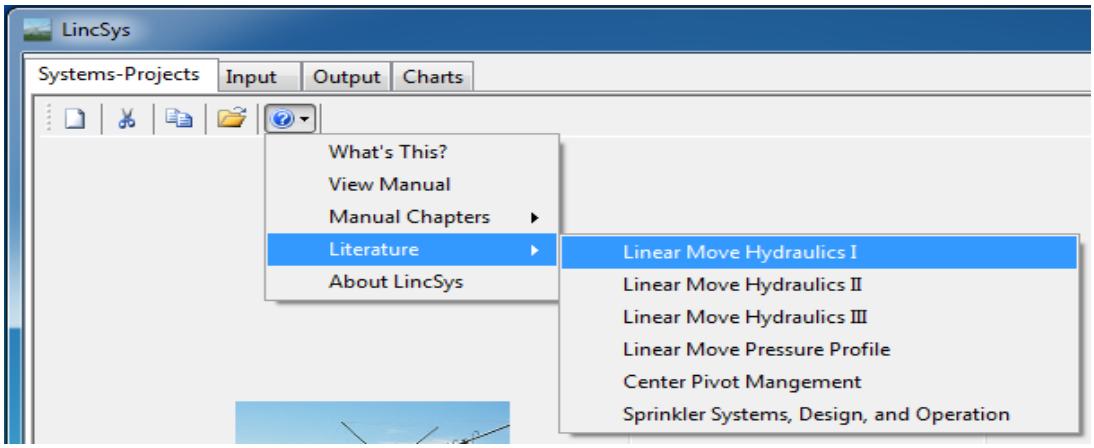

(c)

Figure 8. (a) The Help menu of *LincSys*, (b) The Help menu of *LincSys* displaying the submenu items under the menu title Manual Chapters, and (c) The Help menu of LincSys displaying the submenu items under the menu title Literature

describing in sufficient detail the design and operation of sprinkler systems, including center-pivot and linear-move systems (Martin et al., 2007), and is considered a standard reference on the subject.

About LincSys: Moving the cursor to the About *LincSys* menu title and clicking opens the *About LincSys* window (Figure 9), which provides a concise description of the core program capability. It also contains program developers' name, their institutional affiliations, their coordinates, and information on the proper citation of the model. Clicking on the Ok button returns program control to the Systems-Projects tabpage.

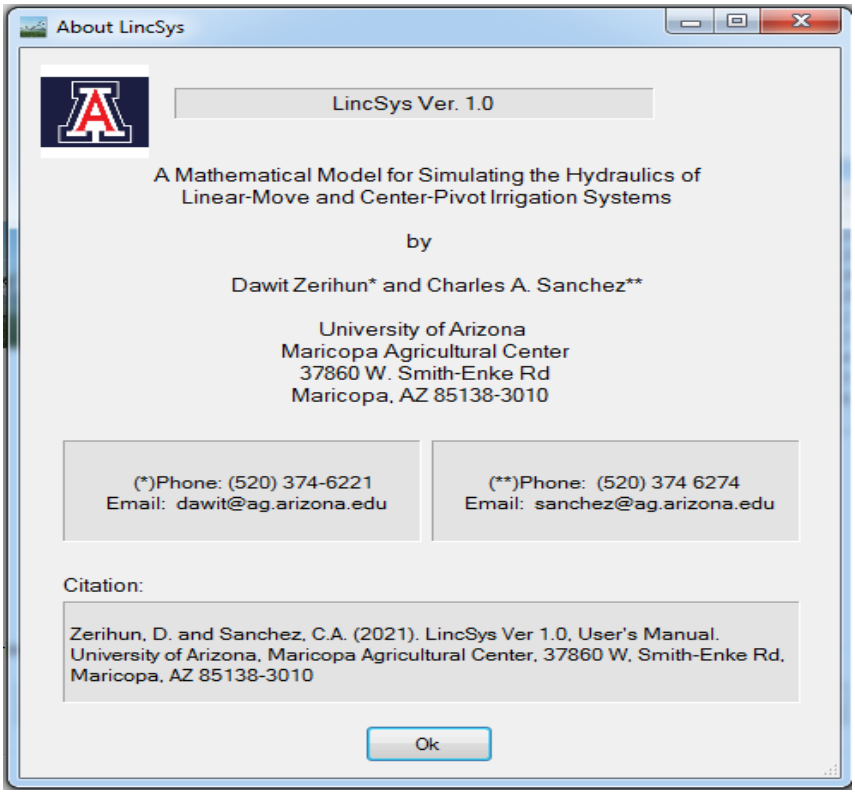

Figure 9. The About *LincSys* window

4.2.3.c. Navigation buttons

The Input, Output, and Charts tabpages cannot be accessed from the System-Projects tabpage through the respective tabcontrols. Instead, the navigation buttons displayed in the lower half of the window (Figure 5) are the only access points to each of the tabpages.

Three navigation buttons (namely: Input, Output, Charts) and an Exit button are displayed in the lower half of the System-Projects tabpage (Figure 5). Activating the Exit button closes *LincSys*. The Input, Output, and Charts buttons provide access to the respective tabpages, although with some conditionalities.

Input button

Clicking on the Input button with the mouse or pressing the Alt+I keys from the keyboard opens the Input tabpage. The Input window displays the current projects input data in

tabular and non-tabular format. In addition, the input tabpage provides the functionality for editing input data and conducting simulation runs, if necessary. Descriptions of the features and layout of the Input tabpage and *LincSys* user interface functionalities that are accessible from the Input tabpage are provided in Section 4.3.

Output button

The Output tabpage can be accessed from the Systems-Projects window by clicking on the Output button, provided the currently selected project is complete. A *LincSys* project is considered complete, if the project subfolder contains the input data file and all the output data files, except those output data files whose contents are not displayed in the Output or Charts windows (i.e., EmitterDischargePressure.Dat and Lat_hElvHglEgl_Comp.Dat files), Section 5.1.1.c.

In other words, a complete project implies that a successful simulation of the currently selected project had been conducted in an earlier simulation event and the input-output data files were not deleted or moved to a different folder subsequently.

To open the Output tabpage from the Systems-Projects window just click on the Output button with the mouse or press the Alt-O keys from the keyboard. Assuming the project is complete, this opens the Output window which displays the output data for the current project. A detailed description of the features, layout, and functionalities of the Output tabpage is provided in Section 4.4.

Charts button

The Charts tabpage as well can be opened from the Systems-Projects tabpage, provided the current project represents a complete project. Assuming that the current project is complete, then clicking on the Charts button in the Systems-Projects window or pressing the Alt+C keys from the keyboard opens the Charts tabpage. At any one time the Charts tabpage displays 1 of 11 charts (i.e., graphical rendering of output hydraulic parameters). Discussion on the features, layout, and functionalities of the Charts tabpage is provided in Section 4.5.

4.3. The *Input* tabpage

4.3.1. Features and layout of the Input tabpage

The Input tabpage features a titlebar, a statusbar, user interface controls consisting of input boxes and an input data table (to display and enable the editing of input data), navigation buttons, and tabcontrols. The features and layout of the Input tabpage are depicted in Figure 10 for systems with Droptube-Prv-Emitter configuration and in Figures 11 and 12 for systems with Droptube-Emitter and Emitter-On-Lateral configuration options, respectively.

The titlebar of the Input page has exactly the same content as that of the Systems-Project tabpage, described in Section 4.2 (Figure 4). The content of the statusbar in the Input page is the same as that of the Systems-Projects tabpage, except that the currently active tabpage is set to the Input tabpage instead of the Systems-Projects tabpage.

In the Input tabpage, the tabcontrols are depicted with the Input tabpage highlighted. While the Systems-Projects tabpage can be accessed from the Input window by tapping on the Systems-Projects tabcontrol with the (left) mouse button, the other tabcontrols (i.e., Output and Charts) can be used to open the respective tabpages only if the tabpage or tabpages have already been activated through navigation buttons earlier in the current simulation event.

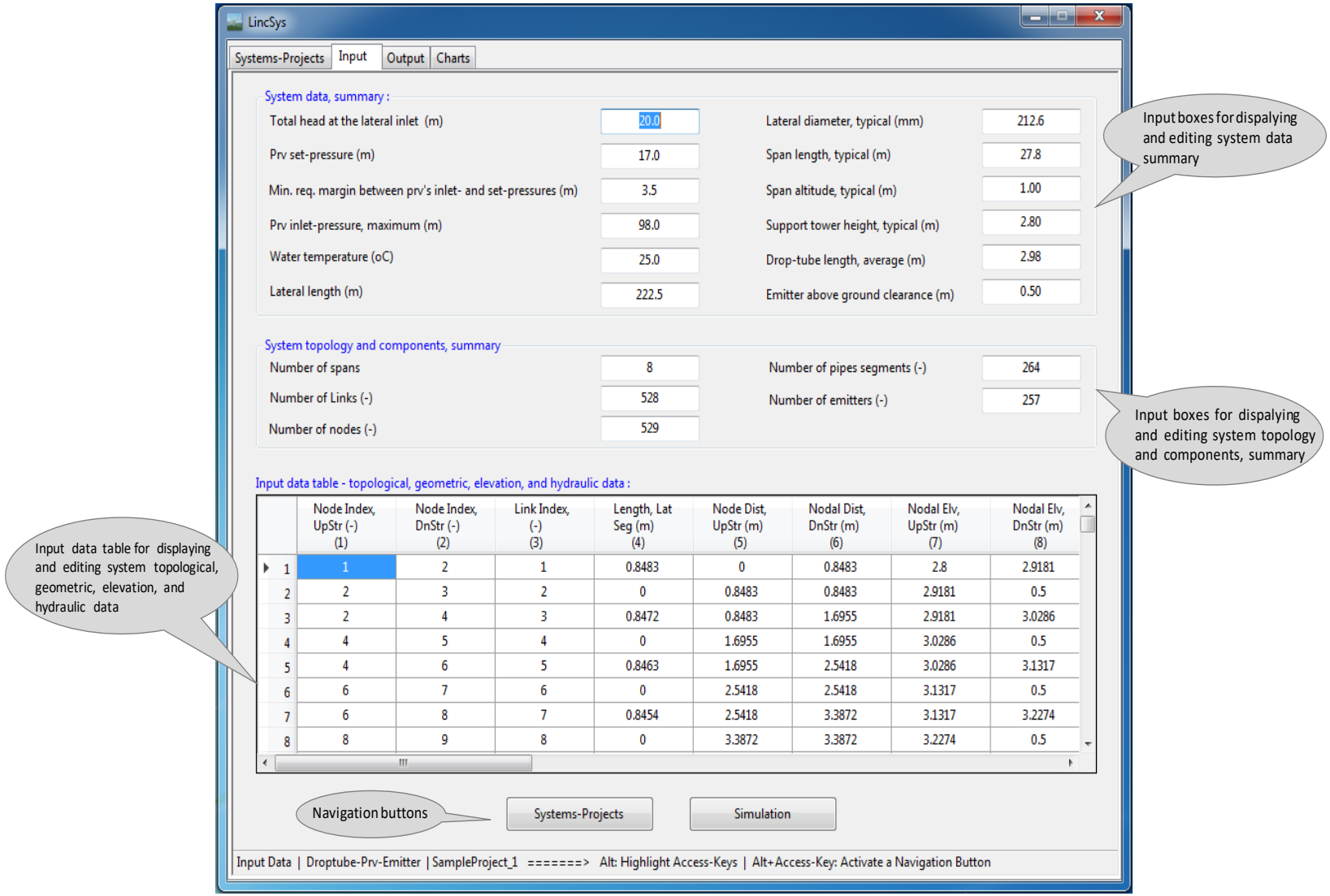

Figure 10. The Input tabpage displaying non-tabular input data, tabular input data, and navigation buttons, for the Droptube-Prv-Emitter system configuration option

Note that the term simulation event is used here to describe the duration between the time that a navigation button on the Systems-Projects tabpage is activated, and program control is transferred to any one of the other three tabpages from the Systems-Projects tabpage, and the time that program control reverted back to the Systems-Projects tabpage. Thus, during a simulation event either input data are edited and/or simulation runs are conducted for the currently selected project from the Input tabpage or simply the output data and/or charts of a selected project, from an earlier simulation event, are displayed in the Output and/or Charts tabpages, possibly, for further examination and analysis.

By comparison, a simulation session consists of all the activities that occur in the time interval between the start of the *LincSys* program and the time that the program is closed.

As can be noted from Figure 10, the input data of *LincSys* consists of tabular and non-tabular data sets. The non-tabular input data are displayed in, and can be edited from within, input boxes. The input boxes are displayed in two separate groupboxes: The System data, summary and the System topology and components, summary.

An input data table for displaying and editing tabular input (consisting of lateral topological, geometric, elevation profile, and hydraulic data) is shown right under the Input boxes (Figure 10).

Furthermore, the Input window features a pair of navigation buttons placed above the status bar: Systems-Projects and Simulation. The functions of these buttons will be discussed in Section 4.3.4.

4.3.2. Displaying and editing non-tabular input data

4.3.2.a. Displaying non-tabular input data

Input boxes are used to display non-tabular input data in the Input tabpage (Figures 10 to 12). An input box is in fact what is technically called a textbox (Table 1). To facilitate data entry and editing, *LincSys* treats the data in an input box as a concatenated set of characters, i.e., a string type variable. The string will then be converted to numerical values before data validation and computation commences.

The non-tabular input data set depicted in Figure 10 is for the Droptube-Prv-Emitter system configuration option. It consist of a total of 17 data items displayed in a pair of groupboxes: The System data, summary and the System topology and components, summary. A complete list of the non-tabular input data, corresponding units, and allowable ranges are presented in Table 2.

The input boxes in the System data, summary groupbox are arranged in two columns. The left-hand column consists of input boxes for total head at the lateral inlet, *prv* hydraulic parameters, water temperature (which is related to the effect of viscosity on the Darcy-Weisbach friction coefficient), and lateral length. On the other hand, the right-hand column displays input boxes for lateral diameter, span geometric parameters, support tower height, drop-tube length, and emitter above ground clearance.

The input boxes in the System topology and components, summary groupbox are also arranged in two columns. The inputs in this groupbox consist of numbers of system components (such as number of spans, number of lateral pipe segments, and emitters) and lateral topological data summary (number of links and nodes).

The Input data tabpages for the Droptube-Emitter and Emitter-On-Lateral system configurations are shown in Figures 11 and 12, respectively. For these system configuration

Table 2. Non-tabular input data of *LincSys*: parameter names, units, and acceptable range

Parameter name	Unit	Acceptable range	
		Lower limit	Upper limit
Total head at the lateral inlet	*m*	5.0	150.0
prv-set pressure [(a)]	*m*	2.5	100.0
Minimum required margin between the inlet and set-pressures of the *prv*[(a)]	*m*	0.1	15.0
Prv inlet pressure, maximum[(a)]	*m*	5.0	150.0
Water temperature	^oC	5.0	50.0
Lateral length	*m*	20.0	800.0
Lateral diameter, typical	*mm*	38.1	381.0
Span length, typical	*m*	20.0	70.0
Span altitude, typical	*m*	0.75	2.25
Support tower height, typical	*m*	1.75	6
Drop-tube length, average[(b)]	*m*	1.5	7.5
Emitter above ground clearance[(b)]	*m*	0.25	8.0
Number of spans	-	1	12[(c)]
Number of links	-	10	2000
Number of nodes	-	11	2001
Number of lateral pipe segments	-	5	1000
Number of emitters	-	5	1000

[(a)] Applies to Droptube-Prv-Emitter system configuration option only, [(b)]applies only to Droptube-Prv-Emitter and Droptube-Emitter system configuration options only, and [(c)]there is no limit on the maximum number of spans, but more than 12 spans in a lateral seems to be unrealistic.

options, *prv* parameters are impertinent and hence the input boxes for *prv* hydraulic parameters are deactivated (Figures 11 and 12). Furthermore, for systems with Emitter-On-Lateral configuration option, Figure 12 shows that the input boxes for the average drop-tube length and emitter above ground clearance are also deactivated.

4.3.2.b. Editing non-tabular input data with input boxes

User interface focus

When the Input window is opened, the uppermost input box in the left-hand column of the System data, summary groupbox is highlighted (Figure 10), indicating that this input box has

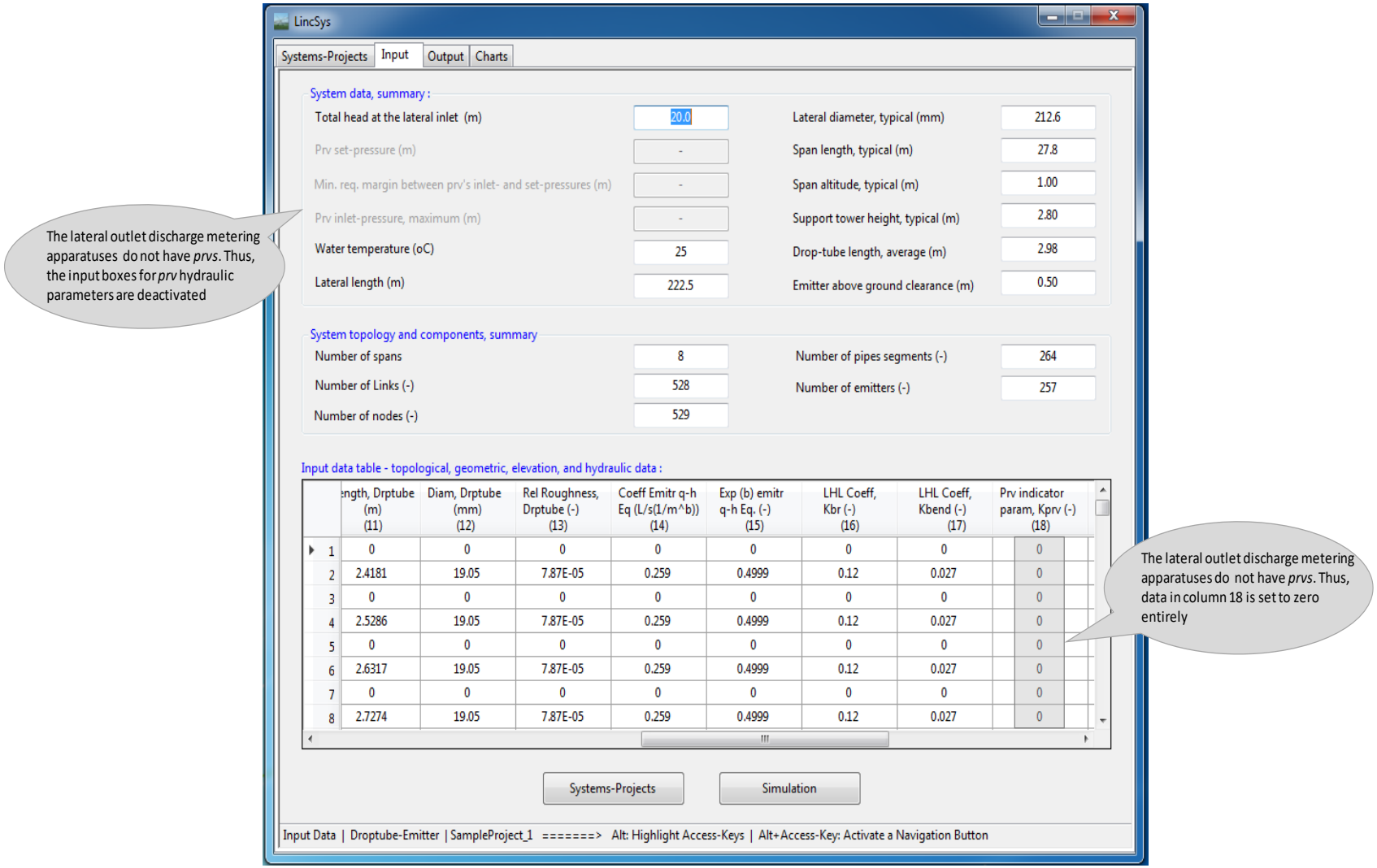

Figure 11. The Input tabpage showing non-tabular input data, tabular input data, and navigation buttons for the system configuration option of Droptube-Emitter

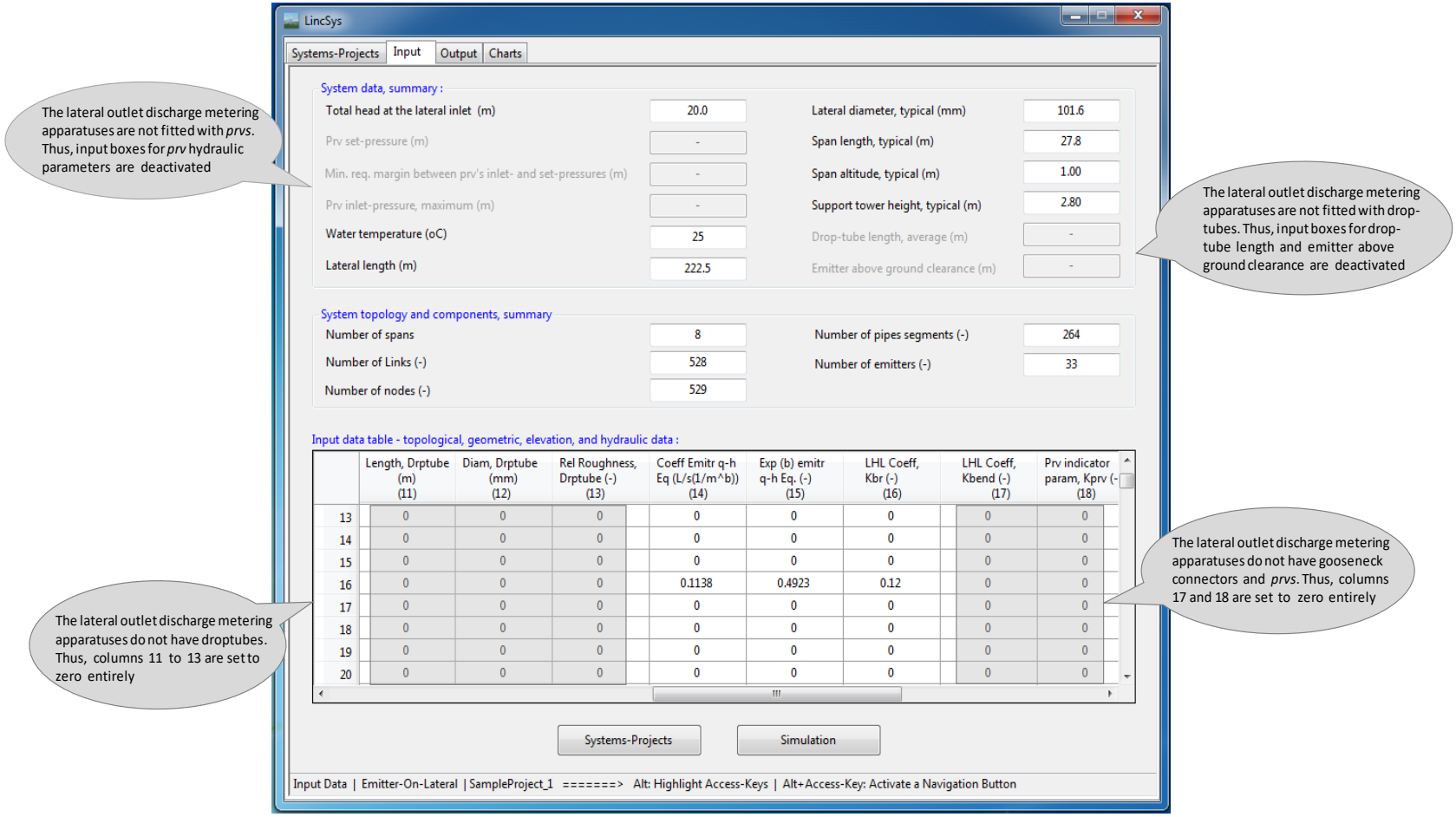

Figure 12. The Input tabpage displaying non-tabular input data, tabular input data, and navigation buttons for the system configuration option of Emitter-On-Lateral

the user interface focus. In other words, the input box for total head at the lateral inlet is the default active input box for user interaction with the program (i.e., data editing), when the Input tabpage is opened.

The user interface focus can be reset from an input box to another by moving the mouse pointer to an input box that is to get the focus and then clicking on the (left) mouse button. The cursor position (the user interface focus) can also be shifted from an input box to another that is immediately below it, by pressing the Tab key from the keyboard. Alternatively, pressing the Shift+Tab key moves the cursor up through the input boxes, one box at a time.

Data editing

To edit the data displayed in an input box, first set the focus in that box (in which case the content of the input box will be highlighted). Then there are two ways to start editing the data. One option is to simply start typing the new input data from the keyboard. Following the first key stroke, the data that was in the input box will then be cleared and replaced by the character corresponding to the first key stroke, provided the key corresponds to a valid keyboard input. The user can then continue entering the new value.

For the input boxes in the System data, summary groupbox, valid keyboard inputs consist of the numerals 0 to 9 and the decimal point, because the corresponding input parameters are real numbers. The input parameters in the System topology and components, summary groupbox are integer, hence the corresponding input boxes accept only numerals as valid keyboard inputs.

Alternatively, data editing in an input box with the focus can start by simply tapping on any of the arrow keys in the keyboard. In which case, a blinking cursor will appear on the right-hand/left-hand side of the current data in the active input box (depending on the type of arrow key), signaling that the content of the box can now be edited.

Note that during data editing in an input box, the Backspace, Delete, and Arrow keys of the keyboard have the same function as in any other Windows application software. The only exception here is that the Upwards and Downwards arrow keys also function as the leftwards and rightwards arrow keys, respectively.

4.3.3. Input data table for displaying and editing hydraulic and geometric parameters and lateral elevation profile data

Figures 10, 11, and 12 depict a partial view of the input data tables of *LincSys* corresponding to the Droptube-Prv-Emitter, Droptube-Emitter, and Emitter-On-Lateral system configuration options, respectively. Note that the input data table is what is described as a DataGridView control in the technical literature (Table 1). It displays the hydraulic network topological indexes along with the lateral hydraulic and geometric parameters and elevation profile in a tabular format and it also allows editing of the data in the individual cells.

The input data table has 24 columns. The number of rows in an input data table is equal to the number of hydraulic links in the lateral, hence it can vary from one lateral to another. *LincSys* has the capability to simulate laterals with up to 2000 links, and hence 2001 nodes, which corresponds to 2000 rows in the input data table.

The columns in an input data table represent a data type. It could be network topological parameters such as link and node indexes, lateral elevation profile data or input data related to the dimensions and/or hydraulic characteristics of system components such as lateral pipe segments, drop-tubes, emitters, *prvs*, and pipe appurtenances. A row of the input data table, on

the other hand, represents data related to a network link and delimiting nodes, which include topological data, nodal distances from the lateral inlet, nodal elevations, and pertinent input geometric and hydraulic parameters.

The column headings define the contents of the columns of the input data table (Figures 10 to 12). Because of space limitations most column headings are abbreviations. However, a more complete description of the column headings are provided through tooltips. A column heading tooltip can be activated by letting the cursor hover over the heading of the column whose data type is to be queried.

At any one time the input data table can display only a small subset of the tabular input data (consisting of 8 rows by 8 columns), Figures 10 to 12. However, the input data table has horizontal and vertical scroll bars that can be used to browse through the rest of the data table. In addition, keys from the keyboard can be used to browse through the input data table. Further discussion on this is provided in Section 4.3.3.h.

The rows and columns of the output data table are numbered sequentially starting from the top row and the left most data column (Figures 10 to 12), respectively, to help the user browse through the table to a particular cell quickly. Note that the width of the row header column (i.e., the column containing the row indices) can be increased to view the row indexes with more than one digit. To do so just let the mouse button hover over the border between the row header column and the first data column and wait until a double headed arrow straddling the border between the two columns appear on the screen and then press the left mouse button and slide the mouse to the right.

For convenience, subsequent discussion on the input data table will be based on Tables 3a and 3b, which present a sufficiently detailed sample input data table for a system with Droptube-Prv-Emitter system configuration option. Because of space limitations the table is divided into two halves. Table 3a depicts a sample of the first 12 columns of the input data table and Table 3b depicts a sample of the second half of the input data table. Note that the first column in Table 3b is not part of the input data table, it is added here to help the user relate the rows in the second half of the table (Table 3b) with those of the first (Table 3a) more readily. As noted earlier the column headings in Tables 3a and 3b are abbreviations and a more complete description of each column headings are provided in Table 4.

4.3.3.a. Topological data of a lateral schematized as a branched hydraulic network (columns #1 to 3)

Relationship between data and network configuration

Columns #1 to 3 contain topological data consisting of numerals identifying links and delimiting nodes, which resulted from the schematization of a linear-move or center-pivot lateral as a branched hydraulic network (Section 3.5.1 and Figure 3). Thus, the first three columns of the input data table constitute the basic network configuration data to which the lateral hydraulic, geometric, and elevation data in the other columns (i.e., columns #4 to 24) are related. The implication is that understanding the structure, meaning, and interrelationship of the data in columns #1, 2, and 3 and their relationship with data in the other columns is key to

Table 3a. Sample input data table of *LincSys* for a Droptube-Prv-Emitter system configuration option with 936 hydraulic links and 937 nodes (columns #1 to 12)

Row index	Column headings											
	Node Index UpStr (-) (1)	Node Index DnStr (-) (2)	Link Index (-) (3)	Length, Lat Seg (m) (4)	Nodal Dist, UpStr (m) (5)	Nodal Dist, DnStr (m) (6)	Nodal Elv, UpStr (m) (7)	Nodal Elv, DnStr (m) (8)	Diam, Lat Seg (mm) (9)	Rel roughness, Lat (-) (10)	Length, Drptube (m) (11)	Diameter, Drptube (mm) (12)
1	1	2	1	0.6026	0	0.6026	6.5233	6.5874	162.1	2.468×10^{-5}	0	0
2	2	3	2	0	0.6026	0.6026	6.5874	3.5819	0	0	3.0055	19.05
3	2	4	3	1.9076	0.6026	2.5102	6.5874	6.7832	162.1	2.468×10^{-5}	0	0
4	4	5	4	0	2.5102	2.5102	6.7832	3.6104	0	0	3.1728	19.05
5	4	6	5	0.5018	2.5102	3.012	6.7832	6.8329	162.1	2.468×10^{-5}	0	0
6	6	7	6	0	3.012	3.012	6.8329	3.6179	0	0	3.215	19.05
7	6	8	7	1.1038	3.012	4.1158	6.8329	6.9397	162.1	2.468×10^{-5}	0	0
8	8	9	8	0	4.1158	4.1158	6.9397	3.6344	0	0	3.3053	19.05
9	8	10	9	0.5719	4.1158	4.6877	6.9397	6.9937	162.1	2.468×10^{-5}	0	0
.	.	.	.	.	.	.	.	.	.	.	.	.
.	.	.	.	.	.	.	.	.	.	.	.	.
.	.	.	.	.	.	.	.	.	.	.	.	.
55	54	56	55	1.4003	26.5277	27.928	8.3356	8.3738	162.1	2.468×10^{-5}	0	0
56	56	57	56	0	27.928	27.928	8.3738	3.9911	0	0	4.3827	19.05
.	.	.	.	.	.	.	.	.	.	.	.	.
.	.	.	.	.	.	.	.	.	.	.	.	.
.	.	.	.	.	.	.	.	.	.	.	.	.
.	.	.	.	.	.	.	.	.	.	.	.	.
500	500	501	500	0	249.0128	249.0128	3.9521	0.796	0	0	3.1561	19.05
.	.	.	.	.	.	.	.	.	.	.	.	.
.	.	.	.	.	.	.	.	.	.	.	.	.
.	.	.	.	.	.	.	.	.	.	.	.	.
933	932	934	933	0.6043	465.7337	466.338	6.0421	6.1137	101.6	0.00003937	0	0
934	934	935	934	0	466.338	466.338	6.1137	2.6319	0	0	3.4818	19.05
935	934	936	935	1.917	466.338	468.255	6.1137	6.3687	101.6	0.00003937	0	0
936	936	937	936	0	468.255	468.255	6.3687	2.6319	0	0	3.7368	19.05

Table 3b. Sample input data table of *LincSys* for a Droptube-Prv-Emitter system configuration option with 936 hydraulic links and 937 nodes (columns 13 to 24)

Row index	Column headings and index											
	Rel roughness, Drptube (-) (13)	Coeff Emitr q-h Eq L/s(1/m^b) (14)	Exp(b), Emitr q-h Eq (-) (15)	LHL Coef, Kbr (-) (16)	LHL Coef, Kbend (-) (17)	Prv Indicator Param (-) (18)	LHL Coef, Klf (-) (19)	LHL Coef, Kcpl (-) (20)	LHL Coef, Kct (-) (21)	LHL Coef, Kexp (-) (22)	LHL Coef, Kval (-) (23)	LHL Coef, Keq (-) (24)
1	0	0	0	0	0	0	0	0	0	0	0	0
2	5.25×10^{-5}	0.0429	0.5018	0.2	0.06	1	0	0	0	0	0	0
3	0	0	0	0	0	0	0.1	0	0	0	0	0
4	5.25×10^{-5}	0.0429	0.5018	0.2	0.06	1	0	0	0	0	0	0
5	0	0	0	0	0	0	0.1	0	0	0	0	0
6	5.25×10^{-5}	0.0429	0.5018	0.2	0.06	1	0	0	0	0	0	0
7	0	0	0	0	0	0	0.1	0	0	0	0	0
8	5.25×10^{-5}	0.0429	0.5018	0.2	0.06	1	0	0	0	0	0	0
9	0	0	0	0	0	0	0.1	0	0	0	0	0
.	.	.	.	.	.	.	.	.	.	.	.	.
.	.	.	.	.	.	.	.	.	.	.	.	.
.	.	.	.	.	.	.	.	.	.	.	.	.
55	0	0	0	0	0	0	0.1	0	0	0	0	0
56	5.25×10^{-5}	0.0429	0.5018	0.2	0.06	1	0	0	0	0	0	
.	.	.	.	.	.	.	.	.	.	.	.	.
.	.	.	.	.	.	.	.	.	.	.	.	.
.	.	.	.	.	.	.	.	.	.	.	.	.
.	.	.	.	.	.	.	.	.	.	.	.	.
500	5.25×10^{-5}	0.0429	0.5018	0.2	0.06	1	0	0	0	0	0	0
.	.	.	.	.	.	.	.	.	.	.	.	.
.	.	.	.	.	.	.	.	.	.	.	.	.
.	.	.	.	.	.	.	.	.	.	.	.	.
933	0	0	0	0	0	0	0.1	0	0	0	0	0
934	5.25×10^{-5}	0.0429	0.5018	0.2	0.06	1	0	0	0	0	0	0
935	0	0	0	0	0	0	0.1	0	0	0	0	0
936	5.25×10^{-5}	0.0429	0.5018	0.2	0.06	1	0	0	0	0	0	0

Table 4. Complete description of column headings of the input data table (Tables 3a and 3b) and units and ranges of the respective input parameters

Column index	Column headings in Tables 3a and 3b	Complete description of column headings	Unit	Acceptable range	
				Lower limit	Upper limit
1	Node Index, UpStr	Index of the upstream-end node of a link	-	1	200
2	Node Index, DnStr	Index of the downstream-end node of a link	-	2	2001
3	Link Index	Index of a hydraulic link	-	1	2000
4	Length, Lat seg	Length of a lateral segment	*m*	0.5	2.5
5	Node Dist, UpStr	Distance from lateral inlet of the upstream-end node of a link	*m*	0.0	797.5
6	Node Dist, DnStr	Distance from the lateral inlet of the downstream-end node of a link(i.e., a lateral pipe segment)	*m*	0.5	800.0
7	Node Elv, UpStr	Elevation of a links upstream-end node	*m*	0.0	1500.0
8	Node Elv, DnStr	Elevation of a links downstream-end node	*m*	0.0	1500.0
9	Diam, Lat Seg	Diameter of a lateral pipe segment	*mm*	38.1	381.0
10	Rel Roughness, Lat Seg	Relative roughness of a lateral pipe segment	-	10^{-10}	0.1
11	Length, Drptube	Length of a drop-tube	*m*	0.0	8.0
12	Diameter, Drptube	Diameter of a drop-tube	*mm*	0.0	50.8
13	Rel roughness, Drptube	Relative roughness of a drop-tube	-	10^{-10}	0.05
14	Coeff Emitr q-h Eq	Coefficient of the emitter head-discharge equation	$L/s(1/m^b)$	0.0	1.0
15	Exp (b) of Emitr q-h Eq	Exponent (labeled here as *b*) of the emitter head-discharge equation	-	0.0	1.0
16	LHL Coeff, Kbr	Local head loss coefficient, associated with the branching flow at outlet ports	-	10^{-6}	5.0
17	LHL Coeff, Kb	Coefficient associated with bending losses at the gooseneck connector	-	0.0	5.0
18	Prv indicator Param, Kprv[(a)]	*prv* indicator parameter, indicates whether an outlet discharge metering apparatus is fitted with a *prv* or not	-	0	1
19	LHL Coeff, Klf	Coefficient for local head losses associated with through-flow across an outlet	-	0.0	5.0
20	LHL Coeff, Kcpl	Coefficient for local losses associated with pipe couplers	-	0.0	5.0
21	LHL Coeff, Kct	Coefficient for local head losses associated with sudden contraction	-	0.0	5.0
22	LHL Coeff, Kexp	Coefficient for local head losses associated with sudden expansion	-	0.0	5.0
23	LHL Coeff, Kval	Coefficient for local head losses associated with a valve	-	0.0	5.0
24	LHL Coeff, Keq	Equivalent coefficient for local head losses associated with more than one appurtenances arranged in series and in close proximity	-	0.0	5.0

(a) The *prv* indicator parameter is set to a value of 0 for Droptube-Emitter or Emitter-On-Lateral system configuration options. For a system with a Droptube-Prv-Emitter configuration it is set to 1 in all even-numbered rows that represent outlet discharge metering apparatuses and is set to 0 in the even-numbered rows that represent virtual links and in all odd-numbered rows.

understanding the structure and content of the input data table. Note that in subsequent discussion, row and column indexes refer to the data rows and columns of the input data table (i.e., they do not include the column header row and the row header column).

The data in the first and second data columns of the input data table represent the node indexes at the upstream-end and downstream-end, respectively, of the corresponding link, which is displayed in the third column. To explain the structure of the data in these columns, a schematics of the four different types of junction nodes and attached links (that resulted from the representation of an irrigation lateral as a branched hydraulic network) are depicted in Figure 13.

A junction node located immediately downstream of the inlet-end node of the lateral and attached links is shown in Figure 13a. Figure 13b and 13c depict offtake and non-offtake junction nodes, respectively, and attached links upstream of the distal-end. Figure 13d shows a junction node at the distal-end of a lateral. Note that the junction nodes in Figures 13b to 13d are connected to only one fixed head node, located downstream, compared to that of Figure 13a where the junction node is connected to two fixed head nodes, one located upstream and another downstream. Also notable is that the distal-end node, Figure 13d, has only one link attached to it that carry discharge from it, as opposed to two, which is the case with the other nodes (Figures 13a to 13c).

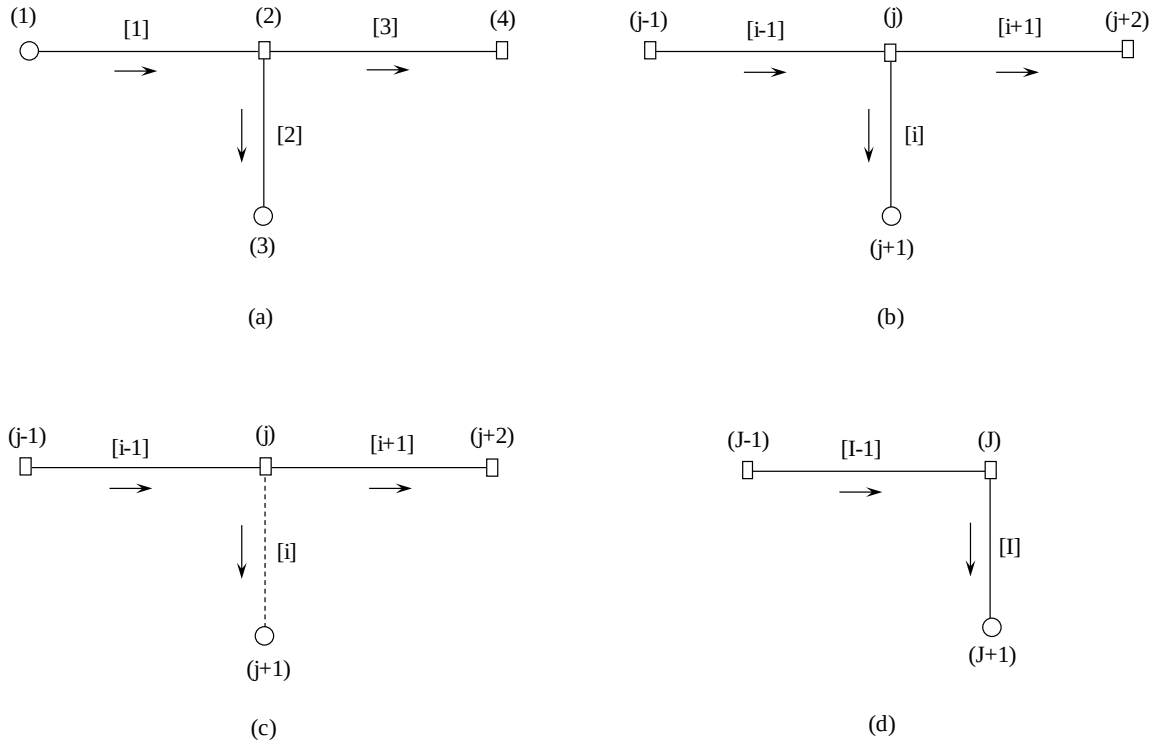

Figure 13. Schematics of junction nodes and attached links: (a) an offtake junction node immediately downstream of the inlet-end node, (b) an offtake junction node located between the inlet and distal-ends of the lateral, (c) a non-offtake junction node located between the inlet and distal-ends of the lateral, and (d) distal-end junction node (Notations: (j) is node index, [i] is link index, –– is link, ○ is fixed head node, and □ is junction node)

Now, from Figure 13a, it can be observed that the inlet-end of the lateral, which is a fixed head node, is labeled as node #1 and the junction node immediately downstream of the inlet-end node is marked as node #2. Furthermore, the link connecting nodes #1 and 2 is labeled as link #1. In Table 3a, link #1 and delimiting nodes (i.e., nodes #1 and 2) are entered in the first three columns of the first data row of the table. The link index is shown in column #3 and the corresponding upstream- and downstream-end nodes of the link are depicted in columns #1 and 2 of row #1, respectively.

Considering link #2, which is a lateral outlet discharge metering assembly, it can be observed that it is delimited by a junction node at its upstream-end (node #2) and a fixed head node at its downstream-end (node #3), Figure 13a. In Table 3a, the link number (i.e., link #2) is recorded in the third column and the upstream-end node index (node #2) and downstream-end node index (node #3) are entered in the first and second columns, respectively, of the second row of the table. Similarly, for link #3 it can be observed from Figure 13a that the link is delimited by node #2 at its upstream-end and by node #4 at its downstream-end. Note that the data in the first three columns of the third data row of the table relates to link #3 and delimiting nodes: nodes #2 and 4.

The preceding discussion highlights how the arrangement of the topological data in columns #1 to 3 (Table 3a) relate to the actual structure of the branched hydraulic network shown in Figure 3a. Note that the same approach noted, above, in relation to the three upstream-end links of the lateral can be used to deduce the topological data for an entire lateral based on Figures 13b to 13d, regardless of the number of links.

Nodal and link indexes, patterns of variation (Tables 3a and 3b), and explanations

A close look at the hydraulic network topological data shows that each fixed head node index, which is always an odd-number, appears only in the second column of the table and only once (Table 3a). The exception here is the inlet-end node label, which appears at the top of the first column.

By comparison, each junction node index (which is even-numbered), for both offtake and non-off take nodes, appears first in the second column and then repeated twice in the subsequent rows of the first column. In other words, each junction node label appears in columns #1 and 2 for a total of three times. However, there is an exception here as well, as can be noted from Table 3a, the label for the distal-end junction node appears in the second column and once in a subsequent row of the first column (i.e., it appears for a total of two times in the table). The reason for the observed patterns in the topological data of the input data table will now be explained.

As can be noted from Figure 13a, all intermediate junction nodes (i.e., junction nodes upstream of the distal-end) are shared by three links that are joined at the node. A link that carries discharge to the node and a pair of links that carry discharge from the node. Given that the network nodes and links are numbered sequentially starting from the upstream-end of the lateral, the label of a junction node appears for the first time in the second column of the input data table, as the downstream-end node of the link that carries discharge to it (Table 3a). It then appears in two subsequent rows of the first data column as the upstream-end node of the links that carry discharge from it.

By comparison, fixed head nodes (which represent the inlet-end of the lateral and the downstream-ends of the links associated with outlet discharge metering apparatuses or their virtual variants, Figures 13a to 13d) are boundary nodes and are associated with only a single

link. Thus, their labels appear only once in the input data table, either in the first column, as in the case of the inlet-end node, or in the second column as in the case of all the other fixed head nodes (Table 3a). Note that the inlet-end node delimits the upstream-end of link #1, thus its label appears in the first column. By contrast, all the other fixed head nodes are shown in the second column, because they are the nodes that delimit the downstream-ends of the respective links (which correspond to lateral outlet discharge metering apparatuses).

Furthermore, it can be observed that the nodal and link indexes increase as one moves from the top row to the bottom row of the table. However, the change in the data in each of the first three columns follow a different pattern (Table 3a).

The data in column #1, which shows the nodes delimiting the upstream-ends of the respective links, start with a node index of 1 in row #1. It then increased to 2 in the second row and remains unchanged in the third row, which represent an increment of 1 with respect to the nodal index in row #1. The node index then increases to 4 in the fourth row and stays unchanged in the fifth row, which represents an increment of 2 with respect to the nodal index in row #3. In the sixth row, the nodal index increased by 2 to 6 and stays the same in the seventh row. As can be noted form Table 3a, the pattern observed over rows 2 to 6 continue through the table down to the penultimate row.

Note that the difference between the nodal indexes in the penultimate row and the bottom row, where the label of the distal-end junction node appears, is also 2. However, the corresponding nodal index appears only once in the first data column. Evidently, this is different from all the junction nodes upstream, for which the respective nodal indexes appear twice in column #1. The reason for this is that, unlike the upstream junction nodes where a pair of links carry discharge from each node, in the case of the distal-end junction there is only one link that carries discharge from the node (Figure 13d). Hence, the label of the distal-end junction node appears only once in the penultimate row of the second column as the downstream-end node of the link that carries discharge to the node and once more in the bottom row of the first column as the upstream-end node of the link that carries discharge from the node.

The data in column #2, which represent indexes of the nodes delimiting the downstream-ends of the respective links, start with the index for the downstream-end node of link #1, which is node #2, and increases steadily by 1 as one moves through the table from the top to the bottom row. The node index at the bottom row of column #2, which corresponds to the downstream-end fixed head node, is equal to the total number of nodes in the hydraulic network (which is 937).

The link indices, shown in column #3, start with the label of the upstream-end link, link #1, and increases steadily by 1 as one moves from the top to the bottom row of the table. The index at the bottom row (i.e., 936) is equal to the total number of links in the hydraulic network.

Evident from the preceding discussion is that each link is uniquely associated with a pair of nodes. Thus, nodal distances, elevations, and local head loss coefficients defined at network nodes can be considered properties of the link at its delimiting nodes. Other inputs in the input data table (such as diameter and hydraulic resistance) can be considered as properties spanning the link. It can thus be observed that a hydraulic link is the basic topological data to which the data in each row of the input data table (consisting of nodal indices, hydraulic, geometric, and elevation data) are referenced to.

4.3.3.b. Nodal distances and length of a lateral pipe segment (columns #4 to 6)

Data in column #4 represents the length of the lateral pipe segment corresponding to each link. The data in columns #5 and 6 represent the distances (from the lateral inlet) of the nodes delimiting the upstream- and downstream-ends, respectively, of each link. It can thus be observed that in each row, the sum of the values shown in columns #4 and 5 is equal to the corresponding data item in column #6.

Note that the lateral pipe segment lengths for the even-numbered rows are set to zero (column #4), throughout the table, to indicate that the links in these rows represent flow metering apparatuses, instead of lateral pipe segments and hence impertinent.

An important point here is that a lateral pipe segment length is determined along the centerline of the lateral, which is marginally different from distances measured along the horizontal. A close look at the data in columns #5 and 6 and columns #1 and 2 shows that for the junction nodes (i.e., the even-numbered nodes), the variation in the nodal distances from the lateral inlet (i.e., data shown in columns #5 and 6) follow the same pattern as that observed with respect to nodal indexes in the first and second columns of the table.

For instance, the value in the first row of column #6 is 0.6026m and the value in the second and third rows of column #5 are both 0.6026m. Now, scanning through rows #1 through 3 of columns #1 and 2 it can be observed that each of the corresponding values, in columns #5 and 6, represent the distance from the lateral inlet of the same node, node #2. A similar observation can be made for other nodes throughout the input data table, which explains the one to one correspondence in data pattern (associated with junction nodes) between columns #1 and 5, on one hand, and those of columns #2 and 6, on the other.

Furthermore, for the even-numbered rows of the input data table, which corresponds to the even-numbered links (Table 3a), the nodal distances shown in columns #5 and 6 are equal. The explanation for this lies in the fact that even-numbered links represent outlet discharge metering apparatus, which are vertical. Thus, the nodes delimiting the upstream-end and downstream-end of these links are located at the same distance from the lateral inlet.

The relationship between the data in columns #5 and 6 and those of columns # 1 and 2 are self-evident. Nonetheless, they are discussed here, because they are important in preparing a correct input data table for *LincSys*. Overall, a quick preview of the consistency of data in columns #4 to 6 can be made based on: *(i)* for each row (link) the sum of the values in columns #4 and 5 must be equal to the value in column #6, *(ii)* the pattern of variation of the even-numbered nodes in the first and second columns need to be replicated, in the corresponding nodal distance data given, in columns #5 and 6, and *(iii)* in the even-numbered rows data items in columns #5 and 6 must be equal. Note that *LincSys* has data validation routines that use these patterns in the input data to check input data consistency.

4.3.3.c. Nodal elevation data (columns #7 and 8)

The nodal elevation data of the lateral is shown in columns #7 and 8 of the input data table (Table 3a). Each row of data in column #7, represents the elevation of a node that delimits the upstream-end of the corresponding link. Column #8, on the other hand, contains elevation data of the downstream-end nodes of each link.

A practically more useful way of looking at the data in these columns is that column #7 consists of elevation data of the lateral inlet node and all the junction nodes. Thus, when it is paired with the data in column #5, it represents the elevation profile of the lateral centerline. By

comparison, column #8 contains the elevation data of each junction node and fixed head nodes in the hydraulic network, except that at the lateral inlet. Notably, a graphical rendering of the data in columns #6 and 8 will then show the outline of the lateral elevation profile and the elevation profile of the emitter along the lateral. Evidently, the nodal distance in columns #5 and 6 are not horizontal distances and hence, the elevation profiles, noted here, are not exact. Nonetheless, they are sufficiently accurate representations, because the differences between the distances along the lateral centerline and those along the horizontal are marginal, they are in the order of < 0.5%.

Note that the elevation data of the junction nodes, i.e., the even-numbered nodes, shown in columns #7 and 8 also replicates the pattern observed for the corresponding nodal indexes in the first and second columns.

In summary, a quick preview of the elevation profile data for consistency can be made based on: (1) The pattern of the even numbered nodes in the first and second columns need to be replicated, in the corresponding nodal elevation data, in columns #7 and 8 and (2) A graph of the nodal elevation data in column #8 against the nodal distance data in column #6 can be used to make a quick visual assessment of the consistency of the lateral and emitter elevation profiles data. Note that *LincSys* uses these patterns in the input data to check input data consistency.

4.3.3.d. Diameter and relative roughness of lateral pipe segments (Columns #9 and 10)

The diameters and relative roughness of lateral pipe segments are shown in columns #9 and 10, respectively (Table 3a). Note that data in columns #9 and 10 alternate between positive numbers and zero as one moves through the rows of the input data table. Odd-numbered rows, which represent odd-numbered links, and hence lateral pipe segments, contain the diameter and relative roughness values of the respective lateral pipe segments. On the other hand, the even-numbered rows are set to zero, indicating that the associated links are lateral outlet discharge metering devices and hence impertinent.

LincSys allows lateral pipe diameter and the corresponding relative roughness to vary from a lateral pipe segment to the next. While lateral diameter is an input not related to any of the columns in the table, evidently relative roughness is a function of the lateral diameter. Equivalent roughness values for pipes of some widely used materials are summarized by Behave and Gupta (2006) and Boulos et al. (2006).

4.3.3.e. Drop-tube length, dimeter, and relative roughness (columns #11, 12, and 13)

The data consisting of drop-tube length, dimeter, and relative roughness are presented in columns #11 and 12 (Table 3a) and column #13 (Table 3b), respectively. The data in these columns alternate between a value of zero in the odd-numbered rows and positive values in the even-numbered rows of the table. The zeros in the odd-numbered rows indicate that these rows are associated with links representing lateral pipe segments and hence impertinent. On the other hand, the positive values in the even-numbered rows of columns #11, 12, and 13 represent the length, diameter, and relative roughness, respectively, of drop-tubes.

Drop-tube lengths are variable and are functions of the elevation of the lateral outlets (shown in the even-numbered rows of column #8), the field surface elevation, and the above ground clearance of the emitters (typically a constant). *LincSys* allows specification of variable drop-tube diameter. However, it appears that in practice drop-tube diameter is constant across a lateral. Evidently, the drop-tube relative roughness parameters are related to the diameters of the drop-tubes.

Note that drop-tube parameters specified in columns #11 to 13 are relevant only to systems that use drop-tubes to convey water down from the lateral outlet ports to *prv*-emitter assemblies or to emitters (i.e., systems with Droptube-Prv-Emitter and Droptube-Emitter configurations, Figures 10 and 11). However, for Emitter-On-Lateral system configuration option, the drop-tube parameters are impertinent, thus, as shown in Figure 12 these columns are set to zero.

4.3.3.f. Emitter hydraulic parameters (Columns #14 and 15)

In *LincSys*, emitter hydraulic characteristics is defined in terms of an equation that expresses emitter head differential as a power function of emitter discharge (Zerihun and Sanchez, 2019b). For a given emitter, the coefficient and exponent of the head-discharge equation can be obtained by regressing emitter pressure data against the associated discharge data, both of which are provided in manufacturer's catalogue.

The coefficients and exponents of the emitter head-discharge equation are displayed in columns #14 and 15, respectively. Note that the data for the emitter hydraulic characteristics are shown only in the rows that correspond to links, that are attached to offtake nodes and, hence represent outlet discharge metering apparatuses. Thus, they are displayed in most, but not in all, even-numbered rows of the input data table. On the other hand, even-numbered rows representing virtual links, with zero discharge, attached to non-offtake nodes (such as span joints, plugged outlet ports, or other points along the lateral where lateral elevation is known and is used in the schematization of the lateral hydraulic network) and all odd-numbered rows are set to zero.

An important point here is that the model determines whether a junction node is an offtake node or a non-offtake node based on the value assigned to the coefficient of the emitter head discharge function (column #14). A positive value, within the valid range (Table 4) specified in an even-numbered row of column #14, signals to the program that the corresponding junction node is an offtake node. A value of zero, on the other hand, indicates that the corresponding node is a non-offtake node.

The model allows the use of different emitters in each lateral outlet port. Thus, the emitter head-discharge parameters can potentially vary from an outlet port to the next along the lateral.

4.3.3.g. Local head loss coefficients

Localized energy losses occur across lateral pipe appurtenances (such as fittings, tees, bends, valves) where the flow is constrained, changes direction, or changes velocity. These energy losses occur over a relatively short, nonetheless, finite distance and the underlying physical mechanisms are generally complex. However, in practice they are represented as localized point-scale losses and are expressed as the product of an empirical coefficient and the local velocity head (Eq. 6). Thus, the data in columns 16 to 24 of the input data table represent loss coefficients corresponding to eight different forms of local head losses and a column that contains data related to *prv* indicator parameter.

Coefficients in columns #16 to 18

Data in columns #16 to 18 are associated with local head losses that may occur in outlet discharge metering apparatuses (Table 3b). The data in column #16 are coefficients for local head losses associated with branching flow that occurs at offtake nodes where flow division

takes place. This head loss occurs in laterals with any of the three outlet discharge metering apparatuses considered in the model: Droptube-Prv-Emitter, Droptube-Emitter, and Emitter-On-Lateral.

The data in column #17 is a coefficient related to the bending losses that occur in the gooseneck connector and hence it relates only to systems that are equipped with Droptube-Prv-Emitter or Droptube-Emitter outlet discharge metering devices (Table 3b). Note that *LincSys* allows the specification of bending loss coefficients along the lateral as well.

Data in column #18 is not related to local head losses. The local head losses associated with *prvs* are set to a constant equal to the manufacturer recommended minimum pressure head margin between the inlet and set pressure of the *prv* (e.g., Zerihun and Sanchez, 2019a), which is specified by the user in the non-tabular input data section of the Input tabpage (Figure 10). Column #18, thus, contains values that indicate whether a link is fitted with a *prv* or not. Accordingly, the even-numbered cells of column #18 are designed to accept only a binary input consisting of a value of 1 or 0. A value of 1 indicates that the corresponding link is an outlet discharge metering apparatus fitted with a *prv*. A value of 0, on the other hand, indicates the link is a virtual link and hence note fitted with a *prv*. Given that the data in this column pertains only to the Droptube-Prv-Emitter system configuration option, column #18 needs to be set to zero for Droptube-Emitter and Emitter-On-Lateral system configuration options (Figures 11 and 12).

Note that data in columns #16 and 18 are associated with local head losses that occur across outlet discharge metering apparatuses. Thus, they are specified only in a subset of the even-numbered rows of the input data table, where the corresponding links represent outlet discharge metering apparatuses. The even-numbered rows that represent virtual links and all the odd-numbered rows of columns #16 and 18 are set to zero, indicating that these parameters pertain only to links that represent outlet discharge metering apparatuses. The local head loss coefficient associated with bending loss can be specified in both the even- and odd-numbered rows of column #17. However, even-numbered rows that represent virtual links need to be set to zero.

Coefficients in columns #19 to 24

Columns #19 to 22 and 24 contain coefficients that relate only to local head losses that may occur in lateral pipe segments, i.e., odd-numbered links. The data in column #19 contain a line-flow loss coefficient associated with the local energy loss that occurs across an offtake node (outlet port) and it accounts for the part of the head loss that occurs in the through-flow. Given that it is associated with the head loss along the lateral, it is specified in the odd-numbered rows of the input data table, which contains data on lateral pipe segments (Table 3b). The even-numbered rows, on the other hand, are set to zero indicating that line-flow loss coefficient is impertinent to outlet flow metering apparatuses.

The data in columns #20, 21, and 22 represent coefficients associated with local head losses that occur across pipe couplers, sudden contraction, and sudden expansion in the pipe cross-sectional area, respectively. These head losses occur along the lateral only and hence they need to be specified in the odd-numbered rows. The even-numbered rows, on the other hand, need to be set to zero. If a lateral pipe segment does not have one or more of these features, then the corresponding odd-numbered row in columns #20, 21, and 22 need to be set to zero as well. Note that sudden contraction and expansion can occur only at junction nodes. Of course, with the caveat that both sudden contraction and expansion of pipe cross-sectional area cannot occur at a node. The model would not allow it any way.

The data in column #23 represents energy loss across a valve placed in a link, which could be a lateral pipe segment or an outlet discharge metering apparatus. Thus, in the input data table of a project, the valve head loss coefficient can be specified in both the odd- and even-numbered rows of the input data table as necessary. A value of zero in column #23 represents that the corresponding link is not outfitted with a valve, whereas a positive real number within the allowable range (Table 3b) indicates the presence of a valve in the corresponding link.
In principle, the local head losses associated with couplers and valves can occur anywhere along a lateral pipe segment, including at the nodes delimiting a lateral segment. However, the way their effects can be taken into account differ depending on the location of the individual appurtenances with respect to the delimiting nodes of the lateral pipe segment and relative to each other. If these features are placed in series within a lateral pipe segment and if they are sufficiently spaced for the flow in between them to be considered fully developed, then corresponding coefficients need to be specified in the respective columns. The local head losses associated with each will be calculated separately and added to the total energy loss in a link and used in the link energy balance equation.

If, on the other hand, one or more of these features (i.e., coupler and valve) are placed in a node then it is assumed in *LincSys* that their effects are considered additive to that associated with the through-flow head loss across the node. The respective coefficients would be specified the same way as indicated above for the case in which the appurtenances are placed within a link.

If a combination of couplers and valves are placed within a lateral pipe segment and their placement is that they are in such close proximity to one another that the effects of an appurtenance on the flow interacts and merges with that of the adjacent appurtenances, then (within the modeling framework adopted in *LincSys*, i.e., one-dimensional steady pipe flow) there is no mechanism to discern the individual effects of each appurtenance, on link energy balance, from the aggregate effect. Thus, if the placement of some combination of these appurtenances within a link is deemed to fit this description, it is recommended here to use an equivalent local head loss coefficient (column #24), which can be used to calculate the energy loss across appurtenances placed in series, but in close proximity to one another, within a link.

The data in column #24 pertains only to lateral pipe segments and hence need to be specified only in the odd-numbered rows of the input data table. Note that local losses that occur in non-offtake nodes such as span joints can also be specified in this column or in the column for pipe couplers. The sample projects that come with *LincSys* use this column to specify the local head losses associated with span joints.

4.3.3.h. Editing data in the cells of the input data table and browsing the input data table

User interface focus

When the *Input* tabpage opens, the data in the uppermost left-hand corner cell of the input data table is highlighted (Figure 10). However, the input data table is inactive. To activate the input data table and start editing tabular input data, a cell in the input data table should get the user interface focus. To do so simply move the mouse pointer to a cell in the input data table and press the left mouse key. This results in the cell with the focus being highlighted.

The cursor position can also be shifted from a cell to another using the keyboard. It can be moved from a cell to another immediately to the right of it, by pressing the Tab or the

Rightwards arrow key in the keyboard. Alternatively, pressing the Shift+Tab or Leftwards arrow key moves the cursor from an input data table cell to another that is immediately to the left of it. Upwards and Downwards arrow keys can be used to move the cursor up and down a row, respectively, within the same column.

The PgUp and PgDown keys can be used to move the cursor up and down one input data table page within the same column, respectively. The Home and End keys can be used to move the cursor to the first and last columns, respectively, of the input data table within the same row. Pressing the Ctrl+Home keys moves the cursor from any cell in the input data table to the upper left-hand corner cell of the input data table. Alternatively, pressing the Ctrl+End keys moves the cursor from any cell in the input data table to the lower right-hand corner cell of the table.

Data editing

To edit the data displayed in an input data table cell, first set the focus on the cell. There are two ways to start editing data in an input data table. One option is to simply start typing the new input data from the keyboard into a highlighted cell. Following the first key stroke, the data that was in the cell will be cleared and replaced by the character corresponding to the first key stroke, provided the key corresponds to a valid keyboard input. The user can then continue entering the new value.

Alternatively, data editing in the input data table cell can start with a double click on a cell, with the user interface focus, with the left mouth button. A blinking cursor will then appear on the cell with the current value still in display, signaling that the content of the cell can now be edited.

Data editing in an input data table cell with the focus can also start by simply tapping on the F2 key on the keyboard. In which case, a blinking cursor will appear to the right of the data in the active cell, indicating that the content of the cell can now be edited.

For input data table cells of columns #1 to 3 and 18, valid keyboard inputs are only the numerals (0 to 9), because the corresponding input parameters are integers. For input data table cells in columns #4 to 17 and columns #19 to 24, on the other hand, the corresponding parameters are real numbers and hence valid keyboard inputs consist of the numerals 0 to 9 and the decimal point.

Note that during data editing in an input data table cell, the Backspace, Delete, and the Leftward and Rightward arrow keys have the same function as in any other Windows application. One last note is that if the Esc key is pressed immediately, following the editing of an input data table cell, the content that has been edited out will be restored in the cell.

4.3.4. Navigation buttons, Input tabpage

The *Input* window has a pair of navigation buttons displayed right under the *Input* data table, namely: System-Projects and Simulation buttons (Figures 10 to 12).

***System-Projects* button**

Clicking on the System-Projects button with the mouse or pressing the Alt+P keys opens the Systems-Projects tabpage and program control will revert back to the systems configuration and project management window.

***Simulation* button**

Clicking on the Simulation button with the mouse or pressing the Alt+S key initiates a simulation run. Before initiating hydraulic computation, the model input data (possibly edited in the input window) would be validated. This include range test (checks whether all input data items are within permissible range) and consistency test (checks if edited data conform to known relationships between data items).

If the input data is deemed valid, *LincSys* would then update the input data file (InputData_LinLat.Inp) and creates a pair of text files in the current project folder: LatHydrProjectConfiguration.Dat and InputData_LinLat.Dat. These files contain the input data in a format that can be read by the simulation module, *HydrSimLaterals.exe*. LatHydrProjectConfiguration.Dat is a project configuration data file and contains input data on the current project configuration option and the current project name. InputData_LinLat.Dat file contains the same data as the InputData_LinLat.Inp file, only in a format that is simpler and compatible with the input data routines of *HydrSimLaterals.exe*.

Once the system configuration file and a version of the input data file readable by *HydrSimLaterals.exe* are created, *LincSys* would then invoke the simulation module, *HydrSimLaterals.exe*. The simulation module then extracts the input data from LatHydrProjectConfiguration.Dat and InputData_LinLat.Dat files, deletes both files, and proceeds with the simulation run. Thus, the LatHydrProjectConfiguration.Dat and InputData_LinLat.Dat files are generally not visible to the user, except when program exits with runtime error that precedes the deletion of these files.

At the end of a simulation run (whether complete or incomplete), *HydrSimLaterals.exe* creates a hydraulic simulation run time error status report file (HydrSimRunTimeErrStatusReport.Dat) in the current project folder. The simulation error status report file is a text file containing three rows of data. The first row would be an integer value ranging between 0 and 9. A value of zero indicates that the simulation was successfully completed, whereas a value from 1 to 9 indicates that a runtime error has occurred. Each integer numeral between 1 and 9 correspond to a specific type of known runtime error. The data items in the second and third rows provide the link and node numbers, respectively, where runtime error was encountered. *LincSys.exe* would then use these data to report to the user that the simulation has encountered a runtime error along with the type of error, the location along the lateral where the error occurred (link and node indexes), and suggestions on possible remedies.

Note that some combination of input data may cause the simulation to end with a runtime error that is as yet unknown. In such an event, the simulation session may end abruptly and no runtime error report might be displayed on the screen.

Subsequent to a successful simulation, *HydrSimLaterals.exe* creates six output files in the current project folder, in addition to the hydraulic simulation runtime error status report file (HydrSimRunTimeErrStatusReport.Dat). As noted earlier, following a successful simulation the data item in the first row of the runtime error status report file would be set to 0. The data items in the second and third rows of the error status report file are, evidently, impertinent in the event of a successful simulation and hence they are arbitrarily set to 0. *LincSys* would then read the content of the HydrSimRunTimeErrStatusReport.Dat file and deletes the file. It then extracts the output data from the main output file (OutputData_LinLat.Out) and displays it in the Output tabpage. Note that discussion on the OutputData_LinLat.Out file and other output data files is provided in Sections 5.1.1.c to 5.1.1.e.

4.4. The *Output* tabpage

4.4.1. Features and layout of the Output tabpage

Following a successful simulation, the Output tabpage displays the computed outputs in non-editable output boxes and output data table. As noted earlier in Section 4.2.3.c, the output tabpage can also be accessed from the Systems-Projects tabpage, if the currently selected project represents a complete project. A complete project is one in which the project folder contains all project files, including the input and all output data files, except the EmitterDischargePressure.Dat and Lat_hElvHglEgl_Exp.Dat files (Section 5.1.1.c).

The features and layout of the Output tabpage are depicted in Figure 14 for a system with Droptube-Prv-Emitter configuration option and in Figure 15 for a system with Droptube-Emitter configuration option. Note that the general content of the Output tabpage of a system with Emitter-On-Lateral system configuration option would be the same as that shown in Figure 14 for a system with a Droptube-Emitter configuration.

The Output tabpage features a titlebar, a statusbar, user interface controls including output boxes and an output data table (for displaying output data), navigation buttons, and tabcontrols. The titlebar of the Output page features exactly the same content as those of the Systems-Projects and Input tabpages (Figures 4 and 10 to 12). In the statusbar of the Output tabpage, however, the name of the current tabpage is Output (Figures 14 and 15).

In the Output window, the tabcontrols are depicted with the Output tabcontrol highlighted. The Systems-Projects tabpage can be accessed from the Output window by tapping on the Systems-Projects tabcontrol with the (left) mouse button. The Input and Charts tabcontrols on the other hand, can be used to open the respective tabpages only if they have been activated through navigation buttons earlier during the simulation event, either from within the output tabpage or from the Systems-Projects tabpage.

The output data of *LincSys* consists of tabular and non-tabular data sets (Figures 14 and 15). The non-tabular output data is presented in three groupboxes each with a set of output boxes. The tabular data is displayed in the output data table. Note that to distinguish between the Input and Output windows more readily, different background colors are used for the input and output boxes, on one hand, and the input and output data tables, on the other.

The Output window features three navigation buttons: Systems-Projects, Input, and Charts. The functions of each of these buttons will be discussed in Section 4.4.5.

4.4.2. Displaying non-tabular output data

As can be noted from Figures 14 and 15, the Output tabpage uses output boxes to display non-tabular output data. An output box is a Windows Forms user interface control element commonly referred to as a label control (Table 1). Thus, the contents of the output boxes are non-editable.

The output tabpage displays three sets of non-tabular output data each in a separate groupbox: *(i)* emitter discharge and head differential variability indicator parameters, *(ii)* emitter discharge and head differential uniformity indicator parameters, and *(iii)* additional output parameters (Figures 14 and 15).

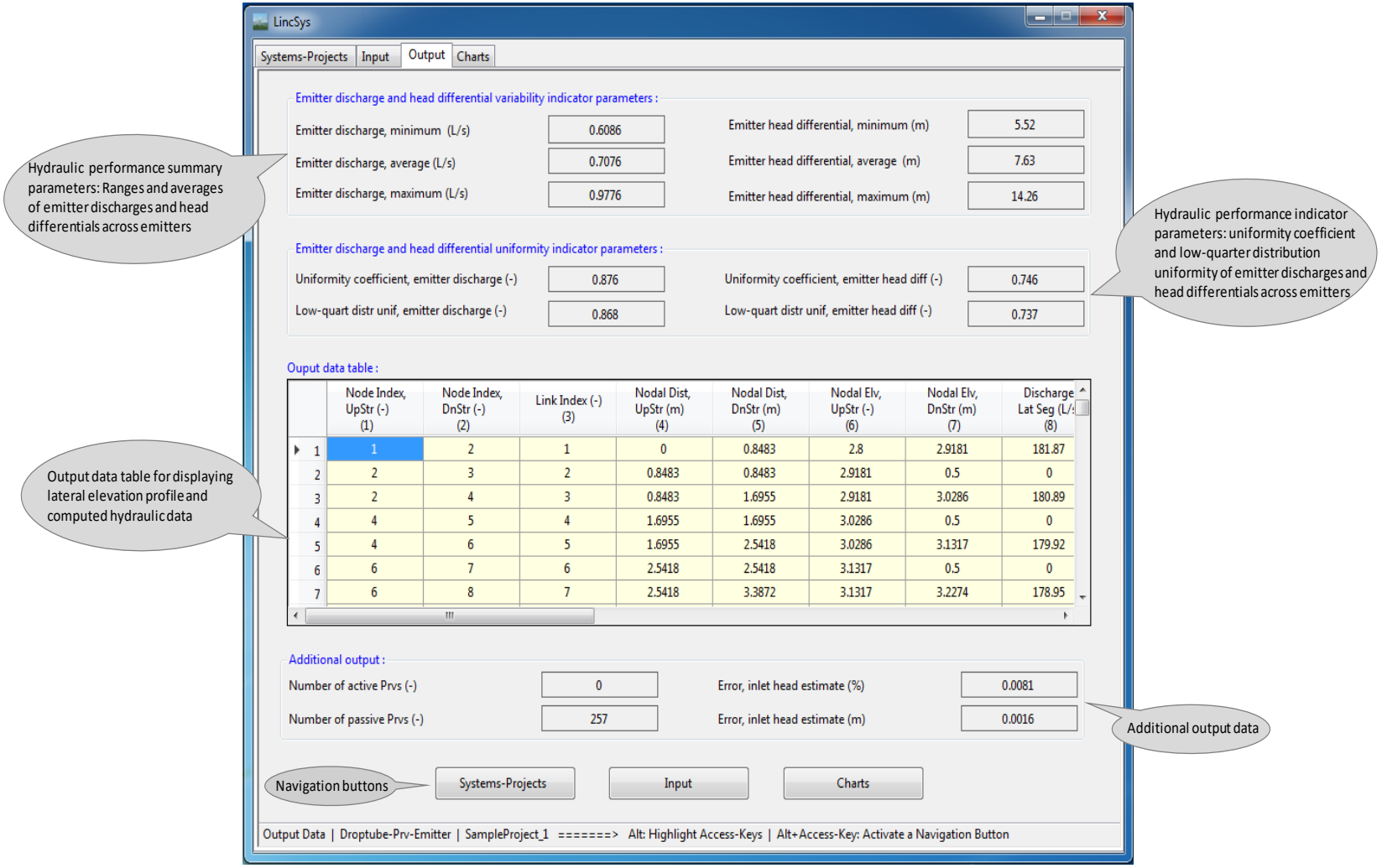

Figure 14. The Output tabpage for the Droptube-Prv-Emitter system configuration option

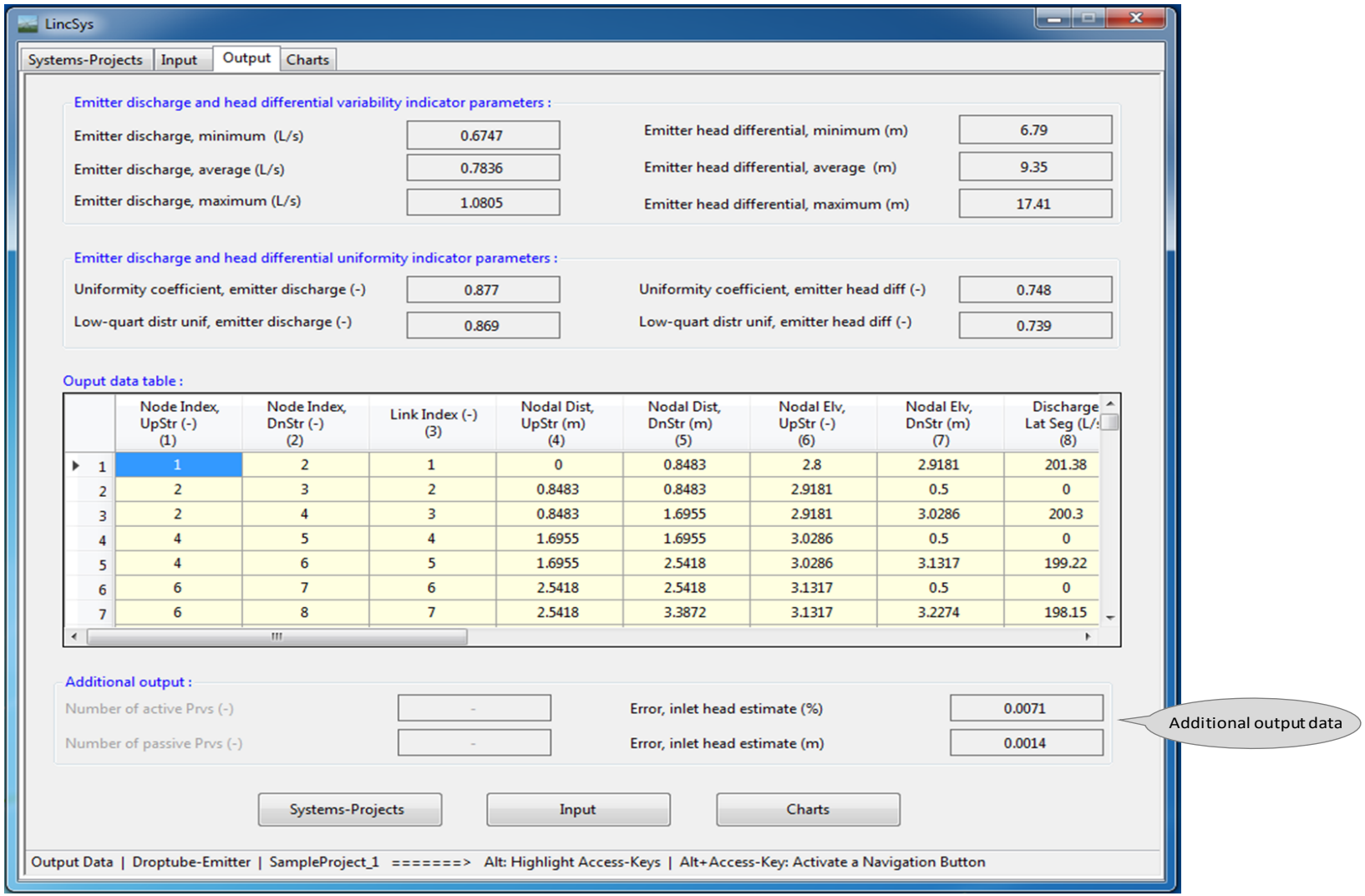

Figure 15. The Output tabpage for a system with Droptube-Emitter configuration option (Note: the general content of the Output tabpage of a system with the Emitter-On-Lateral configuration option is the same as that for a system with Droptube-Emitter configuration)

The emitter discharge and head differential variability indicator parameters groupbox is comprised of six output boxes arranged in two columns. The output boxes display the ranges of variation of the computed emitter discharges and emitter head differentials along with corresponding averages.

The emitter discharge and head differential uniformity indicator parameters groupbox has four output boxes also displayed in a pair of columns. These group of output boxes depict the computed uniformity coefficient and low-quarter distribution uniformity of emitter discharges and emitter head differentials.

In the additional output groupbox as well, output data are shown in two columns (Figures 14 and 15). In the left-hand column, there is a pair of output boxes displaying the number of active and passive *prvs* in the lateral and, on the right-hand side, another pair of output boxes display the error in the computed total head at the lateral inlet in relative and absolute terms. Note that the output data on the number of active and passive *prvs* are impertinent to systems with the Droptube-Emitter or Emitter-On-Lateral configuration option, thus the respective output boxes are deactivated for these options (Figure 15).

4.4.3. Output data table for displaying computed hydraulic parameters and some input data

4.4.3.a Introduction

Figures 14 and 15 depict a partial view of the output data table of *LincSys*. The output data table is actually what is technically known as a DataGridView table (Table 1). It displays computed hydraulic data along with system topological, geometric, and elevation data in a tabular format. Note that the contents of the output data table is non-editable. Furthermore, unlike the non-tabular output data, the format of the tabular output data table does not vary with the system configuration.

The columns in an output data table represent data type. It could be network topological parameters such as link and node indexes, nodal distance from the lateral inlet, elevation profile data or computed hydraulic parameter such as discharge, pressure, hydraulic head, and total head. The row of the output data table, on the other hand, represents data related to a network link and corresponding nodes, which include topological data, nodal distances from the lateral inlet, nodal elevations, and computed hydraulic data relating to the link or the delimiting nodes.

The output data table has 20 columns. The number of rows in an output data table, however, is equal to the number of hydraulic links in the topological representation of the corresponding lateral as a branched hydraulic network. Hence, it can vary from one lateral to another. As noted in Section 4.3.3, *LincSys* has the capability to simulate laterals with up to 2000 links and 2001 nodes, which corresponds to 2000 rows in the output data table.

The top row of the output data table contains column headings that describe the contents of the columns (Figures 14 and 15). Because of space limitations most column headings are abbreviations. However, tooltips can be used to obtain a more complete description of the column headings. A column heading tooltip can be activated by letting the cursor hover over the heading of a column whose content is to be queried.

The rows and columns of the output data table are numbered sequentially starting from the top row and the left most data column, respectively, to help the user browse through the table to a particular cell quickly. Note that in subsequent discussion, row and column indexes refer to

the data rows and columns of the output data table (i.e., they do not include the column header row and the row header column).

At any one time the output data table can only display a small subset of the tabular output data (consisting of 7 rows by 8 columns). However, the table has horizontal and vertical scroll bars that can be used to browse through the rest of the data table. In addition, keys from the keyboard can be used to browse the output data table (Section 4.4.4*)*.

For convenience, subsequent discussion on the output data table will be based on Tables 5a and 5b, which presents a sufficiently detailed sample output data table. Because of space limitations the table is divided into two halves. Table 5a depicts a sample of the first 10 columns of the output data table and Table 5b depicts a sample of the second half of the output data table. Note that the first column in Table 5b is not part of the output data table (Figures 14 and 15) , it is added here to help the user relate the rows in the second half of the table (Table 5b) with those of the first (Table 5a) more readily. A complete description of the column headings of Tables 5a and 5b are provided in Table 6.

4.4.3.b. Topological data of the hydraulic network, distance from lateral inlet, and elevation profile data (columns #1 to 7)

The computed hydraulic data are either nodal or link properties and can only be described in relation to the network nodes and links and nodal distances. Thus, the first five columns of the output data table consist of the network topological data and the nodal distance from the lateral inlet (Table 5a).

Nodal elevations are shown in columns #6 and 7 of Table 5a. Note that the contents of these columns are exactly the same as the corresponding columns of the input data table (Table 3a).

4.4.3.c. Discharge in the lateral pipe segment (column #8)

The data in this column represent the discharge in each of the lateral pipe segments. Note that the output data in this column alternate between positive values in the odd-numbered rows and zero in the even-numbered rows. The values in the even-numbered rows are set to zero, indicating that this data item is impertinent to the links that represent the outlet discharge metering apparatuses.

4.4.3.d. Emitter discharge and head differential across emitter (columns #9 and 10)

The emitter discharges and the head differential across emitters are displayed in columns #9 and 10 of the output data table (Table 5a), respectively.

Note that emitter discharges (column #9) and head differentials across emitters (column #10) are shown only in rows that correspond to links that represent outlet discharge metering apparatuses. Thus, even-numbered rows representing virtual links (links with zero discharges) attached to non-offtake nodes and all the odd-numbered rows are set to zero (Table 5a).

4.4.3.e. Pressure at the upstream- and downstream-ends of a lateral pipe segment (columns #10 and 11)

Within the framework of one-dimensional steady-state pipe flow modeling, the pressure head profile along a lateral is not a continuous function of distance at the network nodes where

Table 5a. Sample output data table of *LincSys* for a project with 937 nodes and 936 hydraulic links (between columns 1 to 10)

Row index	Node Index UpStr (-) (1)	Node Index DnStr (-) (2)	Link Index (-) (3)	Nodal Dist, UpStr (m) (4)	Nodal Dist, DnStr (m) (5)	Nodal Elv, UpStr (m) (6)	Nodal Elv, DnStr (m) (7)	Discharge, Lat Seg (L/s) (8)	Discharge, Emitr (L/s) (9)	Head Diff, Emitr (m) (10)
1	1	2	1	0	0.6026	6.5233	6.5874	52.539	0	0
2	2	3	2	0.6026	0.6026	6.5874	3.5819	0	0.1140	7.008
3	2	4	3	0.6026	2.5102	6.5874	6.7832	52.425	0	0
4	4	5	4	2.5102	2.5102	6.7832	3.6104	0	0.1140	7.008
5	4	6	5	2.5102	3.012	6.7832	6.8329	52.311	0	0
6	6	7	6	3.012	3.012	6.8329	3.6179	0	0.1140	7.008
7	6	8	7	3.012	4.1158	6.8329	6.9397	52.197	0	0
8	8	9	8	4.1158	4.1158	6.9397	3.6344	0	0.1140	7.008
9	8	10	9	4.1158	4.6877	6.9397	6.9937	52.0 83	0	0
.	.	.	.	.	.	.	.	.	.	.
.	.	.	.	.	.	.	.	.	.	.
.	.	.	.	.	.	.	.	.	.	.
55	54	56	55	26.5277	27.928	8.3356	8.3738	49.462	0	0
56	56	57	56	27.928	27.928	8.3738	3.9911	0	0.1140	7.008
.	.	.	.	.	.	.	.	.	.	.
.	.	.	.	.	.	.	.	.	.	.
.	.	.	.	.	.	.	.	.	.	.
.	.	.	.	.	.	.	.	.	.	.
500	500	501	500	0	249.0128	3.9521	0.796	0	0.1140	7.008
.	.	.	.	.	.	.	.	.	.	.
.	.	.	.	.	.	.	.	.	.	.
.	.	.	.	.	.	.	.	.	.	.
933	932	934	933	465.7337	466.338	6.0421	6.1137	0.228	0	0
934	934	935	934	466.338	466.338	6.1137	2.6319	0	0.1140	7.008
935	934	936	935	466.338	468.255	6.1137	6.3687	0.114	0	0
936	936	937	936	468.255	468.255	6.3687	2.6319	0	0.1140	7.008

Table 5b. Sample output data table of *LincSys* for a project with 937 nodes and 936 hydraulic links (between columns 11 to 20)

Row index	Pressure, DnStr (m) (11)	Pressure, UpStr (m) (12)	Velocity Head (m/s) (13)	FHL, Lat Seg (m) (14)	LHL, Lat Seg (m) (15)	Hydr Head, DnStr (m) (16)	Hydr Head, UpStr (m) (17)	Total Head, DnStr (m) (18)	Total Head, UpStr (m) (19)	Prv Opr, Mode (-) (20)
1	22.144	22.063	0.330	0.017	0	28.667	28.650	28.998	28.980	0
2	0	0	0	0	0	0	0	0	0	2
3	22.031	21.781	0.329	0.054	0.033	28.619	28.564	28.947	28.893	0
4	0	0	0	0	0	0	0	0	0	2
5	21.750	21.686	0.327	0.014	0.033	28.533	28.519	28.860	28.846	0
6	0	0	0	0	0	0	0	0	0	2
7	21.655	21.517	0.326	0.031	0.033	28.487	28.456	28.813	28.782	0
8	0	0	0	0	0	0	0	0	0	2
9	21.485	21.415	0.324	0.016	0.033	28.425	28.409	28.750	28.733	0
.	.	.	.	.	.	.	.	.	.	.
.	.	.	.	.	.	.	.	.	.	.
.	.	.	.	.	.	.	.	.	.	.
55	18.808	18.734	0.293	0.036	0.029	27.144	27.108	27.436	27.400	0
56	0	0	0	0	0	0	0	0	0	2
.	.	.	.	.	.	.	.	.	.	.
.	.	.	.	.	.	.	.	.	.	.
.	.	.	.	.	.	.	.	.	.	.
.	.	.	.	.	.	.	.	.	.	.
500	0	0	0	0	0	0	0	0	0	0
.	.	.	.	.	.	.	.	.	.	.
.	.	.	.	.	.	.	.	.	.	.
.	.	.	.	.	.	.	.	.	.	.
933	12.888	12.816	4×10^{-5}	6×10^{-6}	9×10^{-6}	18.930058	18.930042	18.930098	18.930083	0
934	0	0	0	0	0	0	0	0	0	2
935	12.816	12.561	1×10^{-5}	9×10^{-6}	4×10^{-6}	18.93007	18.93006	18.93008	18.93007	0
936	0	0	0	0	0	0	0	0	0	2

Table 6. Complete description of column headings of Tables 5a and 5b and corresponding units

Column index	Column headings in Tables 5a and 5b	Complete description of column headings	Unit
1	Node Index, UpStr	Index of the upstream-end node of a link	-
2	Node Index, DnStr	Index of the downstream-end node of a link	-
3	Link Index	Index of a hydraulic link	-
4	Node Dist, UpStr	Distance from the lateral inlet of the upstream-end node of a link	*m*
5	Node Dist, DnStr	Distance from the lateral inlet of the downstream-end node of a link	*m*
6	Node Elv, UpStr	Elevation of the upstream-end node of a link	*m*
7	Node Elv, DnStr	Elevation of the downstream-end node of a link	*m*
8	Discharge, Let Seg	Discharge in lateral pipe segment	*m*
9	Discharge Emitr	Emitter discharge	*L/s*
10	Head Diff, Emitr	Head differential across emitter	*m*
11	Pressure, UpStr	Pressure at a point immediately downstream of the node that delimits the upstream-end of a link	*m*
12	Pressure, DnStr	Pressure at a point immediately upstream of the node that delimits the downstream-end of a link	*m*
13	Velocity Head	Velocity head in a lateral pipe segment	*m*
14	FHL, Lat Seg	Friction head loss in a lateral pipe segment	*m*
15	LHL, Lat Seg	The local head losses in a lateral pipe segment	*m*
16	Hydr Head, UpStr	Hydraulic head at a point immediately downstream of the node that delimits the upstream-end of a link	*m*
17	Hydr Head, DnStr	Hydraulic head at a point immediately upstream of the node that delimits the downstream-end of a link	*m*
18	Total Head, UpStr	Total head at a point immediately downstream of the node that delimits the upstream-end of a link	*m*
19	Total Head, DnStr	Total head at a point immediately upstream of the node that delimits the downstream-end of a link	*m*
20	Prv Opr Mode	*prv* operating mode	-

local head losses occur (Zerihun and Sanchez, 2019c). However, the pressure at a point immediately upstream and at another point just downstream of a node can be computed. The pressure head profile computed as such, by *LincSys*, is presented in columns #11 and 12 of the output data table (Table 5b).

Considering a link corresponding to a lateral pipe segment, the data in column #11 represents the pressure at a point immediately downstream of the node that delimits the upstream-end of the link (labeled as Pressure, UpStr in Table 5b). Conversely, the data in column #12 represents the pressure at a point immediately upstream of the node that delimits the downstream-end of the link (labeled as Pressure, DnStr in Table 5b). Thus, the data shown in columns #11 and 12 represent the pressure at the upstream- and downstream-ends, respectively, of each lateral pipe segment and are labeled as such in Table 5b.

Note that the continuity property of the lateral pressure head profile noted here applies to the lateral hydraulic head profile (hydraulic grade-line) and the total head profile (the energy grade-line). Thus, each of these hydraulic parameters will also be displayed in the output data table in two columns (see Sections 4.4.3.h and 4.4.3.i).

Both the upstream and downstream lateral pressure head data are shown in the odd-numbered rows, where data related to the links that correspond to the lateral pipe segments are displayed. The even-numbered rows, on the other hand, are set to zero (Tables 5a and 5b), indicating that the data in these columns do not relate to the links corresponding to the lateral outlet metering apparatuses.

4.4.3.f. Velocity head and friction head losses, lateral pipe segments (columns #13 and 14)

The computed velocity head and friction head loss data corresponding to each lateral pipe segment are shown in columns #13 and 14 of the output data table (Table 5b). Velocity heads and friction head losses are displayed in the odd-numbered rows of the output data table. The even-numbered rows of these columns, on the other hand, are set to zero, indicating that the data in these columns do not relate to the links representing lateral outlet metering apparatuses.

4.4.3.g. Local head loss, lateral pipe segment (column #15)

Computed local head losses that occur in lateral pipe segments are displayed in column #15 of the output data table (Table 5b). Although local head losses occur at a point or points along a lateral pipe segment, the data in column #15 represents the cumulative local head loss that may occur over a lateral pipe segment, not the losses attributable to individual appurtenances. In other words, these values are the sum of the losses that occur at a node delimiting a link and all other forms of local losses, if any, that occur within the link.

Accordingly, the data in column #15 are shown only in the odd-numbered rows of the output data table. The even-numbered rows are set zero, indicating that data in column #15 are impertinent to links corresponding to outlet discharge metering apparatuses.

4.4.3.h. Hydraulic head at the upstream- and downstream-ends of a lateral pipe segment (columns #16 and 17)

The computed hydraulic head at the upstream- and downstream-ends of each lateral pipe segment are shown in columns #16 and 17 (Table 5b). As noted earlier in Section 4.4.3.e, the hydraulic head profile (i.e., the hydraulic grade-line) is not a continuous function of distance at junction nodes where local head losses occur. Thus, *LincSys* computes hydraulic heads not at these nodes, but at points immediately upstream and downstream of each node. Accordingly, the

data in columns #16 and 17 are labeled as hydraulic heads at the upstream- and downstream-ends, respectively, of lateral pipe segments (Table 5b).

It then follows, considering a link corresponding to a lateral pipe segment, it can be observed that the data in the odd-numbered rows of column #16 represent the hydraulic head at a point immediately downstream of the node that delimits the upstream-end of the link. Conversely, the data in column #17 represent the hydraulic head at a point immediately upstream of the node that delimits the downstream-end of the link.

Note that the hydraulic head data in the even-numbered rows of columns #16 and 17 are set to zero, indicating that the data in these columns relate only to the lateral pipe segments.

4.4.3.i. Total head at the upstream- and downstream-ends of a lateral pipe segment (columns #18 and 19)

The computed total head at the upstream-end and downstream-end of each lateral pipe segment are shown in columns #18 and 19 (Table 5b). The total head profile (i.e., the energy grade-line) is not a continuous function of distance at junction nodes where local head losses occur (Section 4.4.3.e). Thus, *LincSys* computes the total head not at the nodes, but at points immediately upstream and downstream of each node. Accordingly, the data in columns #18 and 19 are labeled as the total heads at the upstream- and downstream-ends, respectively, of lateral pipe segments (Table 5b).

It then follows, considering a link corresponding to a lateral pipe segment, it can be observed that the data in the odd-numbered rows of column #18 represent the total head at a point immediately downstream of the node that delimits the upstream-end of the link. Conversely, the data in column #19 represent the total head at a point immediately upstream of the node that delimits the downstream-end of the link.

Note that the total head data in the even-numbered rows of columns #18 and 19 are set to zero, indicating that the data in these columns relate only to the lateral pipe segments.

4.4.3.j. The operating status of prvs (columns #20)

The data describing the operating status of the pressure reducing valves, *prvs*, are shown in column #20 of the output data table (Table 5b). The output data displayed in this column can be one of three integer numbers: 0, 1, or 2. A value of 0, in this column, indicates that the link has no *prv* attached to it. A value of 1 signifies that the link has a *prv* attached to it and the *prv* is operating in the passive mode. On the other hand, a value of 2 indicates that the link has a *prv* and is operating in the active mode.

If the current system configuration option is Droptube-Emitter or Emitter-On-Lateral, then the entire column #20 is set to zero. If, on the other hand, the Droptube-Prv-Emitter system configuration is considered, then the even-numbered rows corresponding to virtual links and all the odd-numbered rows would be set to zero. The even-numbered rows corresponding to links that represent discharge metering apparatuses, on the other hand, would display a value of 1 or 2 depending on the mode of operation of the *prv*.

Note that if one or more of the *prvs*, along the lateral, are fully throttled then the simulation is considered unsuccessful and a runtime error message will be printed on the screen with a suggestion on how to remedy the source of the error.

4.4.4. Browsing the output data table

When the Output tabpage opens, the uppermost left-hand corner cell of the output data table is highlighted (Figure 15). However, the output data table is non-editable, thus the cursor function is only navigational. The cursor can be moved from an output data table cell to another through mouse clicks. Alternatively, the keyboard can be used to shift user interface focus from one cell to another.

The cursor can be moved from a cell to one that is immediately to the right of it by pressing the Tab or the Rightwards arrow keys in the keyboard. Alternatively, pressing the Shift+Tab or Leftwards arrow keys moves the cursor from an output data table cell to another that is immediately to the left of it. Upwards and Downwards arrow keys can be used to move the cursor up and down through the table a row at a time.

The PgUp and PgDown keys can be used to move the cursor up and down, respectively, one output data table page within the same column. The Home and End keys can be used to move the cursor to the first and last columns, respectively, of the output data table within the same data row. Pressing the Ctrl+Home keys moves the cursor from any cell in the output data table to the upper left-hand corner cell of the output data table. Alternatively, pressing the Ctrl+End keys moves the cursor from any cell in the output data table to the lower right-hand corner cell of the table.

4.4.5. Navigation buttons, Output tabpage

Three navigation buttons are displayed in the lower half of the Output tabpage, namely: Systems-Projects, Input, and Charts buttons, which can be activated with the mouse click or using access keys from the keyboard.

Clicking on the Systems-Projects button with the mouse or pressing the Alt+P keys from the keyboard shifts the focus from the Output tabpage to the Systems-Projects window.

The Input tabpage can be opened from the Outptut window by tapping on the Input button with a mouse or by pressing Alt+I keys from the keyboard.

Clicking on the Charts button with a mouse or pressing Alt+C keys from the keyboard shifts the focus from the Output tabpage to the Charts tabpage, where computed output parameters are displayed in graphical form.

4.5. The Charts tabpage

4.5.1. Features and related functionalities and layout of the Charts tabpage

The Charts tabpage can be accessed from the Systems-Projects window if the currently selected project represents a complete project. As noted earlier in Section 4.2.3.c, a complete project is one in which the project folder contains all project files, including the input and all output data files, except the EmitterDischargePressure.Dat and Lat_hElvHglEgl_Exp.Dat files (Section 5.1.1.c). Often, however, the Charts tabpage is accessed through the Charts button in the Output window.

The Charts tabpage is designed to display a graphical rendering of a total of 11 computed hydraulic parameters each in a separate charts panel sequentially. Figure 16, depicts the features, layout, and content of the Charts window when it is first opened either form the Systems-Projects or the Output window.

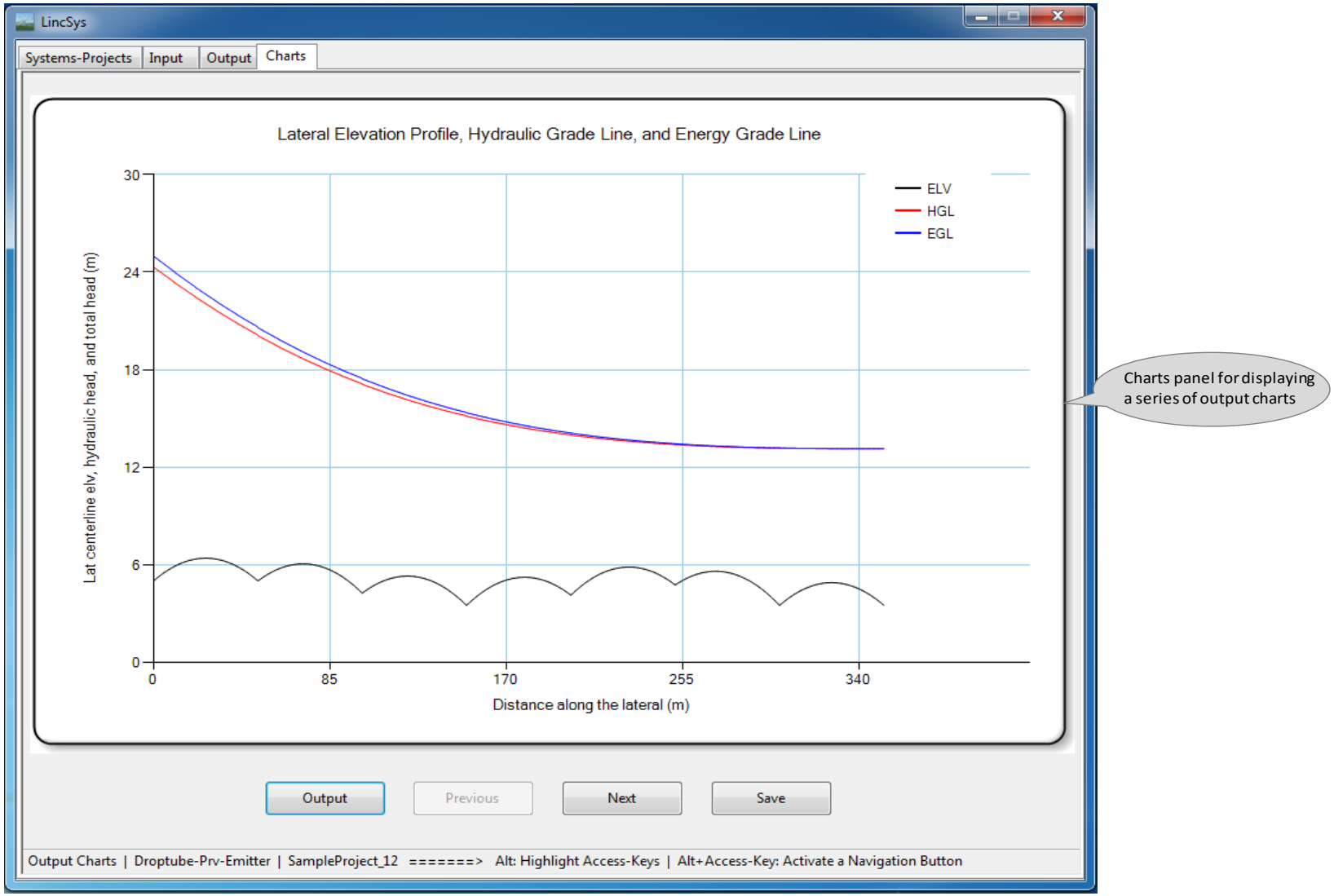

Figure 16. The Charts tabpage showing a graph of the elevation profile of the centerline of the lateral and the computed lateral hydraulic and energy grade-lines

At the top of the window is the titlebar and at the bottom the statusbar. The titlebar of the Charts window is exactly the same as those of the Systems-Projects, Input, and Output pages. In the statusbar of the Charts tabpage, however, the name of the current tabpage is Charts (Figure 16).

Right under the titlebar of the Charts window, the tabcontrols are displayed with the Charts tabcontrol highlighted. The Systems-Projects tabpage can be accessed from the Charts window by tapping on the Systems-Projects tabcontrol with the (left) mouse button. The Input and Output tabcontrols, on the other hand, can be used to open the respective tabpages only if they were activated through navigation buttons earlier during the simulation event (Sections 4.3.1 and 4.4.1). However, unless the Charts tabpage was accessed directly from the Systems-Projects window, the fact that the charts window is open implies that either the Output or both the Output and the Input windows may have already been activated in the current simulation event. Hence, either one or both tabpages can be opened from the Charts window by tapping on their respective tabcontrols.

Directly under the tabcontrols, the Charts window features a rectangular chart panel that displays graphical outputs. When the Charts window is first opened the charts panel displays the graph of the elevation profile of the lateral centerline and the computed hydraulic and energy grade-lines (Figure 16). Other chart panels can be brought into display using the navigation buttons depicted in Figure 16 below the charts panel. Before proceeding to the discussion on the navigation buttons, however, some general chart attributes common to all charts will be discussed next.

A chart's panel has a white background color. The axes are black and the grid lines are set to light green color. A chart consists of at least one curve and at most three curves. Charts with three curves use different colors to draw each curve and the colors used are: red, blue, and black. If a chart contains only one curve, then it is drawn with a blue color. Chart titles, axes titles, and legends are in black color.

The Charts window contains three navigation buttons (Output, Previous, and Next) and a Save button. If the Output button is activated, the user interface focus shifts to the Output tabpage. The Previous and Next buttons allow the user to shift program focus from a chart's panel to the next.

In order to understand the function of the Previous and Next buttons, it is convenient to conceptualize each of the charts as images placed in different pages of a charts album. Now, in any given page, the Previous button allows you to flip a page to the left of the current page and hence bring into view the chart in the page to the left of the current page. By contrast, The Next button allows you to flip a page to the right of the current page and bring into view the chart on the page to the right of the current page.

In the left-most chart panel (which displays the lateral elevation profile and the hydraulic- and energy grade-lines), the Previous button is deactivated, because there is no chart page (panel) to the left of this page. Conversely, when the right-most chart panel (which displays the velocity head profile chart) is reached, the Next button would be deactivated as there is no chart page to the right of that page. In between the left-most and right-most pages, however, both the Previous and Next buttons are active and can be used to browse through the different chart pages.

The Save button can be used to save the chart that is in display in the Charts subfolder under the current project folder. The saved chart can then be opened in any image processing application and incorporated into a report.

4.5.2. Description of the contents of the Charts output

4.5.2.a. Chart depicting elevation profile of the centerline of the lateral and the hydraulic and energy grade-lines

Figure 16 depicts a graph of the lateral elevation profile and computed hydraulic and energy grade-lines. Both the horizontal axis, which represent distance from lateral inlet and vertical axis which shows the lateral elevation, hydraulic head, and total head are in meter. The chart title is shown at the top and the chart legend is shown at the upper right-hand corner of the chart panel.

The lower most curve, shown in black color, is the elevation profile of the lateral. A look at the elevation profile of the lateral shows that the lateral is comprised of seven spans installed in a field with variable slope (along the length of run of the lateral).

The upper most curve, displayed in blue color, is the energy grade-line (or the total head profile) of the lateral. Whereas the middle curve, depicted in red color, is the hydraulic grade-line (or the hydraulic head profile) of the lateral. For this particular problem both of these curves are monotonic decreasing functions of distance from the lateral inlet. Evidently, the energy-grade line should be a decreasing function of distance, unless the lateral has a booster pump, a scenario not considered here. On the other hand, the hydraulic grade-line can have a different monotonic property with respect to distance along the lateral depending on the lateral diameter.

Evidently, the difference between the total head at the inlet and that at any point along the lateral reflects the energy loss (friction and local head losses) that occurred between the inlet and that point. The difference between the energy grade-line and the hydraulic grade-line at any given point along the lateral is the velocity head. Finally, the difference between the hydraulic grade-line and the elevation profile is the pressure head.

The *Save* button can be used to save the current chart. On the other hand, activating the *Next* button would close the current chart panel and open the lateral pressure chart panel (Figure l7).

4.5.2.b. Lateral pressure head profile chart

A sample of the lateral pressure profile is shown in Figure 17. The pressure head profiles of linear-move and center-pivot laterals exhibit a distinctly wavy pattern, which contrasts with the generally smooth pressure profiles of solid-set and set-move irrigation systems lateral. As a result, two different forms of spatial variability attributes, consisting of local span-scale variability patterns (solid-line) and a broader inter-span/lateral-wide trends (dash-dotted line) can be discerned in the pressure head profiles of these laterals (Zerihun et al., 2019 and Zerihun and Sanchez, 2019c). As can be noted from Figure 17, the local span-scale (in-span) pressure head profile variability patterns exhibit some general attributes that are repeated, although with some variation, along the lateral. The pressure differentials across individual spans, when considered over two or more consecutive spans, yields a trend in pressure variability over multiple spans. Such a pressure variability attribute is referred here as the inter-span lateral pressure variability trend.

The in-span pressure variability patterns and the inter-span trends are mainly functions of the geometry of the lateral, the slope of the field in which the lateral is installed, and lateral diameter. More detailed discussion on lateral pressure profile variability attributes will be provided in Chapter 6. Note that, in Figure 17, the curve shown in solid-line (i.e., the actual lateral pressure profile) is computed with *LincSys*, but the curve representing the inter-span trend is added to the chart manually.

The user can save the pressure head chart by activating the *Save* button and/or return to the elevation profile and the hydraulic and energy grade-lines chart by clicking on the *Previous* button. Alternatively, activating the *Next* button will close the lateral pressure head profile chart panel and brings into display the head differential across emitter, *prv*-inlet pressure, and *prv*-set pressure profiles chart.

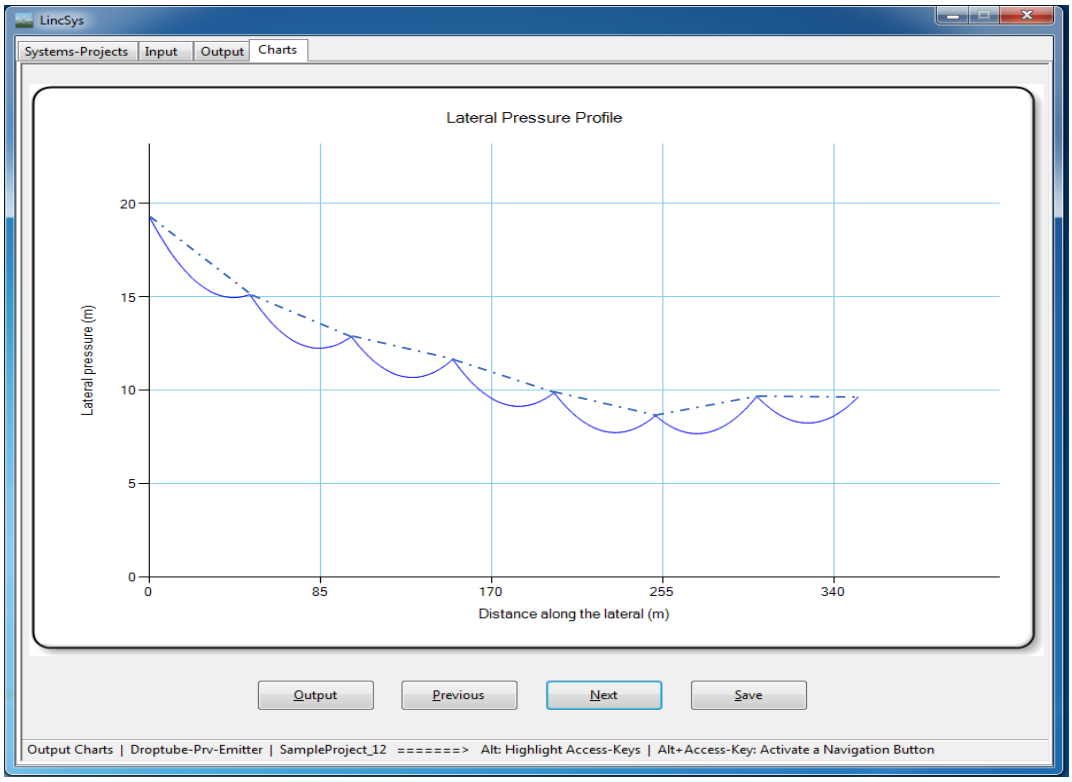

Figure 17. Sample lateral pressure head profile

4.5.2.c. Chart depicting the head differential across emitter, prv-inlet pressure, and prv-set pressure profiles

Figure 18 depicts a sample chart of the head differential across emitter, *prv*-inlet pressure, and *prv*-set pressure profiles along the lateral. The upper most curve (shown in blue color) is the *prv*-inlet pressure, the lower most curve (depicted in black color) is the emitter head differential, and the horizontal curve (displayed in red color) is the *prv*-set pressure. Note that this sample chart is for a system with Droptube-Prv-Emitter configuration option. If, on the other hand, the system configuration option is Droptube-Emitter or Emitter-On-Lateral, then this chart panel will display only the head differential across emitter.

Note that over the upper 173.0m section of the lateral, the *prv*-set pressure and the emitter head differential curves overlap (i.e., the *prv*-set pressure is equal to the emitter inlet pressure over this segment of the lateral). This implies that the *prvs* over this section of the lateral were operating in the active mode. In other words, over the upper 173.0m section of the lateral the *prv*-inlet pressure at least equals to the minimum recommended for the *prv* to operate reliably in the active mode (13.5m) and is less than the maximum allowable (74.0m). Note that the minimum recommended *prv*-inlet pressure is equal to the sum of the *prv*-set pressure and the minimum required margin between the *prv*-set and *prv*-inlet pressures for the *prv* to operate reliably in the active mode. On the other hand, the maximum allowable *prv*-inlet pressure or its range is specified in the manufacture's catalogue.

By comparison, the emitter head differential over the lower 179.0m reach of the lateral fell below the *prv*-set pressure, indicating that *prvs* over this segment of the lateral were operating in the passive mode. Note that the spatial variation in the head differential across emitters over the lower section of the lateral reflects the variation in the field slope.

The current chart can be saved by pressing the *Save* button, if necessary. Alternatively, pressing the *Next* button closes the current chart panel and displays the chart emitter discharge profile.

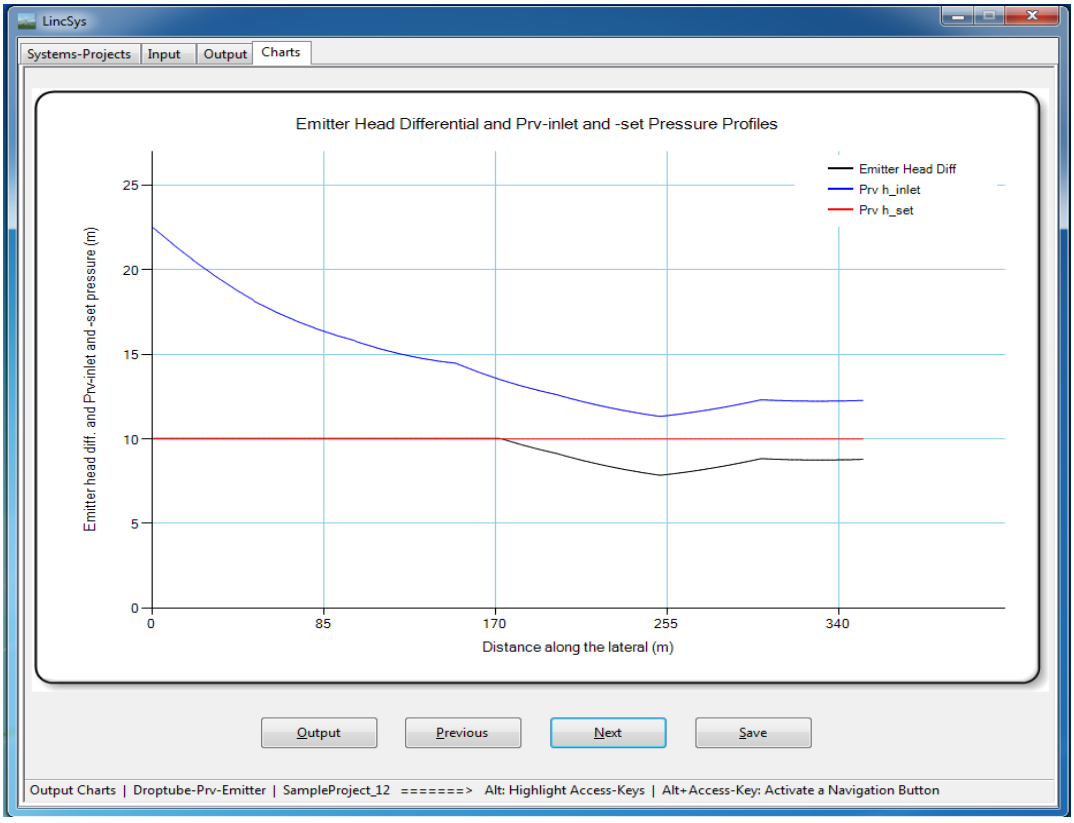

Figure 18. Sample chart of head differential across emitters, *prv*-inlet pressure, and *prv*-set pressure for a Droptube-Prv-Emitter system configuration option

4.5.2.d. Emitter discharge profile chart

Figure 19 displays a sample emitter discharge profile along a lateral. Emitter discharge is in gallons per minute and distance along the lateral is in meter. Note that the emitter discharge is constant over the upper 173.0m section of the lateral, where the *prvs* are operating in the active mode (Section 4.5.2.c). In the lower 179.0m, however, emitter discharges were smaller than those observed in the upstream section and follow the same pattern as the corresponding emitter head differential.

While the *Save* button can be used to save the current chart, activating the *Next* button will close the current chart panel and displays the chart for the lateral discharge profile.

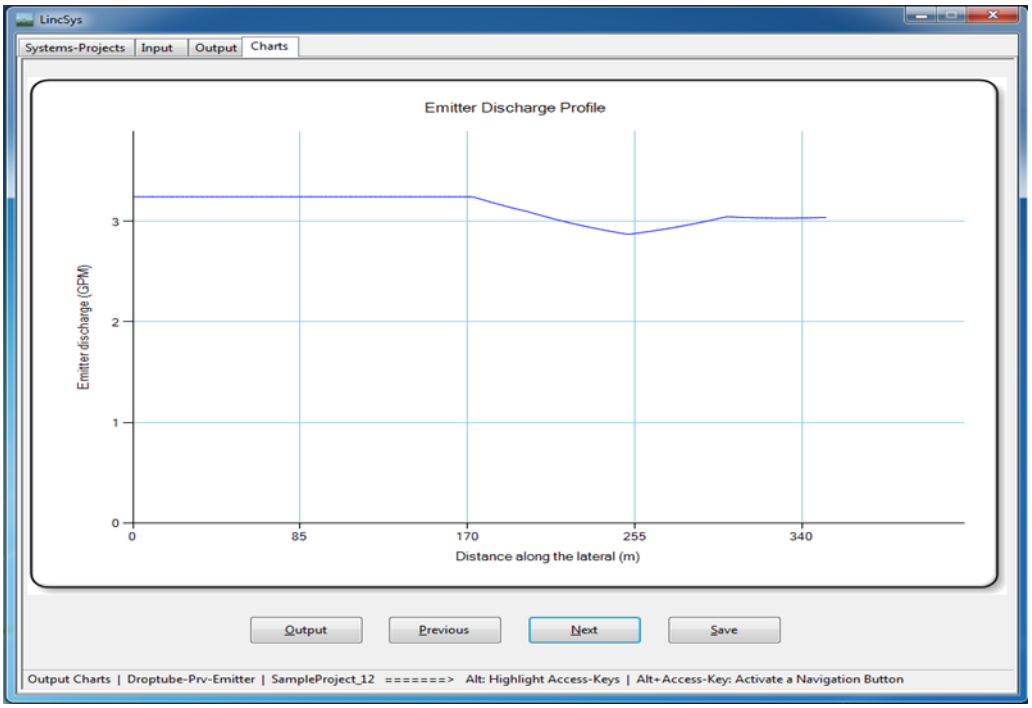

Figure 19. Sample chart of emitter discharge profile

4.5.2.e. Lateral discharge profile chart

A sample lateral discharge profile is depicted in Figure 20. The lateral discharge is in gallons per minute and the distance along the lateral is in meter. The lateral discharge profile for this example is a linear decreasing function of distance from the lateral inlet. However, depending on the hydraulic and geometric parameters of the lateral and the field slope, the rate of decrease in the lateral discharge may not necessarily follow a linear pattern.

The Save button can be used to save the current chart, if necessary. Alternatively, activating the Next button will close the current chart page and brings into display the chart panel for friction head loss in lateral pipe segments.

4.5.2.f. Chart depicting the profile of friction head loss in lateral pipe segments

Figure 21 displays a sample chart of friction head loss profile in lateral pipe segments. Friction head loss in lateral pipe segments, is shown in the vertical axis, in centimeter and distance from lateral inlet, is shown in the horizontal axis, in meter.

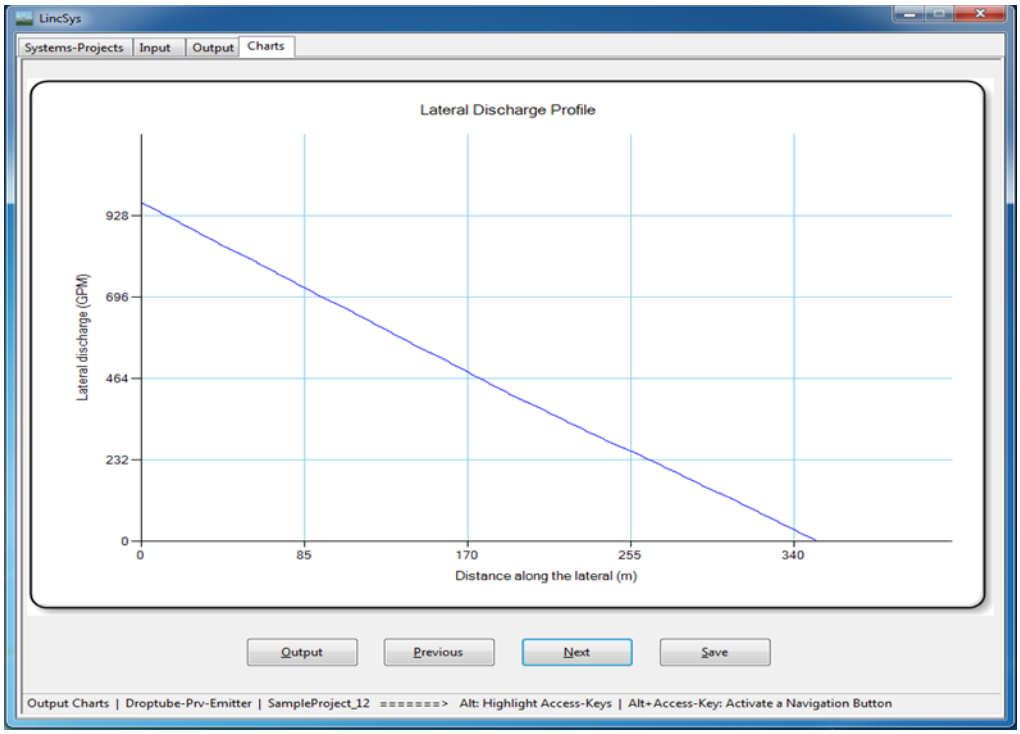

Figure 20. Sample chart of lateral discharge profile

Typically, the profile of friction head loss in lateral pipe segments is a smooth, often monotonically decreasing convex, function of distance from the lateral inlet. However, that behavior of the friction head loss curve holds only if the lateral pipe segments are of equal length and have diameter and hydraulic resistance characteristics that is invariant along the lateral. For the lateral considered here, the length of the lateral pipe segments vary along the lateral, but diameter and hydraulic resistance parameter are constant. Now, considering pipe segments that are adjacent to one another it can be observed that, in such a lateral, a segment with a longer length can have a friction head loss greater than that of a shorter segment, even when the shorter segment is located upstream of the longer segment. Although lateral discharge decreases monotonically with distance from the inlet, the difference in discharge between adjacent segments may not always be sufficient to compensate for the effect of lateral pipe segment length on friction head loss, which explains the series of spikes and dips in the friction head loss curve shown in Figure 18. Nonetheless, overall, the lateral segment friction head loss profile shows a decreasing trend with distance from the lateral inlet.

Now, the Save button can be activated to save the current chart. Alternatively, clicking on the Next button on the current chart panel closes the current page and opens the chart panel for cumulative friction head loss.

4.5.2.g. Chart depicting cumulative friction head loss profile

A sample cumulative friction head loss chart is displayed in Figure 22. The cumulative friction head loss data, shown in the vertical axis, is in centimeter and the distance along the lateral, shown in the horizontal axis, is in meter. Figure 22 shows that the cumulative friction

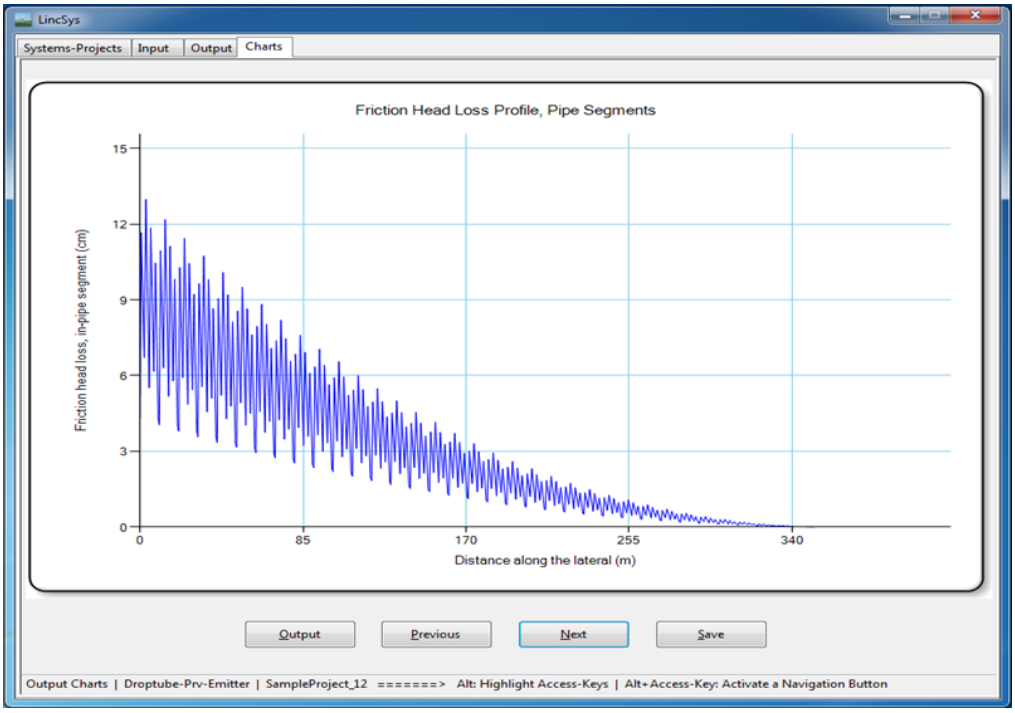

Figure 21. Sample chart depicting the profile of friction head loss in lateral pipe segments

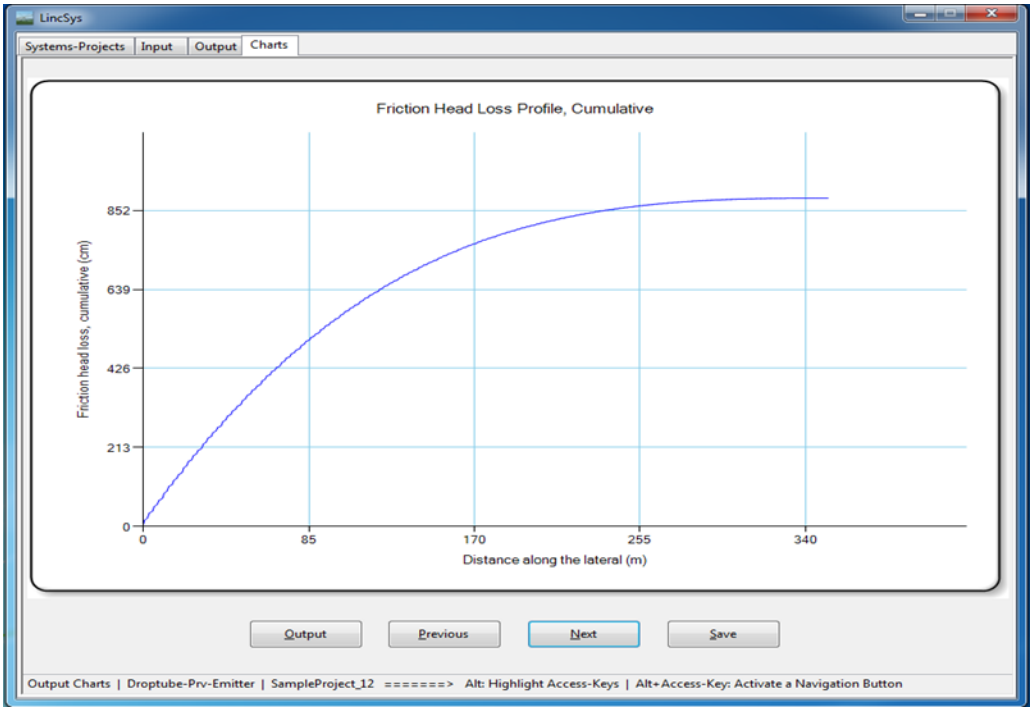

Figure 22. Sample chart of the cumulative friction head loss profile

head loss curve for the current lateral is a monotonic increasing concave function of distance from the lateral inlet.

The current chart can be saved by pressing the *Save* button, if necessary. Alternatively, activating the *Next* button will close the current window and opens the page that displays the Darcy-Weisbach friction factor.

4.5.2.h. Darcy-Weisbach friction factor profile

A sample chart for the Darcy-Weisbach friction factor profile along a lateral is depicted in Figure 23. It is an increasing convex function of distance from the lateral inlet over the upper 350.0m length of the lateral. It then becomes an increasing linear function of distance over the distal two-meter long section of the lateral.

The spatial behavior of the friction factor profile can be explained based on the variation, with distance form lateral inlet, of the flow Reynolds number. Over the upper 350.0m section of the lateral, the Reynolds number is at least equals 4000, thus flow over this section of the lateral stayed in the turbulent zone. Given that the lateral considered here is characterized by spatially invariant diameter, it can be readily reasoned that the flow Reynolds number for this lateral should decrease with distance from the lateral inlet. It then follows from the relationship between friction factor, a constant relative roughness, and Reynolds number in the turbulent zone (given in Moody diagram) that, for such a lateral, the friction factor is an increasing convex function of distance from the lateral inlet. This explains the spatial trend of the friction factor curve over the upper 350.m length of the lateral.

Over the last two-meter segment of the lateral, however, the lateral discharge became sufficiently small for the corresponding Reynolds number to fall under 4000. For Reynolds number less than 4000, *LincSys* computes the friction factor with the laminar flow equation. Note that the change in the trend of the friction factor curve (Figure 19) near the downstream-end of the lateral (characterized by an initial drop in the friction factor followed by a steep increase with a linear form) reflects the behavior of the friction factor equation for laminar flow.

Now, the *Save* button can be used to save the current chart. Alternatively, clicking on the *Next* button will close the current window and open the page that displays the chart showing local head loss in lateral pipe segments.

4.5.2.i. Chart depicting the profile of local head losses in lateral pipe segments

Figure 24 depicts a sample profile of the local head losses in lateral pipe segments. The vertical axis shows the local head loss in lateral pipe segments in centimeter and the horizontal axis represents distance from the lateral inlet in meter.

Except for the occasional localized spikes, the local head losses in lateral pipe segments overall show a decreasing trend along the lateral. This is because the types of local losses considered and the local loss coefficients used (with the exception of those at span joints) are the same along lateral and that the lateral discharges decrease progressively with distance along the lateral. However, this pattern is disrupted by sharp spikes in the local head losses at six points along the lateral, which of course decreased with distance from the inlet. Note that these localized spikes occur at span joints where local head losses are relatively larger than the other nodes.

The Save button can be used to save the current chart. On the other hand, activating the Next button will close the current window and opens the page that displays the cumulative local head loss chart.

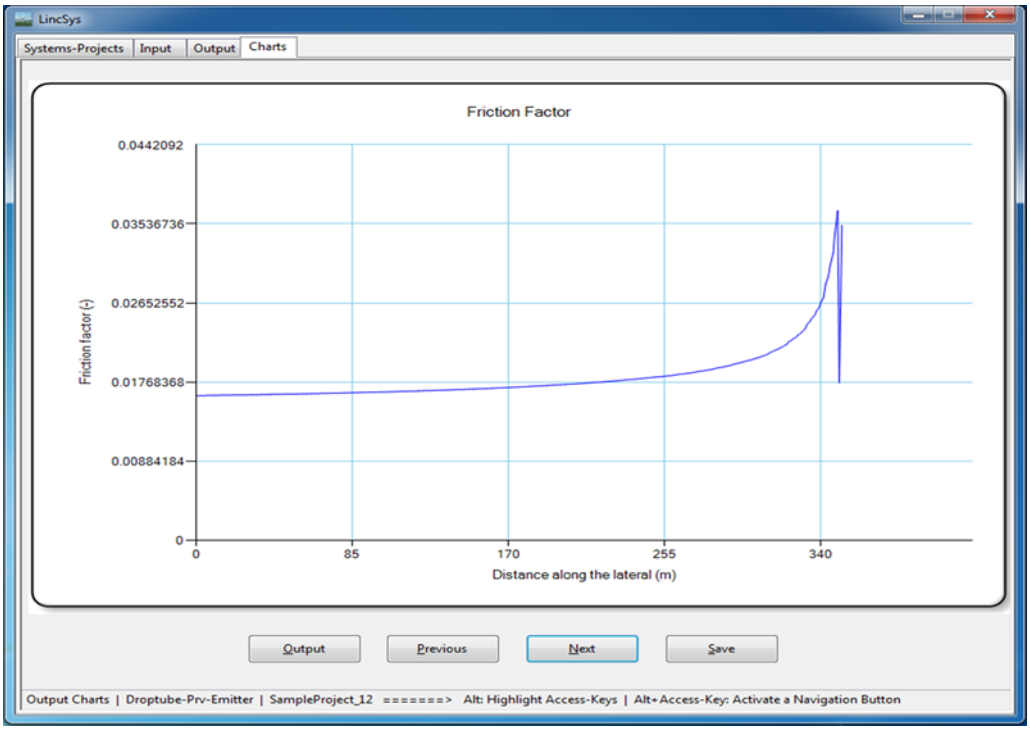

Figure 23. Sample chart of the Darcy-Weisbach friction factor profile

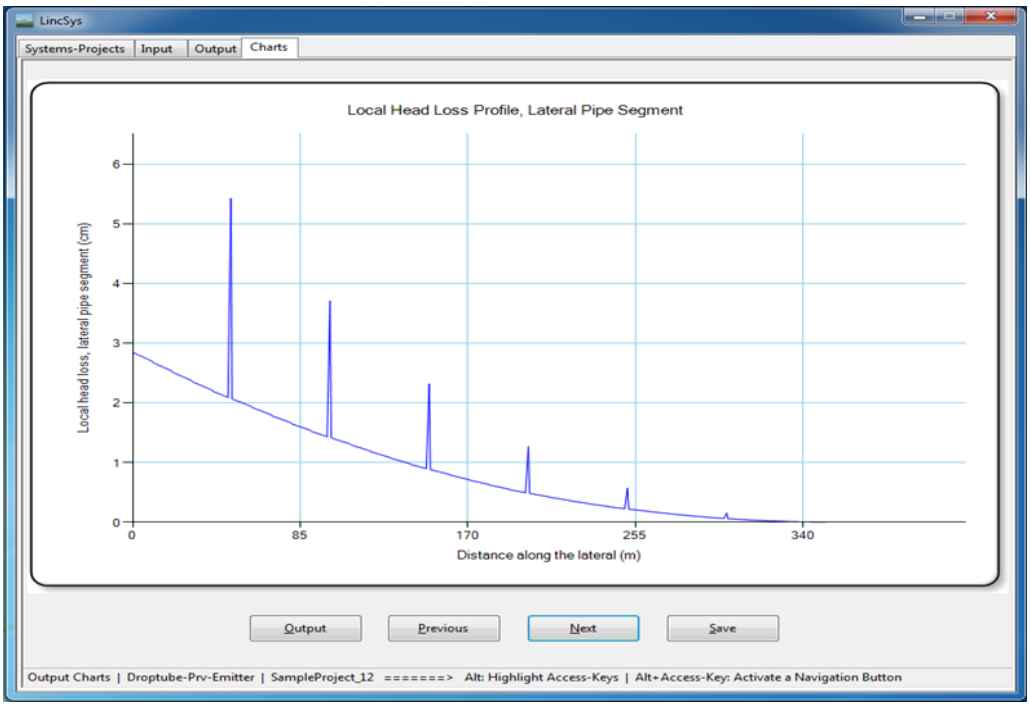

Figure 24. Sample chart depicting the profile of local head losses in lateral pipe segments

4.5.2.j. Chart depicting the cumulative local head loss profile

Figure 25 depicts the cumulative local head loss profile. The cumulative local head loss, shown in the vertical axis, is in centimeter and the distance along the lateral shown in the horizontal axis is in meter. The cumulative local head loss profile is an increasing concave function of distance from the lateral inlet. The loalized spikes that occurred in the span jonts appear as slight jumps at the locations of the three upstream span joints (Figure 25). However, for span joints close to the distal-end their effects on the cumulative local head losses are indicernible.

The current chart can be saved using the *Save* button. On the other hand, the *Next* button can be activated to close the current window and open the panel displaying the velocity head chart.

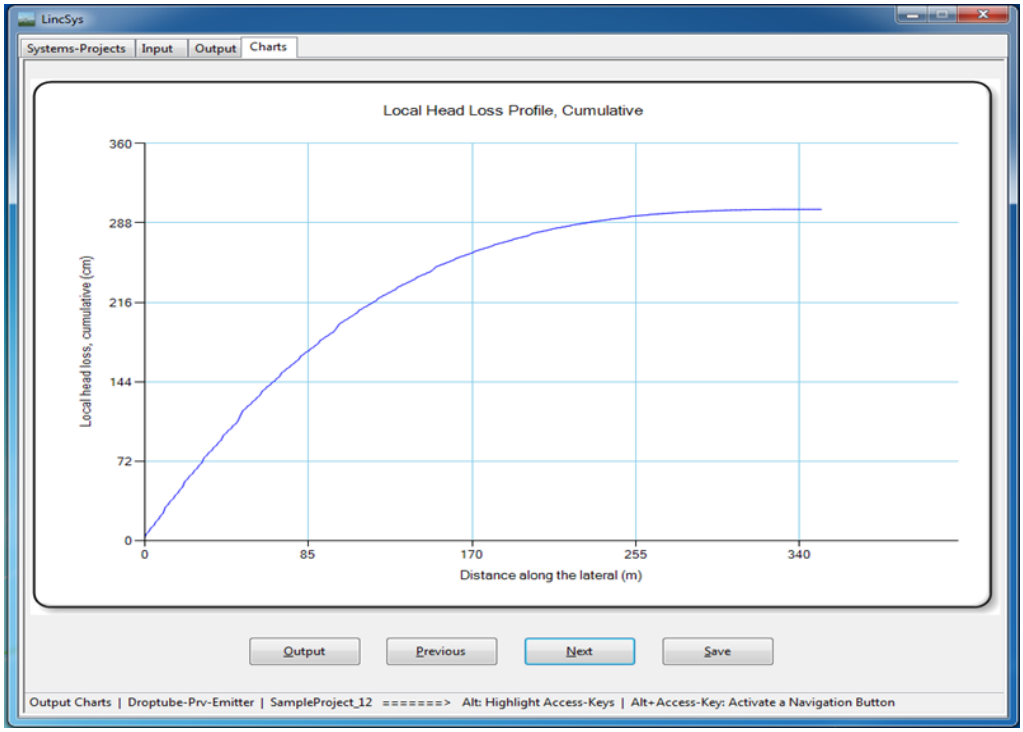

Figure 25. Sample chart of the cumulative local head loss profile

4.5.2.k. Velocity head profile chart

Figure 26 displays the velocity head profile. The velocity head is shown in the vertical axis in centimeter and the distance along the lateral is shown in the horizonatl axis in meter. Because pipe diameter is constant along the lateral, the velocity head profile is a montonic decreasing convex function of distance from the lateral inlet.

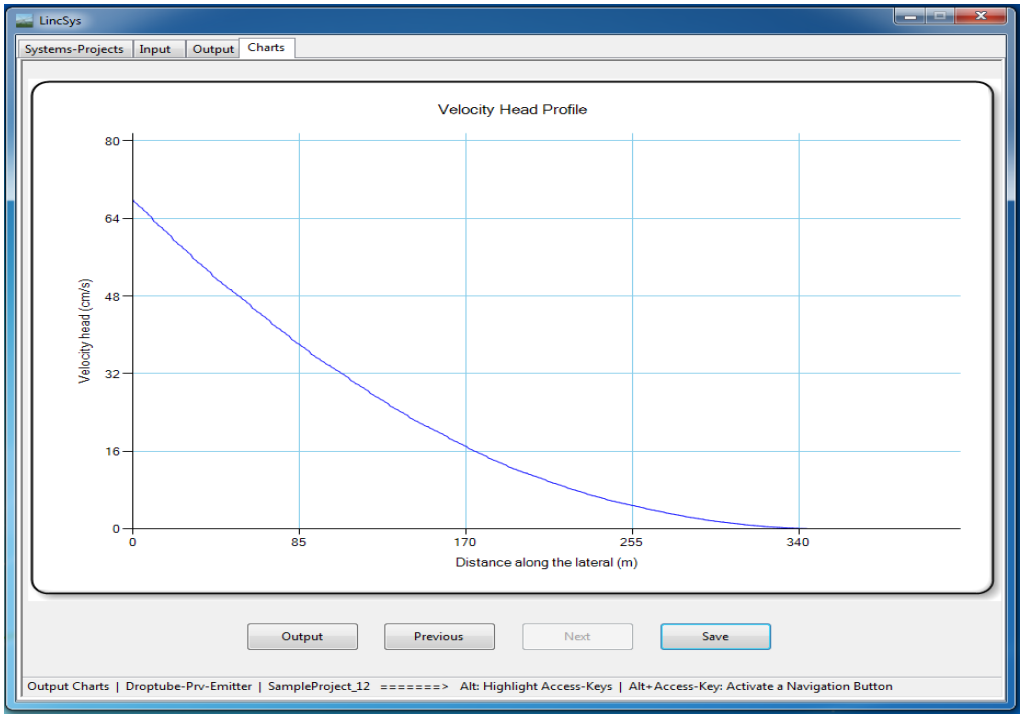

Figure 26. Sample chart of the velocity head profile

Chapter 5. File management (directory structure and input-output data files), data validation, and runtime errors

5.1. File management: directory structure and input-output data files

LincSys uses a specific directory structure to track and manage projects and other program data files. Figure 27 depicts the project management directory structure and its contents at program installation.

As noted in Section 1.2.3.a, directly under the *LincSys* installation folder (which is labeled as the *LincSys* folder in Figure 27) there is the Projects folder. Under the Projects folder there are five subfolders: DrptubePrvEmitter, DrptubeEmitter, EmitterOnLat, HelpDocAndLiterature, and Templates_InputDataFiles. The contents of each of these folders will now be discussed.

5.1.1. The contents of the system configuration option folders

5.1.1.a An overview

The DrptubePrvEmitter, DrptubeEmitter, and EmitterOnLat folders are referred here as system configuration folders and they contain *LincSys* project data corresponding to the Droptube-Prv-Emitter, Droptube-Emitter, and Emitter-On-Lateral system configuration options, respectively. Opening, for instance, the DrptubePrvEmitter folder would show that at installation it contains fifteen sample projects (i.e., folders), named SampleProject_1, SampleProject_2, …, SampleProject_15, each with a complete set of input and output data files, including graphical outputs (Figure 27). The sample projects, cover a wide range lateral hydraulic and geometric

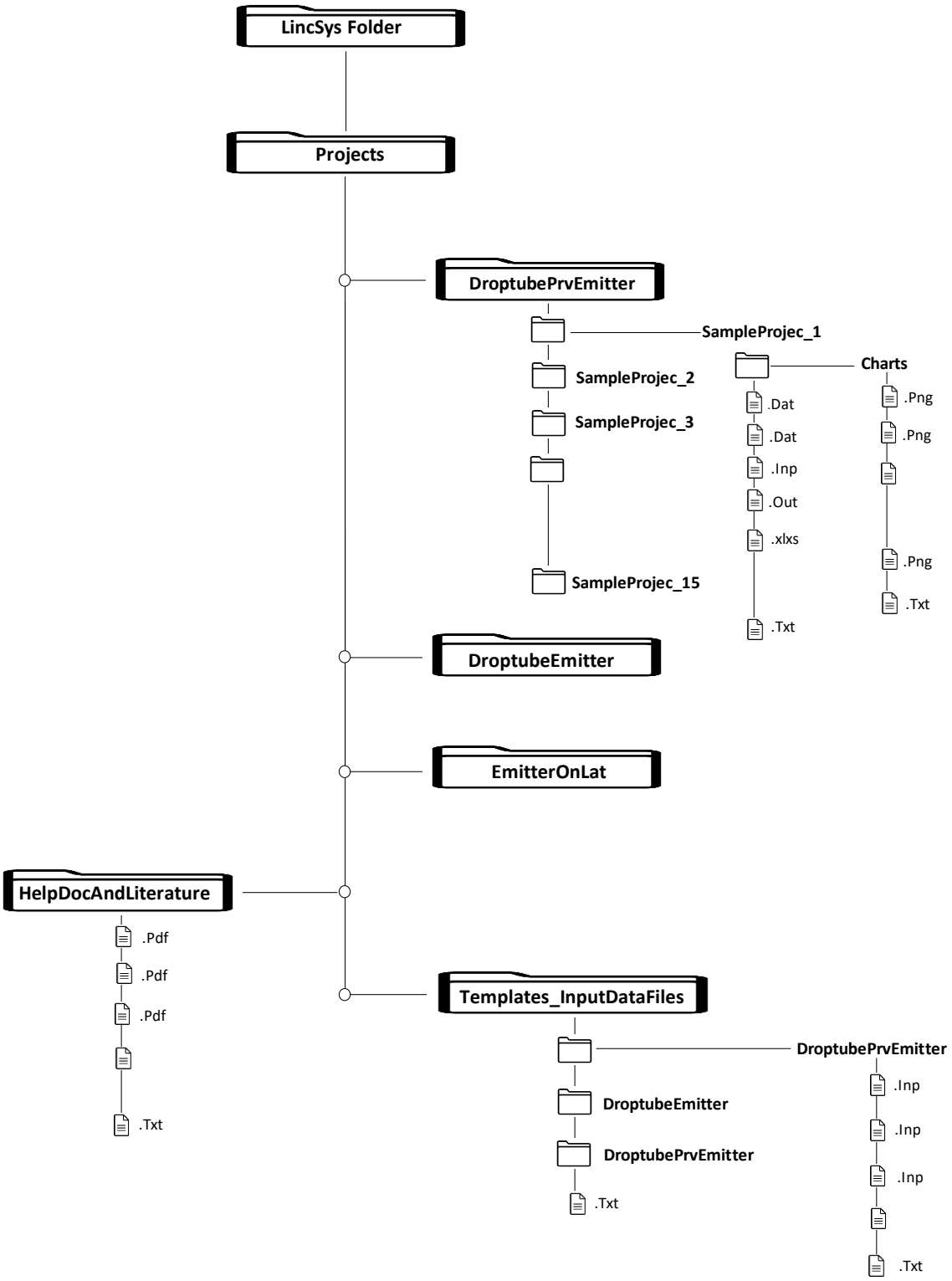

Figure 27. The content and structure of *LincSys'* project management directory

parameter sets and field slopes, and are meant to help users to familiarize themselves with the contents and format of the input-output data files of *LincSys*.

Although only the content of the DroptubePrvEmitter folder is shown in Figure 27, each of the DroptubeEmitter and EmitterOnLat system configuration folders as well contain fifteen sample projects with exactly the same name as those for the DrptubePrvEmitter system configuration folder.

Opening any one of the project folders under the DrptubePrvEmitter system configuration folder, say for instance opening the SampleProject_1 folder, would show that it contains a total of 9 files and a folder named Charts. As can be noted from Figure 27, the project files have the following extensions: Inp, Out, Dat, Txt and Xlxs. The file with the extension Inp is the input data file, while the files with the extensions Dat and Out consist of the output data files. The file with the extension Txt is a Readme file, which is meant to serve as a quick help information resource to the user on the contents of the project folder. Note that all the input and output data files of *LincSys* are space delimited text files. The exception here is the excel file (extension Xlxs), which has the same content as the input data file (InputData_LinLat.Inp) and is intended to be used as an input data template that can be modified and adapted by the user as needed. A list of the input-output files of *LincSys* and a description of the contents of the files are presented in Table 7.

The Charts subfolder contains image files with the extension Png and each file represents one of the eleven output charts created by *LincSys*.

Note that subsequent discussion is based on input-output data files of a system with Droptube-Prv-Emitter configuration. However, where necessary particular attributes of the input-output data associated with the Droptube-Emitter and Emitter-On-Lateral system configurations will be highlighted.

5.1.1.b. Input data file (InputData_LinLat.Inp)

InputData_LinLat.Inp

InputData_LinLat.Inp is the input data file of *LincSys* and it contains both non-tabular and tabular data. Figure 28 depicts a sample of the content of an InputData_LinLat.Inp file, showing the non-tabular data block and a segment of the tabular data section.

The non-tabular input data block includes such items as total head at the lateral inlet, water temperature, lateral length, span geometric parameters, support tower height, summary of the network topological data (i.e., number of links and nodes), number of lateral pipe segments and emitters, and number of spans (Figure 28). For systems with Droptube-Prv-Emitter configuration, the *prv* hydraulic parameters need to be specified in the non-tabular data section. For systems with Droptube-Prv-Emitter and Droptube-Emitter configuration, average drop-tube length and emitter above ground clearance need to be specified as well. A list of the parameter names specified in the non-tabular input data section and corresponding units and ranges are summarized in Table 2.

The tabular data block is where the network topological data, the lateral hydraulic, geometric, and elevation profile data, drop-tube related parameters (if applicable), emitter parameters and local head loss coefficients are specified (Figure 28). As indicated in Section 4.3.3 and also shown in Figure 28, the tabular input data contains 24 columns. Each column represents a data type.

Table 7. Input and output data files of a *LincSys* project

File name	Extension	Description of content
InputData_LinLat	Inp	Input data file. File content consists of network topological and lateral hydraulic, geometric, and elevation data
InputData_LinLat	Xlxs	Excel version of the input data file (InputData_LinLat.Inp)
OutputData_LinLat	Out	The main output data file. This file contains network topological and elevation profile data and computed hydraulic parameters
Chart_ElvHglEgl	Dat	Output date file. The contents of this file consists of the lateral elevation profile and computed hydraulic grade-line, energy grade-line, and lateral pressure profile data. *LincSys* uses data from this file to create: (1) the lateral elevation profile, the hydraulic grade-line, and the energy grade-line chart and (2) the lateral pressure profile chart
Chart_EmitterPrvInletSetPres	Dat	Output data file. This file contains data on *prv*-inlet pressure, *prv*-set pressure, computed head differential across emitter, and emitter discharge profile along the lateral. Output data from these file are used by the program to create: (1) the *prv*-inlet pressure, *prv*-set pressure, and emitter head differential chart and (2) the emitter discharge profile chart
Chart_FhlLhlVelH	Dat	Output data file. Contents of this file consist of the computed lateral discharge, friction head loss in lateral segments, cumulative friction head loss, Darcy-Weisbach friction factor, local head loss in a lateral pipe segment, cumulative local head loss, and velocity head profile data. These data are used by the program to create: (1) the lateral discharge profile chart, (2) chart depicting the profile of friction head loss in lateral pipe segments; (3) the cumulative friction head loss profile chart; (4) the friction factor profile chart; (5) chart depicting the profile of local head losses in lateral pipe segments; (6) the cumulative local head loss profile chart; and (7) the velocity head profile chart
EmitterDischargePressure	Dat	Output data file. The file contents consists of emitter discharge, emitter head differential, lateral discharge, *prv*-inlet pressure, and *prv* operating status. The file contains optional content for users to create professional looking charts with graphical applications.
Lat_hElvHglEgl_Comp	Dat	Output data file. Contains a more complete data on lateral hydraulic head, total head, and pressure head profiles along the lateral. File contains optional content for use in the analysis of the spatial properties of these parameters.
Readme	Txt	Readme file. The file contains a brief summary of the contents of the sample project folder

```
//      INPUT     DATA   OF      LINEAR   MOVE     OR       CENTER   PIVOT  LATERAL,   Prv-EMITTER  ASSEMBLY  PLACED     ON        DROPTUBE
//*************************************************************************************************************************************

Total    head       at     the      lateral  inlet      (m)   =  20
Set      pressure   head,  Prv                          (m)   =  17
Minimum  required   pressurehead     margin,  Prv       (m)   =   3.5
Maximum  inlet      pressurehead,    Prv               (m)   =  98
Water    temperature                                   (oC)  =  25
Lateral  length                                        (m)   =  222.5
Lateral  diameter,  typical                            (mm)  =  212.6
Span     length,    typical                            (m)   =  27.8
Span     altitude,  typical                            (m)   =   1
Support  tower      height, typical                    (m)   =   2.8
Droptube length,    average                            (m)   =   2.98
Emitter  above      ground  clearance                  (m)   =   0.5
Number   of         spans                               ()   =   8
Number   of         links                               ()   = 528
Number   Of         nodes                               ()   = 529
Number   Of         lateral pipe     segments           ()   = 264
Number   Of         emitters                            ()   = 257

//*************************************************************************************************************************************************************************************************************
```

Node Index UpStr	Node Index DnStr	Link index -	Lat seg leng	Node dist UpStr	Node dist DnStr	Node Elv UpStr	Node Elv DnStr	Lat seg diam	Lrel rough	Drop-tube leng	Drop-tube diam	Droptube rel rough	Emitter qhFunc coeff	Emitter qhFunc exp(b)	- Kbr	- Kbend	- Kprv	Local Klf	head Kcpl	loss Kct	Coeffs. Kexp	- Kval	- Keq
()	()	()	(m)	(m)	(m)	(m)	(m)	(mm)	()	(m)	(mm)	()	L/s(1/m^b)	()	()	()	()	()	()	()	()	()	()
1	2	1	0.8483	0	0.8483	2.8	2.9181	212.6	0.00001176	0	0	0	0	0	0	0	0	0	0	0	0	0	0
2	3	2	0	0.8483	0.8483	2.9181	0.5	0	0	2.4181	19.05	0.0000787	0.259	0.4999	0.12	0.027	1	0	0	0	0	0	0
2	4	3	0.8472	0.8483	1.6955	2.9181	3.0286	212.6	0.00001176	0	0	0	0	0	0	0	0	0.042	0	0	0	0	0
4	5	4	0	1.6955	1.6955	3.0286	0.5	0	0	2.5286	19.05	0.0000787	0.259	0.4999	0.12	0.027	1	0	0	0	0	0	0
4	6	5	0.8463	1.6955	2.5418	3.0286	3.1317	212.6	0.00001176	0	0	0	0	0	0	0	0	0.042	0	0	0	0	0
6	7	6	0	2.5418	2.5418	3.1317	0.5	0	0	2.6317	19.05	0.0000787	0.259	0.4999	0.12	0.027	1	0	0	0	0	0	0
6	8	7	0.8454	2.5418	3.3872	3.1317	3.2274	212.6	0.00001176	0	0	0	0	0	0	0	0	0.042	0	0	0	0	0
8	9	8	0	3.3872	3.3872	3.2274	0.5	0	0	2.7274	19.05	0.0000787	0.259	0.4999	0.12	0.027	1	0	0	0	0	0	0
8	10	9	0.8446	3.3872	4.2318	3.2274	3.3155	212.6	0.00001176	0	0	0	0	0	0	0	0	0.042	0	0	0	0	0
10	11	10	0	4.2318	4.2318	3.3155	0.5	0	0	2.8155	19.05	0.0000787	0.259	0.4999	0.12	0.027	1	0	0	0	0	0	0
10	12	11	0.8439	4.2318	5.0757	3.3155	3.3963	212.6	0.00001176	0	0	0	0	0	0	0	0	0.042	0	0	0	0	0
12	13	12	0	5.0757	5.0757	3.3963	0.5	0	0	2.8963	19.05	0.0000787	0.259	0.4999	0.12	0.027	1	0	0	0	0	0	0
12	14	13	0.8432	5.0757	5.9189	3.3963	3.4697	212.6	0.00001176	0	0	0	0	0	0	0	0	0.042	0	0	0	0	0
14	15	14	0	5.9189	5.9189	3.4697	0.5	0	0	2.9697	19.05	0.0000787	0.259	0.4999	0.12	0.027	1	0	0	0	0	0	0
14	16	15	0.8426	5.9189	6.7615	3.4697	3.5356	212.6	0.00001176	0	0	0	0	0	0	0	0	0.042	0	0	0	0	0
16	17	16	0	6.7615	6.7615	3.5356	0.5	0	0	3.0356	19.05	0.0000787	0.259	0.4999	0.12	0.027	1	0	0	0	0	0	0
16	18	17	0.842	6.7615	7.6035	3.5356	3.5942	212.6	0.00001176	0	0	0	0	0	0	0	0	0.042	0	0	0	0	0
18	19	18	0	7.6035	7.6035	3.5942	0.5	0	0	3.0942	19.05	0.0000787	0.259	0.4999	0.12	0.027	1	0	0	0	0	0	0
18	20	19	0.8416	7.6035	8.4451	3.5942	3.6455	212.6	0.00001176	0	0	0	0	0	0	0	0	0.042	0	0	0	0	0
20	21	20	0	8.4451	8.4451	3.6455	0.5	0	0	3.1455	19.05	0.0000787	0.259	0.4999	0.12	0.027	1	0	0	0	0	0	0
20	22	21	0.8411	8.4451	9.2862	3.6455	3.6894	212.6	0.00001176	0	0	0	0	0	0	0	0	0.042	0	0	0	0	0
22	23	22	0	9.2862	9.2862	3.6894	0.5	0	0	3.1894	19.05	0.0000787	0.259	0.4999	0.12	0.027	1	0	0	0	0	0	0
22	24	23	0.8408	9.2862	10.127	3.6894	3.726	212.6	0.00001176	0	0	0	0	0	0	0	0	0.042	0	0	0	0	0
24	25	24	0	10.127	10.127	3.726	0.5	0	0	3.226	19.05	0.0000787	0.259	0.4999	0.12	0.027	1	0	0	0	0	0	0

Figure 28. The content of a sample input data file (InputData_LinLat.Inp) of *LincSys*, for Droptube-Prv-Emitter system configuration option

The number of rows of the tabular data is equal to the number of hydraulic links. The maximum number of links that *LincSys* can accommodated is 2000. The odd-numbered rows of the input data table contains input parameters related to lateral pipe segments. On the other hand, parameters related to outlet discharge metering apparatuses or virtual links attached to non-offtake nodes are displayed in the even-numbered rows. A more detailed sample of the tabular input data table is provided in Tables 3a and 3b.

In preparing the tabular data section of the InputData_LinLat.Inp file, it is important to pay attention to the fact that the hydraulic network topological data should be specified in accordance with the descriptions provided in Section 4.3.3.a. Furthermore, the pattern of variation in the nodal distances and nodal elevations columns of the tabular data need to duplicate the patterns in the nodal index columns.

As noted in Section 4.3.3.f, *LincSys* distinguishes between offtake and non-offtake nodes based on the input data in the column where the coefficient of the emitter head-discharge equation is specified (column #14 of Table 3b). If the data in an even-numbered row of column#14 is set to a valid positive real number (Table 4), then it signals to the program that the corresponding link is attached to an offtake node. If, on the other hand, it is set to zero, the corresponding link is a virtual link attached to a non-offtake node.

If the data in the even-numbered row of column #14 is set to a valid non-zero value and if the selected system configuration option is Droptube-Prv-Emitter or Droptube-Emitter, then the drop-tube parameters in columns #11 to 13 and the branching and bending local head loss parameters in columns #16 and 17 (Tables 3a and 3b) need to be specified. In addition, for a system with Droptube-Prv-Emitter configuration, the *prv* indicator parameter (column #18, Table 3b) needs to be set to 1. Note that this implies that for the Droptube-Prv-Emitter system configuration option each outlet discharge metering apparatus along the lateral is fitted with a *prv*. For Emitter-On-Lateral system configuration option, however, the contents of columns #11 to 13 and columns #17 and 18 (Tables 3a and 3b) need to be set to zero.

Sources of linear-move and center-pivot sprinkler irrigation system data

Hydraulic simulation of a linear-move or center-pivot system requires a substantial volume of data on lateral elevation profile and hydraulic and geometric parameters. For an actual system, a detailed inventory of the system components and specifications along with related hydraulic and geometric parameters can be found in the machine specification documents provided by the manufacturer.

By contrast, the system elevation profile data may not be readily available. A direct way to determine the elevation profile of a lateral is to run a profile leveling survey along the lateral. However, running a profile leveling survey along the centerline of such a lateral requires a slight modification of the conventional field procedure. In this specific application, the height of instrument (i.e., the elevation of the instrument line of sight from a set datum) is lower than the elevation of the lateral centerline. Thus, the setting of the leveling staff during foresight readings and the calculation of the lateral elevation (from the height of instrument and foresight readings) would be different from what is considered conventional.

The leveling staff should be held upside-down in such a way that the 0-mark is placed at a level that matched the lateral centerline. A foresight read as such should then be added to the height of instrument (as opposed to being subtracted from the height of instrument) to determine the elevation of the point on the lateral centerline.

When measuring elevations, the following points may need to be observed for an accurate determination of the elevation profile of the lateral: *(i)* horizontal distance between nodes should be sufficiently small such that the difference between the corresponding arc and chord lengths can be considered negligible, *(ii)* measurements need to be made at or sufficiently close to points of elevation extrema (elevation peaks and lows), and *(iii)* no elevation measurement needs to be made downstream of the distal-end outlet.

For a hypothetical lateral, one can use equations of conic sections and cubic polynomials to accurately model concave and convex spans, respectively. For instance, the elevation profile of a lateral, installed on a level field and consisting of a series of concave spans, can be represented in terms of a concatenated series of arcs defined by the equation of a circle.

Given the span length and altitude, the radius of curvature of the virtual circle that the centerline of a span is a part of can be readily calculated. To calculate the elevation profile of a lateral, first a two-dimensional coordinate system would be established. If the reference datum is set to the field surface, then the horizontal axis of the coordinate system, can be set in it. Furthermore, if the horizontal location of the lateral inlet is marked as the reference point with respect to which horizontal distance along the length of run of the lateral is measured, then the vertical axis (of the coordinate system) would pass through the lateral inlet. The coordinate system would then have its origin on the field surface right under the lateral inlet.

Now, once the radius of curvature of a span, its altitude, and the support tower height of the lateral are specified, then the coordinates of the center of curvature of the virtual circle, of which the span's centerline is a part, can be readily calculated. Assuming a symmetric span, for instance, the horizontal coordinate of the center of curvature of a span would be half the span length plus the distance of the span inlet from the lateral inlet. The vertical coordinate, of the center of curvature, can be calculated as the negative of the difference between the radius of curvature and the sum of the span's altitude and the support tower height.

Given the radius of curvature and the coordinates of the center of curvature of the virtual circle that a span's centerline is a part, it is a straightforward procedure to calculate the elevations of any number of points along the span with the equation of a circle, starting from the inlet-end of the span. The same can be repeated in each concave span across the lateral to determine the lateral elevation profile over all the concave spans.

As noted earlier, for systems with distal-end cantilever type beams, the elevation profile over such a span can be represented accurately with a cubic polynomial function. The curve defined by the cubic polynomial can simply be appended to the downstream-end of the concave segments of the lateral. However, in order to have a smooth fitting curve at the inlet-end of the distal-end span, the cubic function should have as its vertical-intercept the elevation of the distal-end span joint.

For laterals installed on a sloping field, however, one may need to augment the preceding approach (described for a lateral operated on a level field) with trigonometric relationships to approximately take into account slope effects on lateral elevation profiles.

5.1.1.c. Output data files

As can be noted from Table 7, *LincSys* has six output data files saved in the project folder. The main output data file, which contains network topological and elevation profile data and computed hydraulic parameters is the OutputData_LinLat.Out file. In addition, a project

folder contains three more output data files with the extension Dat (Chart_ElvHglEgl.Dat, Chart_EmitterPrvInletSetPres.Dat, and Chart_FhlLhlVelH.Dat). The contents of these files are used by the program to create output charts.

Two additional output data files are created by *LincSys*: EmitterDischargePressure.Dat and Lat_hElvHglEgl_Comp.Dat. As noted in Table 7, the EmitterDischargePressure.Dat file contains optional content meant to be used in creating professional looking charts, with graphical applications, for subsequent use in reports. The data in the Lat_hElvHglEgl_Comp.Dat file, on the other hand, can be used in analyzing the spatial properties of lateral pressure head profiles.

OutputData_LinLat.Out

OutputData_LinLat.Out is the main output data file of *LincSys*. It is a space delimited text file comprised of non-tabular and tabular output data blocks. Figure 29 depicts the content of a sample OutputData_LinLat.Out file showing the non-tabular data block and a segment of the tabular data section.

The non-tabular output data block consists of emitter discharge and emitter head differential variability indicator parameters, emitter discharge and emitter head differential uniformity indicator parameters, and the error in the computed total inlet head (Figure 29). Note that data on the operating modes of *prvs* (if applicable) are shown at the bottom of the input data table and hence not visible in Figure 29.

The tabular output data consists of 20 columns. Each column represents a data type, consisting of network topological data, lateral elevation profile, and computed hydraulic data such as lateral and emitter discharges, lateral pressure, emitter head differential, friction head loss, local head losses, velocity head, hydraulic head, and total head profiles along the lateral.

The number of rows of the tabular output data is variable and is equal to the number of hydraulic links. Each row in the tabular output data contains nodal distances and elevations as well as computed hydraulic data related to a link or associated nodes. The maximum number of rows of the tabular output data, which is equal to the maximum number of links that *LincSys* can simulate, is 2000.

As can be noted from Figure 29, the emitter discharge and emitter head differential are shown in the even-numbered rows of the tabular data indicating that they correspond to the links associated with outflow metering apparatuses. On the other hand, all the other computed outputs are displayed in the odd-numbered rows of the table, indicating that they are related to links that correspond to lateral pipe segments and associated nodes.

A more detailed sample of the output data table is presented in Tables 5a and 5b. The contents of about half of the cells in the output data table are 0 (Tables 5a and 5b and Figure 29). A value of 0 in all the data columns, except column 20, does not indicate that 0 is an output parameter. Instead, they imply that the parameter that a column represents is impertinent to that particular row, specifically, to the corresponding hydraulic link and related nodes. An exception to this is the data in column #20. If a value of 0 appears in an even-numbered row of column #20 and the system configuration option is Droptube-Prv-Emitter, then it implies that the corresponding link is a virtual link attached to a non-offtake junction node. A more detailed discussion on the contents of the tabular output data are provided in Section 4.4.3.j.

```
//      OUTPUT    DATA     OF       LINEAR   MOVE     OR       CENTER   PIVOT    LATERAL,  Prv-EMITTER PLACED   ON       DROPTUBE

Minimum     emitter     discharge                                                    (L/s)  =   0.6086
Average     emitter     discharge                                                    (L/s)  =   0.7076
Maximum     emitter     discharge                                                    (L/s)  =   0.9776
Minimum     emitter     head        differential                                     (m)    =   5.52
Average     emitter     head        differential                                     (m)    =   7.63
Maximum     emitter     head        differential                                     (m)    =  14.26
Uniformity  coefficient emitter     discharge                                        ()     =   0.876
Distr       unif        low         quarter     emitter     discharge                ()     =   0.868
Uniformity  coefficient emitter     head        differential                         ()     =   0.746
Distr       unif        low         quarter     emitter     head      differential   ()     =   0.737
Total       inlet       head        relative    error                                (%)    =   0.00809
Total       inlet       head        absolute    error                                (m)    =   0.00162
```

Node Index UpStr	Node Index DnStr	Link Index	Nodal Dist UpStr	Nodal Dist DnStr	Nodal Elv UpStr	Nodal Elv DnStr	Lat. Disch	Emitr Disch	Emitr H-diff.	Pressure UpStr	Pressure DnStr	VelH Link	FHL Link	LHL Link	HGL - UpStr	HGL - DnStr	EGL - UpStr	EGL - DnStr	PrvOperSt -
-	-	-	-	-	-	-	-	-	-	-	-	-	-	-	-	-	-	-	-
(-)	(-)	(-)	(m)	(m)	(m)	(m)	(L/s)	(L/s)	(m)	(m)	(m)	(m)	(m)	(m)	(m)	(m)	(m)	(m)	-
1	2	1	0	0.8483	2.8	2.9181	181.865686	0	0	15.861637	15.681641	1.336745	0.061896	0	18.661637	18.599741	19.998382	19.936486	0
2	3	2	0.8483	0.8483	2.9181	0.5	0	0.977638	14.255658	0	0	0	0	0	0	0	0	0	1
2	4	3	0.8483	1.6955	2.9181	3.0286	180.888048	0	0	15.63972	15.468018	1.322412	0.061202	0.056254	18.55782	18.496618	19.880232	19.81903	0
4	5	4	1.6955	1.6955	3.0286	0.5	0	0.971879	14.088165	0	0	0	0	0	0	0	0	0	1
4	6	5	1.6955	2.5418	3.0286	3.1317	179.916169	0	0	15.426538	15.262907	1.30824	0.060531	0.055652	18.455138	18.394607	19.763377	19.702846	0
6	7	6	2.5418	2.5418	3.1317	0.5	0	0.966312	13.927204	0	0	0	0	0	0	0	0	0	1
6	8	7	2.5418	3.3872	3.1317	3.2274	178.949858	0	0	15.221864	15.066297	1.294225	0.059867	0.055058	18.353564	18.293697	19.647789	19.587922	0
8	9	8	3.3872	3.3872	3.2274	0.5	0	0.960933	13.772562	0	0	0	0	0	0	0	0	0	1
8	10	9	3.3872	4.2318	3.2274	3.3155	177.988924	0	0	15.025689	14.878372	1.280362	0.059218	0.05447	18.253089	18.193872	19.533452	19.474234	0
10	11	10	4.2318	4.2318	3.3155	0.5	0	0.955743	13.624146	0	0	0	0	0	0	0	0	0	1
10	12	11	4.2318	5.0757	3.3155	3.3963	177.033182	0	0	14.838197	14.698815	1.266649	0.058582	0.053888	18.153697	18.095115	19.420346	19.361764	0
12	13	12	5.0757	5.0757	3.3963	0.5	0	0.950731	13.481599	0	0	0	0	0	0	0	0	0	1
12	14	13	5.0757	5.9189	3.3963	3.4697	176.082451	0	0	14.65907	14.527717	1.253081	0.057953	0.053313	18.05537	17.997417	19.308451	19.250498	0
14	15	14	5.9189	5.9189	3.4697	0.5	0	0.945896	13.344805	0	0	0	0	0	0	0	0	0	1
14	16	15	5.9189	6.7615	3.4697	3.5356	175.136555	0	0	14.488401	14.365163	1.239654	0.057338	0.052743	17.958101	17.900763	19.197755	19.140417	0
16	17	16	6.7615	6.7615	3.5356	0.5	0	0.941237	13.213646	0	0	0	0	0	0	0	0	0	1
16	18	17	6.7615	7.6035	3.5356	3.5942	174.195318	0	0	14.326272	14.210943	1.226365	0.056729	0.052179	17.861872	17.805143	19.088237	19.031509	0
18	19	18	7.6035	7.6035	3.5942	0.5	0	0.936747	13.087866	0	0	0	0	0	0	0	0	0	1
18	20	19	7.6035	8.4451	3.5942	3.6455	173.258571	0	0	14.172476	14.065037	1.213211	0.056139	0.051621	17.766676	17.710537	18.979887	18.923748	0
20	21	20	8.4451	8.4451	3.6455	0.5	0	0.932424	12.967314	0	0	0	0	0	0	0	0	0	1
20	22	21	8.4451	9.2862	3.6455	3.6894	172.326147	0	0	14.026991	13.927542	1.200188	0.055549	0.051069	17.672491	17.616942	18.872679	18.81713	0
22	23	22	9.2862	9.2862	3.6894	0.5	0	0.928267	12.851913	0	0	0	0	0	0	0	0	0	1
22	24	23	9.2862	10.127	3.6894	3.726	171.39788	0	0	13.889915	13.798338	1.187293	0.054977	0.050522	17.579315	17.524338	18.766608	18.711631	0
24	25	24	10.127	10.127	3.726	0.5	0	0.924271	12.74148	0	0	0	0	0	0	0	0	0	1

Figure 29. The content of a sample main output data file (OutputData_LinLat.Out) of *LincSys*, for the Droptube-Prv-Emitter system configuration option

Output files related to charts (Chart_ElvHglEgl.Dat, Chart_EmitterPrvInletSetPres.Dat, and Chart_FhlLhlVelH.Dat)

Chart_ElvHglEgl.Dat

The Chart_ElvHglEgl.Dat file contains data on the elevation profile of the lateral centerline, the hydraulic and energy grade-lines, and the lateral pressure profile. The contents of a section of a sample Chart_ElvHglEgl.Dat file is depicted in Figure 30. The file contains five columns of data. The first column is nodal distance from the lateral inlet, the second column is nodal elevation, the third column is the hydraulic head, and the fourth and fifth columns are total head and lateral pressure data, respectively, all expressed in meter. Note that for all the links (except the distal-end link) the hydraulic head, the total had, and the pressure head values are those computed at the upstream end of each link. For the downstream-end link, however, the parameter values computed both at the upstream- and downstream-ends of the link are included in the profiles of these parameters.

As indicated in Table 7, the data in this file are used by *LincSys* to generate the lateral elevation profile, hydraulic grade-line, and energy grade-line chart (Figure 16) and the lateral pressure profile chart (Figure 17).

Chart_EmitterPrvInletSetPres.Dat

The Chart_EmitterPrvInletSetPres.Dat file is a text file containing data on head differential across emitter, the *prv*-set pressure, and *prv*-inlet pressure profiles along the lateral. Note that the head differential across emitter and *prv*-inlet pressure profiles are model outputs whereas the *prv*-set pressure is an input.

The contents of a part of a sample Chart_EmitterPrvInletSetPres.Dat file is shown in Figure 31. The file contains data arranged in five columns. The first column is emitter distance from the lateral inlet, the second column is head differential across emitter, the third and fourth columns contain data on *prv*-inlet and *prv*-set pressures, respectively, (all measured in meter) and the fifth column contains emitter discharge data in gallons per minute. Data shown in the second, third, and fifth columns are model outputs. Note that the content of the Chart_EmitterPrvInletSetPres.Dat file, shown in Figure 31, is for a system with Droptube-Prv-Emitter configuration option. By comparison, for systems with Droptube-Emitter and Emitter-On-Lateral configuration option the file will contain only three columns: the column consisting of nodal distances from the lateral inlet and the columns for head differential across emitter and the emitter discharge columns.

LincSys uses the data in Chart_EmitterPrvInletSetPres.Dat file to create the emitter head differential, *prv*-inlet and *prv*-set pressure chart (Figure 18) and the emitter discharge chart (Figure 19), described in Section 5.1.1.c.

Chart_FhlLhlVelH.Dat

The Chart_FhlLhlVelH.Dat file contains a set of computed hydraulic parameters, consisting of lateral discharge, friction head loss, friction factor, local head loss, and velocity head in lateral pipe segments. A section of the contents of a sample Chart_FhlLhlVelH.Dat file is depicted in Figure 32.

As can be noted from Figure 32, the file contains eight columns. The first column is the nodal distance from the lateral inlet, the second column lateral discharge (discharge in each lateral pipe segment), the third column is friction head loss in a lateral pipe segment, the fourth

//Lateral elevation (ELV), hydraulic grade line (HGL), energy grade line (EGL), and pressure data

Distance nodal (m)	Elevation (ELV) (m)	Hydraulic grade-line,HGL (m)	Energy-grade line,EGL (m)	Lateral pressure (m)
0	2.8	18.662	19.998	15.862
0.848	2.918	18.558	19.88	15.64
1.696	3.029	18.455	19.763	15.427
2.542	3.132	18.354	19.648	15.222
3.387	3.227	18.253	19.533	15.026
4.232	3.316	18.154	19.42	14.838
5.076	3.396	18.055	19.308	14.659
5.919	3.47	17.958	19.198	14.488
6.761	3.536	17.862	19.088	14.326
7.604	3.594	17.767	18.98	14.172
8.445	3.646	17.672	18.873	14.027
9.286	3.689	17.579	18.767	13.89
10.127	3.726	17.487	18.662	13.761
10.967	3.755	17.396	18.558	13.641
11.808	3.777	17.306	18.455	13.528
12.648	3.792	17.216	18.353	13.425
13.488	3.799	17.128	18.253	13.329
14.328	3.799	17.041	18.153	13.242
15.168	3.792	16.954	18.055	13.162
16.008	3.777	16.869	17.957	13.091
16.848	3.755	16.784	17.861	13.029
17.689	3.726	16.7	17.765	12.974
18.53	3.689	16.617	17.67	12.928
19.371	3.646	16.535	17.577	12.89
20.212	3.594	16.454	17.484	12.86
21.054	3.536	16.374	17.393	12.839
21.897	3.47	16.295	17.302	12.825
22.74	3.396	16.216	17.212	12.82
23.584	3.316	16.138	17.123	12.823
24.429	3.227	16.062	17.035	12.834

Figure 30. The content of a sample Chart_ElvHglEgl.Dat file

//Head differential across emitter (He), Prv-inlet pressure (hprv-i), Prv-set pressure (hprv), and emitter discharge (Qe)

Distance emitter (m)	Emitter-head diff,He (m)	Prv-inlet pressure,hprv-i (m)	Prv-set pressure,hprv (m)	Emitter discharge,Qe (GPM)
0.848	14.256	17.156	17	15.496
1.696	14.088	16.996	17	15.405
2.542	13.927	16.842	17	15.316
3.387	13.773	16.694	17	15.231
4.232	13.624	16.551	17	15.149
5.076	13.482	16.415	17	15.069
5.919	13.345	16.284	17	14.993
6.761	13.214	16.158	17	14.919
7.604	13.088	16.038	17	14.848
8.445	12.967	15.922	17	14.779
9.286	12.852	15.812	17	14.713
10.127	12.741	15.706	17	14.65
10.967	12.636	15.605	17	14.589
11.808	12.535	15.508	17	14.531
12.648	12.439	15.416	17	14.475
13.488	12.347	15.328	17	14.422
14.328	12.26	15.245	17	14.371
15.168	12.177	15.166	17	14.322
16.008	12.099	15.09	17	14.276
16.848	12.025	15.019	17	14.232
17.689	11.955	14.952	17	14.191
18.53	11.889	14.889	17	14.152
19.371	11.827	14.83	17	14.115
20.212	11.77	14.775	17	14.08
21.054	11.716	14.724	17	14.048
21.897	11.666	14.676	17	14.018
22.74	11.621	14.632	17	13.991
23.584	11.579	14.593	17	13.966
24.429	11.542	14.557	17	13.943

Figure 31. The content of a sample Chart_EmitterPrvInletSetPres.Dat file for Droptube-Prv-Emitter system configuration option

column contains data on the cumulative friction head loss, the fifth column is the Darcy-Weisbach friction factor, the sixth column is the local head loss in a lateral pipe segment, the seventh column is the cumulative local head loss, and the eight column contains data on velocity head in lateral pipe segments.

Note that the data on nodal distance do not start from the inlet-end of the lateral, where distance is 0m. Instead, it starts form the distance of the upstream-end junction node from the inlet-end of the lateral. This is to indicate that the friction and local head losses in the Chart_FhlLhlVelH.Dat file are cumulative values (over the respective lateral pipe segments) that correspond to the downstream end of the lateral pipe segments. Furthermore, for consistency, the parameters that are constant over a lateral pipe segment (consisting of lateral discharge, friction factor, and velocity head) are also represented in the Chart_FhlLhlVelH.Dat file at the downstream end of each lateral pipe segment.

Note that the content of the Chart_FhlLhlVelH.Dat file does not vary with the system configuration option.

The data in Chart_FhlLhlVelH.Dat file is used by the program to create seven of the eleven charts described in Sections 4.5.2.e to 4.5.2. These include, the lateral discharge profile chart (Figure 20), the chart showing friction head loss profile in the lateral pipe segments (Figure 21), the cumulative friction head loss profile chart (Figure 22), the friction factor profile chart (Figure 23), the chart showing the profile of the local head losses in lateral pipe segments (Figure 24), the chart for cumulative local head losses (Figure 25), and the velocity head profile chart (Figure 26).

Additional output data files (EmitterDischargePressure.Dat and Lat_hElvHglEgl_Comp.Dat)

A *LincSys* project folder contains two additional output data files, namely: EmitterDischargePressure.Dat and Lat_hElvHglEgl_Comp.Dat. These output data files contain data that was presented in one or more of the files described in the preceding section. However, the data in the current files are presented either in a slightly different format or represent a more complete version compared to the files described earlier and are meant to provide the user an optional content.

EmitterDischargePressure.Dat file

The EmitterDischargePressure.Dat file contains data related to emitters and *prvs* in a space delimited text file format.

The contents of a section of a sample EmitterDischargePressure.Dat file, for Droptube-Prv-Emitter system configuration option, is depicted in Figure 33. The file contains a tabular data with six columns. The first column is the distance of an emitter from the lateral inlet in meter. The second column contains data on emitter discharge, the third column is head differential across emitter, the fourth column contains data on lateral discharge, the fifth column is *prv*-inlet pressure, and the six column contains data on *prv* operating status.

As noted earlier, the content of this file can also be found in some of the other output data files described earlier. However, this file is intended to provide optional content to users for creating professional looking charts with graphical applications, which can eventually be incorporated into a report.

//Lateral discharge (Q), in-pipe friction head loss (Hf_pipe), cumulative friction head loss (Hf_cum), friction factor (f),
//local head losses in lateral pipe segments (Lh_Pipe), cumulative local head loss (Lh_Cum), and velocity head (Vh) chart data

Distance nodal (m)	Lateral discharge (GPM)	Friction-head-loss pipe,Hf_pipe (cm)	Friction-head-loss cumulative,Hf_cum (cm)	Friction factor,f (-)	Local-head-loss pipe,Lh_pipe (cm)	Local-head-loss cumulative,Lh_cum (cm)	Velocity head,Vh (cm)
0.848	2882.63	6.19	6.19	0.011605	5.625	5.625	133.674
1.696	2867.134	6.12	12.31	0.011614	5.565	11.191	132.241
2.542	2851.729	6.053	18.363	0.011623	5.506	16.696	130.824
3.387	2836.413	5.987	24.35	0.011633	5.447	22.143	129.422
4.232	2821.182	5.922	30.271	0.011642	5.389	27.532	128.036
5.076	2806.033	5.858	36.13	0.011651	5.331	32.863	126.665
5.919	2790.964	5.795	41.925	0.011661	5.274	38.138	125.308
6.761	2775.971	5.734	47.659	0.01167	5.218	43.356	123.965
7.604	2761.052	5.673	53.332	0.01168	5.162	48.518	122.637
8.445	2746.204	5.614	58.946	0.011689	5.107	53.625	121.321
9.286	2731.425	5.555	64.5	0.011699	5.052	58.677	120.019
10.127	2716.712	5.498	69.998	0.011708	4.998	63.675	118.729
10.967	2702.062	5.441	75.439	0.011718	4.944	68.619	117.452
11.808	2687.472	5.386	80.825	0.011728	4.891	73.511	116.187
12.648	2672.942	5.331	86.156	0.011737	4.839	78.349	114.934
13.488	2658.466	5.277	91.432	0.011747	4.786	83.135	113.693
14.328	2644.045	5.224	96.656	0.011756	4.735	87.87	112.463
15.168	2629.674	5.172	101.828	0.011766	4.683	92.554	111.243
16.008	2615.352	5.12	106.948	0.011776	4.633	97.186	110.035
16.848	2601.076	5.07	112.018	0.011786	4.582	101.768	108.837
17.689	2586.844	5.02	117.038	0.011796	4.532	106.3	107.649
18.53	2572.653	4.971	122.009	0.011806	4.483	110.783	106.471
19.371	2558.502	4.922	126.932	0.011815	4.434	115.217	105.303
20.212	2544.387	4.875	131.807	0.011825	4.385	119.601	104.145
21.054	2530.306	4.828	136.635	0.011835	4.336	123.938	102.995
21.897	2516.258	4.782	141.417	0.011846	4.288	128.226	101.855
22.74	2502.24	4.736	146.153	0.011856	4.241	132.467	100.723
23.584	2488.249	4.691	150.844	0.011866	4.193	136.66	99.6
24.429	2474.283	4.647	155.491	0.011876	4.146	140.807	98.485

Figure 32. The content of a sample Chart_FhlLhlVelH.Dat file

Lat_hElvHglEgl_Comp.Dat file

The Lat_hElvHglEgl_Comp.Dat file contains data on lateral elevation, hydraulic head, total head, and the lateral pressure profiles. The contents of a part of the Lat_hElvHglEg_Comp.Dat file is depicted in Figure 34. Although the Lat_hElvHglEg.Dat file also contains data on these parameters, the content of the Lat_hElvHglEgl_Comp.Dat file represents a more complete version of the hydraulic head, total head, and lateral pressure profiles compared to those in the Chart_ElvHglEgl.Dat file. Specifically, in the Lat_hElvHglEgl_Comp.Dat file, each of the hydraulic head, total head, and the lateral pressure profiles contain a pair of data points about each junction node along the lateral. For instance, the lateral pressure profile, in the Lat_hElvHglEgl_Comp.Dat file, would be comprised of an array in which pressure about each junction node is defined in terms of a pair of values, consisting of pressure evaluated at a point immediately upstream of a node and another one at a point just downstream of the node. Note that the exception here is the boundary nodes (i.e., the inlet- and distal-end nodes), where pressure can be defined only at a point about the node.

While conceptually important and is useful in the analysis of the spatial properties of the lateral pressure head profiles, the difference between the total head, hydraulic head, and lateral

// Emitter discharge, head differential across emitter, lateral discharge,prv-inlet pressure, and prv-operating status profiles

Dist. emitter - (m)	Emitter discharge - (L/s)	HDiff across emitter (m)	Lateral discharge - (L/s)	PRV inlet h-inlet (m)	PRV oper status (-)
0.8483	0.977637822	14.25565772	181.8656861	17.15645183	Passive
1.6955	0.97187878	14.08816541	180.8880483	16.99599831	Passive
2.5418	0.966311926	13.92720357	179.9161695	16.84180082	Passive
3.3872	0.960933285	13.77256239	178.9498576	16.69365839	Passive
4.2318	0.955742659	13.62414559	177.9889243	16.55147877	Passive
5.0757	0.950730662	13.4815995	177.0331816	16.41492316	Passive
5.9189	0.94589592	13.34480522	176.082451	16.28387765	Passive
6.7615	0.941237012	13.21364605	175.136555	16.15823045	Passive
7.6035	0.93674741	13.08786624	174.195318	16.03773656	Passive
8.4451	0.932424089	12.96731355	173.2585706	15.92225011	Passive
9.2862	0.928266668	12.85191302	172.3261465	15.81169933	Passive
10.127	0.924270679	12.74147975	171.3978799	15.70590705	Passive
10.9675	0.920435886	12.63594943	170.4736092	15.60481168	Passive
11.8078	0.916756634	12.53511205	169.5531733	15.50821204	Passive
12.6479	0.913234824	12.43896818	168.6364167	15.41610868	Passive
13.4879	0.909866953	12.34737306	167.7231818	15.3283629	Passive
14.3279	0.906651481	12.26023859	166.8133149	15.24489031	Passive
15.1679	0.903587235	12.17748932	165.9066634	15.16561864	Passive
16.008	0.900673008	12.09905129	165.0030762	15.09047703	Passive
16.8483	0.897909514	12.02490446	164.1024032	15.01944628	Passive
17.6888	0.895292553	11.95489937	163.2044936	14.95238322	Passive
18.5296	0.892824919	11.88907612	162.3092011	14.88932625	Passive
19.3707	0.890504498	11.82734552	161.4163762	14.83018994	Passive
20.2123	0.888332455	11.76970786	160.5258717	14.77497456	Passive
21.0543	0.886307199	11.71609222	159.6375392	14.72361218	Passive
21.8969	0.884428476	11.66646532	158.751232	14.67607091	Passive
22.7401	0.882700097	11.6209028	157.8668036	14.6324232	Passive
23.584	0.881120595	11.57934286	156.9841035	14.59260987	Passive
24.4286	0.879688861	11.54173536	156.1029829	14.55658287	Passive

Figure 33. The content of a sample EmitterDischargePressure.Dat file for Droptube-Prv-Emitter system configuration option

//Complete sets of lateral elevation, hydraulicgrade line, energy grade line, and pressure data

Distance nodal UpStrm/DnStrm (m)	Elevation (ELV) UpStrm/DnStrm (m)	Hydraulic grade-line,HGL UpStrm/DnStrm (m)	Energy-grade line,EGL UpStrm/DnStrm (m)	Lateral pressure UpStrm/DnStrm (m)
0	2.8	18.66163724	19.998382	15.86163724
0.8483	2.9181	18.59974101	19.93648577	15.68164101
0.8583	2.9181	18.55782049	19.88023226	15.63972049
1.6955	3.0286	18.49661807	19.81902983	15.46801807
1.7055	3.0286	18.45513767	19.76337745	15.42653767
2.5418	3.1317	18.39460671	19.70284649	15.26290671
2.5518	3.1317	18.35356392	19.64778859	15.22186392
3.3872	3.2274	18.29369686	19.58792153	15.06629686
3.3972	3.2274	18.25308922	19.53345163	15.02568922
4.2318	3.3155	18.19387167	19.47423408	14.87837167
4.2418	3.3155	18.15369681	19.42034588	14.83819681
5.0757	3.3963	18.09511477	19.36176384	14.69881477
5.0857	3.3963	18.05537028	19.30845117	14.65907028
5.9189	3.4697	17.99741699	19.25049788	14.52771699
5.9289	3.4697	17.95810054	19.19775476	14.48840054
6.7615	3.5356	17.9007626	19.14041683	14.3651626
6.7715	3.5356	17.86187193	19.0882374	14.32627193
7.6035	3.5942	17.80514306	19.03150853	14.21094306
7.6135	3.5942	17.76667589	18.9798871	14.17247589
8.4451	3.6455	17.71053659	18.9237478	14.06503659
8.4551	3.6455	17.67249071	18.8726788	14.02699071
9.2862	3.6894	17.61694186	18.81712995	13.92754186
9.2962	3.6894	17.57931511	18.76660796	13.88991511
10.127	3.726	17.52433791	18.71163075	13.79833791
10.137	3.726	17.48712817	18.66165048	13.76112817
10.9675	3.7552	17.43271728	18.60723959	13.67751728

Figure 34. The content of a sample of the Lat_hElvHglEgl_Comp.*Dat* file

pressure head profiles given in the Chart_ElvHglEgl.Dat and the profiles in the file Lat_hElvHglEgl_Comp.Dat, are practically marginal for most nodes, except those with significant local head losses.

Note that the data in the Lat_hElvHglEgl_Comp.Dat file is not used by the program to create charts. Instead, it is an optional content meant to be used in the analysis of the spatial properties of linear-move and center-pivot lateral pressure profiles.

5.1.1.d. Readme.Txt file

The Readme.Txt file is a text file that contains help information on the contents of a sample project folder and is intended to be used as a quick-help-info resource for users. The content of a sample Readme.Txt file is shown in Figure 35.

The file contains descriptive information on the contents of each file in a sample project folder. It also provides a summary of key input parameters that are used to create the input data file of the sample project and a qualitative description of the corresponding lateral's elevation profile and geometric and hydraulic characteristics. Although the Readme.Txt file is present in all of the sample project folders, it will not be automatically created by *LincSys* in projects created by the user subsequent to program installation.

5.1.1.e. The Charts subfolder

The Charts subfolder contains eleven image files in Png format, each of which represents a graphical rendering of the lateral elevation profile and computed hydraulic parameters (Figures 16 to 26). The list of the chart file names and a description of their contents is provided in Table 8. The Charts subfolder contains a text file, Readme.Txt, with a brief description of the contents of the folder.

5.1.2. HelpDocAndLiterature folder

The folder HelpDocAndLiterature contains two types of documents that can be accessed by users through the Help menu of *LincSys*: *(i)* files with help information that will be displayed on the screen when a relevant Help menu item is activated (Section 4.2.3.b) and *(ii)* a selected set of technical literature on lateral hydraulics and system design and management in Pdf format, which can be displayed on the screen by activating a Help menu item (Figure 8c). The files in the first category consist of the complete user manual: UserManual.Pdf and a second set of documents comprising each chapter of the manual as a standalone help document for quick access to a specific topic. This include: Chapter_1. Pdf, Chapter_2.Pdf, Chapter_3.Pdf, Chapter_4.Pdf, Chapter_5.Pdf, and Chapter_6.Pdf.

The technical literature consists of journal articles detailing the hydraulic principles and numerical algorithms that formed the basis of the numerical module of *LincSys* and additional reference materials in design and management of center-pivot irrigation systems. The names of the files that constitute the technical literature set are (Section 4.2.3.b): HydrLinIrrigSys_1.Pdf, HydrLinIrrigSys_2.Pdf, HydrLinIrrigSys_3.Pdf, and PressProfLinLat.Pdf, DesignOperationOfSprinklerSystems.Pdf, and CenterPivotIrrigationManagementHandBook.Pdf. The HelpDocAndLiterature folder also contains a text file, Readme.Txt, with a brief description of the contents of the folder.

These files are placed in the HelpDocAndLiterature during program installation and users must not alter the files in any way or move them to a different folder.

\//THIS FOLDER CONTAINS THE INPUT AND OUTPUT DATA FILES FOR THE CURRENT SAMPLE PROJECT

The following provides a description of the project:

Project attributes	Value	Explanation
* Project name	SampleProject_1	One of 15 sample projects that comes with the LincSys model, Verison 1.0
* Project files	Seven text files	Consisting of one input and six output files
.....	....	....
- InputData_LinLat.Inp	-	Project input Data file
- OutputData_LinLat.Out	-	Main project output data file
.....	....	....
- Chart_ElvHglEgl.Dat	-	Lateral elevation, hydraulic grade-line (HGL), and energy grade-line (EGL) data for charting
- Chart_EmitterPrvInletSetPres.Dat	-	Head differential across emitter, prv-inlet and prv-set pressures, and emitter discharge profiles data for charting
- Chart_FhlLhlVelH.Dat	-	Friction head loss, local head loss, and velocity head profiles data for charting
.....	....	....
- EmitterDischargePressure.Dat	-	Emitter discharge, head differential across emitter, lateral discharge, Prv-inlet pressure, and prv operating status data
- Lat_hElvHglEgl_Comp.Dat	-	Complete Lateral elevation, pressure, HGL, and EGL profiles data (Note: the pressure, piezometric head, and total head data in this file contains values corresponding to points immediately upstream and downstream of each node)
* Project subdirectory	Charts	Contains eleven image files consisting of hydraulic parameter charts
* System Configuration Option	DrptubePrvEmitter	This is a system that uses droptube, prv, and emitter assemblies to meter outlet discharges along the lateral
* A relatively short lateral	222.5m	
* Number of spans	8	Concave spans
* Short spans	27.7m	
* Large diameter pipes	212.6mm	
* Absolute roughness,low	0.0025mm	

Figure 35. The content of a sample Readme.Txt file in a sample project folder, for a system with Droptube-Prv-Emitter configuration option

5.1.3. Templates_InputDataFiles folder

The Templates_InputDataFiles folder contains *LincSys* input data files for laterals with number of spans ranging between 6 and 12. The contents and formats of these files are used by *LincSys* as templates for creating the input data file for a new project (Section 4.2.3.b).

Directly under the Templates_InputDataFiles folder are the DrptubePrvEmitter, DrptubeEmitter, and EmitterOnLat subfolders (Figure 27). These subfolders contain the input data template files (text files with extension Inp) for the Droptube-Prv-Emitter, Droptube-Emitter, and Emitter-On-Lateral system configuration options, respectively. Overall, there are a total of eight files in each of these subfolders. The name of the input data file in each subfolder consists of two parts: the basic input data file name (“InputData_LinLat”) and a string (“_6”,

Table 8. List of files in the *Charts* subfolder of a *LincSys* project folder

File name	Description of content
ChartEglHglElv.Png	Lateral elevation profile, hydraulic grade-line, and energy grade-line chart
ChartEmitDischarge.Png	Emitter discharge profile chart
ChartEmitPrvInletSetPres.Png	Emitter head differential, *prv*-inlet, and *prv*-set pressure profiles chart[(a)]
ChartLatDischarge.Png	Lateral discharge profile chart
ChartLatPressure.Png	Lateral pressure profile chart
ChartFhlPipeSeg.Png	Profile of friction head loss in lateral pipe segments
ChartFhlCum.Png	Cumulative friction head loss profile chart
ChartFrictionFactor.Png	Darcy-Weisbach friction factor profile chart
ChartLhlCum.Png	Cumulative local head loss profile chart
ChartLhlPipeSeg.Png	Local head loss in pipe segments profile chart
ChartVelHead.Png	Velocity head profile chart

[(a)] The chart depicts the emitter head differential, *prv*-inlet, and *prv*-set pressure profiles for the Droptube-Prv-Emitter system configuration option. For Droptube-Emitter or Emitter-On-Lateral system configuration option, however, the chart would show only the emitter head differential

"_7", "_8", "_9", "_10", "_11", or "_12"). These strings represent the number of spans (in the lateral) that a specific input data template file constitutes. For instance, the name of the file that contains the input data for a lateral with six spans would be InputData_LinLat_6.Inp.

Note that in all the three subfolders, under the Templates_InputDataFiles folder, the names and extensions of corresponding files are the same. In other words, for instance, the input data template file for a lateral with six spans has the name InputData_LinLat_6.Inp in all the three system configuration option subfolders. However, the contents of the files differ from one system configuration option folder to another.

These files are placed in the Templates_InputDataFiles folder during program installation and must not be altered in any way or moved to a different folder.

5.2. Model functionalities for input data validation and for detecting input data file format and runtime errors

The *LincSys* software has functionalities for detecting and reporting various kinds of errors. The main category of errors are: input data and runtime errors. The input data errors are further divided into four categories: incorrect numeric format, data out of acceptable range, data consistency, and wrong input data file format.

Furthermore, errors associated with input data can occur during the preparation of the input data file and hence are embedded in the input data file. Alternatively, they may occur during data editing in the *Input* window (Figures 10 to 12) of *LincSys*. Each of the input data error categories will now be discussed.

5.2.1. Errors related to input data

5.2.1.a. Incorrect numeric format

If a non-numeric string is inputted in a numeric field, then *LincSys* prints an error message on the screen indicating that an incorrect numeric format error has occurred. A numeric field could be an input box or a cell in the input data table of *LincSys* where a numerical input is expected. It could also be an entry in the input data file. A non-numeric string is comprised of a concatenated series of characters with one or more non-numeric characters, other than a decimal point.

5.2.1.b. Data out of range

Each input parameter of *LincSys* has a fixed feasible range of variation, which was set based on literature data and authors' experience (Table 4). Thus, if a data item specified in the input data file or edited in the Input window of *LincSys* is outside the set feasible interval, then *LincSys* prints on the screen an error message related to the input data range.

5.2.1.c. Data consistency

Data specified in the input data file or inputted in the Input window of *LincSys* needs to meet certain consistency criteria. First, the data in the non-tabular section ought to be in agreement with the corresponding data in the tabular data block. For instance, the length of the lateral, the number nodes, links, and system components specified in the non-tabular data block need to be of the same value as the corresponding entries in the tabular data section. Furthermore, the data variability pattern in many of the input data table columns need to be consistent with the patterns of variability of the topological data, which are specified in the first three columns of the input data table (Sections 4.3.3.a, 4.3.3.b, and 4.3.3.c). In addition, data in the input data table need to meet required relationships between data columns, specifically: between input data table columns #4, 5, and 6; between columns #9 and 10; and between columns # 12 and 13.

Finally, data items related to links that are associated with lateral pipe segments can be specified only in odd-numbered rows of the input data table and input data related links representing outlet discharge metering apparatuses can only be specified in even-numbered rows of the table.

If an input data item (either in the input data file or in the Input window of *LincSys*) violates any of these input data consistency requirements, then *LincSys* will print on the screen an error message related to data consistency.

5.2.1.d. Wrong input data file format

As can be noted from Figure 28, the input data file (InputData_LinLat.Inp) has a specific format that needs to be strictly observed when preparing the input data file. The first three lines of the input data table are non-data rows. The first row is a title row and describes the type of lateral and the system configuration option considered. The second row consists of a string of asterisks and the third row is an empty row.

The non-tabular input data block starts in the fourth row and it would be comprised of 17, 14, or 12 rows depending on whether the system configuration option is Droptube-Prv-Emitter, Droptube-Emitter, or Emitter-On-Lateral, respectively.

The non-tabular input data and the tabular input data blocks are separated by two non-data rows: an empty row followed by a row with a string of asterisks. Furthermore, at the top of the tabular data section there are four non-data rows consisting of the column headings of the tabular data.

If any of these rows are missing, *LincSys* will print on the screen an error message indicating that there is an error in the input data file format and needs to be corrected before a simulation run can be executed. Note that the format of the input data file must not be changed in any way.

5.2.1.e. Occurrences of input data error

As noted earlier, the input data errors described in the preceding sections can occur in the input data file (InputData_LinLat.Inp) during input data preparation or they may be introduced during data editing in the Input window of *LincSys*. Thus, the time that the error message is displayed during a simulation session and the form of the message depends on whether the error is in the input data file or was introduced during data editing.

Input data error in the input data file

In the event that the input data error occurred in the input data file, upon activation of the Input window from the Systems-Projects tabpage, *LincSys* would be unable to populate the input boxes and the input data table of the Input window with data. Thus, under such a scenario, the Input window will be displayed with no data. Superimposed on the Input window would be the input data error dialog box with an error message. An example of such a screen is displayed in Figure 36.

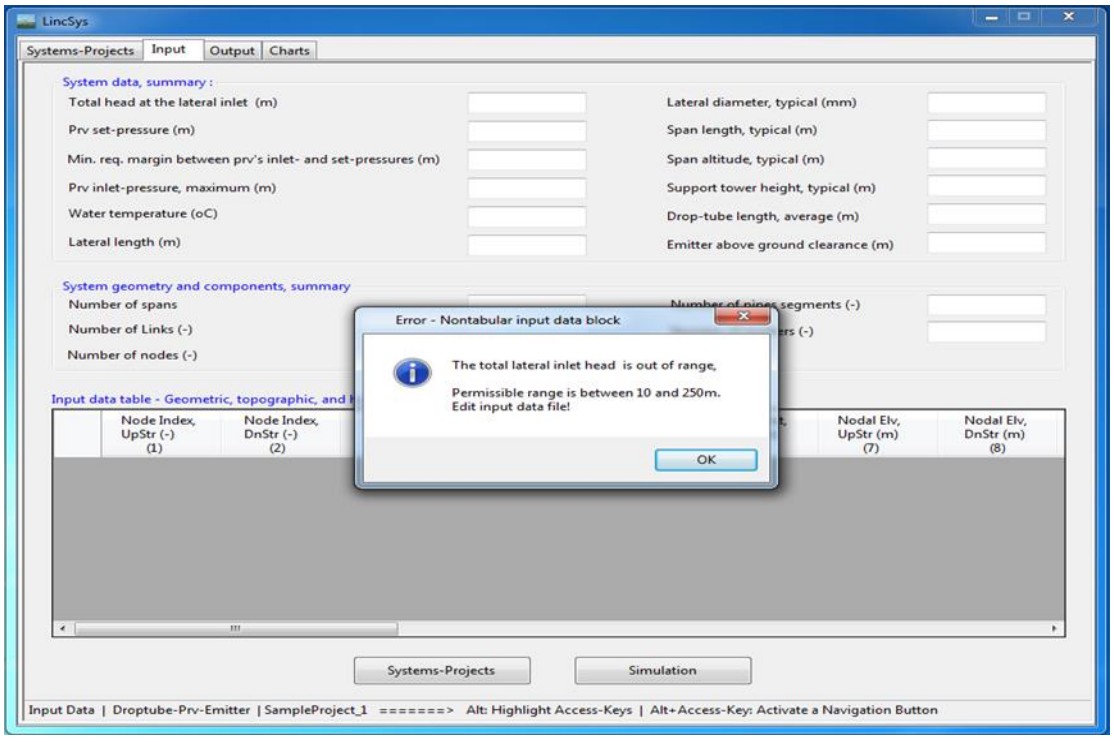

Figure 36. Error message - input data out of range: Input data error that occurred in the input data file (InputData_LinLat.Inp) during data preparation phase

As can be noted from Figure 36, the error dialog box has two components: a title in the titlebar of the dialog box and a message printed in the main body of the dialog box. The tittle indicates that the message in the dialog box is an error message and it also states that the error occurred in the non-tabular data block.

The main body of the dialog box contains the actual error message, which also contains two parts. The first part describes the specific parameter the error relates to, the nature of the error, and possible remedy. The second part, which is displayed at the bottom row of the error message points to where the error occurred (i.e., in the input data file or introduced during data editing in the Input window). For the current project (Figure 36), the error occurred in the input data file and hence the error message states that the user needs to edit the input data file: "Edit input data file".

A click on the Ok button of the dialog box will close the dialog box and returns program control to the Systems-Projects window. The user may then need to open the input data file (InputData_LinLat.Inp) with a suitable application and edit the data item, identified to be in error, in accordance with the suggestion in the error dialog box before initiating a new simulation event.

Input data error introduced during editing of input data in the Input window

If, on the other hand, the input data error is introduced in the Input window during data editing, then error message will be displayed on the screen when the Simulation button, in the Input window, is activated following data editing. Figure 37, for instance, displays an error message related to the range of an input data item.

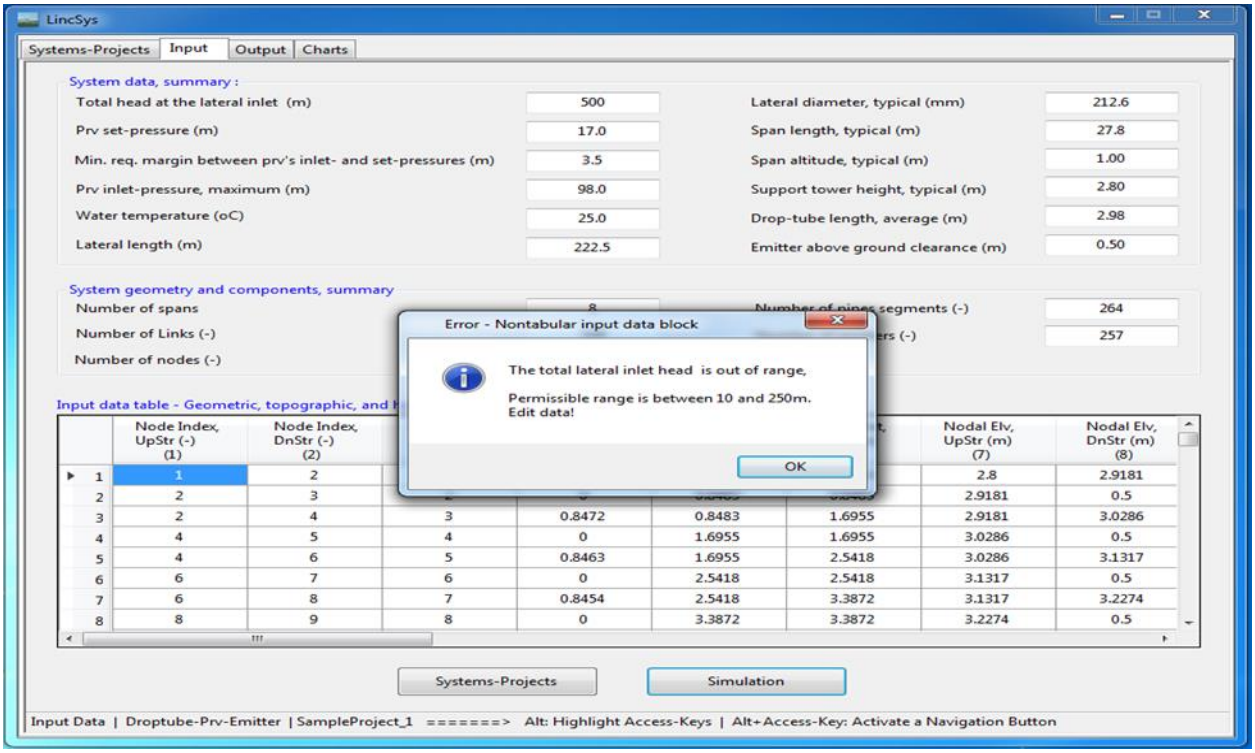

Figure 37. Error message - input data out of range: input data error introduced during data editing in the Input window

Note that the message in the error dialog box of Figure 37 has the same components as that shown in Figure 36. Furthermore, the core error message is the same, because the parameter that the error is associated with, the nature of the error, and possible solutions are the same. However, the error, in the current case, occurred in the Input window during data editing and hence the message at the bottom row of the dialog box is "Edit data", implying that the data in the Input window needs to be corrected.

A click on the Ok button of the dialog box will clear the dialog box and returns program control to the Input window. The new Input window will display the original (i.e., error free data), which can then be edited by the user if need be.

Note that for errors that occur in the input data table, the form of the error dialog box and the time at which the dialog box is displayed on the screen (during a simulation event) also depends on whether the error occurred in the input data file, during the data preparation phase, or is introduced during data editing in the Input window. The only difference is that for errors that occur in the input data table, the specific parameter associated with an input data error is identified in the error message dialog box by the row and column index of the input data table cell where the error occurred.

5.2.2. Model runtime error

LincSys generally produces an output following a simulation run. However, some combinations of input parameters may lead to infeasible hydraulic scenarios, in which case program execution ends with a runtime error. One such error, for instance, arises when a relatively small inlet head is used in a moderate to small diameter lateral that is outfitted with high capacity emitters.

There are nine categories of run time errors (Section 4.3.4) in total that have been identified in the course of the development and testing of *LincSys*. If any of these errors occur during a simulation run, then program execution ends without an output and the program prints an error message on the screen. The error message would be consisting of information on the nature of the error along with a suggestion for possible remedy. An example of a runtime error message is displayed in Figure 38.

As can be seen from Figure 38, the model runtime error dialog box has a title "Runtime Error" displayed in the titlebar of the box and a description of the error message in the main body of the dialog box.

The message displayed in the main body of the dialog box has two components. The first part, which comes under the heading runtime error description, states the nature of the model runtime error. The second part, which is placed under the heading suggested solutions, describes possible solutions that may lead to a successful simulation.

Clicking on the Ok button at the bottom of the dialog box will close the dialog box and returns program control to the Input data table, where the user can edit the input data in accordance with the suggested solution.

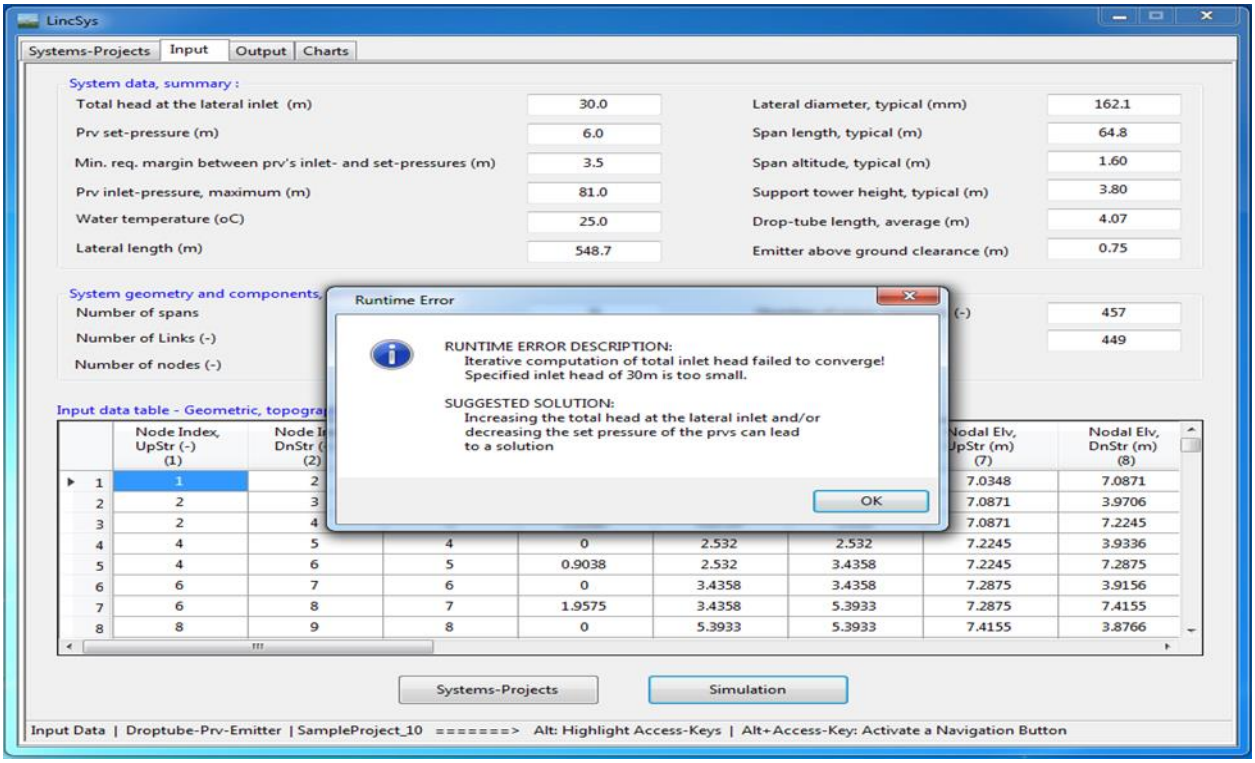

Figure 38. Sample model runtime error dialog box of *LincSys*

Chapter 6. Results of model evaluation and application examples

Results of model evaluation and input-output data from a selected set of application examples (Section 5.1.1.a) are presented in this chapter.

6.1. Model evaluation

6.1.1. Introduction

The current authors and cooperators have conducted a limited evaluation of the hydraulic module of *LincSys*, *HydrSimLaterals.exe*, in which computed lateral pressure head profiles and lateral inlet discharges were compared with measured data (Zerihun et al., 2019). The results of that study is, in large part, reproduced here.

The data was obtained through field measurements performed on a linear-move sprinkler irrigation system with a Droptube-Prv-Emitter system configuration. The system obtained its water supply from a concrete-lined canal and was operated under steady flow conditions. Each span consists of multiple outlet ports placed at variable spacings. Drop-tubes were used to convey water from the overhead outlet ports down to each *prv*-emitter assemblies. Each spray nozzle was coupled to a *prv* at its inlet-end so as to maintain a set nozzle pressure and hence discharge.

Three hydraulic data-sets, consisting of lateral pressure head profiles and inlet discharges, were obtained through the field measurements. One of the data-sets was used in parameter estimation and the remaining two data- sets were used in model verification, i.e., comparison of

measured and simulated lateral pressure head profiles and inlet discharges. Descriptions of the linear-move sprinkler irrigation system used in the study, field measurements, and results of model evaluation will now be presented.

6.1.2. Description of the linear-move sprinkler irrigation system used in model evaluation

Irrigation field evaluations were conducted in the spring of 2018 on a linear-move sprinkler irrigation system installed on the research farm of the Maricopa Agricultural Center of the University of Arizona, Maricopa, AZ. The linear-move system was managed by the USDA-ARS Arid-Lands Agricultural Research Center. The irrigated field, which covers an area of approximately 6ha, was laser leveled in the weeks before the field evaluations. The effective length of the lateral considered for hydraulic modeling purpose was 361.7m, which covered the distance between a point on the lateral just upstream of the first emitter (treated here as the lateral inlet) and the downstream-end outlet of the lateral.

Note that in subsequent discussions, the spans that make up a lateral are numbered sequentially starting from the upstream-end span, which is referred here as span #1, and increasing in the downstream direction along the lateral.

The lateral had seven spans and, as noted earlier, it obtained its water supply from a concrete-lined canal (Figure 39). The effective length of span #1 was 50.8m (Figure 39). Spans #2 to 6 were each 56.8m long. The effective length of span #7 was 27.0m, which was the distance of the distal-end outlet on the lateral from the span inlet. Each of spans #1 to 6 were supported at both ends with wheeled towers. Span #7, on the other hand, was a cantilever type beam and was supported by a wheeled tower at its inlet-end and suspension cables anchored at the tower.

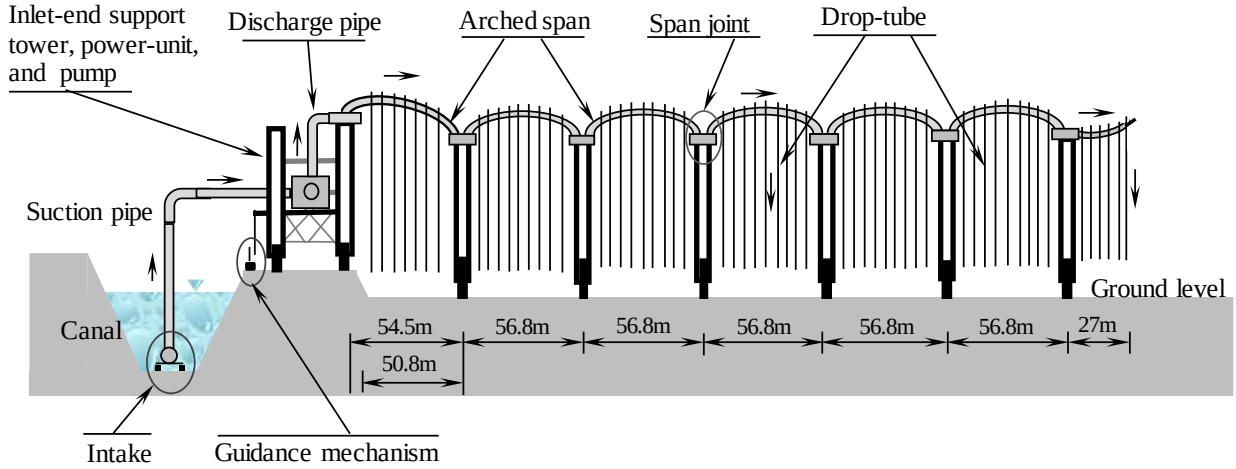

Figure 39. A sketch of the linear-move sprinkler irrigation system used in the field evaluations

The machine was powered by a diesel engine placed on the support-tower at the inlet-end of span #1. This tower travelled on an elevated track along the berm of an embankment of the field supply canal, but the tower attached to the distal-end of the span had its wheels on the field surface (Figure 39). Hence, the upstream-end span was inclined at an appreciable negative gradient between its inlet- and distal-ends. By comparison, spans #2 to 7 were all run on a level

field. Based on machine specification data (Senninger, 2015) and field measurements, it was deemed that spans #2 to 6 had the same geometry. In other words, they had the same length, same maximum in-span elevation differential, and also a curve tracing the centerline of each of these spans was considered here to be symmetric about a vertical line through the span's mid-point. As can be noted from Figure 39, the elevation profile, of each of spans #1 to 6, has a concave form. Thus, for these spans the point of maximum in-span elevation occurred somewhere in between the inlet and distal-end of the spans (Figure 39) and the minimum in-span elevation occurred at the span inlet-end and/or distal-end. In contrast to spans #1 to 6, the elevation profile of span #7 was a convex curve and the point of maximum in-span elevation occurred at the distal-end of the span, and the minimum was somewhere between the inlet and distal-ends of the span.

Except for span #7, pipe diameter was constant along the lateral. A diameter of 162.3mm (6.39″) was used over spans #1 to 6 (Table 9a). Lateral diameter was then reduced to 136.4mm (5.37″) over the upper 13.8m long reach of span #7. It was reduced further to 101.6mm (4.0″) over the distal 13.2m long section of the span. The lateral had a total of 349 emitters, with 49 emitters in span 1; 55 emitters each on spans 2, 4, 5, and 6; 53 emitters on span 3; and 27 emitters on span 7. The emitter model used in this lateral was Super spray UP3 produced by Senninger (Senninger, 2017b). The nozzle size was 4.763mm (3/16)″. The coefficient and exponent of the hydraulic characteristic function of the emitter, obtained based on head-discharge data provided in the manufacturer's catalogue, is summarized in Table 9b. A pressure reducing valve, *prv*, was attached to the inlet-end of each emitter. The *prv* model used in this lateral was *PSR2* (Senninger, 2017a). The *prv*-set pressure, h_{prv}; the maximum allowable inlet pressure for the *prv* to operate reliably in the active mode, h_{max}; and the minimum required pressure head margin between the set pressure and the inlet pressure for the *prv* to operate reliably in the active mode, δh_{prv}, are summarized in Table 9b. Drop-tube lengths vary between 2.6 and 4.4m and they were set such that each *prv*-emitter assembly was suspended from the lateral outlet at a uniform above ground clearance of about 0.76m (2.5ft), when the lateral was installed in a level field (Senninger, 2015). The drop-tubes had a constant diameter of 19.05mm (3/4″).

6.1.3. Determination of lateral elevation profile

The elevation profile of span #1 was different from spans #2 to 6, mainly because of the differences in slopes. The profile of span #7 was also different from the spans upstream, because of the differences in the general concavity structure of the elevation profiles of span #7 and the other spans. As noted earlier, spans #2 to 6 had the same geometry and were running on a level field, thus they had the same elevation profile. This implies that the elevation profile measured along any one of these spans should be applicable to the rest of the spans, after accounting for the differences in the distances of outlet-ports and span joints from the lateral inlet. Thus, determination of the elevation profile of the centerline of the entire lateral was made based on measurements over spans #1, 2, and 7 only. Accordingly, a profile survey was conducted over spans #1, 2, and 7 using the elevation of the field surface (which as noted earlier was considered horizontal) as datum. The measured elevation profile data for spans #1 and 2 were fitted to the equation of an ellipse and a cubic polynomial was fitted to the data for span #7, each with a coefficient of determination (r^2) of 0.99. Note that the elevation profile of span #2 was used to

Table 9a. Lateral hydraulic, geometric, and elevation data used in model evaluation

Lateral parameters		Units	Data-set[(a)]		
			1	2	3
Number of spans		-	7		
Effective span length[(b)]		*m*	27, 50.8, and 56.8		
Lateral length	Horizontal	*m*	361.7		
	along center-line	*m*	362.0		
Support tower height		*m*	3.7		
Elev. differential between span joint and field surface		*m*	3.62		
Maximum in-span elevation differentials[(c)]		*m*	(1.15/1.50)/(0.65/0.74)		
Lateral diameter [(d)]		*mm*	162.3 / 136.4 / 101.6		
Absolute roughness	Lateral pipe	*mm*	0.0015		
	Drop-tube	*mm*	0.0015		
Drop-tube length range		*m*	2.6-4.4		
Emitter spacing, horizontal		*m*	0.59-1.65		
Drop-tube diameter		*mm*	19.05		
Field surface slope		*%*	0.0		
Local head loss parameters	branching, outlet	-	0.03		
	line-flow, outlet	-	0.008		
	bending, connector	-	0.02		
	span joints	-	0.04		
	Contraction [(e)]	-	0.104 / 0.195		
Constant total head at the inlet[(f)]		*m*	19.2, 23.4, and 27.7		
Elev. at the inlet		*m*	4.84		

(a) Data-sets 1, 2, and 3 pertain to an actual linear-move system with six full spans and a cantilever type beam at its downstream-end. Thus, all the lateral parameters are the same for these data-sets except the total head at the inlet.

(b) Effective span lengths, i.e., lengths considered for modeling purpose, are 50.8m for the inlet-end span, 56.8m for spans #2 to 6, and 27m for the distal-end span.

(c) The maximum in-span elevation differentials of the lateral are: 1.5m for the upstream-end span and 1.15m for spans #2 to 6. For span #7, the maximum elevation differentials are 0.65m during irrigation and 0.74m when the lateral is idle.

(d) The linear-move system has a diameter of 162.3mm over spans #1 to 6, span #7 has a diameter of 136.4mm over the upper 13.8m segment of the span and has a diameter of 101.6mm over the lower 13.2m long section of the span.

(e) The local head loss coefficients for sudden contraction of lateral cross-sectional area are obtained from Granger (1995) based on pipe diameter ratios.

(f) The inlet heads for data-sets 1, 2, and 3 are 19.2, 23.4, and 27.7m, respectively.

Table 9b. Emitter and *prv* data of the linear-move system used in model evaluation

Lateral parameters			Units	Data-set		
				1	2	3
Number of *prvs*, emitter, and drop-tubes			-	349		
Emitter data [(a)]	Emitter model		-	Super spray UP3		
	Nozzle size		*mm (in)*	4.763 (3/16)		
	Parameters of emitter head-discharge function	β	$L/s/m^{\lambda}$	0.0771		
		λ	-	0.4998		
prv data[(b)]	*prv* model		-	PSR2		
	prv parameters	h_{prv}	*m*	4.2		
		δh_{prv}	*m*	3.5		
		h_{max}	*m*	90		

[(a)] Emitters are produced by Senninger (Senninger, 2017b), β and λ are coefficient and exponent, respectively, of the emitter head-discharge function obtained by fitting a power function to the data provided in the manufacturer's catalogue. [(b)] *prvs* are from Senninger (Senninger, 2017a), h_{prv} is *prv*-set pressure head; δh_{prv} is the minimum required pressure head margin, between the *prv*-inlet pressure and h_{prv} in order for the *prv* to operate reliably in the active mode; and h_{max} is the maximum allowable pressure at the *prv* inlet for the *prv* to operate reliably in the active mode.

define those of spans #3 to 6 as well. The lateral elevation profile defined in terms of the regression equations was used as model input.

The measured elevation profile showed that span #1 was inclined at an average slope of -1.7% between its inlet- and distal-ends. As a result, the point of maximum in-span elevation was upstream of the span mid-point and was located at a distance of 15.7m from the lateral inlet. The overall elevation increment from the lateral inlet (i.e., the location of the upstream-end pressure gauge) to the highest point in the span was 0.3m. However, the decrement in elevation over the lower 35.1m long reach of span #1 was 1.5m, which is five times the increment in elevation that occurred over the upstream section of the span. By contrast, the elevation profile of each of spans #2 to 6 can be considered symmetrical about a vertical line through the span mid-point. Thus, for each of these spans the increment in elevation over the upper-half was the same as the elevation decrement over the lower-half and was equal to 1.15m. The elevation of the lateral centerline at the span joints (i.e., at points above the support towers) was 3.62m. Note that elevation of lateral centerline was measured with respect to the field surface, which was slightly higher than the wheel tracks of the support towers due to compaction from previous passes of the machine.

Elevation profile measurements were made during an off-time, when the system was idle and parked at a fixed position. The elevation profiles of spans #1 to 6 were considered the same during irrigation as well as when the system was idle, because each of these spans were supported at both ends. By comparison, the elevation profile of span #7 differed slightly depending on whether the machine was idle or irrigating. The maximum elevation of span #7, measured when the system was idle, was 4.16m and it occurred at the distal-end outlet of the span. The corresponding maximum in-span elevation differential was 0.74m. However, during an irrigation event the elevation profile of this span, which was supported only at its inlet end, underwent a vertical deflection under the weight of the irrigation water. As a result, the maximum elevation of the span decreased to about 4.01m and the corresponding maximum in-span elevation differential was 0.65m. Furthermore, a close look at the elevation profile (geometry) of span #7 showed that it was not symmetrical about a vertical line through its mid-

point. Span elevation decreased by 0.26m over the upper 13.8m long reach of the span and then increased by 0.65m over the lower 13.2m section of the span, which represents a more than 2.5 fold rise in elevation over the lower section of the span compared the total decrease in elevation over the upper segment of the span. Differences in the general concavity structure of the spans elevation profiles and the presence or lack of symmetry, in the span elevation profiles, about the mid-point of the spans can have appreciable effects on the spatial trends of the lateral pressure head profiles. A more detailed discussion on these effects is provided by Zerihun and Sanchez (2019c).

6.1.4. Irrigation field evaluations and determination of model parameters

In the spring of 2018, three irrigation field evaluations were conducted on the linear-move system described above (data-sets 1, 2, and 3, Tables 9a and 9b). The goal of the irrigation field evaluations was to collect lateral pressure head profile and inlet discharge data for model verification purposes. Accordingly, a total of thirty-two pressure gauges, five on each of spans #1 to 6 and two on span #7 were installed prior to the irrigation evaluations. Ten of the pressure gauges had data loggers and hence recorded pressure automatically at a preset time interval. Twenty-two of the pressure gauges were analog gauges. The gauges with data loggers were all installed in spans #2 and 3 and the analog gauges were installed on spans #1, 4, 5, 6 and 7. In order to capture the effects of the in-span elevation differential on the span-scale pressure head variations more accurately, the five gauges installed in each of spans #1 to 6 were arranged as follows: one of the gauges was installed close to the span inlet, another one close to the distal-end of the span, and a third one was placed near the mid-point of the span. The remaining two gauges were installed at distances of about one-quarter and three-quarters of the span length from the span inlet. In span #7, the first gauge was placed close to the inlet-end of the span and the second gauge was placed near the span's mid-point, where elevation was minimum.

All system parameters, except for the total head at the lateral inlet, were kept constant during each of the evaluations. Prior to the start of each irrigation evaluation event, pressure at the discharge-end of the pump was adjusted to pre-determined levels by varying the opening of the valve. The corresponding total heads at the lateral inlet were 19.2, 23.4, and 27.7m for data-sets 1, 2, and 3, respectively (Table 9a). Note that these refer to the total heads at the location of the upstream-end pressure gauge and were determined as a function of the measured lateral pressure heads, lateral discharges, and lateral elevation at the upstream-end pressure gauge. Once the pressure at the pump was adjusted to a pre-determined level, the system was operated for a minimum of 5min before a field evaluation event began, to ensure that the flow through the lateral reached a steady-state corresponding to the newly set inlet head.

Each field evaluation event lasted 20min. At each station with an analog gauge, pressure readings were taken manually every 5min. This resulted in a total of six data points per station per evaluation. The pressure gauges with data loggers, on the other hand, were preprogrammed to record pressure every minute, resulting in a total of twenty-one data points per station. For each irrigation evaluation event, the station averages were treated as the local steady state pressure head values. Furthermore, during a field evaluation event discharge at the lateral inlet was measured every 5min with a digital flow meter built into the upstream-end support-tower. The average lateral inlet discharge for an event was considered as the corresponding steady inflow rate into the lateral.

The field measured lateral pressure profiles and inlet discharges were used in model evaluation. Data-set 1 was used in parameter estimation and data-sets 2 and 3 were used in model verification. Lateral parameters estimated based on data-set 1 were lateral pipe absolute roughness and local head loss coefficients. To the best of authors' knowledge there is no modeling capability, that solves the inverse problem of linear-move lateral hydraulics, that can be readily used here to estimate the model parameters. Thus, a simple trial and error approach was used to obtain a parameter set that resulted in a reasonable match between the simulated and measured lateral pressure head profiles. Given a set of parameter estimates, visual comparison of the simulated and measured pressure head profiles was used to qualitatively assess the goodness of fit between the profiles. The parameter (i.e., pipe absolute roughness and local head loss coefficients) estimates obtained as such are summarized in Table 9a. A simple error metric termed, here, as percent absolute residuals or simply as absolute residuals was used to obtain a quantitative measure of the differences between field measurements and model predictions. Note that the absolute residuals of lateral pressure head profiles or inlet discharges were defined, respectively, as the difference between model predicted and measured values, expressed a percentage of those obtained through measurement.

As can be noted from Table 10. the absolute residuals between the simulated and measured lateral pressure head profiles of data-set 1 (i.e., the data-set used in parameter estimation) vary between a minimum of 0.1% and a maximum of 10.9% and the average is 5.1%. Furthermore, the absolute residuals between the simulated and measured lateral inlet discharges of data-set 1 is 8.8% (Table 11). Now, results of model verification obtained, based on the parameter estimates summarized in Table 9a, are presented next.

Table 10. Residuals between measured and computed lateral pressure head profiles

Absolute residuals	Units	Data-set		
		1	2	3
Minimum	(%)	0.1	0.2	0.1
Average	(%)	5.1	3.7	3
Maximum	(%)	10.9	14.3	16

Note: Absolute residuals are calculated as the absolute difference between computed and measured pressure heads expressed as percentage of the measured pressure heads

Table 11. Measured and computed lateral inlet discharges and residuals

Data-set	Lateral inlet discharge (L/s)		Absolute residuals (%)
	Measured	Simulated	
1	50.7	55.2	8.8
2	51.4	55.2	7.5
3	53.5	55.2	3.3

Note: Absolute residuals are calculated as the absolute difference between computed and measured lateral inlet discharges expressed as a percentage of the measured discharges

6.1.5. Results of model verification

6.1.5.a. Comparison of measured and simulated lateral pressure head profiles

Figures 40a and 40b depict the simulated lateral pressure head profiles, for data-sets 2 and 3, superimposed on the corresponding measured pressure head profiles. In Figure 40, the simulated and measured pressure head profiles are shown as dashed-line and circles, respectively, while the elevation profile of the lateral is shown in solid-line.

Visual observations of Figures 40a and 40b suggest that the simulated pressure head profiles of data-sets 2 and 3, for the most part, closely track the respective measured profiles. To provide a quantitative measure of the model prediction errors, the percent absolute residuals between the simulated and measured pressure head profiles are summarized in Table 10. Accordingly, the absolute residuals between the simulated and measured lateral pressure head profiles vary between 0.2 and 14.3% for data-set 2 and between 0.1 and 16% for data-set 3. The average absolute residuals of the lateral pressure head profiles are 3.7% for data-set 2 and 3% for data-set 3. The average absolute residuals obtained for both data-sets suggest a reasonably good agreement between the simulated and measured pressure head profiles. The maximum absolute residuals may not be considered sufficiently small. However, a comparison of the average and maximum absolute residuals, obtained for each data-set, suggests that the maximum absolute residuals may not be good indicators of the overall error levels in the computed pressure head profiles. In fact, it can be shown that if the pair of measured pressure heads corresponding to the maximum absolute residuals are excluded from the respective pressure head profiles, the maximum residuals would be reduced from 14.3 to 8.8% for data-set 2 and from 16 to 8.5% for data-set 3.

6.1.5.b. Linear-move lateral pressure head profile, local in-span patterns and inter-span trends

As can be noted from Figures 40a and 40b, both the simulated and measured pressure head profiles of the linear-move lateral show distinct spatial variability attributes, consisting of local span-scale variability patterns (solid-line) and broader inter-span/lateral-wide trends (dash-dotted line). The implication is that a complete characterization of the pressure head profiles of the lateral requires that both spatial variability attributes be assessed. The local in-span pressure variability patterns are important, because they reflect the actual spatial properties of lateral pressure and also eventually determine the corresponding inter-span lateral pressure variability trends. On the other hand, the significance of the inter-span trend curve stems from the fact that it encapsulates the broader spatial behavior of the lateral pressure head profile, considered over multiple spans, in the form of a curve with a clearly discernible and relatively simple monotonic property. However, it ought to be noted that the curve representing the inter-span trends was not computed, instead it was obtained by simply connecting the inlet- and distal-ends of each span manually (Section 4.5.2.b).

As can be noted from Figures 40a and 40b, the in-span lateral pressure variability patterns have a convex form, over each of spans #1 to 6, and a concave form in span #7. Given that the system parameter set is almost constant across the lateral (Tables 9a and 9b), it can be readily reasoned that the basic forms of the local in-span lateral pressure variability patterns observed in Figure 40 can be attributed to span geometry effects. However, results of an earlier study by Zerihun and Sanchez (2019c) show that field slope and lateral diameter can dampen, amplify, and/or skew the basic span geometry effects on lateral pressure profile. Additional discussion on lateral pressure variability patterns is provided in Section 6.2.1.c.

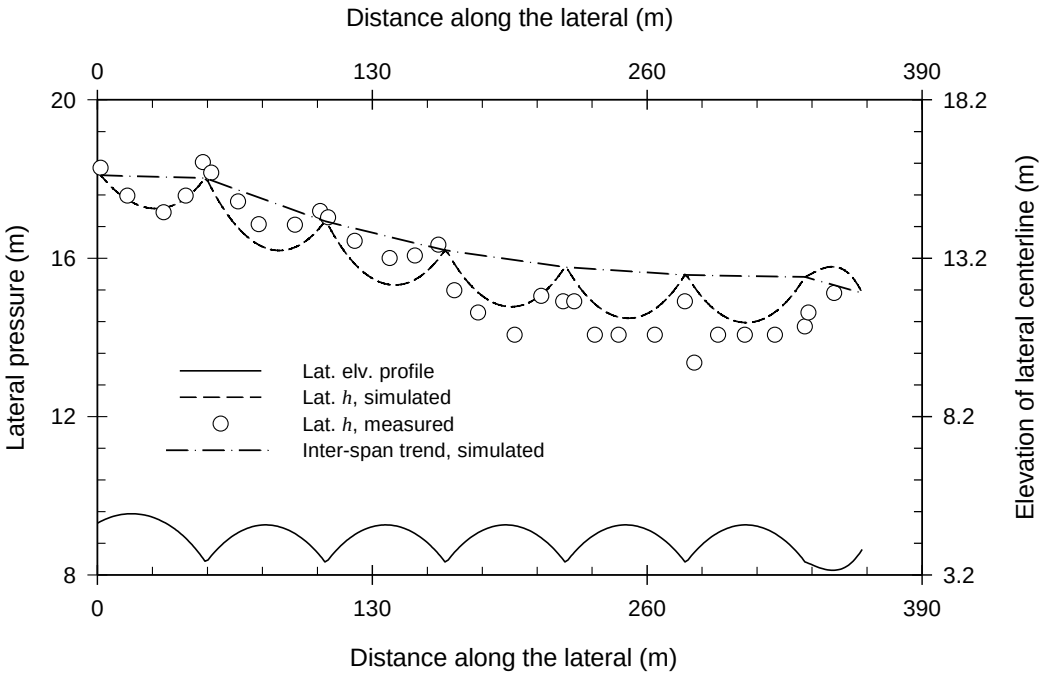

(a)

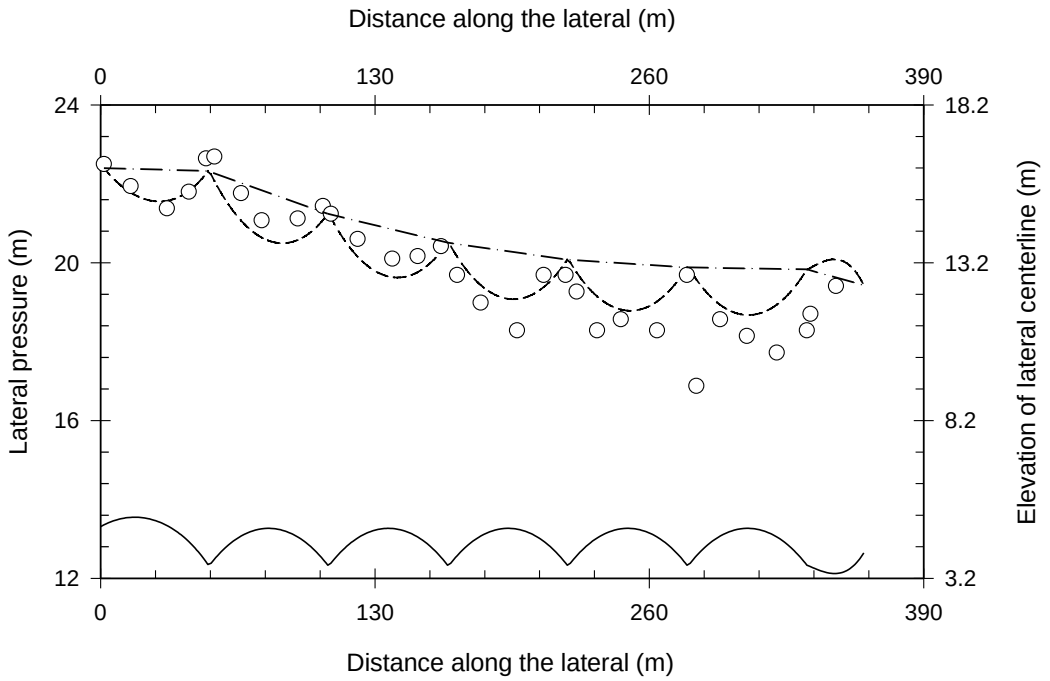

(b)

Figure 40. Comprison of measured and simulated lateral pressure head profiles: (a) Data-set 2 (inlet head of 23.4m) and (b) Data-set 3 (inlet head of 27.7m) [Note: Lat. *h* in Figure 40a is lateral pressure profile]

6.1.5.c. Comparison of measured and simulated lateral inlet discharges

As can be noted form Table 11, the measured lateral inlet discharges are 51.4L/s for data-set 2 and 53.5L/s for data-set 3. By comparison, for both data-sets 2 and 3 the simulated inlet discharge is 55.2L/s. The corresponding absolute residuals between the measured and simulated inlet discharges are 7.5 and 3.3% for data-sets 2 and 3, respectively, which suggests a satisfactory agreement between measurements and model predictions.

6.2.5.d. Lateral-wide operating scenarios of the prvs

The measured lateral inlet discharges for data-sets 1, 2, and 3 vary between 50.7 and 53.5L/s (Table 11). By contrast, the simulated lateral inlet discharge for all the data-sets is 55.2L/s. To gain some insight on the possible sources of the differences between the measured and computed lateral inlet discharges, the simulated lateral-wide operating scenarios of the *prvs* corresponding to all the three data-sets used in model evaluation are examined here.

The profiles of the minimum required inlet pressure heads for the *prvs* to operate reliably in the active mode, h_{min}, the simulated *prv*-inlet pressure heads, h_u, and emitter discharges, Q_s, for data-sets 1, 2, and 3 are depicted in Figure 41. Note that h_{min} is defined as the sum of the *prv*-set pressure, h_{prv}, and the minimum required margin between h_u and h_{prv} for the *prv* to operate reliably in the active mode, δh_{prv}. The values of h_{prv} and δh_{prv} for the *prvs* used in the lateral are given in Table 9b and the h_u and Q_s profiles are outputs of hydraulic simulations. Note that h_{min} is the same for the three data-sets, because the same h_{prv} and δh_{prv} are used in each data-set.

As can be noted from Figure 41, for each of the data-sets the simulated h_u exceeds h_{min} over the entire lateral length. Furthermore, a close look at the simulated h_u profiles of data-sets 1 to 3 show that the maximum h_u is 26.8m (data-set 3), which is well below the 90m threshold given in Table 9b as the maximum allowable inlet pressure head for the *prv* to operate reliably in the active mode, h_{max}. This indicates that for each of the data-sets, $h_{min} < h_u < h_{max}$ over the entire lateral length. The implication is that, for each data-set, all the *prvs* in the lateral were operating in the active mode and hence the *prv*-outlet pressure head was constant along the lateral and was equal to the *prv*-set pressure, which was 4.2m. The corresponding constant emitter discharge along the lateral was 0.158L/s (Figure 41). This shows that the lateral inlet discharge of 55.2L/s, computed for each of the data-sets, corresponds to a hydraulic scenario in which all the *prvs* in the lateral were operating in the active mode. On the other hand, the slightly lower measured lateral inlet discharges, relative to the discharge required for all the *prvs* in the lateral to be considered active, suggest that during the field evaluations some of the *prvs* in the lateral may have actually been operating in the passive mode. However, it ought to be noted that the differences between the measured and simulated lateral inlet discharges could at least partly be attributed to measurement errors, errors related to accuracy of pressure regulation, and possibly to some malfunctioning *prvs* and/or emitters. Naturally, modeling errors, including numerical approximation and mathematical representation of the physical process, may have contributed to a degree.

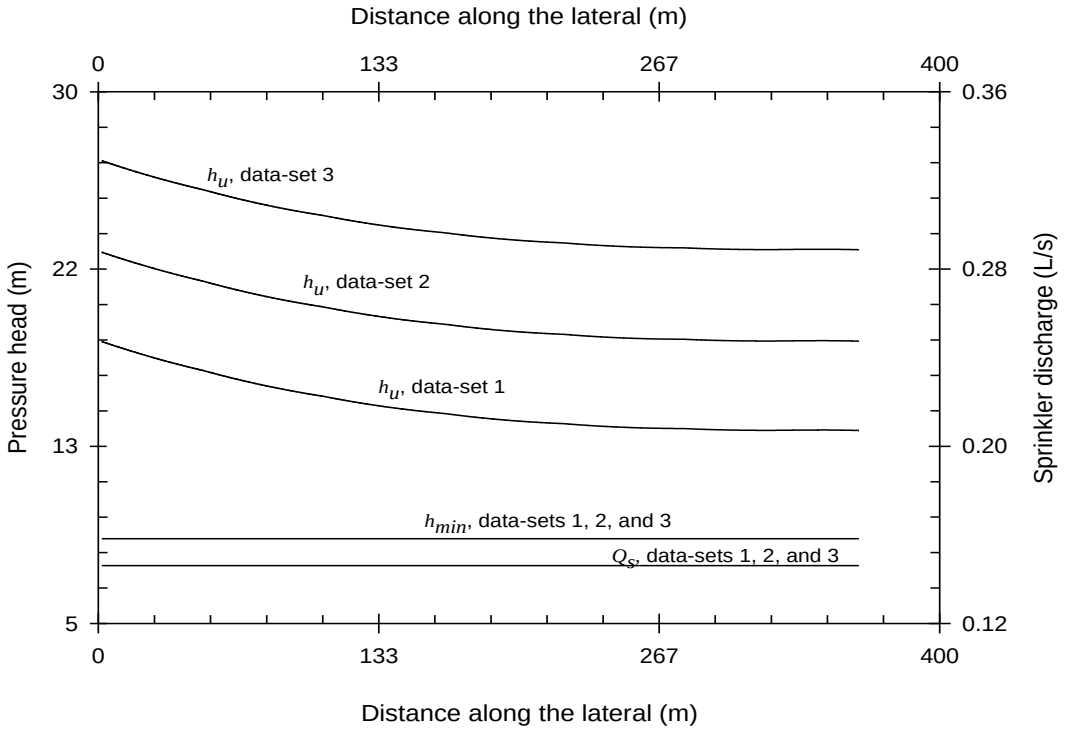

Figure 41. Comparison of h_{min}, h_u, and Q_s profiles of the data-sets used in model evaluation (Notations: h_{min} is the minimum required inlet pressure head for the *prv* to operate reliably in the active mode, h_u is the simulated *prv*-inlet pressure head, and Q_s is the computed emitter discharge)

6.2. Application examples

LincSys produces a range of outputs, given the hydraulic, geometric, and elevation data of a linear-move or center-pivot sprinkler irrigation system as input. The specific input data items include lateral pipe segment lengths and diameters, lateral elevation profile, drop-tube and *prv* parameters (where applicable), emitter parameters, local head loss coefficients, and total head at the lateral inlet, among others. The main outputs of the numerical model are the link discharge, ***Q***, and total head, ***H***, vectors. Additional model outputs include velocity heads and friction head losses in each of the lateral pipe segments, local head losses, hydraulic head profile along the lateral, lateral pressure head profile, inlet pressures of each *prv* and *prv* operating modes (active and/or passive, where applicable), and head differential across each emitter.

As noted in Section 5.1.1.a, 15 sample projects were copied to each of the system configuration option folders during program installation. A summary of the input data-sets for the 15 sample projects, of each system configuration option, are shown in Tables 12 to 15. The basic lateral hydraulic, geometric, and elevation profile data of a sample project is mostly the same for the three system configuration options. In other words, a given sample project, say for instance SampleProject_1, has more or less the same set of basic input parameters across the different system configuration options. However, there are some differences. The differences relate to: *(i)* the emitters used in the Droptube-Prv-Emitter or Droptube-Emitter system

Table 12a. Lateral hydraulic, geometric, and elevation data used in hydraulic simulations

Lateral parameters		**Units**	**Data-set**			
			1	**2**	**3**	**4**
Number of spans		-	8	8	6	8
Span geometry	Concave	-	8	7	6	7
	Convex	-	-	1	0	1
Effective span length		*m*	27.8	36.6/20.1*(a)*	61.3	51.2/46.6/26.9*(b)*
Lateral length	Horizontal	*m*	221.8	275.6	367.5	380.4
	Along center-line	*m*	222.5	276.4	367.9	381.022
Support tower height		*m*	2.8	3.1	3.8	3.3
Maximum in-span elevation differentials *(c)*		*m*	1.0	1.2/0.45	1.2	1.3/0.83
Lateral diameter		*mm*	212.6/101.6*(d)*	203.2, 101.6/88.9*(e)*	162.1	101.6/88.9*(e)*
Absolute roughness	Lateral pipe	*mm*	0.0025	0.0015	0.003	0.0025
	Drop-tube *(f)*	*mm*	0.0015	0.0015	0.001	0.0015
Drop-tube length range*(f)*		*m*	2.3-3.3	2.6-3.8	3.05-4.25	2.3-3.85
Nodal spacing		*m*	0.84	0.5-1.35	1.25	0.5-1.9
Constant above ground clearance of emitter*(f)*		*m*	0.5	0.5	0.75	0.75
Drop-tube diameter*(f)*		*mm*	19.05			
Field surface slope		*%*	0	-0.01	0	-1.2/1.5/ -1.0*(g)*
Local head loss coefficients or related parameters	branching, outlet	-	0.12	0.12	0.2	0.12
	bending, connector*(f)*	-	0.027	0.027	0.1	0.027
	line-flow, outlet	-	0.042	0.042	0.08	0.05
	prv(h)	-	1/0	1/0	1/0	1/0
	span joint*(i)*	-	0.11	0.3	0.3	0.3
	Valve		-	-	-	-
	Coupler		-	-	-	-
	Contraction*(j)*		-	0.34/0.07	-	0.07
Total head at the inlet		*m*	20	22	20	25
Elev. at the inlet		*m*	2.8	5.86	3.8	3.86

(a) The effective span length, of data-set 2, is 20.1m for the distal-end span and 36.5m for all the other spans.
(b) The effective span length, for data-set 4, is 26.9m for the distal-end span, 46.5m for the upstream-end span and 51.2m for all the intermediate spans
(c) The maximum in-span elevation differential in data-set 2 is 0.45m for the distal-end span and 1.2m for all the other spans. The maximum in-span elevation differential in data-set 4 is 0.83m for the distal-end span and 1.3m for all the other spans. **Note**: the maximum in-span elevation differential refers to the elevation differential when the span is on a level surface.
(d) Lateral diameter of data-sets 1 is 212.6mm for the Droptube-Prv-Emitter and Droptube-Emitter system configuration options and 101.6mm for Emitter-On-Lateral system configuration option.
(e) Lateral diameter of data-set 2 is 203.2mm over spans 1 to 7, it is then reduced to 101.6mm over the upper-half of span #8, which is reduced further to 88.9mm over the lower-half of span #8. Lateral diameter of data-set 4 is 101.6mm over spans #1 to 7, it is then reduced to 88.9mm over span #8.
(f) These parameters pertain to Droptube-Prv-Emitter and Droptube-Emitter system configuration options only.
(g) The average field-slope in data-set 4 is also variable. The upstream-end span is set on a slope of -1.2%. Spans #2, 3, and 4 operate on a field with 1.5% slope, and spans #5, 6, 7, and 8 run on a field parcel with -1% slope.

(h) This parameter pertains to Droptube-Prv-Emitter system configuration option only and has to be set to 0 for the other systems

(i) The local head loss coefficient for span joints is specified as Keq on the 24th column of the input data table.

(j) The local head loss coefficients for sudden contraction are obtained from Granger (1995) based on area ratios.

Table 12b. Emitter and *prv* data used in hydraulic simulations (Droptube-Prv-Emitter and Droptube-Emitter system configuration options)

Lateral parameters		**Units**	**Data-sets**			
			1	**2**	**3**	**4**
Number of droptube-*prv*-emitter or droptube-emitter assemblies		-	257	295	289	378
Emitter parameters[(a)]	Model[(b)]	-	Super spray UP3			
	Nozzle size	*(in)*	(11/32)"	(9/32)"	(11/64)"	(3/32)"
	β	$L/s/m^{\lambda}$	0.259	0.1742	0.0646	0.0191
	λ	-	0.4999	0.5	0.5004	0.4993
prv parameter[(c)]	Model[(d)]	-	PSR2			
	h_{prv}	*m*	17	14	10	5.6
	δh_{prv}	*m*	3.5	3.5	3.5	3.5
	h_{max}	*m*	98	85	74	63

[(a)] β and λ are coefficient and exponent, respectively, of the emitter head-discharge function and are derived through regression from the data provided in manufacturer's catalogue. [(b)] Emitters are produced by Senninger (Senninger, 2017b). [(c)] h_{prv} is *prv*-set pressure head; δh_{prv} is the minimum required pressure head margin, between the *prv*-inlet pressure and h_{prv}, in order for the *prv* to operate reliably in the active mode; and h_{max} is the maximum allowable pressure at the *prv* inlet for the *prv* to operate in the active mode. Note that *prv* parameters pertain only to systems with *Droptube-Prv-Emitter* configuration. And [(d)] *prvs* are produced by Senninger (Senninger, 2017a).

Table 12c. Emitter data used in hydraulic simulations (Emitter-On-Lateral system configuration option)

Lateral parameters		**Units**	**Data-sets**			
			1	**2**	**3**	**4**
Number of emitters		-	33	38	59	82
Emitter parameters[(a)]	Model[(b)]	-	30WH	30WH	30FWH	14VH
	Nozzle size	*mm (in)*	(3/16×1/8)"	(3/16×1/8)"	(1/8×3/32)"	(5/64)"
	β	$L/s/m^{\lambda}$	0.1138	0.1138	0.0502	0.0132
	λ	-	0.4923	0.4923	0.5182	0.502
Reference emitter spacing[(c)]		*m*	6.59	6.59	5.67	4.93

[(a)] β and λ are coefficient and exponent, respectively, of the emitter head-discharge function and are derived through regression from the data provided in manufacturer's catalogue. [(b)] Emitters are produced by Rainbird (Rainbird, 2020). [(c)] The reference emitter spacing is the reference horizontal spacing used to place emitters along the lateral. Actual spacings could be off by a margin of up to 1.5m.

Table 13a. Lateral hydraulic, geometric, and elevation data used in hydraulic simulations

Lateral parameters		Units	Data-set			
			5	**6**	**7**	**8**
Number of spans		-	7	7	8	8
Span geometry	Concave	-	7	6	7	7
	Convex	-	-	1	1	1
Effective span length[(a)]		*m*	45.8	56.8/50.8/27.0[(a)]	49.5/25.3[(b)]	62.8/28.4[(b)]
Lateral length	Horizontal	*m*	319.9	361.7	371.4	467.5
	Along centerline	*m*	320.5	362.0	372.1	468.3
Support tower height		*m*	3.2	3.62	3.6	3.7
Maximum in-span elevation differentials[(c)]		*m*	1.2	1.5/1.15/0.65	1.35/0.61	1.45/1.03
Lateral diameter		*mm*	197.1/88.9[(d)]	162.3/136.4/101.6[(e)]	134.9/101.6[(f)]	162.1/101.6[(f)] 101.6/63.5[(g)]
Absolute roughness	Lateral pipe	*mm*	0.0015	0.0015	0.05	0.004
	Drop-tube[(h)]	*mm*	0.0015	0.0015	0.0015	0.001
Drop-tube length range[(h)]		*m*	2.6-3.8	2.59-4.0	2.8-4.2	2.71-4.4
Nodal spacing		*m*	0.5-1.6	0.58-1.65	0.58-1.8	0.5-1.9
Constant above ground clearance of emitter[(h)]		*m*	0.6	0.76	0.75	0.75
Drop-tube diameter[(h)]		*mm*	19.05			
Field surface slope		-	-1.8/0/-0.5[(i)]	-1.7/0.0[(j)]	1.0	1.5/-2.0/1.5/0[(k)]
Local head loss coefficients and related parameters[(i)]	branching, outlet		0.12	0.03	0..4	0.2
	bending, connector[(h)]		0.027	0.02	0.1	0.06
	line-flow, outlet		0.042	0.008	0.125	0.1
	prv[(l)]		1/0	1/0	1/0	1/0
	span joint[(m)]		0.3	0.04	0.35	0.35
	Valve		-	-	-	-
	Coupler		-	-	-	-
	Contraction[(n)]	-	-	0.1/0.195	0.195	0.26
Total head at the inlet		*m*	23.0	27.7	30	29
Elev. at the inlet		*m*	4.71	4.84	3.6	6.52

(a) The effective span length of data-set 6 is variable. The cantilever type distal-end span has an effective length of 27m, the upstream-end span is 50.8m long, and all spans in between are 56.8m long.

(b) Data-sets 7 and 8 also have cantilever type distal-end spans that are 25.3 and 28.4m in long, respectively. The seven upstream spans of data-set 7 are 49.5m long each and those of data-set 8 are each 62.8m long.

(c) The maximum in-span elevation differential for data-sets 6, 7, and 8 vary. For data-set 6, it is 1.5m for the upstream-end span, 1.15m for spans #2 to 6 each, and 0.65m for span #7. For data-set 7, the maximum in-span elevation differential is 0.61 for the distal-end span and 1.35 for each of the other spans. For data-set 8, the maximum in-span elevation differential is 1.03m for span #8 and 1.45m for all the other spans. **Note**: the maximum in-span elevation differential refers to the elevation differential when the span is on a level surface.

(d) For data-set 5, the lateral diameter of the Droptube-Prv-Emitter and Droptube-Emitter system configuration options is 197.1mm. However, for Emitter-On-Lateral system configuration option, lateral dimeter is 88.9mm.

(e) The lateral diameter for data-sets 6 vary. It is 162.3mm over spans 1 to 6, it is then reduced to 136.4mm over the upper-half of the distal-end span, which is further reduced to 101.6mm over the lower-half of the span.

(f) For data-set 7, the lateral diameter over spans #1 to 7 is 134.9mm. It is then reduced to 101.6mm in span #8. For data-set 8 of the Droptube-Prv-Emitter and Droptube-Emitter system configuration options, the diameter of all the spans except the distal-end is 162.1mm and the distal-end span has a diameter of 101.6mm.

(g) For data-set 8 of the Emitter-On-Lateral system configuration option, the diameter of all the spans except span #8 is 101.6mm and the diameter of the distal-end span is 63.5mm.

(h) These parameters pertain to Droptube-Prv-Emitter and Droptube-Emitter system configuration options only.

(i) The average field-slope in data-set 5 is variable. The upstream-end span is set on a slope of -1.8%. Spans #2, 3, and 4 operate on a level section of the field and spans #5, 6, and 7 run on a segment with -0.5% slope.

(j) The field-slope in data-set 6 is variable. The upstream-end span is set on a slope of -1.7% and spans #2 to 7 are installed on a level field.

(k) The field-slope of data-set 8 is also variable. The upstream-end span runs on a parcel of the field that has a slope of 1.5%, spans #2, 3, and 4 are installed on a section where the slope is -2.0%, span 5 and 6 have an average slope of 1.5%, and spans #7 and 8 are set on a level section of the field.

(l) This parameter pertains to Droptube-Prv-Emitter system configuration option only and has to be set to 0 for the other systems.

(m) The local head loss coefficient for span joints is specified as Keq on the 24th column of the input data table.

(n) The local head loss coefficients for sudden contraction are obtained from Granger (1995) based on area ratios.

Table 13b. Emitter and *prv* data used in hydraulic simulations (Droptube-Prv-Emitter and Droptube-Emitter system configuration options)

Lateral parameters		Units	Data-sets			
			5	**6**	**7**	**8**
Number of droptube-*prv*-emitter or droptube-emitter assemblies		-	330	349	354	461
Emitter head-discharge function *(a)*	Model*(b)*	-	Super Spray UP3			
	Nozzle size	*mm (in)*	(7/32)”	(3/16)”	(5/32)”	(9/64)”
	β	$L/s/m^{\lambda}$	0.105	0.0771	0.0534	0.0429
	λ	-	0.5004	0.4998	0.4999	0.5018
prv parameters *(c)*	Model*(d)*		PSR2			
	h_{prv}	*m*	12	4.2	8.5	7.0
	δh_{prv}	*m*	3.5	3.5	3.5	3.5
	h_{max}	*m*	81	70.3	70	67

(a) β and λ are coefficient and exponent, respectively, of the emitter head-discharge function and are derived through regression from the data provided in manufacturer’s catalogue. *(b)* Emitters are produced by Senninger (Senninger, 2017b). *(c)* h_{prv} is *prv*-set pressure head; δh_{prv} is the minimum required pressure head margin, between the *prv*- inlet pressure and h_{prv}, in order for the *prv* to operate reliably in the active mode; and h_{max} is the maximum allowable pressure at the *prv* inlet for the *prv* to operate in the active mode. Note that *prv* parameters pertain only to systems with *Droptube-Prv-Emitter* configuration. And *(d)* *prvs* are produced by Senninger (Senninger, 2017a).

Table 13c. Emitter data used in hydraulic simulations (Emitter-On-Lateral system configuration option)

Lateral parameters		**Units**	**Data-sets**			
			5	**6**	**7**	**8**
Number of emitters		-	51	60	60	89
Emitter parameters *(a)*	Model*(b)*		30WH	30WH	30FWH	30H
	Nozzle size	*mm (in)*	(5/32×3/32)”	(5/32×3/32)”	(1/8×3/32)”	(9/64)”
	β	$L/s/m^{\lambda}$	0.0721	0.0721	0.0502	0.0434
	λ	-	0.5016	0.5016	0.5182	0.4978
Reference emitter spacing *(c)*		*m*	6.29	6.29	5.67	5.18

(a) β and λ are coefficient and exponent, respectively, of the emitter head-discharge function and are derived through regression from the data provided in manufacturer’s catalogue. *(b)* Emitters are produced by Rainbird (Rainbird, 2020). *(c)* The reference emitter spacing is the reference horizontal spacing used to place emitters along the lateral. Actual spacings could be off by a margin of up to about 1.5m.

Table 14a. Lateral hydraulic, geometric, and elevation data used in hydraulic simulations

Lateral parameters		Units	Data-set			
			9	**10**	**11**	**12**
Number of spans		-	7	9	10	7
Span geometry	Concave	-	6	8	10	7
	Convex	-	1	1	0	0
Effective span length		*m*	61.4/32.5[(a)]	64.8/30.3[(b)]	60.1	50.3
Lateral length	Horizontal	*m*	400	547.7	600	351.4
	Along center-line	*m*	400.7	548.7	601.0	352.2
Support tower height		*m*	3.8	3.8	4	3.5
Maximum in-span elevation differentials		*m*	1.5/1.0[(c)]	1.6/0.81[(d)]	1.5	1.4
Lateral diameter[(e)]		*mm*	162.1/101.6	162.1/101.6, 88.9/50.8	203.2	145.8
Absolute roughness	Lateral pipe	*mm*	0.01	0.005	0.0015	0.045
	Drop-tube[(f)]	*mm*	0.0015	0.0015	0.0015	0.0015
Drop-tube length range[(f)]		*m*	2.91-4.7	2.66-4.65	3.25-4.75	2.75-4.15
Nodal spacing		*m*	1.25	0.58-1.95	1.0	0.57-1.75
Constant above ground clearance of emitter[(f)]		*m*	0.6	0.75	0.75	0.75
Drop-tube diameter[(f)]		*mm*	19.05			
Field surface slope		*%*	-1.5	-2.0/1.0/-1.5/3.0[(g)]	-0.5	0/-1.5 /1.25/-2.5/0[(h)]
Local head loss coefficients and related parameters	branching, outlet	-	0.2	0.15	0.12	0.12
	Bending , connector[(f)]	-	0.08	0.05	0.027	0.027
	Line-flow, outlet	-	0.1	0.06	0.042	0.042
	prv[(i)]	-	1/0	1/0	1/0	1/0
	Span joints[(j)]	-	0.3	0.35	0.11	0.11
	Valve	-	-	-	-	-
	Coupler	-	-	-	-	-
	Contraction[(k)]	-	0.26	0.26/0.28	-	-
Total head at the inlet[(l)]		*m*	20	60/50	45	25
Elev. at the inlet		*m*	9.8	7.03	7	5.0

(a) The effective span length of data data-set 9 is variable. The distal-end span has an effective length of 32.5m and all the other spans are 61.4m long each.

(b) Data-set 10 has a 30.3m long distal-end span and each of the other spans are 64.7m long.

(c) The maximum in-span elevation differential for data-sets 9 vary. It is 1.0m for the distal-end span and 1.5m for each of the other spans. **Note**: the maximum in-span elevation differential refers to the elevation differential when the span is on a level surface.

(d) The maximum in-span elevation differential of the distal-end span of data-set 10 is 0.81m. The rest of the spans have a maximum in-span elevation differential of 1.6m.

(e) The lateral diameter for data-sets 9 and 10 vary. For both data-sets 9 and 10 of the Droptube-Prv-Emitter and Droptube-Emitter system configuration options, the pipe diameter in all, but the distal-ends, span was set to 162.1mm and in the distal-end span it was set to 101.6mm. For data-set 9 of the Emitter-On-Lateral configuration option, lateral dimeter was the same as those of the Droptube-Prv-Emitter and Droptube-Emitter system configuration options. However, for data-set 10 of the system with Emitter-On-Lateral configuration option, lateral diameter was set to 88.9mm over spans #1 to 8 and to 50.8mm in span #9.

(f) These parameters pertain to Droptube-Prv-Emitter and Droptube-Emitter system configuration options only.

(g) The average field-slope in data-set 10 is variable. Spans #1 and 2 are set on a slope of -2.0% and spans #3 and 4 run on a field parcel with a slope of 1.0%. Spans #5 and 6 are installed on a section of the field with a slope of -1.5% and spans #7, 8, and 9 are set on a slope of 3.0%

(h) The field-slope of data-set 12 is also variable. The upstream-end span runs on a parcel of the field that is level. and spans #2 and 3 operate on a section with a slope of -1.5%. Spans #4 and 5 are set on a segment with a slope of 1.25%. Span #6 has an average slope of -2.5% and span #7 runs on a level section of the field.

(i) This parameter pertains to Droptube-Prv-Emitter system configuration option only and it has to be set to 0 for the other systems.

(j) The local head loss coefficient for span joints is specified as Keq on the 24th column of the input data table.

(k) The local head loss coefficients for sudden contraction are obtained from Granger (1995) based on area ratios. For data-set 10, it is 0.26 for systems with Droptube-Prv-Emitter and Droptube-Emitter configuration options and 0.28 for Emitter-On-Lateral system configuration option.

(l) The total head at the lateral inlet was 60m for the Droptube-Prv-Emitter system configuration option and it was set to 50m for the Droptube-Emitter and Emitter-On-Lateral system configuration options.

Table 14b. Emitter and prv data used in hydraulic simulations (Droptube-Prv-Emitter and Droptube-Emitter system configuration options)

Lateral parameters		**Units**	**Data-sets**			
			9	**10**	**11**	**12**
Number of prvs, emitters, and drop-tubes		-	314	449	591	309
Emitter parameters [(a)]	Model[(b)]	-	Super Spray UP3			
	Nozzle size	mm (in)	(9/64)"	(7/32)"/(3/16)"	(3/16)"	(11/64)"
	β	L/s/m$^{\lambda}$	0.0429	0.105[(b)]/0.0771[(c)]	0.0771	0.0646
	λ	-	0.5018	0.5004[(b)]/0.4998[(c)]	0.4998	0.5004
prv parameters [(c)]	Model [(d)]		PSR2			
	h_{prv}	m	5.6	6	12	10
	δh_{prv}	m	3.5	3.5	3.5	3.5
	h_{max}	m	63	81	78	74

(a) β and λ are coefficient and exponent, respectively, of the emitter head-discharge function and are derived through regression from the data provided in manufacturer's catalogue. *(b)* Emitters are produced by Senninger (Senninger, 2017b), *(c)* h_{prv} is *prv*-set pressure head; δh_{prv} is the minimum required pressure head margin, between the *prv*- inlet pressure and h_{prv}, in order for the *prv* to operate reliably in the active mode; and h_{max} is the maximum allowable pressure at the prv inlet for the prv to operate in the active mode. And *(d)* prvs are produced by Senninger (Senninger (2017a). Note that prv parameters pertain only to systems with Droptube-Prv-Emitter configuration.

Table 14c. Emitter data used in hydraulic simulations (Emitter-On-Lateral system configuration option)

Lateral parameters		**Units**	**Data-sets**			
			9	**10**	**11**	**12**
Number of emitters		-	80	85	100	59
Emitter parameters[(a)]	Model[(b)]		30H	30WH	30WH	30FWH
	Nozzle size	*(in)*	(9/64)"	(3/16×3/32)"	(5/32×3/32)"	(1/8×1/32)"
	β	$L/s/m^{\lambda}$	0.0434	0.0961	0.0721	0.0502
	λ	-	0.4978	0.4993	0.5016	0.5182
Reference emitter spacing [(c)]		*m*	5.18	6.29	6.29	5.67

(a) β and λ are coefficient and exponent, respectively, of the emitter head-discharge function and are derived through regression from the data provided in manufacturer's catalogue. *(b)* Emitters are produced by Rainbird (Rainbird, 2020). *(c)* The reference emitter spacing is the reference horizontal spacing used to place emitters along the lateral. Actual spacings could be off by a margin of up to about 1.5m.

Table 15a. Lateral hydraulic, geometric, and elevation data used in hydraulic simulations

Lateral parameters		**Units**	**Data-set**		
			13	**14**	**15**
Number of spans		-	11	12	6
Span geometry	Concave	-	10	11	6
	Convex	-	1	1	0
Effective span length[(a)]		*m*	64.8/23.7	64.8/23.7	61.3
Lateral length	Horizontal	*m*	670.5	735.2	367.5
	Along center-line	*m*	671.8	736.6	367.9
Support tower height		*m*	3.8	3.8	3.8
Maximum in-span elevation differentials [(b)]		*m*	1.6/1.4	1.6/1.4	1.2
Lateral diameter		*mm*	162.1	162.1	127/76.2/50.8[(c)] , 162.1/88.9/63.5[(d)], 88.9/50.8/38.1[(e)]
Absolute roughness	Lateral pipe	*mm*	0.01	0.002	0.003
	Drop-tube[(f)]	*mm*	0.0015	0.0015	0.001
Drop-tube length range[(f)]		*m*	2.47-4.65	2.63-4.8	3.05-4.25
Spacing		*m*	0.64-1.95	0.64-1.95	1.25
Constant above ground clearance of emitter[(f)]		*m*	0.75	0.6	0.75
Drop-tube diameter[(f)]		*mm*	19.05		
Field surface slope [(g)]		*%*	-2.0/1.0/-1.5	-2.0/1.0/-1.5	0
Local head loss coefficient and related parameters	Branching, outlet	-	0.12	0.12	0.2
	Bending, connector[(f)]	-	0.04	0.3	0.1
	Line flow	-	0.06	0.1	0.08
	prv[(h)]	-	1/0	1/0	1/0
	Span joint[(i)]	-	0.5	0.5	0.3
	Valve	-	-	-	-
	Coupler	-	-	-	-
	Contraction	-	-	-	0.29/0.248[(j)], 0.32/0.22[(k)], 0.34/0.195 [(l)]
Total head at the inlet		*m*	45	50	35[(m)]/15[(n)]
Elev. at the inlet		*m*	11.27	11.27	3.8

(a) The effective span lengths of data data-sets 13 and 14 are variable. In each case, cantilever type distal-end span has an effective length of 23.7m and all the other spans are 64.8m long each.

(b) The maximum in-span elevation differential is the same for data-sets 13 and 14. It is 1.4m for the distal-end span and 1.6m for each of the other spans. **Note**: the maximum in-span elevation differential refers to the elevation differential when the span is on a level surface.

(c) Lateral diameter for the Droptube-Prv-Emitter system configuration option of data-set 15 vary along the lateral. The pipe diameter over spans #1 to 4 is 127.0mm, it is then reduced to 76.2mm over span #5, which is further reduced to 50.8mm in span #6.

(d) Lateral diameter for the Droptube-Emitter system configuration options of data-set 15 vary along the lateral. The pipe diameter over spans #1 to 4 is 162.1mm, it is then reduced to 88.9mm over span #5, which is further reduced to 63.5mm in span #6.

(e) Lateral diameter for the Emitter-On-Lateral system configuration option of data-set 15 also vary along the lateral. It is 88.9mm over spans #1 to 4, it is then reduced to 50.8mm over span #5, which is further reduced to 38.1mm over the span #6.

(f) These parameters pertain to Droptube-Prv-Emitter and Droptube-Emitter system configuration options only.

(g) Field slope along the lateral consists of three segments for each of data-sets 13 and 14.

(h) This parameter pertains to Droptube-Prv-Emitter system configuration option only and it has to be set to 0 for the other systems.

(i) The local head loss coefficient for span joints is specified as Keq on the 24th column of the input data table.

(j) The local head loss coefficients for sudden contraction are for the system with Droptube-Prv-Emitter configuration. These parameters were obtained from Granger (1995), based on area ratios.

(k) The local head loss coefficients for sudden contraction are for the system with Droptube-Emitter configuration.

(l) The local head loss coefficients for sudden contraction are for the system with Emitter-On-Lateral configuration.

(m) The total head for Droptube-Prv-Emitter and Droptube-Emitter system configuration options

(n) The total head for the Emitter-On-Lateral system configuration option

Table 15b. Emitter and prv data used in hydraulic simulations (Droptube-Prv-Emitter and Droptube-Emitter system configuration options)

Lateral parameters		**Units**	**Data-sets**		
			13	**14**	**15**
Number of droptube-*prv*-emitter or droptube-emitter assemblies		-	555	608	349
Emitter parameters *(b)*	Model*(a)*	-	Super Spray UP3		
	Nozzle size	*mm (in)*	(3/32)"	(3/32)"	(11/64)"
	β	$L/s/m^{\lambda}$	0.0191	0.0191	0.0646
	λ	-	0.4993	0.4993	0.5004
prv model is PSR *(c)*	Model*(d)*	-	PSR2		
	h_{prv}	*m*	8.5	8.5	10
	δh_{prv}	*m*	3.5	3.5	3.5
	h_{max}	*m*	80	80	74

(a) β and λ are coefficient and exponent, respectively, of the emitter head-discharge function and are derived through regression from the data provided in manufacturer's catalogue. *(b)*Emitters are produced by Senninger (Senninger, 2017b), *(c)*h_{prv} is *prv*-set pressure head; δh_{prv} is the minimum required pressure head margin, between the *prv*- inlet pressure and h_{prv}, in order for the *prv* to operate reliably in the active mode; and h_{max} is the maximum allowable pressure at the *prv* inlet for the *prv* to operate in the active mode. And *(d)*prvs are produced by Senninger (Senninger, 2017a). Note that *prv* parameters pertain only to systems with Droptube-Prv-Emitter configuration.

Table 15c. Emitter data used in hydraulic simulations (Emitter-On-Lateral system configuration option)

Lateral parameters		**Units**	**Data-sets**		
			13	**14**	**15**
Number of emitters		-	125	137	59
Emitter parameters *(a)*	Model*(b)*	-	14VH	14VH	30WH
	Nozzle size	in	(5/64)"	(5/64)"	(1/8×3/32)"
	β	$L/s/m^{\lambda}$	0.0132	0.0132	0.0502
	λ	-	0.502	0.502	0.5182
Reference emitter spacing*(c)*		m	4.93	4.93	6.29

(a)β and λ are coefficient and exponent, respectively, of the emitter head-discharge function and are derived through regression from the data provided in manufacturer's catalogue. *(b)* Emitters are produced by Rainbird (Rainbird, 2020). *(c)* The reference emitter spacing is the reference horizontal spacing used to place emitters along the lateral. Actual spacings could be off by a margin of up to about 1.5m.

configuration option are low pressure spray nozzles from Senninger (Senninger, 2017b), while those used in the Emitter-On-Lateral system configuration option are high pressure impact sprinklers from Rainbird (Rainbird, 2020). As a result lateral outlet port spacings used in the sample projects of the Emitter-On-Lateral system configuration option are significantly greater than those used in the other system configuration options (Tables 12a,b,c; 13a,b,c; 14a,b,c; and 15a,b,c). *(ii)* Drop-tube data (i.e., drop-tube geometry and its hydraulic resistance parameter) and the local head loss coefficient associated with bending at the gooseneck connector are specified only for systems with Droptube-Prv-Emitter and Droptube-Emitter system configuration options. *(iii) prv* hydraulic data are specified only for systems with Droptube-Prv-Emitter configuration option. And *(iv)* while the preceding list accounts for the main differences in input data of the sample projects, as related to differences in system configuration options, there are also additional differences in lateral diameter and total head in a couple of the sample projects. Note that Tables 12 to 15 make extensive use of footnotes to highlight the differences in the input data-sets of the sample projects.

The following sections present a description of the model input-output data of three application examples (sample projects), one application example corresponding to each system configuration option of *LincSys*.

6.2.1. Droptube-Emitter system configuration option

6.2.1.a. Input data: SampleProject_9 of the Droptube-Emitter system configuration option

Among the 15 sample projects in the DroptubeEmitter system configuration option folder, SampleProject_9 is presented here as an example. A summary of the input data for SampleProject_9 is provided in Tables 14a and 14b. In addition, the nontabular input data and a part of the tabular input data of the sample project are depicted in Figure 42.

SampleProject_9 considers a lateral with 6 concave spans, each about 61.35m long, and a distal-end cantilever type span of 32.54m (Table 14a). The lateral length is 400.7m. The lateral is installed in a field with a uniform slope of -1.5%. The maximum in-span elevation differential is 1.5m for the concave spans and 1.0m in the distal-end convex span, if the lateral was to be installed on a level field. There are seven support towers each 3.8m in height. Using a horizontal surface that passes through the point of minimum field elevation along the length of run of the lateral as a reference datum, the elevation of the lateral inlet is set at 9.8m. The total head at the lateral inlet is 20.0m (Table 14a and Figure 42).

Lateral diameter is 162.1mm over spans #1 to 6 and 101.6mm in the distal-end span. The lateral has 314 outlet ports (Table 14b) and water is conveyed from each outlet port down to the *prv*-emitter assemblies with drop-tubes. Drop-tube lengths vary between 2.91 and 4.7m (Table 14a) and emitters are placed at a constant above ground clearance of 0.6m (Figure 42). The emitter used in the SampleProject_9 is a spray nozzle (Super spray UP3 model) with a nozzle size of 3.572mm (9/64)” from Senninger (Senninger 2017b). The emitter hydraulic parameters are summarized in Table 14b.

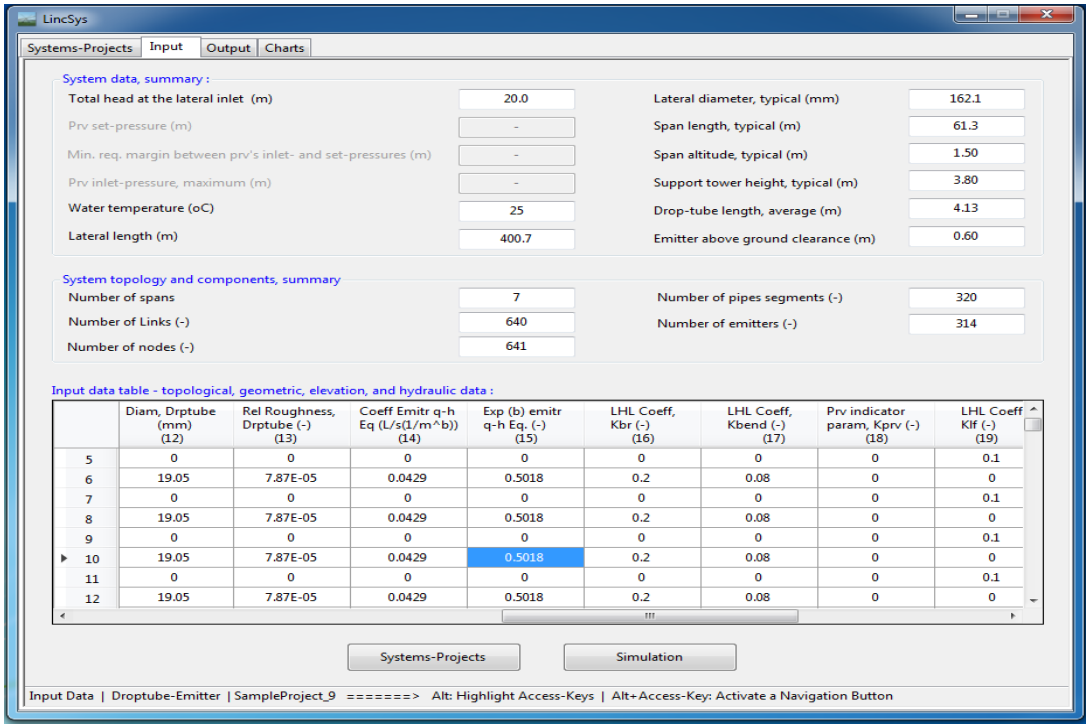

Figure 42. The Input window: SampleProject_9 of the Droptube-Emitter system configuration option

Note that, in Figure 42, the input boxes for the *prv* hydraulic parameters are deactivated and the *prv* indicator parameter column of the input data table is set to zero, indicating that the lateral considered in the current sample project is not fitted with *prvs*.

A section of the tabular input data of SampleProject_9 is displayed in the input data table (Figure 42). The input data table for the current sample project consists of 24 columns and 640 rows. Note that the complete input data-set for the current sample project is saved in the "InputData_LinLat.Inp" file, and also in the excel version of the input data file, "InputData_LinLat.Xlxs". Both of these files were placed in the current sample project folder during program installation.

6.2.1.b. Output data: SampleProject_9 of the Droptube-Emitter system configuration option

The output data for the current sample project, which contains both nontabular and tabular data, are displayed in Figure 43.

A summary of the computed emitter discharge variability data shows that emitter discharges along the lateral vary between a minimum of 0.143L/s and a maximum of 0.1569L/s and the average is 0.1479L/s. On the other hand, the emitter head differential profile varies between a lower limit of 11.02m and an upper limit of 13.25m and the mean value is 11.79m (Figure 43).

The system hydraulic performance summary shows that the emitter discharge uniformity coefficient and the low-quarter distribution uniformity are 0.975 and 0.969, respectively, which suggests a highly uniform emitter discharge profile. With a uniformity coefficient of 0.951 and a

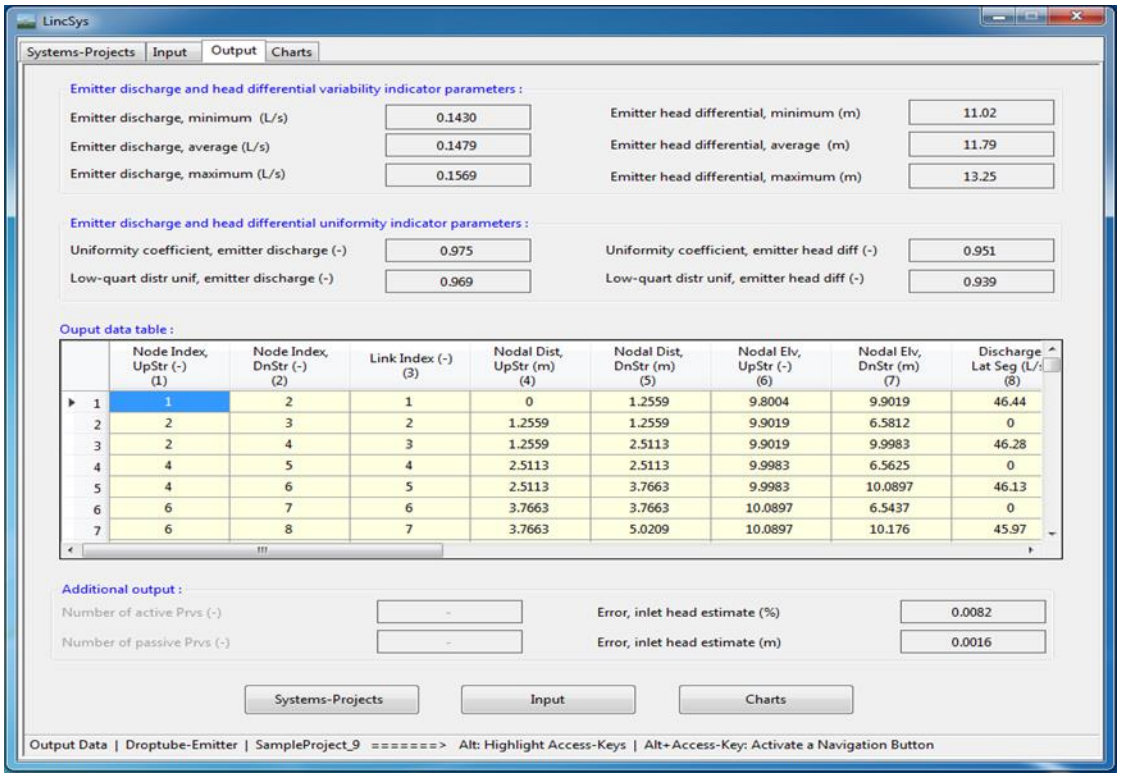

Figure 43. The Output window: SampleProject_9 of the Droptube-Emitter system configuration option

low-quarter distribution uniformity of 0.939, the emitter head differential profile as well shows high uniformity.

Furthermore, the output data in the additional output groupbox show that the error in the computed inlet-head estimate is 0.0016m or 0.0082% of the imposed inlet head. Figure 43 also shows that the output boxes for the *prv* operating modes are deactivated, indicating that the lateral considered here is not fitted with *prvs*.

A section of the tabular output data for the current sample project is displayed in the output data table (Figure 43). The output data table consists of 20 columns and 640 rows. Note that the complete set of computed hydraulic parameters (i.e., output data) can be found in the "OutputData_LinLat.Out" file and the additional output data files listed in Table 7, all of which were placed in the current project folder during program installation.

6.2.1.c. Output charts: SampleProject_9 of the Droptube-Emitter system configuration option

Among the 11 charts generated by *LincSys* for the current project, a sample set of output charts consisting of: *(i)* the lateral elevation profile and the hydraulic and energy grade-lines, *(ii)* the lateral pressure profile, and *(iii)* the emitter discharge profile will now be presented.

Chart depicting the lateral elevation profile and the hydraulic and energy grade-lines

As can be noted from Figure 44, the energy grade-line (i.e., the upper most curve) steadily declines with distance along the lateral from a maximum value of 20.0m at the lateral

inlet to 13.87m at the distal-end of the lateral. On the other hand, the hydraulic grade-line (the curve that is right under the energy grade-line) varies between a minimum of 13.87m at the distal-end to 19.74m at the inlet. The total head and the hydraulic head at the distal-end appear to be identical, which suggests that the computed velocity head in the distal-end lateral pipe segment is zero. However, that is not correct. The computed total head and the hydraulic head at the distal-end of the lateral are different, but the two parameters appear identical only because the significant digits of the values reported here are less than those used in the numerical computation.

The lower most curve, in Figure 44, with a series of concave segments and a distal-end convex section is the elevation profile of the lateral centerline, which is installed on a field with an average slope of -1.5%.

Note that the data used in this chart is saved in the "Chart_ElvHglEgl.Dat" file within the current project folder (Table 7).

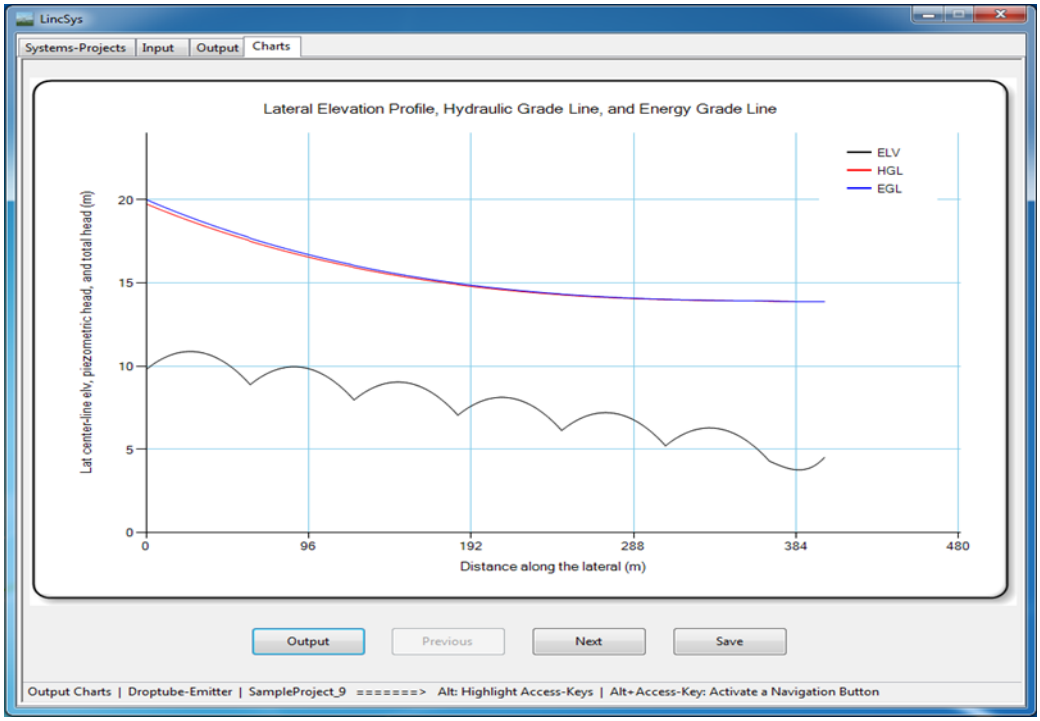

Figure 44. Chart depicting the lateral elevation profile and the hydraulic and energy grade-lines: SampleProject_9 of the Droptube-Emitter system configuration option

Lateral pressure head profile chart

The lateral pressure head profile for SampleProject_9 of the Droptube-Emitter sample project is depicted in Figure 45. Consistent with earlier observations, the pressure profile of the lateral considered here as well exhibits both local span-scale variability patterns (solid-line) and broader inter-span/lateral-wide trends (shown in dash-dotted line). A more detailed discussion on in-span pressure variability patterns and inter-span trends and their relationship with span geometry, field slope, and lateral diameter is provided by Zerihun and Sanchez (2019c). Thus, only a brief description appertaining to the pressure head profile patterns of the current sample project will be presented here.

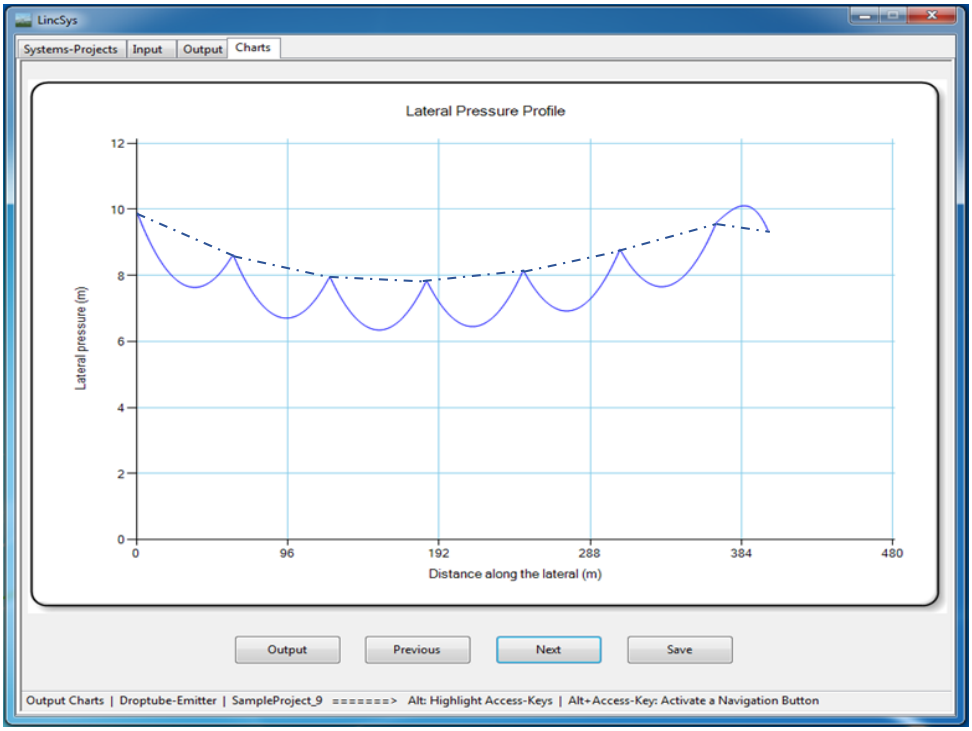

Figure 45. Lateral pressure profile chart: SampleProject_9 of the Droptube-Emitter system configuration option (the solid-line represents the actual pressure head profile and the dash-dotted line depicts the inter-span variability trend)

As can be noted from Figure 45, the in-span lateral pressure profile variability patterns exhibit some general attributes that are repeated along the lateral, although with some variation. For the six (upstream) concave spans, the corresponding local in-span lateral pressure head variability patterns follow a convex form, consisting of an upstream section over which pressure decreases with distance from the lateral inlet to a local minimum somewhere within the span and a downstream section over which pressure increases with distance from the lateral inlet (Figure 45). By comparison, over the distal-end span (i.e., a span with a convex elevation profile), the in-span pressure variability pattern exhibits a concave form. Thus, the lateral pressure profile shows an increasing trend over an upstream section of the span, followed by a decreasing trend in the lower section of the span.

Furthermore, a closer look at Figure 45 reveals that over the upper 184.1m section of the lateral, i.e., over spans #1 to 3, the inter-span pressure variability trends down as one moves downstream from the lateral inlet. Thereafter, over spans #4 to 6 (i.e., over a segment of the lateral measuring 184.1m), the inter-span pressure variability tends upwards with distance from the lateral inlet. The results of an earlier study by Zerihun and Sanchez (2019c) suggests that the inter-span lateral pressure variability trend observed over the six upstream spans, in Figure 45, is likely attributable to the field slope, which is -1.5%.

Now, considering spans #6 and 7, the inter-span pressure variability trend changed slightly from one of increasing with distance along the lateral (in span #6) to that of decreasing in span #7. This change in the inter-span trend is related to changes in the span concavity structure and lateral diameter over span #7. Span geometry changed from concave (over the six

upstream spans) to convex form over the distal-end span and lateral diameter was reduced from 162.1mm (over the upstream spans) to 101.6mm over the distal-end span. As can be noted from Figure 45, these changes, in span geometry and diameter, did have some (although not significant) effect on the overall inter-span pressure variability trend.

Note that, in Figure 45, the curve shown in solid-line (i.e., the actual lateral pressure profile) was computed with *LincSys*, but the curve representing the inter-span trend (dash-sotted line) was added to the chart manually.

Emitter discharge profile chart

Figure 46 depicts the emitter discharge profile. Note that the emitter discharge profile exhibits a spatial trend that is, for the most part, analogous in form to the overall inter-span pressure variability trend, described in the preceding paragraph. It decreased with distance from the lateral inlet over the upper 165.3m section of the lateral, it then rose with distance from the inlet-end in the lower 235.4m long segment.

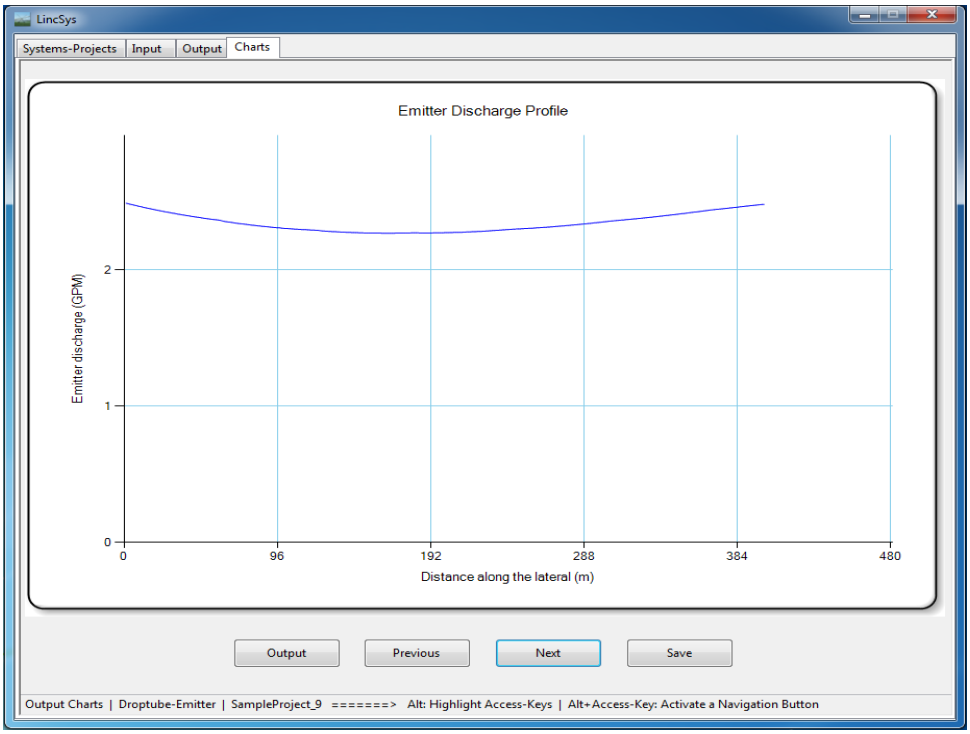

Figure 46. Emitter discharge profile: SampleProject_9 of the Droptube-Emitter system configuration option

Remarkably, the emitter discharge profile depicted in Figure 46 is a nearly smooth and almost convex function of distance from the later inlet. In other words, the effects of span-scale elevation differentials are not evident in the emitter discharge profile. The explanation for this observation relates to the position of emitters with respect to the lateral centerline and the spatial invariance of emitters above ground clearance along the lateral.

In the lateral considered in current sample project, emitters are placed at a significantly lower elevation relative to the lateral outlet ports. For instance, for the current lateral, the average drop-tube length is 4.1m, which translates into a hydrostatic pressure of about the same amount

on the emitters, on the average. As a result, pressure at the inlet of the emitters are not only different from the respective lateral outlet pressures, but they are also significantly larger. Furthermore, owing to the positioning of emitters at a uniform above ground clearance from the field surface, the pressure differential between emitter inlets and the respective lateral outlets vary in a pattern that nearly even-out the in-span elevation differential effects on emitter pressure heads. Consequently, the span-scale wiggly patterns that are prominent in the lateral pressure profile, and are attributable to the in-span lateral elevation differential effects, are barely discernible on the corresponding emitter discharge profile (Figure 46).

6.2.2. *Droptube-Prv-Emitter system configuration option*

6.2.2.a. Input data: SampleProject_5 of the Droptube-Prv-Emitter system configuration option

Among the 15 sample projects under the DroptubePrvEmitter system configuration option folder, SampleProject_5 is presented here as an example (Tables 13a and 13b). The nontabular input data and a part of the tabular input data of SampleProject_5 are depicted in Figure 47.

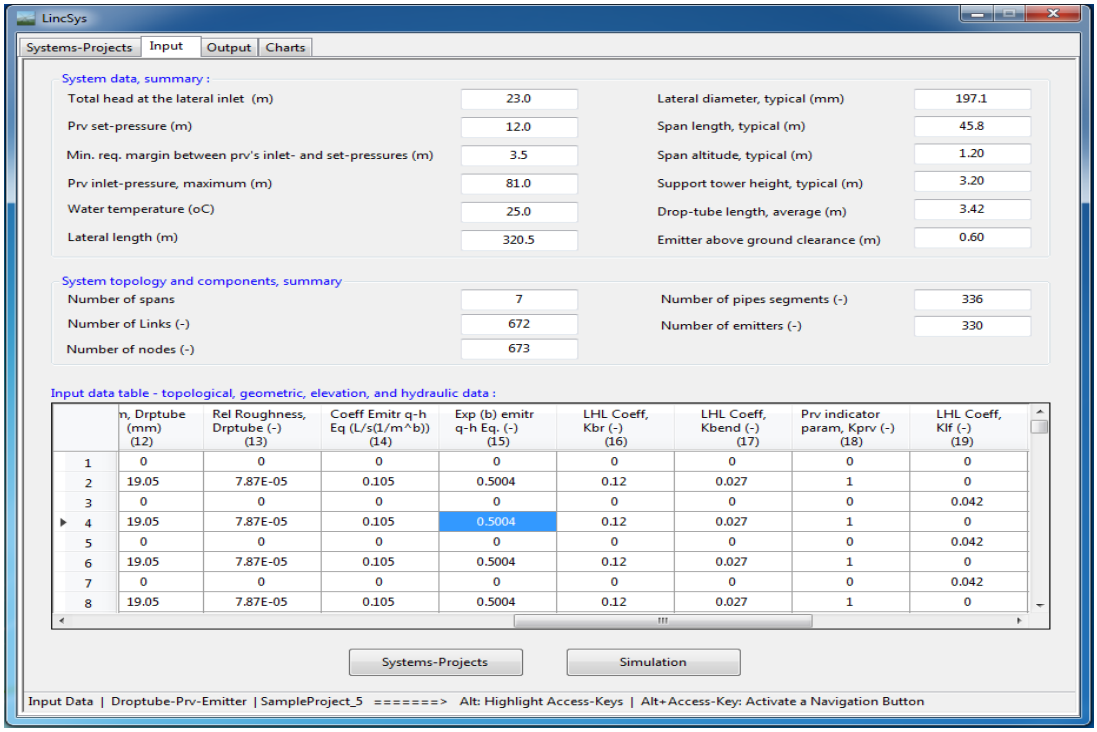

	n, Drptube (mm) (12)	Rel Roughness, Drptube (-) (13)	Coeff Emitr q-h Eq (L/s(1/m^b)) (14)	Exp (b) emitr q-h Eq. (-) (15)	LHL Coeff, Kbr (-) (16)	LHL Coeff, Kbend (-) (17)	Prv indicator param, Kprv (-) (18)	LHL Coeff, Klf (-) (19)
1	0	0	0	0	0	0	0	0
2	19.05	7.87E-05	0.105	0.5004	0.12	0.027	1	0
3	0	0	0	0	0	0	0	0.042
4	19.05	7.87E-05	0.105	0.5004	0.12	0.027	1	0
5	0	0	0	0	0	0	0	0.042
6	19.05	7.87E-05	0.105	0.5004	0.12	0.027	1	0
7	0	0	0	0	0	0	0	0.042
8	19.05	7.87E-05	0.105	0.5004	0.12	0.027	1	0

Figure 47. The Input window: SampleProject_5 of Droptube-Prv-Emitter system configuration option

The lateral considered in the current sample project has 7 concave spans each about 45.79m long along the centerline of the lateral. The lateral length is 320.5m. The lateral is operated on a field with variable slope. The upstream-end span is set on a slope of -1.8%, spans #2, 3, and 4 operate on a level section of the field, and spans #5, 6, and 7 run on a segment with

-0.5% slope. The maximum in-span elevation differential, if the lateral were to run on a level field is 1.2m. There are eight support towers, each 3.2m in height. Using a horizontal surface (that passes through the point of minimum field elevation along the length of run of the lateral) as the reference datum, the elevation of the lateral inlet is set to 4.71m. The total head at the lateral inlet is 23.0m.

Lateral diameter is 197.1mm. The lateral has 330 outlet ports and drop-tubes are used to convey water from the overhead outlet ports down to the respective *prv*-emitter assemblies. Drop-tube lengths vary in the range 2.6 to 3.8m and the constant above ground clearance of the emitter is 0.6m. The emitter used in the SampleProject_5 is a spray nozzle (Super spray UP3 model) with a nozzle size of 5.556mm (7/32)" from Senninger (Senninger, 2017b). The emitter hydraulic parameters are summarized in Table 13b.

The model of the *prv* used in the lateral considered here is PSR2 (Senninger, 2017a). The *prv*-set pressure, the maximum allowable inlet pressure for the *prv* to operate reliably in the active mode, and the minimum required pressure head margin between the *prv*-inlet pressure and the *prv*-set pressure for the *prv* to operate reliably in the active mode are summarized in Table 13b and also in Figure 47.

A section of the tabular input data of the current sample project is displayed in the input data table (Figure 47). The input data table consists of 24 columns and 672 rows. In contrast to the input data table of SampleProject_9 (of the Droptube-Emitter system configuration option) where the entire column for the *prv* indicator parameter is set to zero, for the current sample project the even-numbered rows of the *prv* indicator parameter column are set to 1 (Figure 47). This indicates that the lateral considered in the current sample project is fitted with *prvs*.

Note that the complete input data-set for the current sample project is saved in the "InputData_LinLat.Inp" file, and also in an excel version of the input data file, "InputData_LinLat.Xlxs". Both of these files were placed in the SampleProject_5 folder during program installation.

6.2.2.b. Output data: SampleProject_5 of the Droptube-Prv-Emitter system configuration option

Figure 48 depicts the output data for SampleProject_5 of the Droptube-Prv-Emitter system configuration option. The output data consists of both nontabular and tabular data blocks.

A summary of the emitter discharge variability data, displayed in the output window, shows that emitter discharges along the lateral vary between a minimum of 0.3293L/s and a maximum of 0.3654L/s and the average is 0.3464L/s. On the other hand, the emitter head differential profile ranges between a lower limit of 9.82m and an upper limit of 12.08m, with a mean value of 10.88m.

A summary of the system hydraulic performance shows that with a uniformity coefficient of 0.958 and a low-quarter distribution uniformity 0.954, the computed emitter discharge profile along the lateral can be considered highly uniform. The uniformity coefficient and low-quarter distribution uniformity of the emitter head differential profile are 0.917 and 0.909, respectively, which also suggests a high degree of uniformity.

Furthermore, the output data in the additional output groupbox show that 104 of the 330 *prvs* are operating in the active mode and the remaining 226 *prvs* are operating in the passive mode and the error in the computed inlet-head estimate is 0.0011m or 0.0046% of the imposed inlet head.

A section of the tabular output data for SampleProject_5, of the Droptube-Prv-Emitter system configuration option, is displayed in the output data table (Figure 48). The output data table consists of 20 columns and 672 rows. Note that the complete set of computed lateral hydraulic parameters (i.e., output data) is saved in the "OutputData_LinLat.Out" file and the additional output files listed in Table 7, all of which were placed in the current sample project folder during program installation.

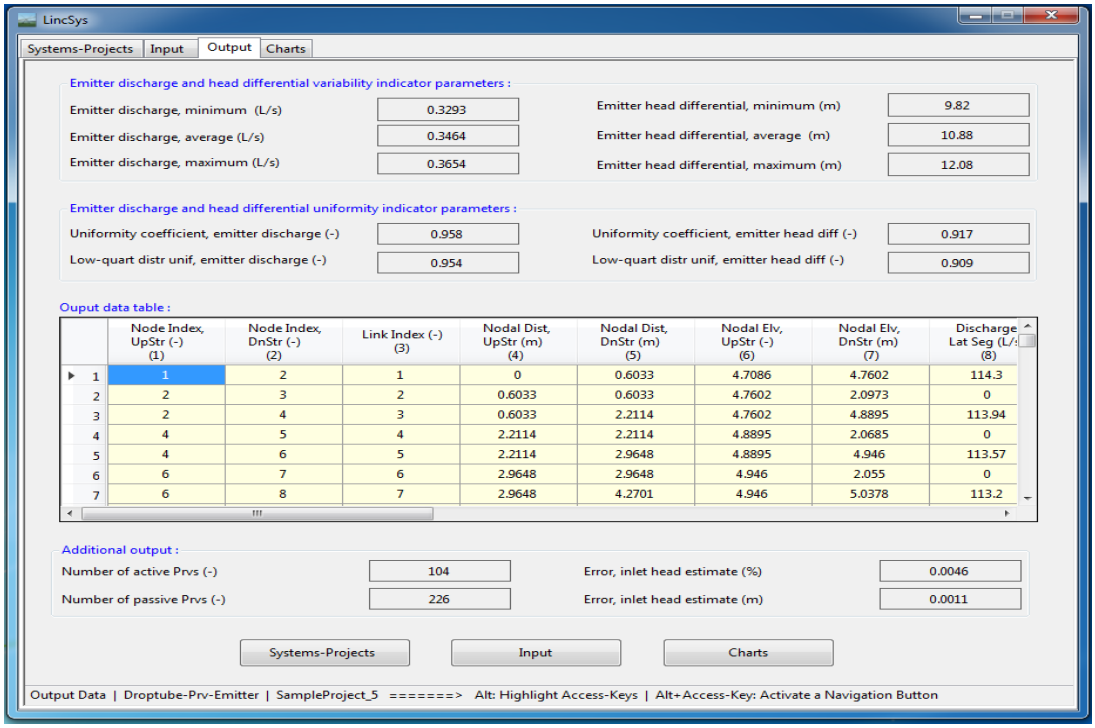

Figure 48. The Output window: SampleProject_5 of Droptube-Prv-Emitter system configuration option

6.2.2.c. Output charts: SampleProject_5 of the Droptube-Prv-Emitter system configuration option

Three of the eleven output charts of SampleProject_5, consisting of *(i)* the lateral pressure head profile, *(ii)* the emitter head differential, *prv*-inlet pressure, and *prv*-set pressure profiles, and *(iii)* the emitter discharge profile are presented next.

Lateral pressure profile chart

The lateral pressure profile for the current sample project is shown in Figure 49. The lateral pressure profile of the current sample project as well exhibits both in-span (shown in solid-line) and inter-span trends (depicted in dash-dotted line). A closer look at Figure 49 shows that the inter-span pressure variability trends down, but at a decreasing rate, over spans #1 to 5 and then inches upwards over spans #6 and 7 as one moves downstream along the lateral. The main explanatory factor for the slight rise in the inter-span pressure variability trend curve observed over spans #6 and 7 is the field slope, which varies along the lateral between a negative gradient (over the upstream-end span and spans #5 to 7) and a level section (over spans #2 to 4).

A more detailed discussion on the relationship between the inter-span pressure variability trends and field slope is provided by Zerihun and Sanchez (2019c).

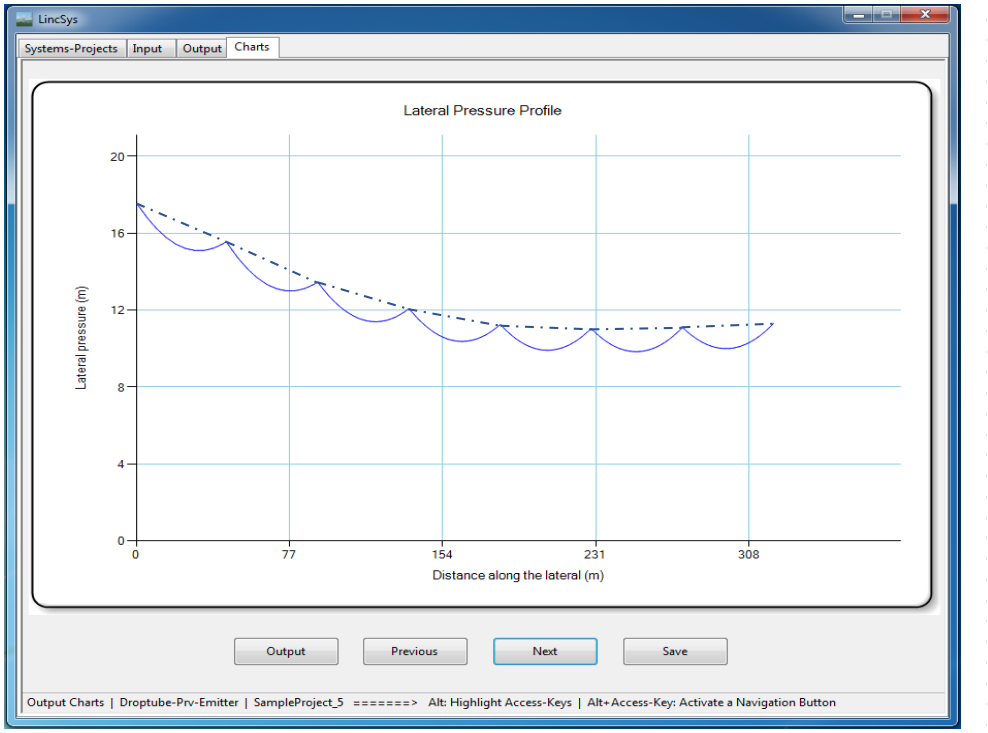

Figure 49. Lateral pressure profile chart: SampleProject_5 of the Droptube-Prv-Emitter system configuration option (the solid-line represents the actual pressure head profile and the dash-dotted line depicts the inter-span variability trend)

Chart depicting emitter head differential, prv-inlet pressure, and prv-set pressure profiles

Figure 50 depicts the profiles of the *prv*-set pressure along with the computed emitter head differential and *prv*-inlet pressure for the current sample project. The upper most curve is the *prv*-inlet pressure profile. The lower most curve is the emitter head differential profile and the horizontal line in between is the *prv*-set pressure profile, which is constant at 12.0m. The inlet pressure at the upstream-end *prv* is 20.42m, which is well above the minimum required for the *prv* to operate reliably in the active mode, i.e., 15.5m (note that the minimum required *prv*-inlet pressure is the sum of the *prv*-set pressure and the minimum required margin between the *prv*-inlet and *prv*-set pressures for the *prv* to operate reliably in the active mode, which is 3.5m).

As can be noted from Figure 50, the *prv*-inlet pressure generally trends down with distance from the lateral inlet. It falls under the 15.5m mark at a distance of 101.5m from the inlet and thereafter it continues to decline at a decreasing pace over the next 127.9m segment of the lateral. Then, the *prv*-inlet pressure inches slightly upwards over the lower 91.0m section (i.e., over spans #6 and 7) of the lateral, mainly because of the negative gradient of the field that this section of the lateral is installed in. Nonetheless, the *prv*-inlet pressure profile stays under 15.5m over the lower 219.0m reach of the lateral.

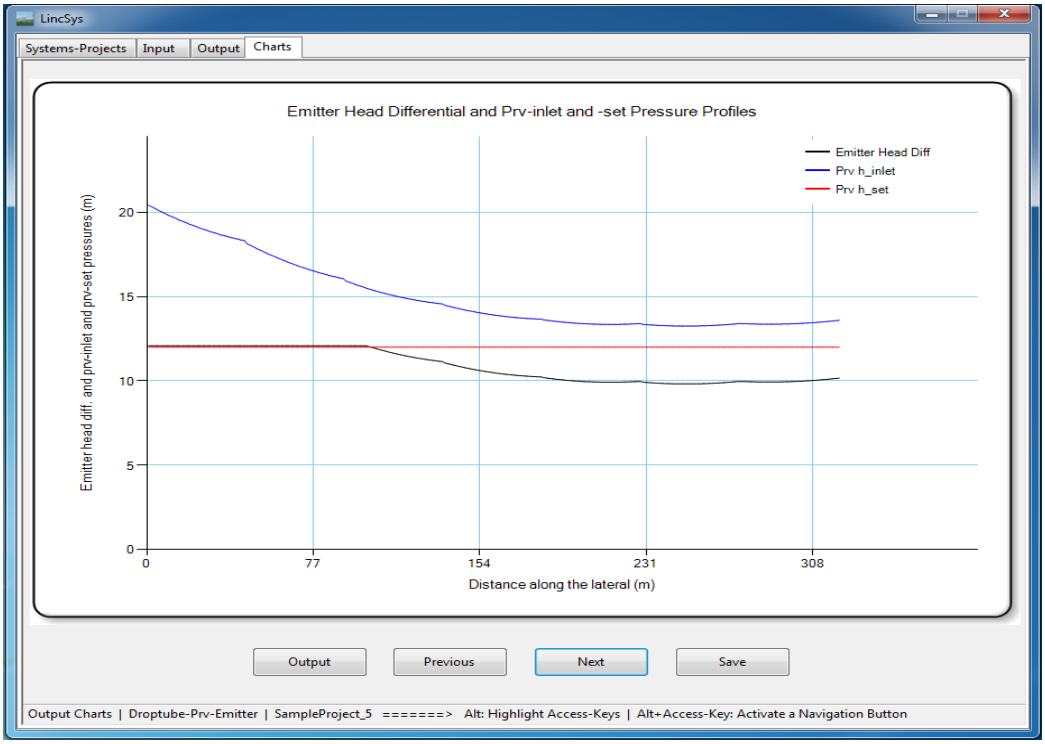

Figure 50. Chart depicting head differential across emitter, *prv*-inlet pressure, and *prv*-set pressure profiles: SampleProject_5 of the Droptube-Prv-Emitter system configuration option

The implication is that over the upper 101.5m section of the lateral (which contains 104 of the 330 *prv*-emitter assemblies in the lateral) the *prv*-inlet pressures are at least equal to the minimum required inlet pressure for an active *prv*. Considering that the maximum allowable *prv*-inlet pressure is 81.0m (Table 13b), which exceeds the computed maximum *prv*-inlet pressure of 20.42m, it can be readily observed that in the upper 101.5m reach of the lateral, the *prv*-inlet pressure varies within the range required for the *prv* to operate reliably in the active mode (i.e., between a minimum of 15.5m and a maximum of 81.0m). It, thus, follows that the *prvs* in this lateral segment operate in the active mode and hence the corresponding emitter pressures are constant at the *prv*-set pressure. As a result, in Figure 50 the *prv*-set pressure and the emitter head differential profiles are overlapped over this section of the lateral.

By comparison, over the lower 219.0m reach of the lateral the *prv*-inlet pressures are less than the minimum required for an active *prv* (i.e., 15.5m). Consequently, the emitter head differentials, over this segment of the lateral, are less than the corresponding *prv*-set pressures (Figure 50) and hence all the 226 *prvs* there are operating in the passive mode.

Notably, the *prv*-inlet pressure profile is a nearly smooth and almost convex function of distance from the lateral inlet (Figure 50). In other words, the effects of the in-span elevation differentials, on the *prv*-inlet pressure profile, are not as evident as they are in the lateral pressure head profile (Figure 49). The explanation for this observation relates to the position of the *prvs* relative to the lateral centerline and the spatial invariance of the *prv*-emitter above ground clearance.

Because of the positions of the *prv*-emitter assemblies relative to the lateral centerline, the *prv*-inlet pressures are significantly greater than the corresponding lateral outlet pressures. For instance, the lateral-wide average pressure differential between the *prv*-inlet pressure and the corresponding lateral outlet pressure for the current sample project is about 3.42m (which is the average drop-tube length). Furthermore, because of the positioning of the *prv*-emitter assemblies at a uniform above ground clearance from the field surface, the pressure head differentials between the *prv*-inlets and the respective lateral outlets vary in a pattern that nearly even-out the in-span elevation differential effects on the *prv*-inlet pressure head profile. Consequently, the span-scale wiggles that are prominent in the lateral pressure profile (Figure 50) are barely discernible over a section of the *prv*-inlet pressure profile spanning the lower 219.0m segment of the lateral.

Furthermore, over the lower 219.0m segment of the lateral where *prvs* are operating in the passive mode (and hence the emitters interact directly with the flow dynamics upstream of the *prv*) the emitter head differential profile shows a spatial variability pattern that is analogous in form to that of the *prv*-inlet pressure profile. Given that the emitter head differential differs from the *prv*-inlet pressure by a constant amount (an amount equal to the required pressure head margin between the *prv*-set pressure and the *prv*-inlet pressure, 3.5m), it stands to reason that these profiles exhibit a similar spatial pattern over the lower 219.0m section of the lateral.

Note that the data used to create this chart is saved in the "Chart_EmitterPrvInletSetPres.Dat" file.

Emitter discharge profile chart

The emitter discharge profile for SampleProject_5 of the Droptube-Prv-Emitter system configuration option is depicted in Figure 51. A closer look at the emitter discharge profile reveals that it is analogous in form to that of the emitter head differential profile (Figure 50). It is constant at 5.792GPM (0.3654L/s) over the upper 101.5m segment of the lateral (which is the segment of the lateral in which *prvs* are operating in the active mode) and thereafter it generally trends down with distance from the lateral inlet over the next 127.9m segment of the lateral. It then inches slightly upwards over the distal 91.0m section (i.e., spans # 6 and 7) of the lateral. Nonetheless, emitter discharge over the lower 219.0m reach of the lateral stays under that corresponding to the *prv*-set pressure.

Note that the slight wiggles evident in the emitter discharge profile over the lower 219.0m section of the lateral (Figure 51) represent traces of the effects of the spans' curvature on the emitter discharge profile, as was the case with the emitter head differential profile (Figure 50). Given that emitter discharge is a direct function of emitter head differential, it can be readily observed that the similarity in the spatial pattens of the emitter head differential and emitter discharge profiles is consistent with intuitive reasoning.

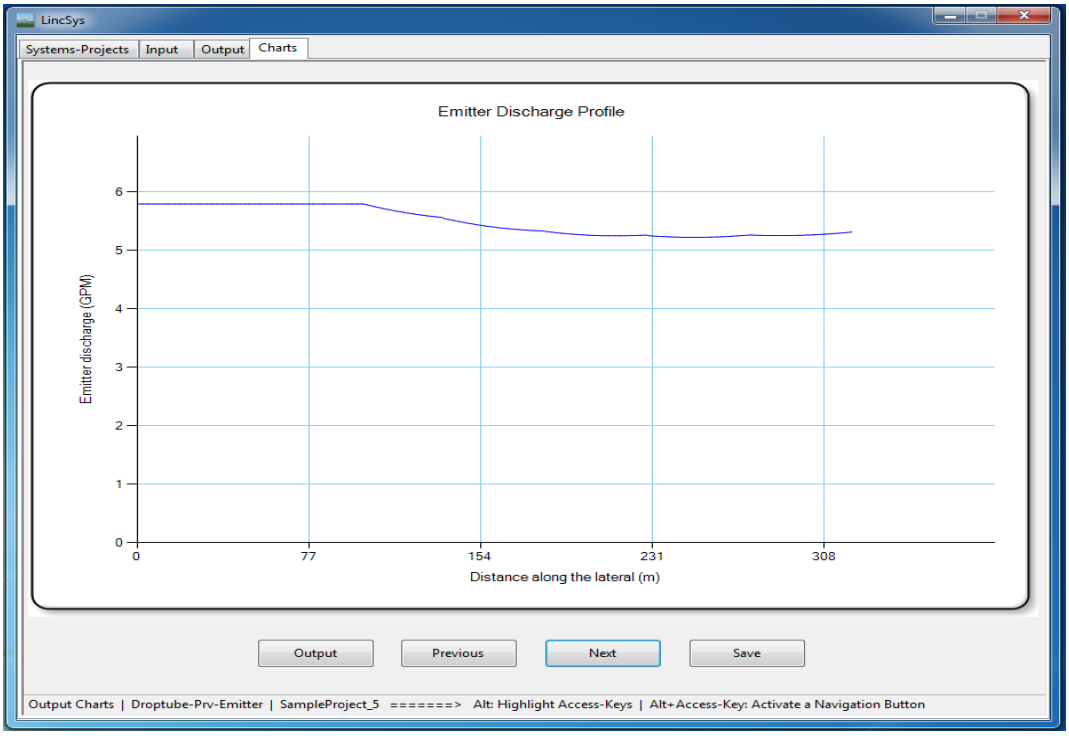

Figure 51. Emitter discharge profile: SampleProject_5 of the Droptube-Prv-Emitter system configuration option

6.2.3. Emitter-On-Lateral system configuration option

6.2.3.a. Input data: SampleProject_15 of the Emitter-On-Lateral system configuration option

Among the 15 sample projects under the EmitterOnLat system configuration option folder, SampleProject_15 is presented here as an example (Tables 15a and 15c). The nontabular input data and a part of the tabular input data for SampleProject_15 are depicted in Figure 52.

The current sample project considers a lateral with 6 concave spans, each 61.3m long along the centerline of the lateral (Table 15a). The lateral is 367.9m long and is installed in a level field. The lateral is supported by seven wheeled towers each 3.8m in height. Thus, using the field surface as the reference datum, the elevation of the lateral inlet is 3.8m. The total head at the lateral inlet is 15.0m (Figure 52).

Pipe diameter varies along the lateral. A diameter of 88.9mm was used over spans #1 to 4, which is then reduced to 50.8mm in span #5 and to 38.1mm over span #6 (Table 15a). A total of 59 outlet ports with a reference emitter spacing of 6.29m are used to distribute water along the length of the lateral (Table 15c). Emitters used in the current lateral, which are placed directly on the outlet ports, are high pressure impact sprinklers (30WH model) with a spreader nozzle (nozzle size of 3.175×2.381mm [1/8”×3/32]”) from Raindbird (Rainbird, 2020). The emitter hydraulic parameters, obtained by fitting a power function to the pressure-discharge data

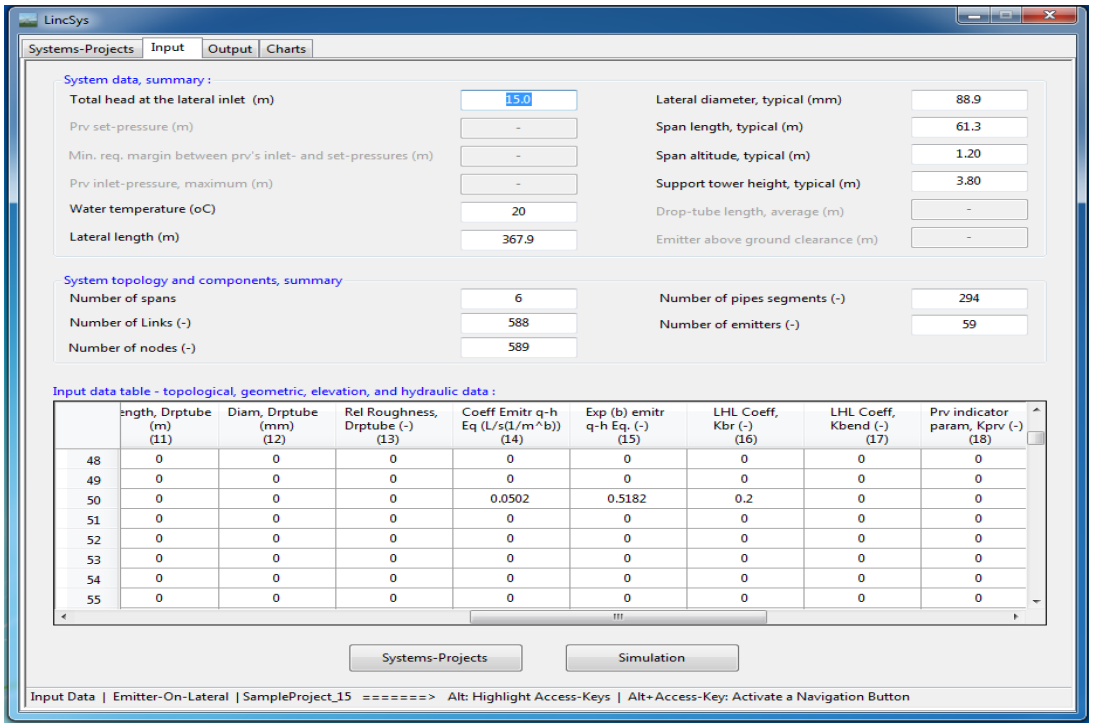

Figure 52. The Input window: SampleProject_15 of the Emitter-On-Lateral system configuration option

provided in the manufacturers' catalogue, are summarized in Table 15c. Note that the input data boxes for the *prv* hydraulic parameters (Figure 52) are deactivated, because the lateral considered in the current sample project does not have *prvs*. In addition, input boxes for the average drop-tube length and emitter above ground clearance are also deactivated, indicating that the lateral has no drop-tubes and the above ground clearance of emitters is not constant along the lateral.

A section of the tabular input data for SampleProject_15 of the Emitter-On-Lateral system configuration option is displayed in the input data table (Figure 52). The complete input data table for the current sample project consists of 24 columns and 588 rows. Note that the drop-tube parameter columns (columns #11 to 13) and the columns for the local head loss coefficient associated with bending losses and the *prv* indicator parameter (i.e., columns #17 and 18, respectively) are set to zero, indicating that the lateral considered in the current sample project is not fitted with drop-tubes and *prvs*.

The complete input data-set for the current sample project is saved in the "InputData_LinLat.Inp" file, and also in an excel version of the input data file, "InputData_LinLat.Xlxs". Both these files were placed under the current project folder during program installation.

6.2.3.b. Output data: SampleProject_15 of the Emitter-On-Lateral system configuration option

Output data for SampleProject_15 of the Emitter-On-Lateral system configuration option are depicted in Figure 53. The output data consists of both nontabular and tabular data blocks.

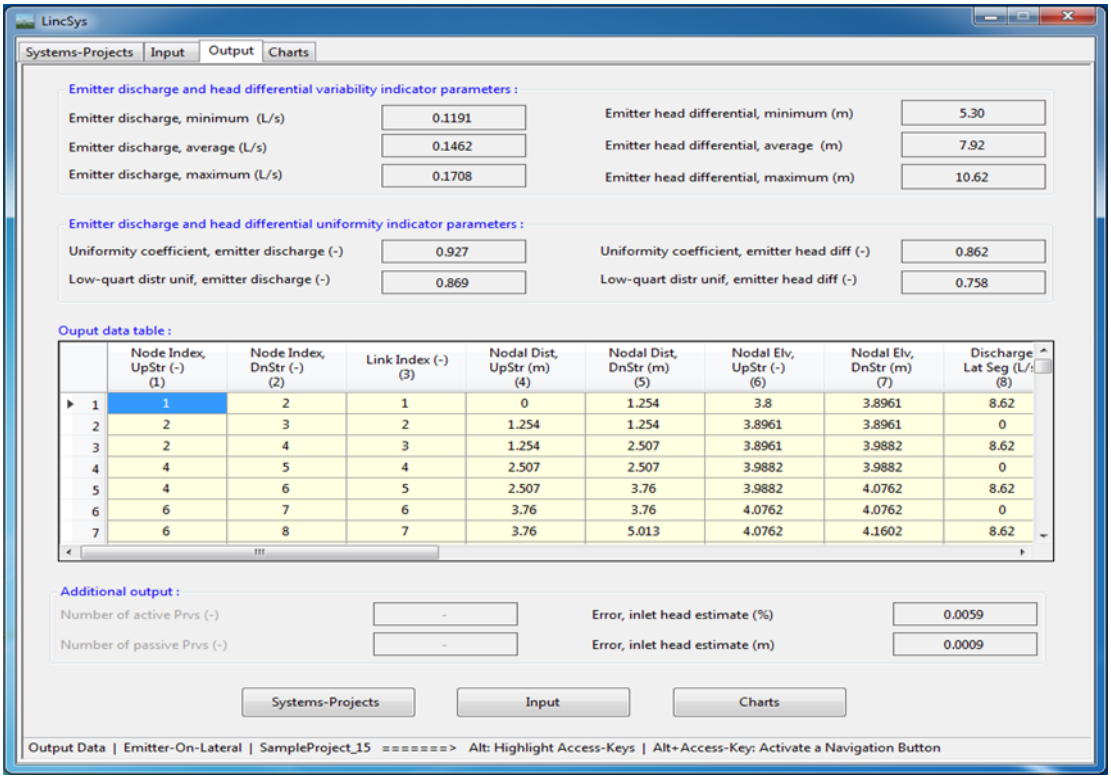

Figure 53. The Output window: SampleProject_15 of the Emitter-On-Lateral system configuration option

The computed emitter discharge variability data, displayed in Figure 53, shows that emitter discharges along the lateral vary over a relatively wider range from a lower limit of 0.1191L/s to a maximum of 0.1708L/s and the average is 0.1462L/s. On the other hand, the emitter head differential profile vary between 5.30 and 10.62m and the mean value is 7.92m.

The system hydraulic performance summary shows that the emitter discharge uniformity coefficient is 0.927 and the low-quarter distribution uniformity is 0.869, which suggests a fairly high emitter discharge uniformity along the lateral. With a uniformity coefficient of 0.862 and a low-quarter distribution uniformity of 0.759, the emitter head differential profile is rather less uniform compared to the discharge profile.

Furthermore, the output data in the additional output groupbox show that the error in the computed inlet-head estimate is 0.0009m or 0.0059% of the imposed inlet head. Note that the input boxes, for the operating modes of the *prvs*, are deactivated, indicating that the lateral considered here is not fitted with *prvs*.

A section of the tabular output data for the current sample project is displayed in the output data table (Figure 53). The output data table consists of 20 columns and 588 rows. Note that the complete set of computed hydraulic parameters (i.e., output data) can be found in the "OutputData_LinLat.Out" file and the additional output files listed in Table 7, all of which were placed in the current sample project folder during program installation.

6.2.3.c. Output charts: SampleProject_15 of the Emitter-On-Lateral system configuration option

A set of output charts of SampleProject_15, consisting of: *(i)* the lateral elevation profile and the computed lateral hydraulic and energy grade-lines, *(ii)* the lateral pressure profile, and *(iii)* the emitter discharge profile will be presented next.

Chart depicting lateral elevation profile and hydraulic and energy grade-lines

As can be noted from Figure 54, the energy grade-line (i.e., the upper most curve) decreased steadily with distance along the lateral from a maximum value of 15.0m at the lateral inlet to 10.15m at the distal-end of the lateral. The hydraulic grade-line (which is right under the energy grade-line) varies between a minimum of 10.15m at the distal-end to 14.9m at the inlet. The total head and the hydraulic head, near the distal-end of the lateral, appear to be identical for the current sample problem as well. These data suggest that the velocity head at the distal-end is zero, which actually is not the case. It appears so, only because the velocity head at the distal-end, in particular (and over the entire lateral in general), is of a much smaller order of magnitude compared to the hydraulic and the total heads.

Note that both the energy and the hydraulic grade-lines have three segments. Over the upper 245.2m segment (covering spans #1 to 4) of the lateral both parameters decrease with distance from the lateral inlet at a decreasing rate. However, in the upper reach of span #5, the trend observed in the upstream spans is reversed and both the energy and hydraulic grade-lines begin to decline at a faster pace with distance from the lateral-inlet, although the rate of decrement slows down with distance within span #5 as well. Once again in the upper section of

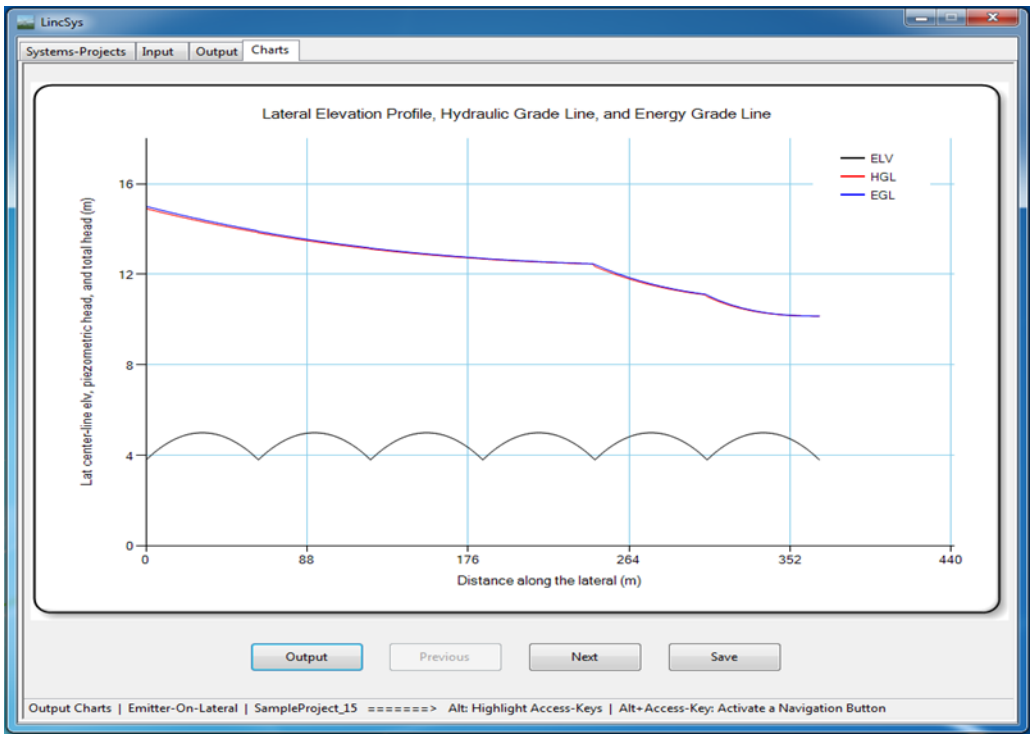

Figure 54. Chart depicting the lateral elevation profile and the hydraulic and energy grade-lines: SampleProject_15 of the Emitter-On-Lateral system configuration option

span #6, the rate of decrement in both the energy and hydraulic grad-lines tend to accelerate compared to the lower section of span #5. Evidently, the observed pattern of variability in the lower reaches of the energy and hydraulic grad-lines is related to the progressive decrement in lateral diameter from 88.9mm over spans #1 to 4 to 50.8mm in span #5 and then to 38.1mm in span #6.

Note that in Figure 54, the lower most curve, with a series of concave segments, represents the elevation profile of the lateral centerline, which shows that the lateral is installed on a level field.

Lateral pressure profile chart

The lateral pressure profile for the current sample project is depicted in Figure 55. Consistent with the results described earlier for the other sample projects, here as well the lateral pressure profile exhibits both in-span patterns (solid-line) and inter-span trends (dash-dotted line). A closer look at Figure 55 shows that the inter-span pressure variability trends down over spans #1 to 4, but at a decreasing rate, as one moves downstream from the lateral inlet (note that this trend is consistent with the fact that the lateral is installed on a level field). By contrast, over spans #5 and 6 the inter-span pressure variability continue to trend down with distance from the lateral inlet, but at an accelerated pace compared to spans upstream, which evidently is related the progressive reduction in lateral diameter over these spans. A more detailed discussion on the effects of lateral diameter on in-span and inter-span trends of lateral pressure profiles is provided by Zerihun and Sanchez (2019c).

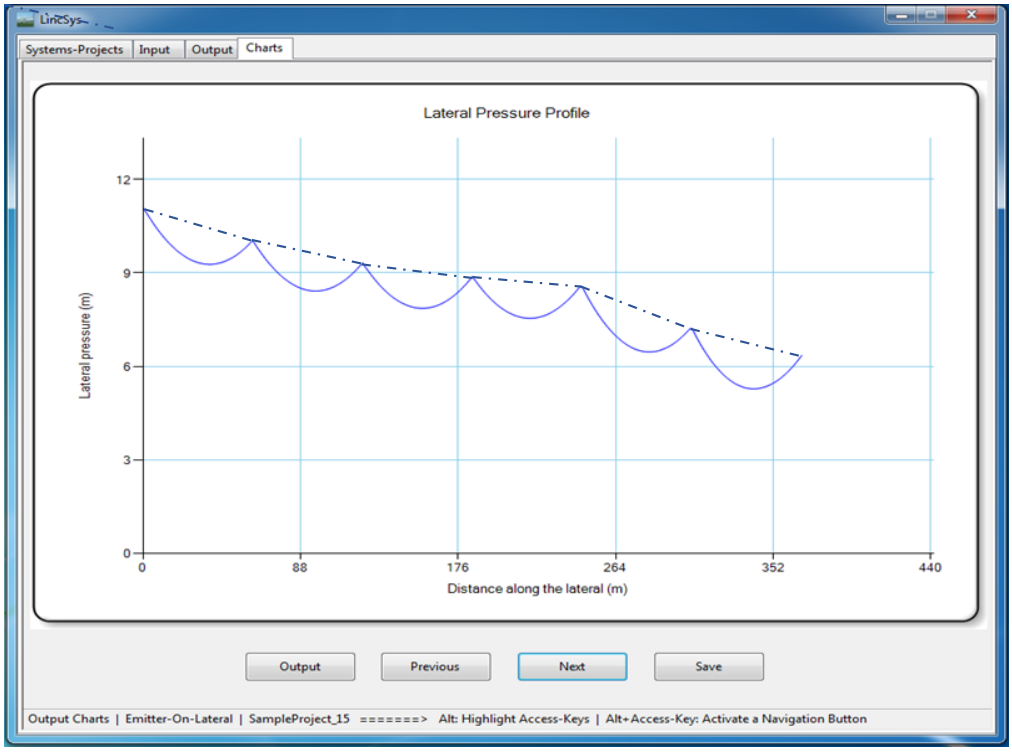

Figure 55. Lateral pressure profile chart : SampleProject_15 of the Emitter-On-Lateral system configuration option

Emitter discharge profile chart

The emitter discharge profile for SampleProject_15 of the Emitter-On-Lateral system configuration option is shown in Figure 56. In contrast to the sample projects of the Droptube-Emitter and Droptube-Prv-Emitter system configuration options, the in-span emitter discharge variability patterns for the current sample project are of the same general form as those of the corresponding lateral pressure profile variability patterns. Given that (in the lateral considered here) emitters are placed directly on the lateral outlets, it can be readily observed that for each emitter, the emitter inlet pressure is nearly the same as the local lateral pressure. The implication is that the emitter discharge profile is a strong function of the lateral pressure profile, which explains the observed similarity in profile patterns between the lateral pressure and emitter discharge profiles.

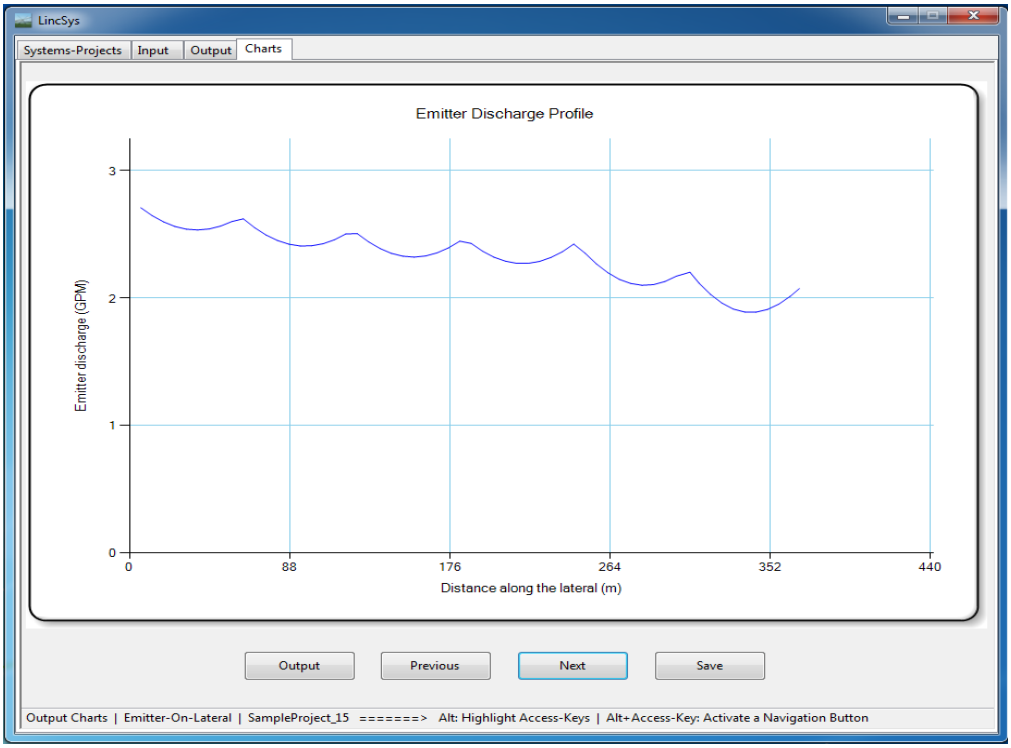

Figure 56. Emitter discharge profile: SampleProject_15 of the Emitter-On-Lateral system configuration option

Although the emitter discharge profile, shown in Figure 56, has the same general form as that of the lateral pressure profile depicted in Figure 55, a closer look at Figure 56, nonetheless, reveals that the local in-span variability patterns of the emitter discharge profile do not precisely follow that of the lateral pressure profile. This is particularly evident in sections of the lateral around some of the span joints (particularly the span joints that are near the upstream-end), where the changes in the slope of the emitter discharge profile (Figure 56) are not as sharp those of the pressure head profile (Figure 55).

The explanation for this observation is related to the significant differences in the nodal and outlet (emitter) spacings used in this lateral. While the reference outlet (emitter) spacing for

the current lateral (a lateral that uses high pressure sprinklers) is set at about 6.29m (Table 15c), the nodal spacing was set to a constant value of 1.25m along the lateral. Thus, the lateral pressure profile, evaluated at each of the computational nodes, has a sufficiently fine resolution to track the form of the lateral elevation profile more closely, even near span joints where the rate of change in lateral elevation is at its maximum. By contrast, the relatively large emitter spacings used in the current lateral meant that for at least some of the span joints emitter placements are such that distances between the location of a span joint and those of the closest emitters are relatively large for the resultant emitter discharge profile to closely track the form of the lateral pressure profile near such a span joint. As a result, sections of the emitter discharge profile, about some of the span joints, appear to be not as sharp as the lateral pressure profiles (Figure 56).

References

Anwar, A.A. (1999). "Friction Correction Factors for Center-Pivots." *J. Irrig. Drain. Eng*., ASCE, 125(5):280-286.

Behave, P.R. and Gupta, R. (2006). *Analysis of Water Distribution Networks*. Alpha Science International Ltd., Oxford, UK.

Boulos, P.F., Lansey, K.E., and Karney, B.W. (2006). *Comprehensive Water Distribution Systems Analysis Handbook for Engineers and Planners.* 2nd Ed., MWH Soft, Pasadena, CA.

Chu, S.T. and Moe, D.L. (1972). "Hydraulics of a Center Pivot System." *Trans ASAE,* 15(5):894-896.

Fraisse, C.W., Heermann, D.F., and Duke, H.R. (1995). "Simulation of Variable Water Application with Linear-Move Irrigation System." *Trans ASAE,* 38(5):1371-1376.

FRIS. (2008). Farm and Ranch Irrigation Survey. Volume 3 – Special studies part 1 – AC-07-SS-Washington, D.C. USDA National Agricultural Statistics Service. Available at: www.agcensus.usda.gov/Publications/2007/Online-Highlights/Farm_Ranch_and_ranch_Irrigation_Survey/FRIS.txt

Gregg, T. (2004) "Water Conservation Best Management Practice Guide." *Report 362, Texas Water Development Board,* Austin, TX.

Granger, R.A. (1995). *Fluid Mechanics*. Dover Publications Inc., New York, NY.

Hathoot, H.M., Abo-Ghobar, H.M., Al-Amudi, A.I. (1994). Analysis and Design of sprinkler irrigation laterals. *J. Irrig. Drain Eng*., ASCE, 120(3):534-549.

Heermann, D.F. and Stahl, K.M. (2006). CPED: Center Pivot Evaluation and Design. https://www.ars.usda.gov/plains-area/fort-collins-co/center-for-agricultural-resources-research/water-management-and-systems-research/docs/cped/

Keller, J. and Bleisner, R. 1990. *Sprinkle and Trickle Irrigation*. Van Nostrand Reinhold, New York, NY.

Keller, J., Corey, F., Walker, W.R., and Vavra, M.E. (1980). Evaluation of Irrigation Systems. In Irrigation: Challenges of the 80's. *Proc. Second Nat'l Irrigation Symp*., 95-105. St. Joseph, MI, ASAE.

Kincaid, D.C., and Heermann, D.F. (1970). "Pressure Distribution on a Center-Pivot Sprinkler Irrigation System." *Trans. ASAE,* 13(5):556-558.

Martin, D.L., Denis, C. K., and Lyle, W.M. (2007). *Chapter 16. Design and Operation of Sprinkler Systems. (eds. Hoffmann, G.J., Evans, R.G., Jensen, M.E., Martin, D.L., Elliott, R.L). 2nd ed, ASABE, St. Joseph, MI,* pp.557-631.

Martin, D., Kranz, W., Smith, T., Irmak, S., Charles, B., and Yoder,. R. (2017). Center Pivot irrigation Handbook. Department of Biological Systems Engineering, University of Nebraska-Lincoln, Lincoln, NE 68583-0726.

Microsoft Corportaion (2017). Microsoft Visual Studio Community 2017.

Microsoft Corportaion (2019). Microsoft Visual Studio Community 2019, Version 16.4.

New, L and Fipps, G. (2020). Center Pivot Irrigation. Texas Agricultural Extension Service . Texas A&M University System. https://oaktrust.library.tamu.edu/bitstream/handle/1969.1/86877/pdf_1181.pdf?sequence=1&isAllowed=y

Scaloppi, E. J. and Allen, R.G. (1993). "Hydraulics of Center-Pivot Laterals." *J. Irrig. Drain. Eng*., ASCE, 119(3):554-567.

Senninger (2015). Chart No. MK-923-13B. Senninger Irrigation Inc., Clermont, FL.

Senniger.com (Accessed 2017a). "Super Spray Customizable Field Proven Technology." https://www.senninger.com/sites/senninger.hunterindustries.com/files/super-spray-up3-brochure.pdf.

Senninger (Accessed 2017b) "Pressure Regulator Guide." (https://www.senninger.com/sites/senninger.hunterindustries.com/files/pressure-regulator-guide.pdf.).

Tabuada, M.A. (2014). "Friction Head Loss in Center-Pivot Laterals with Single Diameter and Multidiameter." *J. Irrig. Drain. Eng.* ASCE, 10.1061/(ASCE)IR.1943-4774.0000755.

Valiantzas, J.D. and Dercas, N. (2005). "Hydraulic Analysis of Multidiameter Center-Pivot Sprinkler Laterals." *J. Irrig. Drain. Eng.* ASCE, 10.1061/(ASCE)0733-9437(2005) 131:2(137).

Zerihun, D. and Sanchez, C.A. (2014). Field-scale sprinkler irrigation system hydraulic model. II, Hydraulic Simulation. *J. Irrig. Drain Eng.,* 10.1061/(ASCE)IR.1943-4774.0000723, 04014020.

Zerihun and Sanchez (2017). Irrigation Lateral Hydraulics with the Gradient Method. *J. Irrig. Drain Eng.*, 10.1061/(ASCE)IR.1943-4774.0001195.

Zerihun, D. and Sanchez, C.A. (2019a). Hydraulics of linear-move sprinkler irrigation systems, I. System Description, Assumptions, and Definition of the Hydraulic Simulation Problem. *Irrig. Drainage. System Eng.* 8:235.

Zerihun, D. and Sanchez, C.A. (2019b). Hydraulics of linear-move sprinkler irrigation systems, II. Model Development. *Irrig. Drainage. System Eng.* 8:236.

Zerihun, D. and Sanchez, C.A. (2019c). Pressure head profile of Linear-Move Sprinkler Irrigation Lateral: Analysis, Equation, and Profile Patterns. *Irrig. Drainage. System Eng*. 8:239.

Zerihun, D. and Sanchez, C.A., Thorp, K.R., Thorp, and Hagler, M.J. (2019). Hydraulics of linear-move sprinkler irrigation systems, III. Model evaluation. *Irrig. Drainage. System Eng.* 8:237.